D 2022

U.PORTO
FEUP FACULDADE DE ENGENHARIA
UNIVERSIDADE DO PORTO

THERMAL INSULATION SOLUTIONS FOR HISTORIC BUILDINGS:
FEASIBILITY, EFFICACY, COMPATIBILITY

MAGDA POSANI
TESE DE DOUTORAMENTO APRESENTADA
À FACULDADE DE ENGENHARIA DA UNIVERSIDADE DO PORTO EM
ENGENHARIA CIVIL

SUPERVISORS

Supervisor:
Doctor Maria Do Rosário Veiga,
Senior Researcher (Investigadora Principal com Habilitação) at the Department of Buildings at the National Laboratory of Civil Engineering National Laboratory for Civil Engineering (LNEC).

Co-supervisor:
Professor Vasco Manuel Araújo Peixoto de Freitas,
Full Professor at the Department of Civil Engineering at FEUP - Faculty of Engineering of the University of Porto (FEUP).

Supervisor	Co-supervisor

ASSESSMENT COMMITTEE

Professor Humberto Salazar Amorim Varum (President of the committee)**,**
Full Professor at the Faculty of Engineering of the University of Porto (FEUP);

Doctor María del Mar Barbero Barrera,
Associate Professor (Profesor Contratado Doctor), Department of Architectural Construction and Technology at Higher Technical School of Architecture of Madrid (ETSAM), Technical University of Madrid (UPM);

Doctor Maria Isabel Morais Torres,
Assistant Professor at the Department of Civil Engineering, Faculty of Science and Technology of the University of Coimbra (FCTUC);

Doctor Maria Paulina Faria Rodrigues,
Associate Professor at the Department of Civil Engineering, Faculty of Science and Technology of Universidade Nova de Lisboa (FCTUNL);

Doctor Maria do Rosário Veiga (Supervisor),
Senior Researcher (Investigadora Principal com Habilitação) at the Department of Buildings at the National Laboratory of Civil Engineering National Laboratory for Civil Engineering (LNEC);

Doctor Nuno Manuel Monteiro Ramos,
Associate Professor at the Department of Civil Engineering at the Faculty of Engineering of the University of Porto (FEUP).

Defense: May 24th 2022

EUROPEAN DOCTORATE

Experts from higher education institutions of two European countries, other than the one where the thesis was defended, who assessed the thesis:

Professor Juan José Sendra

Full Professor at the Higher Technical School of Architecture of Seville, University of Seville (Spain);

Doctor Barbara Lubelli

Associate Professor, Delft University of Technology – TU Delft (The Netherlands).

DOCTORAL PROGRAM IN CIVIL ENGINEERING

Phone +351-22-508 1901

Fax +351-22-508 1446

✉ prodec@fe.up.pt

Edited by

FACULDADE DE ENGENHARIA DA UNIVERSIDADE DO PORTO

Rua Dr. Roberto Frias

4200-465 PORTO

Portugal

Phone +351-22-508 1400

Fax +351-22-508 1440

✉ feup@fe.up.pt

http://www.fe.up.pt

To my beloved family,
to my friends Michela, Federica, and Nicole,
and to the amazing people I met on the international journey.

ACKNOWLEDGMENTS

I hereby would like to thank for the financial support provided by FCT and CONSTRUCT, and the institutions hosting the research: FEUP and LNEC.

Furthermore, I would like to express my appreciation for the professional and personal support provided by my supervisor and co-supervisor, together with all the time they devoted to improving and correcting my doctoral research. It was a tough, but extremely rewarding, journey.

I would also like to highlight the cooperation and friendship that I found in the colleagues from LNEC and LFC – FEUP, especially Cinthia, Eleonora, Alessandra, Teresa, Mafalda, Giovanni and Sofia.

In addition, I acknowledge the technical assistance provided by the technicians of LNEC for the experimental tests, especially Acàcio Monteiro, whose help was precious.

I express my appreciation for the opportunity I had to spend a period abroad, at the Eindhoven University of Technology (TU/e), in the Netherlands. For this chance, I have to thank the collaboration of my supervisor, co-supervisor and the increased funding provided by FCT. Furthermore, I would like to thank TU/e for hosting me and Prof. Schellen and Dr Kompatscher for the guidance they provided me with. Additionally, I recognize the great personal support and friendship found in Dr Katarina Katìk at TU/e.

Finally, I would like to acknowledge the collaboration of the public institutions that allowed for the indoor monitoring of the case studies and that provided documentation concerning the buildings:

- the staff of the Municipal Library of Porto, especially Dr Lucinda Oliveira,
- the staff of Corucheus' Library, especially Dr Hélder Ferreira,
- *Fondazione Carisbo* and *Genus Bononiae* corporation, in particular its President Prof. Fabio Roversi-Monaco, Dr Pierangelo Bellettini and Dr Daniela Schiavina, for providing the authorization to monitor the Library of San Giorgio in Poggiale. Additionally, I express my appreciation for the assistance provided by the technical staff, namely Arch. Francisco Giordano and the technicians Dr. Giovanni Palladini and Dr. Claudio Fiorini.

Finally, I would like to thank ARPAE and IPMA for providing the meteorological data of Porto, Lisbon, and Bologna.

ABSTRACT

Historical heritage represents a not renewable nor replaceable resource that we have the duty to preserve and deliver to future generations. It is therefore fundamental to keep it in use and to carefully analyse the possible risks involved in rehabilitation interventions. In this context, energy-efficient interventions can pass through the addition of thermal insulation to exterior walls, which is an intervention whose adaptability and compatibility with historic valuable constructions is typically difficult to obtain. Thus, it is extremely important to define the most appropriate solutions for application in this specific scenario.

As a consequence, this study aims to investigate the feasibility, efficacy and compatibility of thermal insulation for the rehabilitation of thick masonry walls of historic buildings located in temperate climates. The research is composed of a literature review and two experimental parts, one focused on indoor climate monitoring in three case studies, and one on the hygrothermal characterization of some thermal insulation solutions considered suitable for applications in historic buildings. In addition, the study adopts validated numerical models to study the efficacy and compatibility of the aforementioned solutions, by means of dynamic hygrothermal simulations.

This research offers a view on the feasibility of adopting thermal insulation to retrofit historic walls, while underlining the restraints affecting the intervention. All considered, thermal mortars emerge to be very suitable for the scope, for several reasons. Among them, the great flexibility of their thickness, their adaptability to uneven surfaces, the gap-filling ability, and the competitive thermal performance. In terms of compatibility, it seems that a general criterion for choosing suitable insulation solutions does not exist, yet. Nonetheless, this study indicates that solutions complying with specific requirements on capillary water absorption and water vapour permeability appear compatible with the case studies considered. Furthermore, this investigation suggests that these recommendations might be more generally applicable for interventions on "thick masonry walls of historic buildings with temporary occupation, located in areas with temperate climates with warm or hot summers and mild winters, where heating systems are adopted". Thermal mortars appear very promising for retrofitting historic walls even when a relatively-thin layer of insulation, such as a 4cm-thick one, is considered. Indeed, numerical simulations showed that thermal mortar can provide for reductions of up to 60% in the intensity of annual thermal discomfort, and up to 40% in the energy demands for heating and cooling, when the buildings are considered in free-floating or under intermittent climate control, respectively. Finally, experimental results indicate the importance of testing not only single materials but also complete thermal rendering and plastering systems, due to the relevant influence of interface phenomena and layered structure.

Overall, thermal mortar-based systems proved to be potentially viable, compatible, and efficient solutions. In addition, the solutions available on the market can be suitable for intervention on historic walls when their hygrothermal properties are clearly and properly defined in the technical documentation.

KEYWORDS: Thermal mortars, massive walls, historic buildings, moisture-related risks, energy savings, thermal comfort.

RESUMO

O património histórico representa um recurso não renovável nem substituível que temos o dever de preservar e entregar às gerações futuras. Por isso, é fundamental mantê-lo em uso e analisar cuidadosamente os possíveis riscos envolvidos nas intervenções de reabilitação. A melhoria do desempenho energético pode passar pela adição de isolamento térmico nas paredes exteriores, dificilmente compatível com as soluções construtivas e arquitetónicas das paredes dos edifícios com valor patrimonial, pelo que é de crucial importância definir os sistemas mais adequados para essas construções.

Este estudo visa investigar a viabilidade, eficácia e compatibilidade de sistemas de isolamento térmico para a renovação de paredes de alvenaria de elevada espessura de edifícios históricos localizados em climas temperados. O estudo é composto por várias partes: revisão de literatura, campanha experimental de monitorização do microclima interior em três casos de estudo, caracterização higrotérmica de algumas soluções de isolamento térmico julgadas viáveis para a intervenção, e simulações através de modelos numéricos validados.

Os resultados da pesquisa oferecem uma visão sobre a viabilidade da adoção de isolamento térmico para a renovação das paredes de edifícios históricos, sublinhando as condicionantes que afetam a intervenção. As argamassas térmicas surgem como uma solução a considerar por vários motivos: grande flexibilidade da espessura, adaptabilidade a superfícies irregulares, capacidade de preenchimento de lacunas, e desempenho térmico elevado. No que se refere à compatibilidade, ainda não existe um critério geral para a escolha de uma solução de isolamento térmico otimizada. No entanto, este estudo indica que as soluções que atendem aos requisitos específicos de absorção capilar de água e permeabilidade ao vapor de água se afiguram aceitáveis para os casos de estudo considerados. Por outro lado, esta investigação sugere que as recomendações formuladas em termos de compatibilidade possam ser aplicáveis para intervenções no cluster “paredes espessas de alvenaria em edifícios históricos com ocupação temporária localizados em áreas de clima temperado, com verões mornos ou quentes e invernos amenos, onde se adotam sistemas de aquecimento ”. As argamassas térmicas são promissoras para este tipo de intervenção, evidenciando as simulações numéricas que tal isolamento pode conduzir a reduções até 60% no desconforto térmico quando os edifícios estão em flutuação livre, e até 40% nas necessidades energéticas para climatização quando se leva em conta o uso intermitente dos sistemas de aquecimento e arrefecimento, nos climas considerados. Finalmente, os resultados experimentais indicam a importância de testar não apenas materiais únicos, mas também sistemas completos baseados em argamassas termicas, devido à influência significativa dos fenômenos de interface e da estrutura em camadas.

Globalmente, os sistemas à base de argamassa térmica podem ser soluções viáveis, compatíveis e eficientes, existindo soluções comerciais paras as quais as propriedades devem ser claramente definidas na documentação técnica.

PALAVRAS-CHAVE: Argamassas térmicas, paredes maciças, edifícios históricos, riscos relacionados com humidade, economia de energia, conforto térmico.

CONTENTS

4. EXPERIMENTAL CHARACTERISATION OF THERMAL MORTAR-BASED INSULATION SOLUTIONS.

6.THERMAL INSULATION FOR HISTORIC WALLS: THE EFFECT ON THERMAL COMFORT AND ENERGY DEMANDS

7. CONCLUSIONS AND FUTURE WORKS

ANNEXES

ANNEX I

ANNEX II

INDEX OF FIGURES

INDEX OF TABLES

NOMENCLATURE

GREEK-LETTER NOTATIONS:

δ	[kg/ (m.s.Pa)]	Permeability to water vapour
μ	[-]	Water vapour diffusion resistance factor
λ	[W/(m.K)]	Thermal conductivity
ρ	[kg/m^3]	Bulk density
ψ	[°]	Angle between the wind direction and the normal to the façade
θ	[°C]	Temperature
f	[-]	Relative humidity

ROMAN-LETTER NOTATIONS:

a	[-]	Short-wave absorption coefficient
A_w	[kg/(m^{2}s$^{1/2}$)] or [kg/(m^{2}min$^{1/2}$)] or [kg/(m^{2}h$^{1/2}$)]	Capillary water absorption coefficient
c	[J/(kg K)]	Specific heat capacity
d	[m]	Thickness
D_w	[m^2/s]	Liquid transport coefficient
D_{ws}	[m^2/s]	Liquid transport coefficient, suction
D_{ww}	[m^2/s]	Liquid transport coefficient, redistribution
H	[J/m^3]	Volumetric enthalpy
I	[W/m^2]	Short wave radiation at the component surface
Is	[W/m^2]	Normal component of the short wave radiation incident on the surface
p	[Pa]	Air pressure
P_0	[%]	Open porosity
p_{sat}	[Pa]	Water vapour saturation pressure
R_1	[-]	Rain coefficient dependent on the studied surface inclination
R_2	[s/m]	Rain coefficient dependent on the vertical distance from the ground
R^2	[-]	Coefficient of determination
RH	[%]	Relative humidity
R_h	[mm/h]	Rainfall on horizontal surfaces
R_{wdr}	[mm/h]	Wind driven rain intensity
s_d	[-]	Equivalent air thickness
T	[°C]	Temperature
t	[s]	Temporal variable (time)
T_{OC}	[°C]	Operative temperature of comfort
T_{RM}	[°C]	Running mean outdoor temperature
u	[m^3/m^3]	Water content mass by mass
V	[m/s]	Average hourly wind speed at 10 meters height
w	[kg/m^3]	Volumetric water content

w_f	[kg/m^3]	Free saturation water content
x	[m]	Spatial variable (distance)

ACRONYMS AND ABBREVIATIONS:

CEN		European Committee for Standardization
CO_2		Carbon dioxide
CV(RMSE)	[%]	Coefficient of Variation of the Root Mean Square Error
EAD		European Assessment Document
EOTA		European Organisation for Technical Approvals
ETICS		External Thermal Insulation Composite Systems
GHGs		Greenhouse gases
HVAC		Heating, Ventilation and Air Conditioning
NMBE	[%]	Normalized Mean Bias Error
PIR		Polyisocyanurate
PUR		Polyurethane
TRY		Test Reference Year
VIP		Vacuum Insulation Panels
WDR		Wind-driven rain
XPS		Extruded polystyrene

CODES USED FOR MATERIALS AND SYSTEMS:

A1	Thermal mortar 1 (with cork aggregates)
A2	Thermal mortar 2 (with cork aggregates)
A3	Thermal mortar 3 (with EPS aggregates)
B1	Regularization Mortar
B2	Regularization and Finishing Mortar
C1	Paint – Indoor use
C2	Paint – Outdoor use
MW	Hydrophobic mineral wool
EPS	Expanded polystyrene

S1	Whole system: A1+B1+C1– Indoor use
S2	Whole system: A1+B1+C2 – Outdoor use
S3	Whole system: A2+B1+C1– Indoor use
S4	Whole system: A2+B1+C2 – Outdoor use
S5	Whole system: A3+B2 – Indoor/Outdoor use
S_MW	Whole system: MW+B2 – Indoor/Outdoor use
S_EPS	Whole system: EPS+B2 – Indoor/Outdoor use
S5_mu	Whole system for parametric study): A3 (imposed μ=50) +B2
S5_Aw	Whole system for parametric study): A3 (imposed A_w=0) +B2
S5_Aw_mu	Whole system for parametric study): A3 (imposed μ=50, A_w=0) +B2

1
INTRODUCTION

1.1. MOTIVATION

Our global climate is changing as a consequence of human activity (Balibar, 2017) and the problem has become so serious that it is believed to be one of the defining issues of the current century (Jordan et al., 2010).

The attention given to the problem resolution has grown since the 1992 United Nations Framework Convention on Climate Change (UNFCCC), passing through the Kyoto Protocol and arriving at the Paris Agreement (Pischke et al., 2019), thus achieving an international collaboration aimed at fighting the climate change (United Nations, 2018). Despite the common commitment to the cause, in 2019 the European parliament declared the climate and environment emergency (European Parliament, 2019), because of the inadequacy of the progress made worldwide towards the objectives of the Paris Agreement (European Commision, 2020). Consequently, the European Commission decided to lead the way by example with the European Green Deal (European Commission, 2019), through which the EU committed to make Europe the first climate-neutral continent by 2050, i.e. the first one with net-zero greenhouse gases (GHGs) emissions. What is more, in 2020 the EU legally embraced the urgency and importance of cutting GHGs emissions via introducing the first-ever European Climate Law (European Commision, 2020), making the sustainable strategy of the Union legally binding for all member states.

Hence, the EU is pursuing an ambitious policy on climate actions and it is urgently calling to accelerate and underpin the transition needed in all sectors, focusing particularly on resource-intensive ones, and among them, the construction industry. The building sector was identified in 2017 as the largest single energy consumer in Europe, with 40% of the total energy use. Given that 75% of the existing stock is energy inefficient and that a very small percentage (0.4-1.2%) of it is renovated each year (European Commission, 2017), existing buildings offer vast potential for energy use reduction, which the EU is addressing through the 'renovation wave' initiative introduced with the European Green Deal (European Commission, 2017).

The urgency of retrofitting existing constructions in Europe is thus clear and the specific case of historic buildings has great importance for several reasons.

First, 14% of existing buildings date to before 1919 in Europe, and this percentage reaches 26% if the ones built before 1945 are also considered (Ascione et al., 2015). Hence, a considerable share of the existing stock is composed of historic buildings (Arayici et al. 2017, Hao, Herrera, and Troi, 2018), defined as

traditional constructions (Wood, Brocklebank and Pickles, 2010) from before 1945, as they use some technologies, materials and solutions that are no longer being used, thus acting as testimonies of technical and architectural historic paradigms. As a consequence, retrofitting historic constructions can play a key role in reducing global energy consumptions (Brandt, 2017) and consequent GHGs emissions, thus collaborating in the mitigation of climate change, as widely underlined by cultural heritage experts in Europe (Sesana et al., 2018).

What is more, beyond the opportunity for energy savings, retrofits can improve indoor comfort (Pracchi and Buda, 2018) while lowering operational costs (Troi and Bastian, 2015), factors that are fundamental to ensure the continued use of historic constructions over time, and, with that, improving their preservation and durability. It is indeed well known that keeping in use heritage buildings is the most effective tool of protection, in accordance with the integrated conservation strategies (Council of Europe, 1975), as it ensures continuous maintenance while avoiding leaving the building in a state of neglect (Carbonara, 2015).

Likewise, retrofitting historic heritage plays a crucial role in sustainable development. Indeed, having comfortable, retrofitted buildings that are suitable for being kept in use means reducing the need for new constructions, which is a highly sustainable intervention in terms of reduction of GHGs emissions (Rosales Carreón, 2015). What is more, heritage buildings represent a non-renewable nor replaceable resource that we have the duty to deliver to future generations (Franco and Magrini, 2017). For this reason, adapting, reusing and preserving historic buildings appear as key elements in the field of sustainability, as already underlined by the United Nations through the 2030 Agenda for Sustainable Development (Appendino, 2017).

1.2. RESEARCH GAP: THERMAL INSULATION SOLUTIONS FOR HISTORIC WALLS, AN OPEN QUESTION.

Given the growing urgency and importance of the topic, the scientific interest in energy efficiency and thermal comfort in historic buildings has strongly increased in the last decades (Martínez-Molina et al., 2016). Several solutions are thus provided in the literature, and, among the others, the use of thermal insulation appears as a very debated intervention.

In a preliminary literature review (Posani, Veiga and Freitas, 2018) it was observed that thermal insulation solutions can be applied to roofs, floors and walls in historic buildings. Nonetheless, the last intervention appeared to be the most discussed in the literature, due to the difficult feasibility, the unclear efficacy and the high moisture-related hazards entailed, especially when the intervention concerns the indoor-facing side of walls. Consequently, the focus of this research is put on thermal insulation solutions for external walls, since this field appears to need further investigations. Some of the main concerns and opens questions are discussed in the following text.

The use of thermal insulation in historic buildings represents a very complex intervention. It cannot be a performance-based adjustment, but it should be used as a preservation tool (Carbonara, 2015) that does not alter the unique character of the construction. Hence, the adoption of insulation in historic buildings is not always feasible because of the need of preserving their original appearance. The aspect of external walls is usually one of the most important characteristics of a historic building and it contributes to creating its unique and local character. Consequently, interventions at the indoor-facing

side of walls are generally more suitable than the ones at its external side, especially when a complete internal re-plastering is needed. Nonetheless, external-side applications cannot be excluded a priori and the choice depends on the features characterizing the construction, as well as the legal-technical regulations protecting the specific building. Another problem concerns the thickness of the insulation system, which is subjected to restrictions related to the dimensional changes entailed in the envelope geometry. Indeed, the perception of internal spaces and outdoor shapes should be preserved, avoiding marked changes in the wall thickness, especially at window and door openings and near surfaces with valuable details. Thus, relatively thin insulation solutions should be taken into account.

The former restriction leads to a second concern, which is the effectiveness of applying a thin layer of insulation to a (typically thick) historic wall, in terms of operational energy savings and indoor comfort. The wonderings that arise in this context are two. First, whether the reduction of heat losses provided by a thin layer of insulation, in winter, may be relevant when thick masonry walls are considered. And, even if this reduction is noticeable, how does the intervention influence the annual dynamic behaviour of walls, when the effect of thermal inertia is taken into account? The first issue can be explained through the concept of thermal resistance. This parameter can be adopted to discuss, in first approximation, the heat losses through a building component. Theoretically, the higher the thermal resistance, the better the heat loss reduction. The estimation method based on thermal resistance and temperature boundary conditions refers to specific hypothetical, simplified conditions (e.g. steady-state, neglecting the effect of thermal inertia and temporal changes in the direction of heat flux) that are far from the operational ones of historic buildings. Leaving aside the strong simplification implied, the concept of thermal resistance helps to give a perception of the problem previously introduced. Thermal resistance depends on both the thickness and the thermal conductivity of the layers composing the wall. Hence, the improvement of resistance provided by applying a new, thin layer of insulation might be not relevant when compared to the original performance of a wall that has a very thick section, even when the construction is originally made of poorly performing materials.

A third concern regards the effect of insulation on the thermal inertia of historic walls. Historic walls are traditionally thick and massive, built of bricks or stones, and, as a result, they are largely characterized by a high thermal mass (Rosales Carreón, 2015). This feature can provide passive cooling during summer in climates characterized by high temperatures during daytime and cool nights. Indeed, thermally heavy constructions can absorb heat during the “hot peak” of the day and release it when the temperature falls down (Godwin, 2011). Thus, walls with high thermal inertia provide lower indoor temperatures during the daytime and they release the buffered heat at night, when it can be effectively mitigated through natural ventilation. Thermal insulation does typically reduce winter heat losses through the walls, but it can have detrimental effects during summer, thus increasing cooling demands and overheating discomfort. Hence, insulation solutions should be carefully analysed by comparing winter benefits with summer drawbacks. What the best solution is for insulating massive porous walls is still an open question (Pfluger and Baldracchi, 2011; Verbeke and Audenaert, 2018) and the best choice might be not to insulate them at all, depending on the situation. The final decision strongly depends on the geometry of the building, involved materials, and boundary conditions, i.e. indoor comfort requirements, building usage and outdoor climate.

Finally, when intervening on historic buildings, compatibility must be guaranteed in order to avoid introducing degradation risks for the original materials (Veiga et al., 2010). When it comes to insulation, the main concern regards physical compatibility, from the hygric point of view (Posani, Veiga, and Freitas, 2019). Historic buildings are generally constructed with porous, vapour permeable materials

that allow both the wetting and drying of construction components. Hence, moisture is not prevented from entering the envelope and its disposal relies on the good drying capacity of historic components (Webb, 2017). The introduction of new materials on walls surfaces can strongly alter these mechanisms (Hansen, 2018), potentially leading to deterioration risks (Rasmussen and Møller, 2015; Hao, Herrera and Troi, 2018) related to the changes introduced in the original moisture dynamics. Defining what type of solutions and materials are more compatible than others is a very arduous task, both for internal and external interventions. It is clear that all choices, vapour permeable or vapour-tight, capillary active or not, offer pros and cons depending on the side of retrofit intervention (internal or external), wall thickness, materials adopted, and boundary conditions involved. Due to this dependency of compatibility on the specific situation considered, no general and absolute recommendations were found in the literature for compatible insulation solutions.

Overall, the thermal retrofit of historic walls appears promising in terms of lowering energy consumptions and reaching a climate-neutral Europe by 2050. Even though the interest and studies on this type of intervention have strongly grown in the last decades, there are still open questions on its feasibility, efficacy and compatibility. The efforts of the scientific community are leading towards a more complete understanding of the implication of insulating historic envelopes, as testimonied by several European projects that include this topic, and in particular by the project RIBuild (Robust Internal Thermal Insulation of Historic Buildings, 2015-2020). Certainly, the topic still needs to be investigated, especially within the scope of providing the tools for defining whether or not it is effective and risk-free to intervene. Such tools are needed to allow the technicians operating in the heritage sector, as well as all the public entities responsible for the preservation of historic buildings, to proceed on evaluating effectively whether and how to retrofit our built heritage. Finally, further investigations are needed to clarify the impact of the interventions in the specific scenario of Southern-European countries, where the complexity is increased by the presence of hot and warm summers, with the over-heating risk that those entail.

1.3. RESEARCH GOAL

Historic buildings must be treated with particular attention and every thermal retrofit should be evaluated with an integrated approach that considers energy efficiency and users-comfort while guaranteeing the preservation of the cultural value of the building and compatibility with the original materials.

According to the literature, it appears that a general, qualitative criterion for defining efficient, hygric-compatible insulation solutions for historic envelopes is not available (Caro and Sendra, 2021). This lack is likely to be related to the dependence of the risks and benefits on several factors. Nonetheless, it seems possible to define specific clusters of situations for which a similar behaviour of walls is forecastable, thus opening the possibility of defining target solutions that appear suitable, at least at a first approximation.

For this reason, this research investigates thermal insulation solutions for the specific cluster of “thick masonry walls of historic buildings with temporary occupation, located in areas with temperate climates with warm or hot summers and mild winters, where heating systems are adopted”. The choice of considering thick masonry walls and temperate climates with warm or hot summers and mild winters, is taken because those are typical characteristics of historic buildings located in Southern Europe. In addition, the combination of these two parameters allows for evaluating the effect of insulation on

buildings with high thermal inertia, and quite extreme summer conditions. Mild winters are also typical of southern Europe, and they imply a different evaluation of moisture-related risks than northern European countries, namely frost damages are not a concern of the compatibility analysis. The use of heating systems is common in southern European climates, despite the mild winters. More in detail, three climates are considered, namely those of Porto and Lisbon, in Portugal, and Bologna, in northern Italy. All cities are characterized by temperate climates, with moderate temperature in winter and hot (Lisbon and Bologna) or warm (Porto) summers. Those three climates are classified, respectively, as "Csa", "Cfa" and "Csb" according to Köppen–Geiger system (Peel, Finlayson and McMahon, 2007).

Finally, temporary usage was considered typical of historic buildings adopted for public usage. More in detail, public libraries are selected for the investigation, because they represent a type of building where conditioning systems may be intensively applied and where guaranteeing thermal comfort appears important. Furthermore, they seem representative of many other buildings such as those hosting public offices, and also of private buildings having a moderate number of users, whose main activity is sedentary and occupation patterns are temporary, such as banks and private offices.

The question addressed in the research are the following:

- Is it feasible to adopt thermal insulation on historic walls? When is it reasonable to do so? Are there solutions that appear suitable for the scope, on the market?
- Do feasible insulation solutions appear compatible with historic walls? Is it possible to define some recommendations for choosing solutions that are compatible with historic walls, in the cluster considered?
- Are feasible solutions effective for reducing thermal discomfort and energy demands, when massive historic walls and temperate climates are taken into account? Is one side of the application preferable to the other?

1.4. RESEARCH METHODOLOGY

The methodology defined for this doctoral research is composed of several steps, which can be overall divided into four categories: literature review, experimental investigations, numerical simulations, and conclusions. The methodology is schematically represented in Figure 1.1.

First, a state of art concerning the feasibility of thermal retrofit interventions in historic construction is performed. The insulation materials adopted in research are reviewed and the important characteristics to consider for hygric compatibility are discussed. Consequently, some commercially available insulation systems that appear suitable for the scope are selected and experimentally tested, namely thermal mortar-based solutions.

The experimental campaign on materials and systems is developed to determine the hygrothermal properties of materials and complete systems chosen for the investigation. The second experimental part consists of an indoor climate monitoring campaign (temperature and relative humidity) in the three case studies, together with some further measurements related to thermal stratification and superficial temperatures. The experimental campaigns are intended to provide the input data needed for numerical simulations, in terms of materials properties of the insulation and boundary climatic conditions. In

addition, the measurements followed in the three case studies provide the means for validating the simulations model developed in the following steps of the research.

The numerical part consists is composed of two types of analyses. Compatibility is studied at the component level, through 1D simulations, and it aims to evaluate moisture-related risks in detail. Then, the hygrothermal behaviour of the case studies is studied by means of whole-building simulations, which are used to evaluate the effects of insulation on energy demands and indoor thermal comfort.

Finally, some remarks and recommendations are be defined according to the results obtained from the literature review, and the experimental and numerical work. The outcomes are then used to reply to the research questions previously defined and to draw some conclusions on the feasibility, efficacy and compatibility of thermal insulation solutions for historic walls.

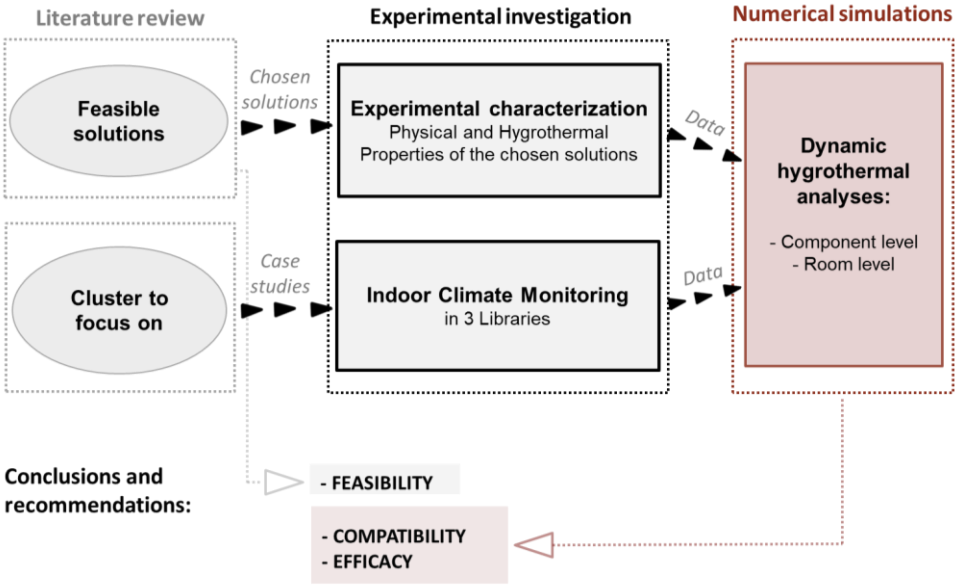

Figure 1.1 – Research methodology.

1.5. RESEARCH ORGANIZATION

The research thesis is organized in the following chapters:

1. Introduction
2. Thermal insulation for historic walls: An overview of possible solutions and a discussion on feasibility, efficacy and compatibility
3. Experimental monitoring of three case studies
4. Experimental characterisation of thermal mortar-based insulation solutions.
5. Hygrothermal behaviour of retrofitted walls: the impact of thermal insulation.
6. Thermal insulation for historic walls: The effect on thermal comfort and energy demands
7. Conclusions

1.6. REFERENCES

Appendino, Federica. 2017. “Balancing Heritage Conservation and Sustainable Development - The Case of Bordeaux.” *IOP Conference Series: Materials Science and Engineering* 245 (6). doi:10.1088/1757-899X/245/6/062002.

Ascione, Fabrizio, Nicla Cheche, Rosa Francesca De Masi, Francesco Minichiello, and Giuseppe Peter Vanoli. 2015. “Design the Refurbishment of Historic Buildings with the Cost-Optimal Methodology: The Case Study of a XV Century Italian Building.” *Energy and Buildings* 99: 162–76. doi:10.1016/j.enbuild.2015.04.027.

Balibar, Sébastien. 2017. “Energy Transitions after COP21 and 22.” *Comptes Rendus Physique* 18: 479–87. doi:10.1016/J.CRHY.2017.10.003.

Brandt, Mark Thompson. 2017. “Buildings and stories: Mindset, climate change and mid-century modern. ” *Journal of Architectural Conservation* 23.1-2: 36-46.

Carbonara, Giovanni. 2015. “Energy Efficiency as a Protection Tool.” *Energy and Buildings* 95: 9–12. doi:10.1016/j.enbuild.2014.12.052.

Caro, Rosana, and Juan José Sendra. 2021. “Are the Dwellings of Historic Mediterranean Cities Cold in Winter? A Field Assessment on Their Indoor Environment and Energy Performance.” *Energy and Buildings*. doi:10.1016/j.enbuild.2020.110567.

Council of Europe. 1975. *The Declaration of Amsterdam(1975)*. Directorate of Press and Information of the Council of Europe: Strasburg, France, 1975. Available online at: https://www.icomos.org/en/and/169-the-declaration-of-amsterdam (accessed on June 1, 2021)

European Commission. 2017. “Commission Welcomes Agreement on Energy Performance of Buildings”. Available online at: https://ec.europa.eu/commission/presscorner/detail/en/IP_17_5129 (accessed on March 30, 2020)

European Commission. 2019. “Communication on The European Green Deal”. 2019. Available online at: https://ec.europa.eu/info/files/communication-european-green-deal_en (accessed on March 30, 2020)

European Commision. 2020. “Commission Proposal for a Regulation: European Climate Law”. 04 March 2020. Available online at: https://ec.europa.eu/info/files/commission-proposal-regulation-european-climate-law_en (accessed on March 30, 2020)

European Parliament. 2019. “European Parliament Resolution of 28 November 2019 on the Climate and Environment Emergency (2019/2930(RSP))”. Available online at: https://www.europarl.europa.eu/doceo/document/TA-9-2019-0078_EN.html (accessed on March 30, 2020)

Franco, Giovanna, and Anna Magrini. 2017. *Historical Buildings and Energy*. doi: 10.1007/978-3-319-52615-7.

Godwin, P J. 2011. “Building Conservation and Sustainability in the United Kingdom.” *Procedia Engineering* 20: 12–21. doi: 10.1016/j.proeng.2011.11.135

Hansen, Tessa Kvist. 2018. “Hygrothermal Performance of Internal Insulation in Historic Buildings.”

PhD thesis. Technical University of Denmark.

Hao, L, D Herrera, and A Troi. 2018. “The Effect of Climate Change on the Future Performance of Retrofitted Historic Buildings A Review.” In *The 3rd International Conference on Energy Efficiency in Historic Buildings (EEHB2018)*. Visby, Sweden: Uppsala University.

Jordan, Andrew, Dave Huitema, Harro Van Asselt, Tim Rayner, and Frans Berkhout. 2010. *Climate Change Policy in the European Union: Confronting the Dilemmas of Mitigation and Adaptation?* Cambridge University Press: Cambridge, UK. doi: 10.1017/CBO9781139042772.

Martínez-Molina, Antonio, Isabel Tort-Ausina, Soolyeon Cho, and José Luis Vivancos. 2016. “Energy Efficiency and Thermal Comfort in Historic Buildings: A Review.” *Renewable and Sustainable Energy Reviews* 61: 70–85. https://doi.org/10.1016/j.rser.2016.03.018.

Pfluger, Rainer, and Paolo Baldracchi. 2011. “Report on Energy Efficiency Solutions for Historic Buildings - Deliverable 3.1 of 3encult.” 3encult - Europen Project. Available online at: https://www.3encult.eu/en/project/workpackages/energyefficientsolutions/Documents/3ENCULT_3.1.pdf (accessed January 15, 2022).

Posani, Magda, Maria Do Rosário Veiga, and Vasco Peixoto De Freitas. 2018. “Historic Buildings Resilience: A View over Envelope Energy Retrofit Possibilities. .” *8th International Conference on Building Resilience. November 14-16, 2018. Lisbon, Portugal*.

Pracchi, V, and A Buda. 2018. “Potentialities and Criticalities of Different Retrofit Guidelines in Their Application on Different Case Studies.” In *The 3rd International Conference on Energy Efficiency in Historic Buildings (EEHB2018), Visby, Sweden, September 26th to 27th, 2018.*, 283–93. Uppsala University.

Rasmussen, T. Valdbjørn, Eva B. Møller, and Thomas Cornelius Buch-Hansen. 2015. "Extensive renovation of heritage buildings-reduced energy consumption and CO2 emissions." The Open Construction and Building Technology Journal. doi: 10.2174/1874836801509010058

Rosales Carreón, Jesús. 2015. “Review on Techniques, Tools and Best Practices for Energy Efficient Retrofitting of Heritage Buildings.” ReFoMo, EU Project. Universiteit Utrecht: Netherlands. Available online at: https://refomo.eu/wp-content/uploads/sites/105/2015/11/Review-on-techniques-for-energy-efficient-retrofitting-of-heritage-buildings_Final.pdf.

Sesana, Elena, Alexandre S. Gagnon, Chiara Bertolin, and John Hughes. 2018. “Adapting Cultural Heritage to Climate Change Risks: Perspectives of Cultural Heritage Experts in Europe.” *Geosciences (Switzerland)* 8 (8). doi:10.3390/geosciences8080305.

Troi, A., and Z. Bastian. 2015. “Building Energy Efficiency Solutions: A Handbook. Chapter 2.3: Cultural Heritage.” In *Birkhauser*. doi:10.1017/CBO9781107415324.004.

Veiga, Maria Do Rosário, Ana Fragata, Ana Luisa Velosa, Ana Cristian Magalhães, and Goreti Margalha. 2010. “Lime-Based Mortars: Viability for Use as Substitution Renders in Historical Buildings.” *International Journal of Architectural Heritage*. doi: 10.1080/15583050902914678.

Verbeke, Stijn, and Amaryllis Audenaert. 2018. “Thermal Inertia in Buildings: A Review of Impacts across Climate and Building Use.” *Renewable and Sustainable Energy Reviews*. doi: 10.1016/j.rser.2017.08.083.

Webb, Amanda L. 2017. “Energy Retrofits in Historic and Traditional Buildings: A Review of Problems

and Methods." *Renewable and Sustainable Energy Reviews*. doi: 10.1016/j.rser.2017.01.145.

Wood, C, I Brocklebank, and D Pickles. 2010. "ENERGY EFFICIENCY AND HISTORIC BUILDINGS. Application of Part L of the Building Regulations to Historic and Traditionally Constructed Buildings." English Heritage: UK.

Yusuf, Arayici, John Counsell, Lamine Mahdjoubi, Gehan Ahmed Nagy, Soheir Hawas, Khaled Dweidar. 2017. "HBIM and Environmental Simulation." In *Heritage Building Information Modelling*. Taylor & Francis. ISBN: 978-1-138-64568-4.

2

THERMAL INSULATION FOR HISTORIC WALLS: AN OVERVIEW OF POSSIBLE SOLUTIONS AND A DISCUSSION ON FEASIBILITY, EFFICACY AND COMPATIBILITY.

2.1. INTRODUCTION

This chapter gives an overview of the types of thermal insulation solutions mentioned in the literature, for interventions on historic walls. The feasibility, efficacy and compatibility of the intervention is then discussed accounting for the information found in the literature.

Parts of this chapter have been presented in:

- Posani, Magda, Rosário Veiga, and Vasco Peixoto de Freitas. 2018. "Historic buildings resilience: A view over envelope energy retrofit possibilities." In *8th ICBR International Conference on Building Resilience*, Lisbon, November 14-16;

- Posani, Magda, Rosário Veiga, and Vasco Peixoto de Freitas. 2019. "Towards Resilience and Sustainability for Historic Buildings: A Review of Envelope Retrofit Possibilities and a Discussion on Hygric Compatibility of Thermal Insulations." *International Journal of Architectural Heritage*: 1-17. Doi: 10.1080/15583058.2019.1650133;

- Posani, Magda, Rosário Veiga, and Vasco Peixoto de Freitas. 2021. "Retrofitting Historic Walls: Feasibility of Thermal Insulation and Suitability of Thermal Mortars." *Heritage*: 4(3). Doi: /10.3390/heritage4030114.

2.2. THERMAL INSULATION FOR HISTORIC WALLS: SOLUTIONS IN THE LITERATURE.

In this section of the study, the solutions adopted in the literature for improving the thermal performance of historic walls are reported and organized according to their frequency. The frequency of the interventions is accounted as follows: when a solution is considered in a general study or review, such result is accounted once; when an analysed paper contains one or more case studies, the solution is accounted once more for every time the measure is considered in a different case study.

The review performed on energy-efficient insulation solutions for historic walls takes into account some guidelines published by Historic England on the thermal retrofit of historic components (Pickles, Ian, and Wood, 2010) as well as the outcomes of the European Project ReFoMo (Reduced Footprints of Monumental Structures, Landscapes & Buildings) presented by Rosales Carreón (2015) in a report on best practices for retrofitting the European Heritage. The measures adopted in the European project RIBuild (Robust Internal Thermal Insulation of Historic Buildings) for the retrofits of several case studies located in Belgium, Denmark, Germany, Italy, Latvia, Sweden and Switzerland (Blumberga et al., 2016) are considered, and the infrared-reflective coatings developed through the EFFESUS project (Becherini et al., 2018) are also accounted. Some theoretical studies and investigations that adopt energy simulation tools are additionally reviewed. Most of them consider retrofits of historic buildings situated in central and southern Italy (Ascione, Bianco, et al., 2015; Ascione, Cheche, et al., 2015; Ascione, De Rossi, and Vanoli, 2011; De Berardinis et al., 2014; Di Ruocco, Sicignano, and Sessa, 2017; Mancini et al., 2017; Cornaro, Puggioni, and Strollo, 2016; Cirami et al., 2017), as well as in the cities of Bolzano (Roberti et al., 2017) and Treviso (Baggio et al., 2017), in Northern Italy. Other studies accounted in the review, consider the energy savings obtained via simulating retrofits of historic buildings in Riga (Biseniece et al., 2017), Latvia, and the hygric impact of thermal renders on wall retrofits in the climate of Essen, Germany (Govaerts et al., 2018). Further reviewed papers account for the energy savings resulting from real interventions on historic buildings located in Sweden (Johansson, Donarelli, and Strandberg, 2018) and northern Italy (Dalla Mora et al., 2015). Lastly, studies that compare the results obtained by applying different insulations in a monastery located in Germany (Krus, Kilian and Pfundstein, 2016) and in a case study in Dublin (Walker and Pavía, 2015), Ireland, are considered.

For external insulation solutions, 26 mentions were found, and the results are shown in Figure 2.1. As long as internal insulation is concerned, 71 mentions were identified, and the outcomes are presented in Figure 2.2. In the two figures, aerogel-based mortars are distinguished from thermal renders and plasters having more typical insulation materials in their formulations (e.g. Perlite, cork, and expanded polystyrene). All in all, thermal mortars, reflective coatings, mineral wool and EPS appear to be very common solutions.

The solutions found in the literature can be divided into three typologies, according to their effect on heat transfer:

- reflective insulations, which reduce the heat transferred by radiation;
- phase change materials, that rely on latent heat storage;
- thermal insulations, which increase the thermal resistance to heat conduction.

The last type of insulation is the traditional typology considered for insulating buildings, it offers a large variety of solutions, and it is widely adopted in common practice. This is the one type of insulation solution that is considered in this research.

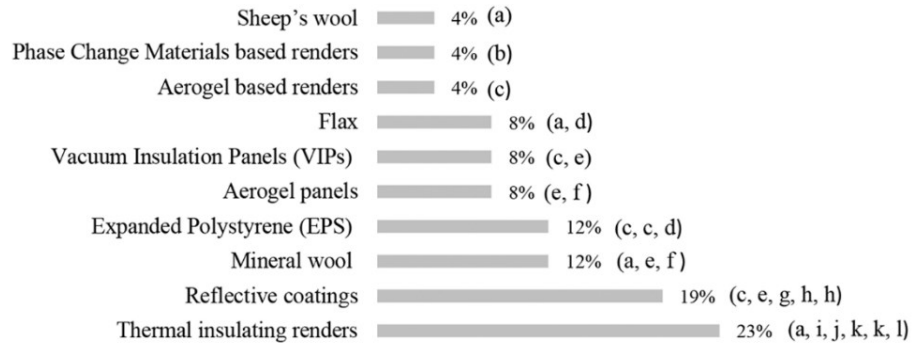

Figure 2.1 – External insulation solutions for walls in historic buildings, frequency in literature. References: (a) Pickles, Ian, and Wood (2010a), (b) Ascione, Bianco, et al. (2015), (c) De Berardinis et al. (2014), (d) Blumberga et al. (2016), (e) Baggio et al. (2017) ,(f) Roberti et al. (2017), (g) Rosales Carreón (2015), (h) Becherini et al. (2018), (i) Ascione, Cheche, et al. (2015), (j) Cornaro, Puggioni, and Strollo (2016), (k) Johansson, Donarelli, and Strandberg (2018), (l) Govaerts et al. (2018).

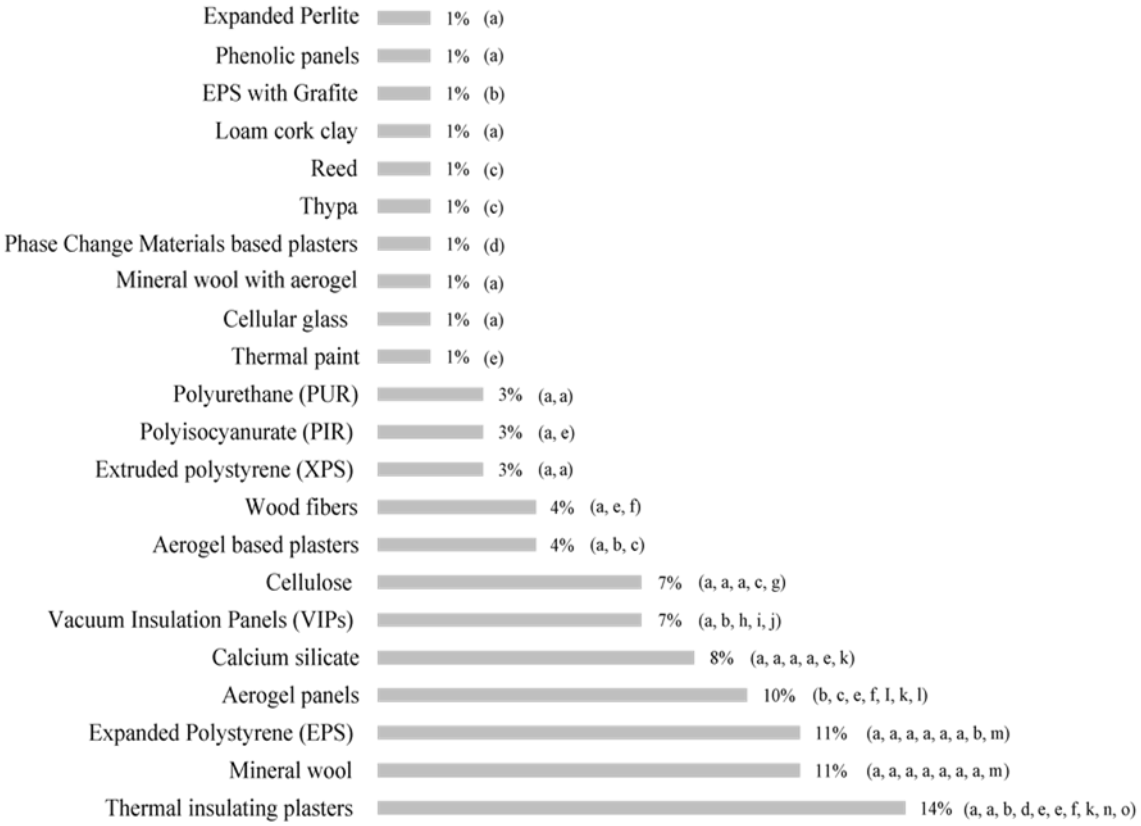

Figure 2.2 – Internal insulation solutions for walls in historic buildings, frequency in literature. References: (a) Blumberga et al. (2016), (b) De Berardinis et al. (2014), (c) Krus, Kilian (2016), (d) Ascione, Bianco, et al. (2015), (e) Walker and Pavía (2015), (f) Di Ruocco, Sicignano, and Sessa (2017), (g) Pickles, Ian, and Wood (2010c), (h) Rosales Carreón (2015), (i) Biseniece et al. (2017), (j) Johansson, Donarelli, and Strandberg (2018), (k) Cirami et al. (2017), (l) Mancini et al. (2017), (m) Dalla Mora et al. (2015), (n) Ascione, Cheche, et al. (2015), (o) Ascione, De Rossi, and Vanoli (2011).

2.3. FEASIBILITY

The adoption of thermal insulation on the walls of historic constructions is not always feasible, because of the need to preserve their valuable and characteristic features. On the contrary, no similar concern affects interventions on existing buildings with no cultural value (Alfano and de Santoli, 2017).

Furthermore, for heritage buildings, European standard EN16883:2017 requires a first phase of recognition of the significance and specific values of the construction, based on which unsuitable measures should be excluded from the intervention design. Then, depending on the level of heritage significance, on-site visits from third parties such as heritage or planning officers may be needed (EN16883:2017). Finally, even when the adoption of thermal insulation appears feasible, attention must be paid to the integration of the retrofit with the original construction, and the designer may be required to justify the technological and scenic integration of the chosen measures with the specific historic building considered (e.g., a document on this regard is required by the Italian Cultural Heritage offices, as highlighted by Alfano and de Santoli, 2017).

In the context of heritage conservation, four aspects appear very relevant for evaluating the suitability of thermal retrofit interventions on historic buildings: authenticity, integrity, reversibility (Troi and Bastian, 2015) and compatibility (Ganobjak, Brunner and Wernery, 2019). The first three concepts are hereby discussed in detail to evaluate the feasibility of introducing insulation in historic walls, whereas "compatibility" is treated in a separate section. Some concepts that appear useful for the discussion are excerpted from the international charters on conservation and restoration of the cultural heritage and reported in Table 2.1.

Table 2.1 – References from the international charters on conservation and restoration of the cultural heritage.

The Venice Charter (ICOMOS 1964) Art.5	*The conservation of monuments is always facilitated by making use of them for some socially useful purpose. Such use is therefore desirable but it must not change the lay-out or decoration of the building. It is within these limits only that modifications demanded by a change of function should be envisaged and may be permitted.*
The Venice Charter (ICOMOS 1964) Art.6	*The conservation of a monument implies preserving a setting which is not out of scale. […] No new construction, demolition or modification which would alter the relations of mass and colour must be allowed.*
The Venice Charter (ICOMOS 1964) Art.13	*Additions cannot be allowed except in so far as they do not detract from the interesting parts of the building, its traditional setting, the balance of its composition and its relation with its surroundings.*
The Nara Document on Authenticity (ICOMOS 1994) Art.13	*Depending on the nature of the cultural heritage, its cultural context, and its evolution through time, authenticity judgements may be linked to the worth of a great variety of sources of information. Aspects of the sources may include form and design, materials and substance, use and function, traditions and techniques, location and setting, and spirit and feeling, and other internal and external factors. [...]*
ICOMOS Charter Ratified at Zimbabwe general assembly (ICOMOS, 2003) Art. 1.3	*The value of architectural heritage is not only in its appearance, but also in the integrity of all its components as a unique product of the specific building technology of its time. In particular the removal of the inner structures maintaining only the façades does not fit the conservation criteria.*
The New Zealand Charter (ICOMOS, 2010)	*Conservation maintains and reveals the authenticity and integrity of a place, and involves the least possible loss of fabric or evidence of cultural heritage value. Respect for all forms of*

Art. 5	*knowledge and existing evidence, of both tangible and intangible values, is essential to the authenticity and integrity of the place. […]*
The New Zealand Charter (ICOMOS, 2010) Art. 6	*[…] Intervention should be the minimum necessary to ensure the retention of tangible and intangible values and the continuation of uses integral to those values. The removal of fabric or the alteration of features and spaces that have cultural heritage value should be avoided.*
the Burra Charter (ICOMOS, 2013) Art. 15.1	*[…] The amount of change to a place should be guided by the cultural significance of the place and its appropriate interpretation. When change is being considered, a range of options should be explored to seek the option which minimizes the reduction of cultural significance.*
the Burra Charter (ICOMOS, 2013) Art. 15.2	*Changes that reduce cultural significance should be reversible and be reversed when circumstances permit.* *Reversible changes should be considered temporary. Non-reversible change should only be used as a last resort and should not prevent future conservation action.*

2.3.1. POSITION OF THE INSULATION

Accounting for the authenticity principle, the appearance of original structures should not be changed. From this point of view, the location of the insulation can be discussed.

External façades are usually one of the most important aspects of a historic building, and they contribute to creating its unique and local character (Pickles, Ian, and Wood, 2010b). Consequently, it is often preferable to intervene at the indoor facing side of historic envelopes rather than on exterior façades. Nevertheless, a large share of the European historic heritage is composed of constructions whose value is mainly related to the role they play as "groups of buildings" (UNESCO, 1972) to form the cultural identity of townscapes or cities. Those cases often allow for external retrofits if the façade's appearance is reconstructed to conserve its identity (Govaerts et al., 2018). In any case, the impact on cultural values from both the interior and exterior sides should be assessed (Art. 13 of the Nara Document on Authenticity, 1994) when planning the intervention, and for listed buildings, it should be discussed with the local monument preservation services (Ganobjak, Brunner and Wernery, 2019). For obvious reasons, external interventions are excluded for all buildings whose façades are subjected to integral protection (Govaerts et al., 2018). When wall surfaces are recognized not to hold cultural or tangible values, or when they are so damaged they require a complete replastering (Pickles, Ian, and Wood, 2010b), the introduction of insulation is viable.

From the point of view of the dimensional changes introduced, the intervention should not strongly alter the proportions and spatial perception of the building, its parts and its relation with the surroundings (Art 6. and Art. 13 of the Venice Charter, 1964). Dimensional changes may be unacceptable at window and door openings (Pickles, Ian, and Wood, 2010b) or where original surface details are valuable (Art 5. of the Venice Charter, 1964). Thus, it is often necessary to limit the thickness of the insulation adopted in the intervention. Consequently, insulation systems that offer a wide range of available thicknesses and systems that can provide good thermal performance with a very small thickness appear more viable than others.

2.3.2. FEASIBILITY OF DIFFERENT THERMAL INSULATION SOLUTIONS

According to the principle of integrity: removal, damage and replacement of original materials should be minimized to reduce the loss of original fabric (Art. 1.3 of the ICOMOS Charter ratified at the Zimbabwe general assembly, 2003, and Art. 5 of the New Zealand Chapter, 2010). Thus, the damages introduced in the walls by the insulation fastening supports should be minimized. For this reason, insulating plasters and renders are preferable over boards and blankets relying on mechanical fastening systems (Ganobjak, Brunner and Wernery, 2019). When the fastenings can be substituted by an adhesive layer, the intervention appears feasible, as long as the adhesive can be safely removed (Baiani, Lucchi and Pascucci, 2018) or a protective system is used between historic materials and new ones, like laminated interlayers or protective films of Japanese tissue paper (Krus, Killan and Pfundstein, 2016).

When accounting for reversibility (Art. 15.2 of the Burra Charter, 2013), new additions to historic buildings should be recognizable and removable with minimal or absent damage to the original fabric. They should not be so different that they stand out, but they should be distinguishable from authentic materials (Ganobjak, Brunner, and Wernery, 2019) so that in the future, the unoriginal materials can be removed. Anyway, the theoretical principle of reversibility is an ideal to aim to, but it is never achievable, as total reversibility cannot be obtained in practice. Thus, interventions must offer a "certain degree", preferably high, of reversibility (Petzet, 2004). From this point of view, thermal mortars appear to be a very suitable solution, as they offer a texture that is similar to original renders and plasters, differently from other insulation materials. Furthermore, they are expected to be distinguishable from the original mortars because of the presence of lightweight aggregates, which is typically recognizable. In addition, they are considered to be easily removable (Del Curto and Cinieri, 2020). Nevertheless, other thermal insulation materials can also be suitable for the scope if finished with rendering and plastering systems that recall the original appearance of historic surfaces.

Another important concept in heritage conservation is minimal intervention, meaning that retrofits should "do as much as necessary and as little as possible" (Bond and Worthing, 2016). Thus, a range of options (Art 15.1 of the Burra Charter, 2013) should always be considered to evaluate what interventions can better respond to the circumstantial necessities while minimizing the loss of original fabric, especially when it is considered to hold cultural value (Art. 6 of the New Zealand Charter, 2010). These considerations suggest that in historic buildings, insulation is feasible only when all the interventions involving a smaller impact on the original structures are proven to not be enough to meet the goal of the retrofit (Pickles, Ian, and Wood, 2010a).

Apart from heritage conservation needs, the feasibility of the intervention can be considered from the constructional point of view. In this context, insulation systems that can adapt to uneven surfaces are preferable, as historic walls may present irregularities. Thus, thermal mortars and flexible blankets are more feasible than stiff boards, as the first two can adapt to irregular surfaces while the latter cannot (Ganobjak, Brunner, and Wernery, 2019). In addition, thermal mortars allow for gap filling, thus providing for continuous contact between the insulation layer and the substrate (Guizzardi, 2014) even when the walls are affected by cracks or other damages. Finally, thermal mortars also offer the additional advantage of being applicable by mechanical spraying, which noticeably eases the retrofitting intervention (Maia, Ramos, and Veiga, 2018).

2.3.3. MAIN OUTCOMES OF THE REVIEW ON THE FEASIBILITY OF ADOPTING THERMAL INSULATION TO RETROFIT HISTORIC WALLS

Concerning the feasibility of adopting thermal insulation to retrofit historic walls, some overall indications emerged from the literature, and they can be summarized as follows:

- Intervention is excluded for surfaces holding cultural or tangible values or subjected to integral protection. When these circumstances do not occur, insulation may be installed, especially if the original rendering or plastering is so damaged that it needs to be replaced;
- It is generally preferable to use internal rather than external insulation to maintain the exterior appearance of buildings. However, external interventions are often feasible if the façade's appearance is reconstructed to conserve the building's identity, especially for buildings whose importance is related to the cultural value of "groups of buildings" or landscape and not to the singular construction;
- Interventions that cause dimensional changes at window and door openings or where original surface details are valuable should be avoided. In all cases, the original proportions and spatial perception of the building and its parts should be preserved by adopting moderate thicknesses of insulation. Thus, solutions providing good thermal performance with a small thickness of insulation appear more viable than other solutions. Furthermore, insulations offering a wide range of available thicknesses appear to be preferable.

Furthermore, thermal mortars arose as a very feasible solution for historic walls because of the following reasons:

- Unlike insulation boards and blankets, they do not need any anchoring points or adhesive layers;
- They offer great flexibility for the thickness, which can be easily adapted to the dimensional restriction that the intervention may require, and it can be adjusted near valuable decorations to leave them clearly visible;
- They adapt to uneven surfaces and provide gap-filling abilities, consequently allowing for continuous contact between the insulation layer and the substrate, even in the case of irregularities, cracks, and other damages which are quite commonly found in historic components;
- They can be applied by mechanical spraying, noticeably easing the intervention;
- They are more able than insulation boards and blankets to offer a texture similar to original renders and plasters.

2.4. EFFICACY

This section of the literature review aims to investigate what are the indicators to consider for evaluating the efficacy of thermal insulation in the context of historic buildings. Furthermore, different insulation materials are compared and discussed, and the different impact of adopting insulation on the interior or exterior side of the walls is considered.

It is worth underlining that in all cases, retrofit solutions cannot ever be evaluated on merely efficacy-based considerations. The retrofit goes as far as heritage preservation restraints allow it to, meaning that the importance of achieving high performances is secondary to safeguarding buildings' significance. When it comes to historic constructions, the aim is not to comply with modern buildings standards

(Govaerts et al., 2018) but to obtain comfort and energy enhancements that improve the usability and sustainability of buildings, while safeguarding their significance, in accordance with the Amsterdam declaration (Di Ruocco, Sicignano and Sessa, 2017).

2.4.1. THERMAL CONDUCTIVITY OF INSULATION MATERIALS

When insulation materials are analysed and compared in terms of efficacy, their thermal properties are the parameters that lead the discussion. Several studies consider thermal conductivity and specific heat capacity (Walker and Pavía, 2015; Zhao et al., 2017; De Berardinis et al., 2014; Asdrubali, D'Alessandro and Schiavoni, 2015). The first parameter can be adopted to evaluate the improvement of thermal resistance obtainable in a retrofitted component. The latter may be used to discuss thermal mass and the effect of thermal inertia. Nonetheless, thermal conductivity is considered to be the one key thermal parameter for insulations (Blumberga et al., 2016a), and the lower the thermal conductivity, the higher the theoretical reduction of heat losses.

A comparison among the values of dry thermal conductivity found in the literature for several common insulation solutions is provided in Figure 2.3. In the same image, the threshold values of 0.026 W/(m·K), 0.065 W/(m·K) and 0.2 W/(m·K) are indicated with dash-dotted lines. These values provide a useful indication because of the following reasons:

- the first one represents the thermal conductivity of still air, at typical indoor temperatures. Systems with a thermal conductivity lower than this value are defined as super insulators (Nosrati and Berardi, 2018);
- the second value is the threshold thermal conductivity adopted in the European Guidelines for External Thermal Insulation Composite Systems (ETICS) with renderings (EOTA, 2020);
- the last one indicates the maximum thermal conductivity of thermal mortars according to EN 998-1:2017: "Specification for mortar for masonry - Part 1: Rendering and plastering mortar." (CEN, 2017).

The graphical comparison shows that thermal mortars can have much higher thermal conductivities than traditional insulations. For instance, Walker and Pavía (2015) performed a field investigation on the thermal performance of insulation materials suitable for historic buildings and obtained a thermal conductivity of about 0.07 and 0.09 W/(m·K) for lime plasters containing cork and hemp, respectively. Govaerts et al. (2018) tested a lime–perlite insulating render for heritage buildings and observed a dry thermal conductivity of around 0.10 W/(m·K). Bouzit et al. (2021) considered gypsum plasters with EPS and detected dry thermal conductivities spanning 0.12–0.22 W/(m·K).

More competitive performances were observed by other authors testing renders containing EPS aggregates (i.e., minimum values of about 0.05 W/(m·K) were found by Maia, Ramos and Veiga, 2018, and 0.06 W/(m·K) by Gomes et al., 2019). The best thermal properties were observed with aerogel plasters. Ganobjak, Brunner and Wernery (2019) adopted an aerogel render with a declared conductivity of 0.03 W/(m·K) for a field study on aerogel materials for heritage buildings, and Nosrati and Berardi (2018) measured minimum values of around 0.025 W/(m·K) (and a maximum of 0.11 W/(m·K)) for lime-based plasters with additions of granular silica aerogel, at 10 °C and 50% RH.

All the thermal mortars considered had much better thermal conductivities than standard gypsum and lime mortars, typically in the range of 0.4–0.8 W/(m·K) according to standard EN 12524:2000. Some

of the solutions emerged as competitive with traditional insulations, having a thermal conductivity lower than 0.065 W/(m·K), even though most thermal mortars seemed to exceed this value.

All in all, thermal mortars appear to be interesting for further investigation and application in temperate climates which have moderately cold winters.

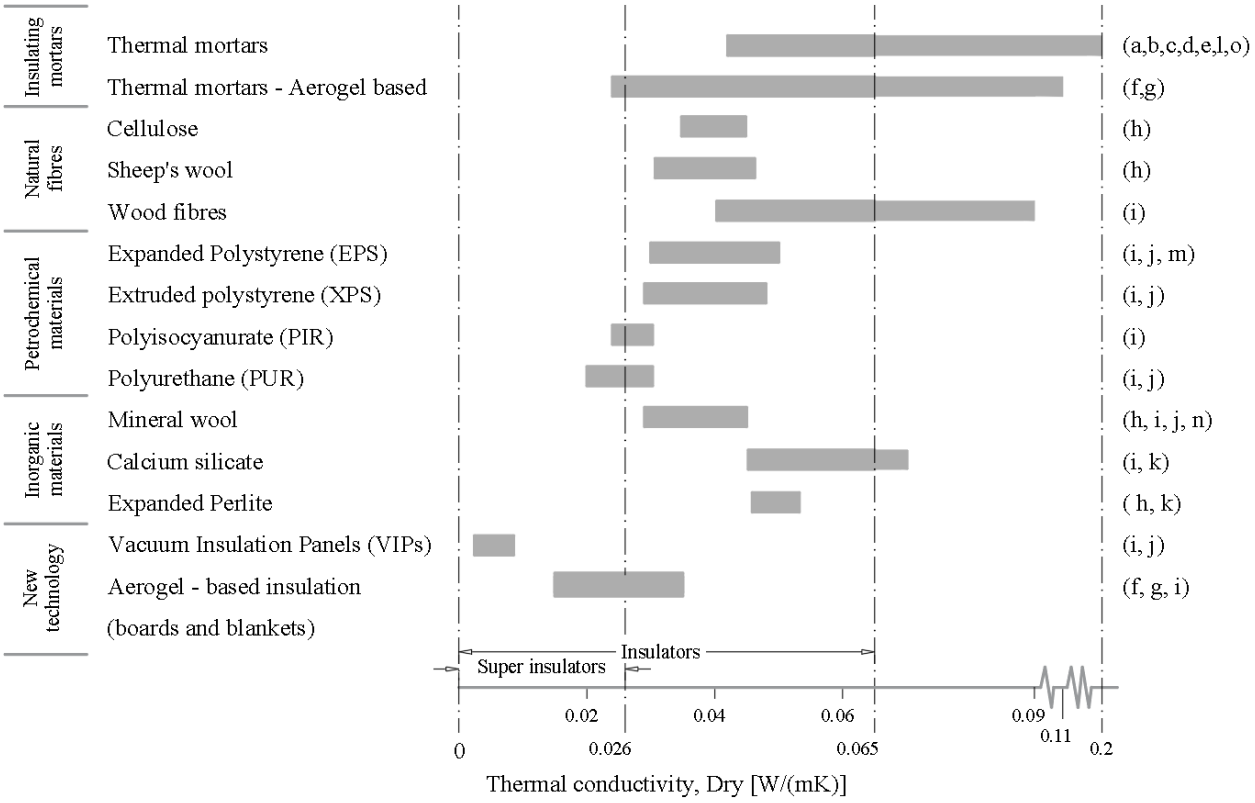

Figure 2.3. Comparison of thermal conductivity of common thermal insulation materials.
References: (a) Walker and Pavía (2015), (b) Govaerts et al. (2018), (c) Maia, Ramos and Veiga (2018), (d) EN 12524:2000, (e) Gomes et al. (2019), (f) Ganobjak, Brunner and Wernery (2019), (g) Nosrati and Berardi (2018), (h) Lekavicius et al. (2015), (i) Blumberga et al. (2016a), (j) Cuce et al. (2014), (k) Zhao et al. (2017), (l) EN 998-1: 2017, (m) Malanho, Veiga and Farinha (2021), (n) Parracha et al. (2021) and (o) Bouzit et al. (2021).

2.4.2. TOOLS AND INDICATORS FOR EFFICACY AT THE COMPONENT LEVEL

Thermal conductivity is a very important parameter for evaluating the improvement of thermal performance obtained with the thermal retrofits of building envelopes. For instance, it is fundamental for evaluating the U-value of a building component after the intervention, which is a parameter largely considered in international standards and national building codes (Portaria 379-A/2015, Dlgs 73/2020; ISO 6946:2017). The U-value of building components is generally required to comply with a maximum value defined in the standards, but for historic buildings this parameter is typically very flexible.

The U-value quantifies the heat that passes through one square meter of the wall when a difference of 1°C is applied at the boundary layers of air (Hegger et al., 2013). Thus, with a lower U-value, a larger

reduction of heat losses is theoretically achieved. Even though this parameter proved to be very representative for modern, lightweight structures, it poorly adapts to the context of historic walls, especially massive ones. Indeed, it accounts for the behaviour of the component under steady-state conditions, which is very far from representing the real behaviour of thermally heavy constructions under operational circumstances. For this reason, the U-value alone can give just a rough indication of the potential benefits of the retrofit, but it is still useful for comparing different types of insulation materials and thicknesses at a preliminary stage of the project.

More detailed calculations can be performed by means of mono-dimensional dynamic hygrothermal simulations, which account for realistic outdoor and indoor climatic conditions and the influence of moisture changes on the thermal properties of building materials (Bottino-Leone et al., 2019; Amorim et al., 2020), while accounting for the thermal mass of the building element. Dynamic simulations can be adopted to have an accurate representation of the heat losses through the walls, before and after the retrofit intervention.

2.4.3. TOOLS AND INDICATORS FOR EFFICACY AT THE BUILDING LEVEL

When more detailed analyses are needed, dynamic whole-building hygrothermal simulations can be adopted. These tools allow for accounting realistic outdoor conditions, reductions of thermal performances due to moisture accumulation and thermal inertia. Based on outdoor climate, envelope characteristics, HVAC (Heating, Ventilation, and Air Conditioning) usage and interior loads, whole-building simulations calculate the indoor climate and energy use, thus allowing for a detailed analysis of the effect of different retrofit strategies on indoor comfort and energy demands.

For conditioned buildings, the improvements obtained in terms of energy consumption is often performed by considering the annual energy savings of the retrofitted scenario versus the original configuration, and sometimes those results are translated into annual CO_2 emissions avoided (Webb, 2017). When it comes to buildings whose usage occurs under free-floating conditions, i.e. without the adoption of HVAC systems, the discussion is focused on the possible comfort improvements by considering comfort indexes and indoor environmental quality (Roberti et al., 2017). Furthermore, for some Mediterranean countries, Magalhães and Freitas (2017) observed that the reluctance to use heating systems can lead to reduced use of building services, if not completely absent. For those cases, these authors suggest focusing the efficiency evaluation on the analysis of thermal discomfort in free-floating scenarios or with intermittent use of technical systems, aiming at its minimization.

2.4.4. POSITION OF THE INSULATION

From the building physics point of view, external insulation is always preferable to internal insulation (Künzel 1998). Indeed, internal insulation leads to a decrease in the temperature of the walls during the heating season, which entails a reduction of their drying ability, thus leading to colder and damper walls. This condition results in reduced thermal performance and durability concerns, as high moisture levels can lead to degradation risks (Flores-Colen et al., 2016; Stingl Freitas et al., 2020). Furthermore, interior thermal insulation may result in moisture problems when applied to walls exposed to wind-driven rain, if not adequately protected with hydrophobic treatments or if relatively too thin (Bjarløv, Finken, and Odgaard, 2015).

From the point of view of energy saving in insulated massive constructions, the effects of thermal inertia and night-time cooling must be considered. The combination of these two aspects is recognized to be very effective within the Mediterranean context (Baiani, Lucchi and Pascucci, 2018). High thermal inertia is a typical feature of historic envelopes in Europe (Rosales Carreón, 2015), where traditional constructions with massive walls made of stone or brick masonry are diffused (Blumberga et al., 2016). This characteristic can provide for passive cooling during summer in climates having high temperatures during daytime and cool nights. Indeed, thermally heavy constructions have the ability to absorb heat during the "hot peak" of the day and release it when the temperature drops (Godwin, 2011). Thus, walls with high thermal mass provide lower indoor temperatures during the daytime and release the buffered heat at night when it can be effectively mitigated through natural ventilation, if adequate conditions are provided. On the other hand, when historic constructions are conditioned with intermittent heating, the high thermal mass of the envelope gives some disadvantages in terms of energy demands. During the heating season, massive walls may absorb a relevant part of the energy provided by the heating system for warming up the indoor environment, thus increasing the energy needed to reach indoor comfort conditions in the building and extending the preheating period.
In this context, the introduction of insulation impacts the envelope in different ways according to its position. Internal solutions decouple the thermal capacity of the wall from the indoor air, which is good in terms of heating demands in buildings with temporary use but counterproductive in terms of passive summer cooling (Pfluger and Baldracchi, 2011). In addition, the use of internal insulation reduces thermal bridges to a lesser extent than exterior insulation. Specifically, interior insulation decreases heat losses at cracks and corners in the walls, but it typically leaves uninsulated areas at the conjunctions with transverse walls (Bjarløv, Finken and Odgaard, 2015) and floor structures (Odgaard, Bjarløv and Rode, 2018), whereas external coating systems can reduce thermal bridging also in these areas.
Apart from energy savings, thermal insulation can improve indoor thermal comfort during the heating season, raising the surface temperatures of walls on their interior side (Kienzlen et al., 2014) while reducing draughts and asymmetries in radiant temperatures (Blumberga et al., 2016), but it may lead to overheating risks during summer, especially in southern European countries (Chvatal and Corvacho, 2009). From this point of view, internal insulation is more effective than exterior insulation for reducing radiant temperature asymmetries (Lucchi and Pracchi, 2013), but it is also likely to lead to higher risks of summer discomfort because of its stronger impact on the thermal inertia (Al-Sanea, Zedan, and Al-Hussain, 2012).

Hence, insulation solutions and the side of the intervention should be carefully analysed, comparing the benefits gained in winter against the potentially increased cooling demands and the amplified risk of overheating during summer.

2.4.5. MAIN OUTCOMES OF THE REVIEW ON EFFICACY OF THERMAL INSULATION FOR HISTORIC WALLS

The main information obtained in the literature review on the efficacy of thermal insulation for historic walls are the following ones:

- the efficacy of adopting thermal insulation can be evaluated at the material, component and building level;
- for thermal insulation materials, thermal conductivity can be used to compare different solutions and the lower the thermal conductivity, the better performance can be expected;

- at the component level, a largely adopted parameter is the U-value. This parameter poorly adapts to thermally heavy constructions but it can be used to have a first perception of the improved thermal performance of building components. The analysis performed through dynamic mono-dimensional or bi-dimensional simulations appears to offer a more detailed view on the thermal performance of retrofitted components, while accounting for the effect of moisture content on thermal conductivity, realistic climatic conditions and thermal inertia;
- whole-building dynamic hygrothermal simulations appear particularly suitable to evaluate the changes of indoor comfort and energy demands obtainable with thermal retrofits of historic constructions;
- finally, adopting thermal insulation on the exterior or interior side of thermally heavy walls can have a very different effect on thermal comfort and energy demands. Internal insulation reduces the benefits of thermal inertia to a higher extent than exterior insulation, potentially increasing thermal discomfort during summer. Nonetheless, it may have a positive effect in reducing winter energy demands for buildings subjected to intermittent heating because it decouples the thermal capacity of the wall from the indoor air. Additionally, it is more effective than exterior insulation for reducing radiant temperature asymmetries. Thus, the choice of application side of the insulation should be carefully evaluated considering the specific scenario under analysis.

2.5. COMPATIBILITY

A very challenging aspect of thermal retrofits lies in forecasting the effect of post-insulation strategies on the moisture dynamics of historic envelopes. The need for combining old and new components makes the intervention challenging, and the likelihood of unforeseen circumstances is far greater than in new constructions (EN 16883:2017).

As explained by Little, Ferraro and Aregi (2015), post-insulating existing constructions is very different from adopting thermal insulation in new ones. Indeed, in most new buildings, the insulation is introduced from the design phase, and it is assessed to avoid moisture-related degradation risks for the building components. Modern constructions are largely designed to block moisture entrance (capillary breaks, membranes for the reduction of vapour transport, vented cavities, etc.). Consequently, trapped moisture is supposed not to be an issue, while the main focus is put on preventing the occurrence of condensation. On the contrary, traditionally constructed buildings are largely characterized by porous, capillary-active materials and no waterproofing layers (Little, Ferraro and Aregi, 2015). Hence, traditional walls generally absorb liquid water (e.g., rain and rising damp), buffer it and then dry out thanks to their typically good vapour permeability (Little, Ferraro and Aregi, 2015). Consequently, the choice of insulation should be very careful because of the risk of altering the original water transport dynamics, potentially leading to degradation issues related to moisture accumulation (Johansson et al. 2019). What is more, in existing construction, on-site inspections are generally needed, and mandatory for heritage buildings (EN 16883:2017), to gain awareness and information on existing components and their state of conservation. Walls may present high initial moisture levels and various types of damage, which should be critically evaluated and eventually resolved before the retrofit, to avoid post-intervention problems (Blumberga et al., 2020).

The main hazards involved by post-insulation of traditional and historic walls are frost damages (Künzel, 1998), interstitial and superficial condensation, mould growth and salt crystallization (Rasmussen,

Møller and Buch-Hansen, 2015; Hao, Herrera and Troi, 2018), together with the possible deterioration of elements embedded in walls, such as wooden beam ends (Webb, 2017). These hazards are all related to the moisture dynamics of walls. Hence, the type of compatibility to refer to is the physical one, from the hygric point of view. As a consequence, the impact of new materials on historic components should consider moisture transport, via vapour diffusion and capillary action, as pointed out by Maurenbrecher (2012) while studying performance requirements for mortars for historic masonry. In this context, two material properties appear to be fundamental for analysing the issue: Vapour permeability, δ_p, and Capillary water absorption coefficient, A_w (Veiga et al., 2010). The importance of these two properties and their influence on the behaviour of insulation materials and retrofitted components is further examined in the next sections.

As long as tools and indicators are concerned, the analysis of deterioration risks related to the use of thermal insulation in historic walls is widely assessed through the use of monodimensional or bidimensional dynamic hygrothermal simulations (Vereecken et al., 2015; Little, Ferraro and Aregi, 2015a; Robert and Piotr, 2017; Grunewald, Ruisinger and Häupl, 2006; Govaerts et al., 2018; Bottino-Leone et al., 2019). The outputs typically considered for assessing the risks are temperature, relative humidity and moisture content (Bottino-Leone et al., 2019). Dynamic hygrothermal models, appear suitable for the scope of analysing moisture dynamics in historic envelopes as they can account for realistic outdoor and indoor climatic conditions, for the combined transport of heat and moisture, and for the movement of water through porous media, in both the vapour and liquid form.

2.5.1. Vapour permeability (δ_p) and hygric compatibility

The drying capacity of building materials depends on their vapour permeability, δ_p (Künzel, Künzel, and Holm, 2004). Materials having a high vapour permeability are usually referred to as vapour permeable (Walker and Pavía, 2015) or vapour open (Vereecken and Roels, 2016) whereas materials with a high vapour resistance (low δ_p) are defined as vapour impermeable (Troi and Bastian, 2015) or vapour proof (Vereecken and Roels, 2017). Typically, traditional porous materials are vapour permeable (Little, Ferraro and Aregi, 2015) and it is good practice to maintain this specific feature (Pickles, Ian, and Wood, 2010a) as it improves the evaporation of moisture out of the envelope, thus decreasing long-term decay problems related to water accumulation (Rosales Carreón, 2015). As a result, the "good drying capacity" (Little, Ferraro and Aregi, 2015) of traditional envelopes should be safeguarded by adopting insulation systems characterized by a higher (or very similar) vapour permeability than the adjacent historic materials.

Hence, literature largely indicates vapour permeable insulations as suitable solutions for preserving the original drying ability of historic components.

Position of the insulation

When internal insulation of walls is considered, the use of vapour permeable systems can introduce some disadvantages. This type of intervention decreases walls temperature, at the inner side, during the heating season. In this scenario, internal condensation is more likely to occur if a vapour open system is chosen over a vapour proof one (Vereecken and Roels, 2014). It is therefore possible to find studies that account for the adoption of vapour-proof systems for internal insulation of walls. For instance, Vereecken et al. (2015) considered vapour impermeable systems as competitive solutions for retrofitting

masonry walls in temperate climates (the weather of Bremerhaven, Essen and München were considered). Nevertheless, the authors also indicated that the use of these systems reduces the inward drying of walls, potentially leading to degradation risks for frost-sensitive facades and embedded wooden beam ends. What is more, this type of solution is very hazardous when liquid water finds a way to reach the walls. Indeed, even though this solution reduces the vapour flux from the indoor environment to the wall, moisture can still reach the wall through rising damp or envelope defects like cracking. In these cases, degradation risks become very high as the original drying capacity is strongly reduced by the retrofit, thus moisture accumulation can be expected. Another study (Vereecken and Roels, 2015), considered different types of internal insulations for masonry walls in the temperate climate of Essen. The outcomes showed that for sufficiently thick walls or walls protected against wind-driven rain, a vapour-permeable, capillary active insulation system performs better than a vapour tight one.

When external insulation is considered, literature appears to indicate vapour permeable solutions as a general suitable choice. Indeed, facades exposed to outdoor weather are subjected to wind-driven rain and so, the moisture vehiculated inside the wall via liquid transport appears much more relevant than the one moved by vapour transport. As a result, the main concern lies in reducing the absorption of liquid water while enhancing the good original drying ability of walls. For walls protected against wind-driven rain or equipped with a final layer that is water-proof, vapour proof insulations might be considered. Nonetheless, also in these cases, liquid water can find secondary ways to enter the envelope and this possibility should be accounted for when assessing the long-term risk of the intervention.

All in all, both choices, vapour permeable and vapour-tight insulations, appear to offer pros and cons. The choice depends on the position of the insulation system, boundary conditions involved, component type, geometry and exposition to outdoor weather.

2.5.2. Capillary water absorption (A_w) and hygric compatibility

The capillary absorption capability of a material can be quantified through the water absorption coefficient (A_w), which describes the speed of water uptake that results from capillary suction when the material is in direct contact with liquid water (Radu et al., 2012). Thus, this coefficient rules the wetting process of the material when it is covered by a film of liquid water (Künzel, Künzel, and Holm, 2004), i.e. the typical scenario that occurs when facades are subjected to wind-driven rain. A high capillary water absorption coefficient is typical of porous, capillary-active materials.

Position of the insulation

As long as internal insulation is concerned, some studies indicate that the adoption of capillary active insulation may be a suitable solution for retrofit interventions. First of all, traditional materials are often porous and capillary active. Therefore, the adoption of insulation solutions characterized by a high water absorption coefficient contributes to the scope of avoiding strong alterations in the original moisture dynamics of historic components (Pickles, Ian, and Wood, 2010a). Secondly, Vereecken and Roles (2016) highlighted that high capillary absorption in insulation materials offers some advantages for buffering and managing moisture. The researchers studied internal insulation of walls, a type of intervention that increases the risk of condensation at the inner surface of the original wall, during the heating season. In this scenario, it was pointed out that when condensation occurs, capillary active

materials absorb the resulting liquid water, buffer it and then dry out through the surface exposed to the indoor air. Nonetheless, a high-water absorption coefficient cannot be assumed as a sure choice for internal insulation. It offers some advantages, but it can also lead to an excessively high moisture content behind the insulation, as observed by Finken, Bjarløv, and Peuhkuri (2016) for thin walls exposed to high rain loads.

Concerning external insulation systems, it is a good choice to regulate the intake of wind-driven rain by adopting coating systems characterized by a low water absorption coefficient, as highlighted in two studies concerning respectively stucco coatings (Künzel, Künzel and Holm, 2004) and external thermal renders (Maia, Ramos and Veiga, 2018). On the other hand, it is good practice to safeguard the overall drying ability of historic components (David; Pickles, Ian, and Wood, 2010b) by adopting insulation materials having hygric properties that are similar to those of the historic materials involved.

Therefore, the adoption of external insulation with moderate water absorption appears as a proper choice to avoid an excessive penetration of rainwater. At the same time, it should not be overly lower than the ones of the original, adjacent materials, in order not to strongly alter the hygric behaviour of historic components. When external insulation is protected against wind-driven rain through the use of water-resistant coating or water-repellent treatment, it might be possible to consider insulation materials with higher water absorption coefficients.

In conclusion, thermal insulation materials characterized by both high and low capillary absorption coefficients may appear appropriate for retrofit interventions, and the preference for one over the other depends on the specific situation taken into analysis.

2.5.3. Hygric behaviour of insulation materials: a classification

Given the importance of vapour permeability and capillary water absorption of insulations in the context of hygric compatibility, a classification method is hereby defined to rank the two hygric properties of insulation materials in comparison to the ones averagely found in historic envelopes. The hygric properties of traditional materials and the average values found are reported in Tables 2.2 and 2.3.

The criterion thus defined is synthesised in Table 2.4 and is based on the average values found in traditional materials adopted in historic envelopes.

Table 2.2 - Water Absorption Coefficient (A_w) of traditional buildings materials, typical of Historic Envelopes.

	Materials	Water Absorption Coefficient A_w [kg/ ($m^2.s^{1/2}$)]		Reference
		Min	Max	
Traditional building materials	Limestone	0.50	1.5	(Møller, 2018)
	Sandstone	0.02	0.88	(Vejmelková et al., 2013; Krus 1995)
	Historic bricks	0.15	0.24	(Zhao and Meissener, 2017)
	Historic mortars (lime based)	0.040	0.54	(A. Magalhães and Veiga, 2009)
	Gypsum plaster	0.050	0.13	(Freire et al., 2019)
	Wood - Spruce	0.0024	0.05	(Scheiding, Direske, and Zauer, 2016)
	Wood - Pine	0.0090	0.87	(Zelinka et al., 2016)

Average Values:

Av. Min Absorption c. - $A_{w\_min} = 0.11$ kg /($m^2s^{1/2}$);
Av. Max Absorption c. - $A_{w\_max} = 0.60$ kg /($m^2s^{1/2}$);
Av. Absorption c. - $A_{w\_Av} = 0.36$ kg /($m^2s^{1/2}$)

Classification criterion:

High Absorption c. - $A_w > 0.60$ kg /($m^2s^{1/2}$); Moderately High Absorption c. - $A_w = 0.36 \div 0.60$ kg /($m^2s^{1/2}$)
Moderately Low Absorption c. - $A_w = 0.11 \div 0.36$ kg /($m^2s^{1/2}$); Low Absorption c. - $A_w < 0.11$ kg /($m^2s^{1/2}$)

Table 2.3 - Vapour permeability (δp) of traditional buildings materials commonly found in Historic Envelopes.

	Materials	Water vapour permeability δp [10^{-12} kg/ (m.s.Pa)]		Reference
		Min	Max	
Traditional building materials	Limestone	2.1	9.4	(Freitas and Pinto 1998; Møller, 2018)
	Sandstone	15.0*	36.4*	(Vejmelková et al., 2013; Krus 1995)
	Historic bricks	8.9	10.9	(Zhao and Meissener, 2017)
	Historic mortars (lime based)	4.5	33.0	(Freitas and Pinto 1998; Margalha et al., 2011; Veiga et al., 2010)
	Gypsum plaster	17.0	39.2	(Freitas and Pinto 1998; Freire et al., 2019)
	Wood - Spruce	2.6	4.6	(Freitas and Pinto 1998)
	Wood - Pine	0.81	10	(Freitas and Pinto 1998)

Average Values:

Av. Min Permeability - $\delta_{p\_min}=6.0 \cdot 10^{-12}$ kg/ (m s Pa); Av. Max Permeability - $\delta_{p\_max}=17.9 \cdot 10^{-12}$ kg/ (m s Pa) ;
Av. Permeability - $\delta_{p\_Av} = 11.9 \cdot 10^{-12}$ kg/ (m s Pa)

Classification criterion:

High Permeability - $\delta_p > 17.9 \cdot 10^{-12}$ kg/ (m s Pa); Moderately High Permeability - $\delta_p = (11.9 \div 17.9) \cdot 10^{-12}$ kg/ (m s Pa)
Moderately Low Permeability - $\delta_p = (6.0 \div 11.9) \cdot 10^{-12}$ kg/ (m s Pa); Low Permeability - $\delta_p < 6.0 \cdot 10^{-12}$ kg/ (m s Pa)

**Values given in literature as Water Vapour Diffusion Equivalent Air Layer Thickness (S_d) and converted in Water vapour resistance factors (μ) by considering the declared mortar thickness of d=10mm, the definition (Radu et al., 2012) of S_d as the product of the material thickness and its vapour resistance factor $S_d = \mu^* d$.

*Values given in literature as Water vapour resistance factors (μ) and converted in Water vapour permeability (δ_p) by considering the definition (Radu et al., 2012) of resistance factor as the ratio between permeability of the still air and the one of the considered material ($\mu = \delta_{p,a} / \delta_p$), an approximated Water vapour permeability of still air ($\delta_{p,a}$) of, 200 10^{-12} kg/ (m s Pa).

Table 2.4 - Hygric classification criterion: Classes of Vapour Permeability and Water Absorption Coefficient.

	Vapour permeability δ_p [10^{-12} kg/ (m s Pa)]	Water absorption coefficient A_w [kg/ ($m^2 s^{1/2}$)]
High	$\delta p \geq 17.9$ ($\mu^* \leq 11.2$)	$A_w \geq 0.60$
Moderately High	$11.9 \leq \delta p < 17.9$ ($11.2 < \mu^* < 16.8$)	$0.36 \leq A_w < 0.60$
Moderately Low	$6.0 \leq \delta p < 11.9$ ($16.8 < \mu^* < 33.3$)	$0.11 \leq A_w < 0.36$
Low	$\delta p < 6.0$ ($\mu^* < 33.3$)	$A_w < 0.11$

*Values converted from Water vapour permeability (δ_p) by considering the definition (Radu et al., 2012) of resistance factor as the ratio between the permeability of the still air and the one of the considered material ($\mu = \delta_{p,a} / \delta_p$) and an approximated value of Water vapour permeability of still air ($\delta_{p,a}$) of 200 10^{-12} kg/ (m s Pa).

The classification obtained for insulation materials is reported in Table 2.5. The results presented in the table are based on the vapour permeability and capillary water absorption values found in literature, which are not reported in this chapter for the reason of synthesis. Nonetheless, a complete description and list of values can be found in Posani, Veiga and Freitas (2019). In Table 2.5 it is also indicated whether the materials were found in internal and/or external interventions, according to the literature outcomes presented in section 2.2.

According to Table 2.5, all the natural fibres taken into account (Cellulose, Flax, Hemp, Sheep's wool, Wood fibres), as well as inorganic materials (Mineral wool, Calcium silicate, Expanded Perlite), show a High Vapour Permeability. On the contrary, Vacuum Insulation Panels and petrochemical materials appear to have quite low permeability (from Moderately Low to Low).

Some inorganic materials (Hydrophilic Mineral Wool and Calcium Silicate) and Cellulose emerge to have high water absorption coefficients. Expanded Perlite appeared to have an absorption coefficient that can range from High to Moderately Low, and all other insulation materials appeared to have quite low absorption coefficients (Moderately Low to Low).

Overall, from the classification reported in Table 2.5, it is possible to observe the existence of 3 types of hygric behaviour in the analysed thermal insulations:

- materials that are vapour permeable (high/moderately high δ_p) and capillary active (high/moderately high A_w), like cellulose and hydrophilic mineral wool;
- vapour permeable materials with a low/moderately low water absorption coefficient, like most natural fibres and hydrophobic mineral wool;
- materials with a low/moderately low value for both vapour permeability and water absorption coefficient, like petrochemical materials (e.g. EPS) and Vacuum Insulation Panels (VIP).

It is also worth mentioning that the thermal mortars considered show very variable properties, especially in terms of water vapour permeability. This result is very reasonable since those properties depend on the materials adopted in the mix design.

Finally, from the results presented in Table 2.5, it is observed that external insulation is in most cases made of materials with low water absorption coefficients whereas internal insulation solutions adopt materials with all the three hygric behaviours.

Table 2.5 – Hygric Classification of the analysed insulation materials.

Materials		Water Vapour Permeability (δ_p) Classification	Water Absorption (A_w) Classification	Use (in literature)	
				Walls Int.	Walls Ext.
Thermal Renders / Plasters	*Hemp-lime*	*High - Moderately Low* δ_p	*Moderately Low - Low* A_w	x	x
	Cork-lime	*Moderately High - Low* δ_p	*Moderately Low - Low* A_w		
Organic: Natural Fibres	*Cellulose*	*High* δ_p	*High* A_w	x	
	Flax	*High* δ_p	*Low* A_w		x
	Sheep's wool	*High* δ_p	*Low* A_w		x
	Wood fibers	*High* δ_p	*Low* A_w	x	
Organic: Petrochemical Materials	*Expanded Polystyrene (EPS)*	*Moderately Low - Low* δ_p	*Low* A_w	x	x
	Extruded polystyrene (XPS)	*Low* δ_p	*Low* A_w	x	
	Polyisocyanurate (PIR)	*Low* δ_p	*Low* A_w	x	
	Polyurethane (PUR)	*Low* δ_p	*Low* A_w	x	
Inorganic Materials	*Mineral wool (Hydrophilic)*	*High* δ_p	*High* A_w	x	x
	Mineral wool (Hydrophobic)	*High* δ_p	*Low* A_w		
	Calcium silicate	*High* δ_p	*High* A_w	x	
	Expanded Perlite	*High* δ_p	*High - Moderately low* A_w	x	
New Technology Materials	*Vacuum Insulation Panels (VIPs)*	*Low* δ_p	*Low* A_w	x	x
	Aerogel based Plasters/Renders	*High* δ_p	*Moderately Low - Low* A_w	x	x
	Aerogel panels	*High - Moderately Low* δ_p	*Low* A_w	x	x

2.5.4. Main outcomes of the review on compatibility and introduction of a method for preliminary evaluation of compatibility

According to the literature review performed on the compatibility of thermal insulation with historic walls, the main outcomes obtained can be synthesized as follows:

- traditional constructions are typically porous and capillary-active, and water can reach the walls through rainwater intake, rising damp and damages in the envelope. In this context, post-insulation represents a very complex intervention because it can alter the original moisture dynamics of historic walls, leading to trapped moisture;
- since the main hazards introduced by the intervention are moisture-related, the main compatibility concern lies in the physical compatibility, from the hygric point of view. Thus, the main material properties to consider for evaluating physical compatibility seem to be capillary water absorption and water vapour permeability;
- adopting insulation solutions with high vapour permeability is good for avoiding reductions in the original drying ability of walls. Nonetheless, low vapour permeability might be suitable for reducing the risk of interstitial condensation when adopting internal insulation, but it can potentially lead to trapped moisture if water reaches the wall through rising dampness, rainwater penetration or damages in the envelope. When adopting external insulation, it appears important to reduce rainwater intake, for this reason, insulation materials with a low A_w appear suitable for the scope. Anyway, if a protective coating or a water-repellent treatment is adopted to complete the thermal insulation system, insulation materials with a high A_w may be adoptable. Furthermore, for sufficiently thick walls and walls not exposed to wind driven rain, capillary active internal insulation appears beneficial for reducing moisture accumulation due to interstitial condensation.

Overall, it appears that a general criterion for choosing compatible insulation solutions for historic walls does not exist. This lack is likely to be related to the dependence of the risks on the specific type of intervention (internal or external insulation), component type (masonry wall, wooden structure, ...), geometry (thickness of the element) and boundary conditions (climate, exposure to weather, ...) considered. However, it seems possible to define specific clusters of situations for which, at a preliminary-design stage, some solutions appear more compatible than others. For example, according to the results obtained by Vereecken and Roels (2015), for the cluster of "internal insulation of thick, massive masonry walls, in temperate climates, with indoor HVAC systems", it is conceivable to indicate vapour open, capillary active systems as target compatible solutions.

Clearly, more studies are necessary to define specific clusters and the associated appropriate interventions. Within this scope, this PhD research aims at analysing compatible solutions for the cluster of "thick masonry walls of historic buildings with temporary occupation, located in areas with temperate climates with warm or hot summers and mild winters, where heating systems are adopted".

2.6. CONCLUSION

According to the literature review presented in this chapter, thermal mortars, mineral wool and EPS are thermal insulation materials widely considered for post-insulating historic walls. The first type of insulation is the one chosen for being analysed in detail in this PhD research because of the good feasibility it offers (e.g., adaptability to uneven surfaces, gap-filling ability, no need of anchoring points or adhesive layer, and a wide range of possible thicknesses). Based on the hygric classification proposed, thermal mortars with low water absorption coefficients and high vapour permeability are selected for being studied in detail in this research. Then, the effect of different capillary absorption and water permeability of the insulation materials will also be investigated through numerical simulations.

Dynamic hygrothermal simulations are the tools chosen for investigating the compatibility and efficacy of insulation solutions for application in the cluster considered. Compatibility is studied by evaluating the hygrothermal behaviour of the walls of some case studies, before and after the thermal retrofit, via mono-dimensional simulations. Efficacy is analysed by observing the effect of thermal insulation on thermal comfort and energy demands, by means of whole-building simulations.

The three case studies considered in this research are presented in the following chapter, together with the experimental monitoring campaigns performed on-site to obtain the hygrothermal dataset needed for the input, calibration and validation of the simulation models.

2.7. REFERENCES

Alfano, Francesca, R.D.Ambrosio, and Livio de Santoli. 2017. “Energy Efficiency and HVAC Systems in Existing and Historical Buildings.” In *Historical Buildings and Energy*. Springer: Cham, Switzerland. doi:10.1007/978-3-319-52615-7_3.

Al-Sanea, Sami A., M. F. Zedan, and S. N. Al-Hussain. 2012. “Effect of Thermal Mass on Performance of Insulated Building Walls and the Concept of Energy Savings Potential.” *Applied Energy*. doi:10.1016/j.apenergy.2011.08.009.

Amorim, Mafalda, Vasco Peixoto de Freitas, Isabel Torres, Tomasz Kisilewicz, and Umberto Berardi. 2020. “The Influence of Moisture on the Energy Performance of Retrofitted Walls.” *MATEC Web of Conferences*. doi:10.1051/matecconf/202032201035.

Ascione, Fabrizio, Nicola Bianco, Rosa Francesca De Masi, Filippo De’Rossi, and Giuseppe Peter Vanoli. 2015. “Energy Retrofit of an Educational Building in the Ancient Center of Benevento. Feasibility Study of Energy Savings and Respect of the Historical Value.” *Energy and Buildings* 95: 172–183. doi:10.1016/j.enbuild.2014.10.072.

Ascione, Fabrizio, Nicla Cheche, Rosa Francesca De Masi, Francesco Minichiello, and Giuseppe Peter Vanoli. 2015. “Design the Refurbishment of Historic Buildings with the Cost-Optimal Methodology: The Case Study of a XV Century Italian Building.” *Energy and Buildings* 99: 162–176. doi:10.1016/j.enbuild.2015.04.027.

Ascione, Fabrizio, Filippo De Rossi, and Giuseppe Peter Vanoli. 2011. “Energy Retrofit of Historical Buildings: Theoretical and Experimental Investigations for the Modelling of Reliable Performance Scenarios.” *Energy and Buildings* 43 (8): 1925–1936. doi:10.1016/j.enbuild.2011.03.040.

Asdrubali, Francesco, Francesco D’Alessandro, and Samuele Schiavoni. 2015. “A Review of Unconventional Sustainable Building Insulation Materials.” *Sustainable Materials and Technologies*. doi:10.1016/j.susmat.2015.05.002.

Baggio, Marialuisa, Chiara Tinterri, Tiziano Dalla Mora, Alessandro Righi, Fabio Peron, and Piercarlo Romagnoni. 2017. “Sustainability of a Historical Building Renovation Design through the Application of LEED® Rating System.” *Energy Procedia* 113: 382–389. doi:10.1016/j.egypro.2017.04.017.

Baiani, Serena, Elena Lucchi, and Michela Pascucci. 2018. “Old and Innovative Materials Towards a ‘Compatible Conservation.’” In *Analysis, Conservation, and Restoration of Tangible and Intangible Cultural Heritage*. IGI Global: Hershey, USA. p. 170-195. ISBN 9781522569367.

Balibar, Sebastien. "Energy transitions after COP21 and 22." *Comptes Rendus Physique* 18.7-8 (2017): 479-487. doi: 10.1016/J.CRHY.2017.10.003

Becherini, Francesca, Elena Lucchi, Alessandra Gandini, Maria Casado Barrasa, Alexandra Troi, Francesca Roberti, Maria Sachini, et al. 2018. “Characterization and Thermal Performance Evaluation of Infrared Reflective Coatings Compatible with Historic Buildings.” *Building and Environment*. doi:10.1016/j.buildenv.2018.02.034.

Biseniece, Edīte, Gatis Žogla, Agris Kamenders, Reinis Purviņš, Kristaps Kašs, Ruta Vanaga, and Andra Blumberga. 2017. “Thermal Performance of Internally Insulated Historic Brick Building in Cold Climate: A Long Term Case Study.” *Energy and Buildings* 152: 577–586. doi:10.1016/j.enbuild.2017.07.082.

Bjarløv, S. P., G. R. Finken, and T. Odgaard. 2015. “Retrofit with Interior Insulation on Solid Masonry Walls in Cool Temperate Climates - An Evaluation of the Influence of Interior Insulation Materials on Moisture Condition in the Building Envelope.” *Energy Procedia* 78, 1461–1466. doi:10.1016/j.egypro.2015.11.171.

Blumberga, Andra, Dagnija Blumberga, Edite Kamendere, Agris, and Gatis Zogla Kamenders , Kristaps Kass , Reinis Purvins. 2016. EU Project - RIBuild (Robust Internal Thermal Insulation of Historic Buildings, EU Project) – “Deliverable No. D1.1: Report on Historical Building Types and Combinations of Structural Solutions”. doi:10.1002/ejoc.201200111.

Blumberga, Andra, Kristaps Kass, Edite Kamendere, Gatis Žogla, Agris Kamenders, Dagnija Blumberga, Armands Grāvelsiņš, Reinis Purviņš, Marika Rošā, and Lelde Timma. 2016a. EU Project - RIBuild (Robust Internal Thermal Insulation of Historic Buildings, EU Project) – “Deliverable No. D1.2: State of the Art on Historic Building Insulation Materials and Retrofit Strategies”.

Blumberga A., Freimanis R., Blumberga D., Veidenbergs I., Hansen E.J.P., Hansen T.K., Du G., Stöcker E., Sontag H., Freudenberg P., Et al. 2020. EU Project - RIBuild (Robust Internal Thermal Insulation of Historic Buildings, EU Project) - “Deliverable no. D6.2: Written Guidelines for Decision Making Concerning the Possible Use of Internal Insulation in Historic Buildings”. Available online: https://www.ribuild.eu/s/Written-guidelines-for-decision-making-concerning-the-possible.pdf (accessed on 1 June 2021).

Bond, Stephen, and Derek Worthing. 2016. “Managing Built Heritage: The Role of Cultural Values and Significance: Second Edition.” In *Managing Built Heritage: The Role of Cultural Values and Significance: Second Edition*. doi:10.1002/9781118298718.

Bottino-Leone, Dario, Marco Larcher, Daniel Herrera-Avellanosa, Franziska Haas, and Alexandra Troi. 2019. “Evaluation of Natural-Based Internal Insulation Systems in Historic Buildings through a Holistic Approach.” *Energy*. doi:10.1016/j.energy.2019.05.139.

Bouzit, S., F. Merli, M. Sonebi, C. Buratti, and M. Taha. 2021. “Gypsum-Plasters Mixed with Polystyrene Balls for Building Insulation: Experimental Characterization and Energy Performance.” *Construction and Building Materials* 283. doi:10.1016/j.conbuildmat.2021.122625.

CEN. 2017. “EN 16883:2017 - Conservation of Cultural Heritage - Guidelines for Improving the Energy Performance of Historic Buildings.” British Standards Institution: London, UK.

CEN. 2017. “EN 998-1:2017 - Specification for Mortar for Masonry - Part 1: Rendering and Plastering Mortar.” British Standards Institution: London, UK.

CEN. 2000. “EN 12524:2000 - Building Materials and Products. Hygrothermal Properties. Tabulated Design Values.” British Standards Institution: London, UK.

Chvatal, Karin Maria Soares, and Helena Corvacho. 2009. “The Impact of Increasing the Building Envelope Insulation upon the Risk of Overheating in Summer and an Increased Energy Consumption.” *Journal of Building Performance Simulation* 2 (4). doi:10.1080/19401490903095865.

Cirami, Simona, Gianpiero Evola, Antonio Gagliano, and Giuseppe Margani. 2017. "Thermal and Economic Analysis of Renovation Strategies for a Historic Building in Mediterranean Area." *Buildings* 7 (3). doi: 10.3390/buildings7030060.

Cornaro, Cristina, Valerio Adoo Puggioni, and Rodolfo Maria Strollo. 2016. "Dynamic Simulation and On-Site Measurements for Energy Retrofit of Complex Historic Buildings: Villa Mondragone Case Study." *Journal of Building Engineering* 6, 17–28. doi:10.1016/j.jobe.2016.02.001.

Cuce, Erdem, Pinar Mert Cuce, Christopher J. Wood, and Saffa B. Riffat. 2014. "Toward Aerogel Based Thermal Superinsulation in Buildings: A Comprehensive Review." *Renewable and Sustainable Energy Reviews*. doi:10.1016/j.rser.2014.03.017.

Dalla Mora, T., F. Cappelletti, F. Peron, P. Romagnoni, and F. Bauman. 2015. "Retrofit of an Historical Building toward NZEB." *Energy Procedia* 78, 1359–1364. doi:10.1016/j.egypro.2015.11.154.

De Berardinis, Pierluigi, Marianna Rotilio, Chiara Marchionni, and Avi Friedman. 2014. "Improving the Energy-Efficiency of Historic Masonry Buildings. A Case Study: A Minor Centre in the Abruzzo Region, Italy." *Energy and Buildings* 80: 415–423. doi:10.1016/j.enbuild.2014.05.047.

Del Curto, Davide, and Valentina Cinieri. 2020. "Aerogel-Based Plasters and Energy Efficiency of Historic Buildings. Literature Review and Guidelines for Manufacturing Specimens Destined for Thermal Tests." *Sustainability*. doi:10.3390/su12229457.

Di Ruocco, Giacomo, Claudia Sicignano, and Anna Sessa. 2017. "Integrated Methodologies Energy Efficiency of Historic Buildings." *Procedia Engineering* 180: 1653–1663. doi:10.1016/j.proeng.2017.04.328.

European Organisation for Technical Approvals (EOTA). 2020. "EAD 040083-00-0404:2020 - European Assessment Document. External Thermal Insulation Composite Systems (ETICS) with renderings ". EOTA: Brussels, Belgium.

Finken, Gholam Reza, Søren Peter Bjarløv, and Ruut Hannele Peuhkuri. 2016. "Effect of Façade Impregnation on Feasibility of Capillary Active Thermal Internal Insulation for a Historic Dormitory - A Hygrothermal Simulation Study." *Construction and Building Materials* 113:, 202–214. doi:10.1016/j.conbuildmat.2016.03.019.

Flores-Colen, I., L. Silva, J. De Brito, and V. P. de Freitas. 2016. "Drying Index for In-Service Physical Performance Assessment of Renders." *Construction and Building Materials*. doi:10.1016/j.conbuildmat.2016.03.034.

Freire, Maria Teresa, António Santos Silva, Maria do Rosário Veiga, and Jorge de Brito. 2019. "Studies in Ancient Gypsum Based Plasters towards Their Repair: Mineralogy and Microstructure." *Construction and Building Materials*. doi:10.1016/j.conbuildmat.2018.11.037.

Freitas, Vasco Peixoto, and P Pinto. 1998. "Nota de Informação Técnica—NITo002 - Permeabilidade Ao Vapor de Materiais de Construção–Condensações Internas.". *LFC:Porto, Portugal.*

Ganobjak, Michal, Samuel Brunner, and Jannis Wernery. 2019. "Aerogel Materials for Heritage Buildings: Materials, Properties and Case Studies." *Journal of Cultural Heritage*. doi: 10.1016/j.culher.2019.09.007.

Godwin, P J. 2011. "Building Conservation and Sustainability in the United Kingdom." *Procedia Engineering*, 20: 12–21. doi:10.1016/j.proeng.2011.11.135.

Gomes, M. Glória, Inês Flores-Colen, Humberto Melo, and António Soares. 2019. "Physical Performance of Industrial and EPS and Cork Experimental Thermal Insulation Renders." *Construction and Building Materials* 198: 786–795. doi:10.1016/j.conbuildmat.2018.11.151.

Govaerts, Yves, Roald Hayen, Michael de Bouw, Ann Verdonck, Wendy Meulebroeck, Stijn Mertens, and Yves Grégoire. 2018. "Performance of a Lime-Based Insulating Render for Heritage Buildings." *Construction and Building Materials* 159. Elsevier Ltd: 376–389. doi:10.1016/j.conbuildmat.2017.10.115.

Grunewald, J., U. Ruisinger, and P. Häupl. 2006. "The Rijksmuseum Amsterdam - Hygrothermal Analysis and Dimensioning of Thermal Insulation." In *Proceedings of the 3rd International Building Physics Conference - Research in Building Physics and Building Engineering.* Montreal, Canada, 27-31 August, 2006.

Guizzardi, Michela. 2014. "Hygrothermal Performance Assessment of Novel Interior Insulation Solutions." PhD thesis, ETH Zurich.

Hao, L., D. Herrera, and A. Troi. 2018. "The effect of climate change on the future performance of retrofitted historic buildings A review.". In *Proceedings of the 3rd International Conference on Energy Efficiency in Historic Buildings* (EEHB2018), Uppsala University, Visby, Sweden, September 26-27,, 2018.

Hegger, Manfred, Volker Auch-Schwelk, Matthias Fuchs, and Thorsten Rosenkranz. 2013. *Construction Materials Manual*. *Construction Materials Manual*. doi:10.11129/detail.9783034614559.

ICOMOS. 1964. "International Charter for the Conservation and Restoration of Monuments and Sites (The Venice Charter 1964).". In *IInd International Congress of Architects and Technicians of Historic Monuments*, Venice, Italy, May 1964. Available online: https://www.icomos.org/charters/venice_e.pdf (accessed on 1 June, 2021).

ICOMOS. 1994. "*The Nara Document on Authenticity*. *Knowledge Creation Diffusion Utilization*." In *Proceedings of the Nara Conference*: Nara, Japan, November 1994. Available online: https://www.icomos.org/charters/nara-e.pdf (accessed on 1 June, 2021).

ICOMOS. 2003. "Principles for the Analysis, Conservation and Structural Restoration of Architectural Heritage (2003)." In *ICOMOS 14th General Assembly*: Victoria Falls, Zimbabwe,, 2003.56.

ICOMOS. 2010. "ICOMOS New Zealand Charter for the Conservation of Places of Cultural Heritage Value." *ICOMOS New Zealand Charter*: Auckland, New Zealand,, 2010. ISBN 978-0-473-17116-2.

ICOMOS. 2013. "The Burra Charter (The Australia ICOMOS Charter for Places of Cultural Significance)". Australia ICOMOS: Burwood, Australia,, 2013, doi:10.1007/978-1-4419-0465-2_1046.

ISO. 2017. "ISO 6946:2017 - Building Components and Building Elements — Thermal Resistance and Thermal Transmittance — Calculation Methods Properties." British Standards Institution: London, UK.

Johansson, P., A. Donarelli, and P. Strandberg. 2018. "Performance of Insulation Materials for Historic Buildings Case Studies Comparing a Super Insulation Material and Hemp-Lime." In *Proceedings*

of the 3rd International Conference on Energy Efficiency in Historic Buildings (EEHB2018), Uppsala University, Visby, Sweden, September 26-27,, 2018.

Johansson, P.,Lång, L., Capener, C.M., Møller, E.B., Quagliarini, E., D'Orazio, M., Gianangeli, A., Janssen, H., Feng, C., Langmans, J. 2019. EU Project - RIBuild (Robust Internal Thermal Insulation of Historic Buildings, EU Project) "Deliverable no. D2.2 - Report on Threshold Values for Failure, Linked to Types of Building Structures and Failure Modes". Available online: https://www.ribuild.eu/s/RIBuild_D22_v10_1.pdf (accessed on 1 June 2021).

Jordan, Andrew, et al., eds. *Climate change policy in the European Union: Confronting the dilemmas of mitigation and adaptation?* Cambridge University Press, 2010.

Kienzlen, V, H Erhorn, H Krapmeier, T Lutzkendorf, J Werner, and A Wagner. 2014. "The Significance of Thermal Insulation Arguments Aimed at Overcoming Misunderstandings." In *Fraunhofer-Publica: Karlsruhe, Germany*. Vol. 35.

Krus, M. 1995. "Moisture Transport and Storage Coefficients Ofporous Mineral Building Materials." In *Theoretical Principles and New Test Methods*, Fraunhofer IRB Verlag: Germany. ISBN: 139783816745358

Krus, M, R Killan, and B Pfundstein. 2016. "Comparison of Different Systems for Internal Wall Insulation with Reversible Application for Historic Building." In *Energy Efficiency and Comfort of Historic Buildings (EECHB),* Brussels,Belgium, 19-21 October, p.181–190.

Künzel, Hartwig M. 1998. "Effect of Interior and Exterior Insulation on the Hygrothermal Behaviour of Exposed Walls." *Materials and Structures*. doi:10.1007/bf02486471.

Künzel, Hartwig M., Helmut Künzel, and Andreas Holm. 2004. "Rain Protection of Stucco Facades." In *Proceedings of the Thermal Performance of the Exterior Envelopes of Whole Buildings IX–International Conference, Florida, USA*.

Lekavicius, V., P. Shipkovs, S. Ivanovs, and A. Rucins. 2015. "Thermo-Insulation Properties of Hemp-Based Products." *Latvian Journal of Physics and Technical Sciences*. doi:10.1515/lpts-2015-0004.

Little, Joseph, Calina Ferraro, and Benat Aregi. 2015. *Technical Paper 15: Assessing Risks in Insulation Retrofits Using Hygrothermal Software Tools Heat and Moisture Transport in Internally Insulated Stone Walls*. Historic Environment Scotland: Edinburgh, Scotland. doi:10.13140/RG.2.1.2493.3844.

Lucchi, Elena, and Valeria Pracchi. 2013. "Efficienza Energetica e Patrimonio Costruito: La Sfida Del Miglioramento Delle Prestazioni Nell'edilizia Storica." Maggioli Editore: Rimini, Italy. ISBN: 8838762600

Magalhães, A, and R Veiga. 2009. "Physical and Mechanical Characterisation of Historic Mortars. Application to the Evaluation of the State of Conservation." *Materiales de Construcción* 59 (295): 61–77.

Magalhães, Sílvia A., and V.P. Freitas. 2017. "A Complementary Approach for Energy Efficiency and Comfort Evaluation of Renovated Dwellings in Southern Europe." In *Energy Procedia*. doi:10.1016/j.egypro.2017.09.717.

Maia, J., Nuno M.M. Ramos, and M. R. Veiga. 2018. "Evaluation of the Hygrothermal Properties of Thermal Rendering Systems." *Building and Environment*. doi:10.1016/j.buildenv.2018.08.055.

Malanho, Sofia, M. R. Veiga, and Catarina Brazão Farinha. 2021. “Global Performance of Sustainable Thermal Insulating Systems with Cork for Building Facades.” *Buildings* 11 (3). doi:10.3390/buildings11030083.

Mancini, Francesco, Carola Clemente, Elisa Carbonara, and Sara Fraioli. 2017. “Energy and Environmental Retrofitting of the University Building of Orthopaedic and Traumatological Clinic within Sapienza Città Universitaria.” *Energy Procedia* 126:195–202. doi: 10.1016/j.egypro.2017.08.140.

Margalha, Goreti, Rosário Veiga, António Santos Silva, and Jorge De Brito. 2011. “Traditional Methods of Mortar Preparation: The Hot Lime Mix Method.” *Cement and Concrete Composites*. doi:10.1016/j.cemconcomp.2011.05.008.

Maurenbrecher, Paul. 2012. “RILEM TC, 203-RHM: Repair Mortars for Historic Masonry: Requirements for Repointing Mortars for Historic Masonry.” *Materials and Structures* 45. Springer: 1303–1309.

Ministério do Ambiente, Ordenamento do Território e Energia. “Portaria n.o 379-A/2015 de 22 de outubro. Diário da República n.o, 207/2015, 2o Suplemento, Série I de, 2015-10-22”. Diário da República: Lisbon, Portugal,, 2015. Available online: https://dre.pt/application/conteudo/70789581 (National standard, in Portuguese)

Møller, E.B.; EsadA.; Blumberga A.; Ekstrand-Tobin A.; Hansen E. J. P.; Ståh F.l; Finken G.R.; Janssen H.; Grunewald J.; Freudenberg P.; Lasvaux S. EU Project - RIBuild (Robust Internal Thermal Insulation of Historic Buildings, EU Project), “Deliverable No. D2.1 - Report on the material properties.”. Available online: https://www.ribuild.eu/s/RIBuild_D21_v10.pdf (accessed on 1 June, 2021).

Nosrati, Roya Hamideh, and Umberto Berardi. 2018. “Hygrothermal Characteristics of Aerogel-Enhanced Insulating Materials under Different Humidity and Temperature Conditions.” *Energy and Buildings*. doi:10.1016/j.enbuild.2017.09.079.

Odgaard, Tommy, Søren Peter Bjarløv, and Carsten Rode. 2018. “Interior Insulation—Characterisation of the Historic, Solid Masonry Building Segment and Analysis of the Heat Saving Potential by 1d, 2d, and 3d Simulation.” *Energy and Buildings* 162. doi:10.1016/j.enbuild.2017.12.008.

Parracha, J. L., G. Borsoi, I. Flores-Colen, R. Veiga, L. Nunes, A. Dionísio, M. Glória Gomes, and P. Faria. 2021. “Performance Parameters of ETICS: Correlating Water Resistance, Bio-Susceptibility and Surface Properties.” *Construction and Building Materials*. doi:10.1016/j.conbuildmat.2020.121956.

Petzet, Michael. 2004. “Principles of Preservation: An Introduction to the International Charters for Conservation and Restoration 40 Years after the Venice Charter.”, ICOMOS: München, Germany,, 2004. ISBN 3-87490-676-0; pp. 7-29.

Pfluger, Rainer, and Paolo Baldracchi. 2011. EU Project - 3encult “Deliverable No. 3.1 - Report on Energy Efficiency Solutions for Historic Buildings”.

Pickles, David, Brocklebank Ian, and Chris Wood. 2010a. “Energy Efficiency in Insulating Solid Walls.” English Heritage: London, Great Britain.

Pickles, David ;, Brocklebank; Ian, and Chris. Wood. 2010b. *Energy Efficiency and Historic Buildings. Application of Part L of the Building Regulations to Historic and Traditionally Constructed Buildings.* English Heritage: London, Great Britain. doi:10.1108/ss.2011.11029caa.019.

Posani, Magda, Maria Do Rosario Veiga, and Vasco Peixoto de Freitas, 2019. "Towards Resilience and Sustainability for Historic Buildings: A Review of Envelope Retrofit Possibilities and a Discussion on Hygric Compatibility of Thermal Insulations." *International Journal of Architectural Heritage*. https://doi.org/10.1080/15583058.2019.1650133.

Presidente della Repubblica Italiana.2020. Dlgs 73/2020 - DECRETO LEGISLATIVO 14 luglio, 2020, n. 73 - Attuazione della direttiva (UE), 2018/2002 che modifica la direttiva, 2012/27/UE sull'efficienza energetica. (20G00093). Gazzetta Ufficiale Della Repubblica Italiana: Roma, Italy. Available online: https://www.gazzettaufficiale.it/eli/id/2020/07/14/20G00093/sg (National standard, in Italian)

Radu, Adrian, Eva Barreira, Hamed Saber, Hugo Hens, Juha Vinha, Maricica Vasilache, Mark Bomberg, et al. 2012. "Heat , Air and Moisture Transfer Terminology Parameters and Concepts," LFC: Porto, Portugal. ISBN 978-90-6363-070-6

Rasmussen, T Valdbjørn, Eva B Møller, and Thomas Cornelius Buch-Hansen. 2015. "Extensive Renovation of Heritage Buildings-Reduced Energy Consumption and CO2 Emissions." *The Open Construction and Building Technology Journal* 9, 58-67. doi: 10.2174/1874836801509010058.

Robert, Wójcik, and Kosiński Piotr. 2017. "On Rehabilitation of Buildings with Historical Façades." In *Energy Procedia*. doi:10.1016/j.egypro.2017.09.724.

Roberti, Francesca, Ulrich Filippi Oberegger, Elena Lucchi, and Alexandra Troi. 2017. "Energy Retrofit and Conservation of a Historic Building Using Multi-Objective Optimization and an Analytic Hierarchy Process." *Energy and Buildings* 138, 1–10. doi:10.1016/j.enbuild.2016.12.028.

Rosales Carreón, Jesús. 2015. (ReFoMo, EU Project) "Review on Techniques, Tools and Best Practices for Energy Efficient Retrofitting of Heritage Buildings"; Universiteit Utrecht: Utrecht, The Netherlands.

Scheiding, Wolfram, Martin Direske, and Mario Zauer. 2016. "Water Absorption of Untreated and Thermally Modified Sapwood and Heartwood of Pinus Sylvestris L." *European Journal of Wood and Wood Products* 74 (4): 585–589. doi: 10.1007/s00107-016-1044-z.

Stingl Freitas, Teresa, Ana Sofia Guimarães, Staf Roels, Vasco Peixoto de Freitas, and Andrea Cataldo. 2020. "Is the Time-Domain Reflectometry (TDR) Technique Suitable for Moisture Content Measurement in Low-Porosity Building Materials?" *Sustainability* 12 (19). doi:10.3390/SU12197855.

Troi, A., and Z. Bastian. 2015. "Building Energy Efficiency Solutions: A Handbook. Chapter 2.3: Cultural Heritage." Birkhauser: Basel, Switzerland. doi:10.1017/CBO9781107415324.004.

UNESCO. 1972. *Convention Concerning the Protection of the World Cultural and Natural Heritage*. UNESCO Publishing: Paris, France. ISBN 9233010937. Available at: https://whc.unesco.org/archive/convention-en.pdf (accessed on 1 June, 2021).

Veiga, M.D. Rosário, Ana Fragata, Ana Luisa Velosa, Ana Cristian Magalhães, and Goreti Margalha. 2010. "Lime-Based Mortars: Viability for Use as Substitution Renders in Historical Buildings." *International Journal of Architectural Heritage*. doi:10.1080/15583050902914678.

Vejmelková, E., M. Keppert, P. Reiterman, and R. Černý. 2013. “Mechanical, Hygric and Thermal Properties of Building Stones.” In *WIT Transactions on the Built Environment*. doi:10.2495/STR130301.

Vereecken, Evy, and Staf Roels. 2014. “A Comparison of the Hygric Performance of Interior Insulation Systems: A Hot Box–Cold Box Experiment.” *Energy and Buildings* 80. Elsevier: 37–44. doi: 10.1016/j.enbuild.2014.04.033.

Vereecken, Evy, and Staf Roels. 2015. “Capillary Active Interior Insulation: Do the Advantages Really Offset Potential Disadvantages?” *Materials and Structures* 48 (9): 3009–3021. doi: 10.1617/s11527-014-0373-9

Vereecken, Evy, and Staf Roels. 2016. “Capillary Active Interior Insulation Systems for Wall Retrofitting: A More Nuanced Story.” *International Journal of Architectural Heritage*. doi:10.1080/15583058.2015.1009575.

Vereecken, Evy, and Staf Roels. 2017. “ Interior insulation of walls in historical buildings: systems, risks and considerations (original in dutch: Binnenisolatie van muren in historische gebouwen: systemen, risico’s en aandachtspunten)” In *Energetische ingrepen in monumentn: een duurzaam verhaal?! Proceedings*, Antwerpen, Belgium, 17 November.

Vereecken, Evy, Liesje Van Gelder, Hans Janssen, and Staf Roels. 2015. “Interior Insulation for Wall Retrofitting–A Probabilistic Analysis of Energy Savings and Hygrothermal Risks.” *Energy and Buildings* 89: 231–244. doi: 10.1016/j.enbuild.2014.12.031.

Walker, Rosanne, and Sara Pavía. 2015. “Thermal Performance of a Selection of Insulation Materials Suitable for Historic Buildings.” *Building and Environment* 94 (P1): 155–165. doi:10.1016/j.buildenv.2015.07.033.

Webb, Amanda L. 2017. “Energy Retrofits in Historic and Traditional Buildings: A Review of Problems and Methods.” *Renewable and Sustainable Energy Reviews*. doi:10.1016/j.rser.2017.01.145.

Zelinka, Samuel L, Samuel V Glass, Charles R Boardman, and Dominique Derome. 2016. “Moisture Storage and Transport Properties of Preservative Treated and Untreated Southern Pine Wood.” *Wood Material Science & Engineering* 11 (4): 228–238. doi: 10.1080/17480272.2014.973443.

Zhao, Jianhua, John Grunewald, Ulrich Ruisinger, and Shuo Feng. 2017a. “Evaluation of Capillary-Active Mineral Insulation Systems for Interior Retrofit Solution.” *Building and Environment*. doi:10.1016/j.buildenv.2017.01.004.

Zhao, Jianhua, John Grunewald, Ulrich Ruisinger, and Shuo Feng. 2017b. “Evaluation of Capillary-Active Mineral Insulation Systems for Interior Retrofit Solution.” *Building and Environment* 115. Elsevier Ltd: 215–227. doi:10.1016/j.buildenv.2017.01.004.

3

EXPERIMENTAL MONITORING OF 3 CASE STUDIES

3.1. INTRODUCTION

When dealing with valuable, historic constructions, it is important to evaluate the risks and benefits of different retrofit strategies via numerical simulations, before proceeding with real interventions.

To have reliable hygrothermal simulations, the models should rely on realistic climatic boundary conditions and be validated against the hygrothermal data measured on-site. Thus, the main goal of the experimental monitoring presented in this chapter is to obtain the datasets necessary as boundary conditions for mono-dimensional simulations and for their qualitative validation, as well as for the calibration and validation of whole-building simulations.

In this chapter, the three case studies chosen for the investigation are presented, some historic background is provided, and the main characteristics of the envelopes and buildings usage are defined. The building selected are representative of different types of historic constructions, namely a convent, a residential building, and a church. All buildings are characterized by thick masonry walls made of different materials. Those are granite, limestone and solid bricks, thus being representative of typical historic walls in Portugal and Italy, while providing for some interesting differences in terms of hygrothermal properties. The three case studies are currently adopted as public buildings and equipped with heating and cooling systems. They are located in Porto, Lisbon and Bologna. Thus, they offer a suitable chance for analysing the cluster chosen for this research, namely "thick masonry walls of historic buildings with temporary occupation, located in areas with temperate climates with warm or hot summers and mild winters, where heating systems are adopted". As public libraries, they are spaces where indoor thermal comfort is extremely important to correctly meet the needs of individuals and groups for education, information and personal development. Similarly, they are types of spaces where high intermittent use of conditioning systems can be expected, due to their monumental dimensions and temporary occupancy. Thus, these buildings offer a good chance for studying both thermal comfort and energy demands.

After presenting the case studies, the experimental monitoring campaign is introduced, and the equipment and methods adopted are defined. Indoor air temperature, relative humidity, and superficial temperatures are the parameters investigated. Additional tests are performed using infrared thermography, to characterize the vertical thermal stratification in one of the case studies. Then, the results of the experimental campaign are presented, and the outdoor climate data obtained from local

meteorological stations are introduced. Experimental results are analysed and discussed in comparison with outdoor climatic conditions. Indoor comfort is then evaluated.

Part of the results of this chapter was presented in:

- Posani, Magda, Rosário Veiga, Vasco Peixoto de Freitas, Henk Schellen, Karin Kompatscher. 2020. "Dynamic hygrothermal models for historic buildings with indoor HVAC systems: Complexity shown through a case study ", in *12th Nordic Symposium on Building Physics*, Tallinn, Estonia. Doi: 10.1051/e3sconf/202017215007

- Posani, Magda, Rosário Veiga, and Vasco Peixoto de Freitas. 2020. "Thermal retrofit for histroic massive walls in temperate climates: risks and opportunities ", in *ENCORE 2020 – 4º Encontro de Conservação e Reabilitação de Edifícios*, Lisboa, Portugal, 2020. Doi: 10.34638/yzys-hn57

3.2. CASE STUDIES

In order to evaluate the effect of adopting thermal insulation in historic buildings, three case studies were chosen:

• the Municipal Library of Porto, originally Convent of "Santo António da Cidade", in Porto, Portugal (41.15, -8.60);

• the Coruchéus' library, originally Coruchéus' Palace, in Lisbon, Portugal (38.75, -9.14);

• the Library of San Giorgio in Poggiale, in Bologna, Italy (44.49, 11.34), originally built as a church.

The three buildings are characterized by massive masonry walls and they are all conditioned with heating and cooling systems, although cooling devices are not provided in all rooms. The three buildings experienced refurbishments and changes of use through the centuries, ending up being adopted as libraries. Thus, they have public use and intermittent occupancy. Furthermore, they are spaces where it is very important to guarantee proper indoor comfort conditions for the users.

Some historical background, characteristics of the constructions envelopes and information on the usage of the buildings are provided in the following sections.

3.2.1. THE MUNICIPAL LIBRARY OF PORTO (PT)

The Municipal Library of Porto is hosted in an XVIII-century building, as shown in Figure 3.1.

It is one of the first libraries established in Portugal and it hosts a large collection of ancient books, coming from private and religious-orders collections, with documents dating back to the XIII century (JPN, 2008). Among its documental heritage, some very precious exemplars can be found, such as the journal of the first voyage of Vasco da Gama to India, which is part of UNESCO's *international memory of the world register* (UNESCO, 2012).

Figure 3.1 – Aerial view of the municipal library of Porto, from south-East, adapted from Google Earth.

The Municipal Library of Porto was originally constructed as a Convent, "*Convento de Santo António da Cidade*". It was founded in 1783 (Rebelo da Costa, 1788), and it was the last convent built in the city of Porto (Filipe and Sereno, 2012).

Most of the building structure dates back to the original construction, whereas the northern part was modified through the centuries, as observable in Figure 3.2, where three plants from different periods of the XVIII-XIX centuries are displayed. The building was used as a military hospital during the "Peninsular war" (1807-1814), occupied by militants during the Portuguese civil war (1828-1834) and it was left in a state of abandonment and neglection from 1832 (Oliveira, 2015). Since 1942, it has hosted the Municipal library of Porto, together with the School of fine arts and the Municipal Museum (Direção Geral do Património Cultural DGPC,2020).

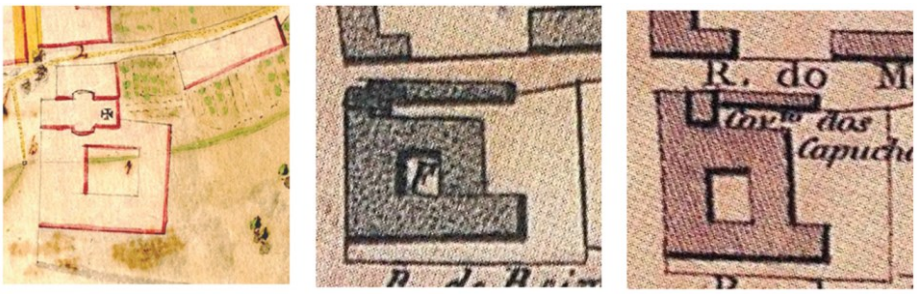

Figure 3.2 – Plants of "*Convento de Santo António da Cidade*". From left to right: plans extracted from historic plants of the city from 1795, 1813, 1833, respectively. Picture adapted from Oliveira (2015)

Between the end of XIX cent. and the beginning of XX cent. the church located in the northern area of the convent was demolished and a new northern wing was constructed (Oliveira, 2015). Then, the building was modified and refurbished several times during the XX century.

The building envelope is composed of massive granite masonry walls, plastered and painted at the indoor and outdoor-facing sides, as shown in Figures 3.3a and 3.3b. Details, pillars and frameworks are made of granite stonework left on sight. Doors are made of wood, while glass doors and windows are composed of wood frames and single glazing (Filipe and Sereno, 2012). Some examples of the glass doors characterizing the building are reported in Figures 3.3b, 3.3c. Insulation was not part of the original design, nor was added to any of the main building components in the refurbishment works.

The building hosts a library and spaces related to this function, such as archives (Figure 3.3d) and exposition rooms. The plans of the building and the usages of its main spaces are reported in Figure 3.4.

Figure 3.3 –Municipal Library of Porto. From left to right: (a) walls overlooking the central cloister, (b, c) reading rooms, (d) deposit in the attic (from Oliveira, 2015).

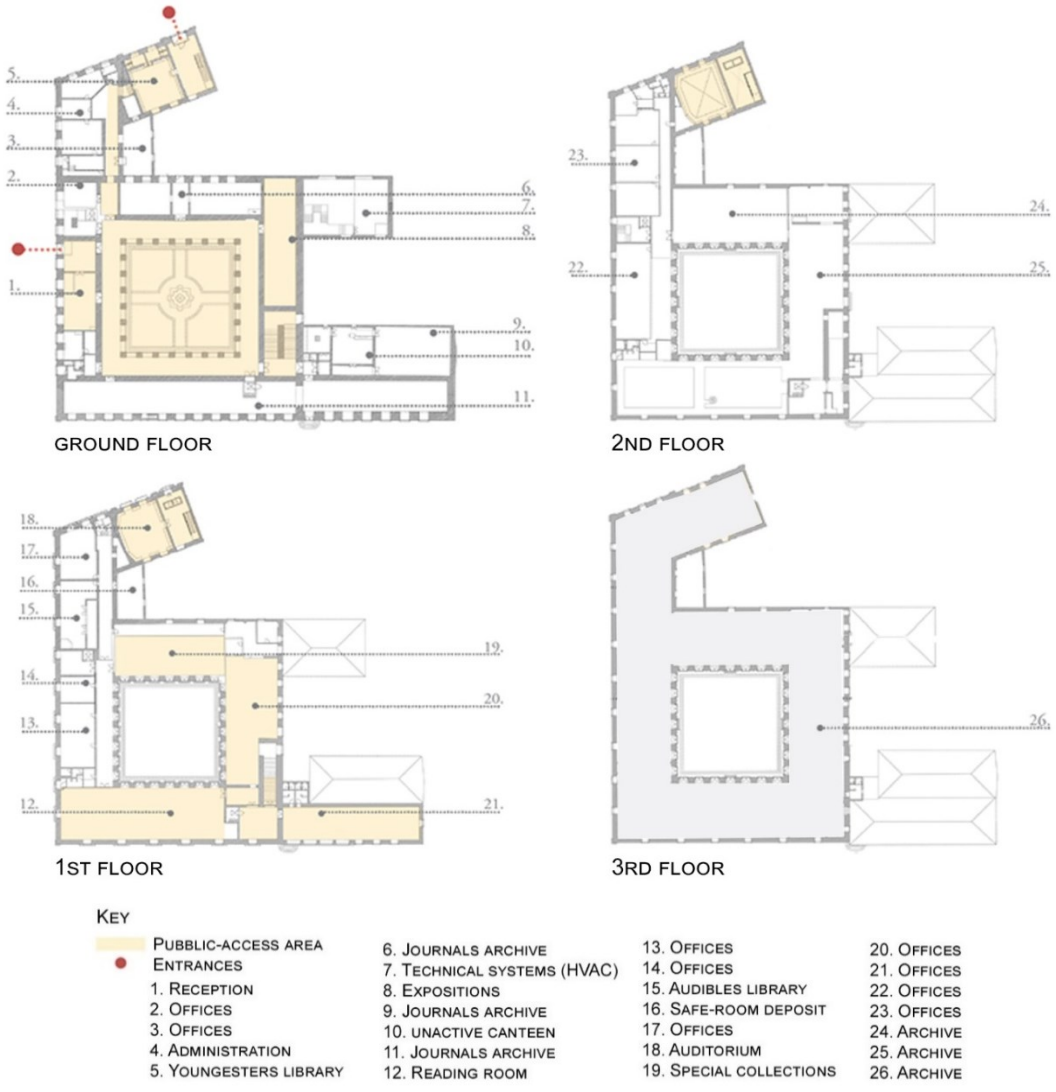

Figure 3.4 – Plans of the Municipal Library of Porto with the usage of the main rooms, adapted from Oliveira (2015).

Archives are conditioned with heating and cooling systems, and most of them are equipped with humidifiers, aiming to provide for a minimum of 50% relative humidity during the heating season. Offices, library rooms and reading rooms are equipped with heating and, in some cases, cooling systems. Most systems were designed and installed in the XX century, and they rely on manual control for the definition of set-point temperatures and working schedules, while the air conditioning is more recent.

The library is open 10 AM - 6 PM on Mondays and Fridays, and 9 AM - 7:30 PM from Tuesday to Friday. During summer, namely 15th July-15th September, the library is open Monday to Friday, 10 AM-6 PM.

3.2.2. CORUCHÉUS' LIBRARY, LISBON (PT)

The Coruchéus' library is located in Lisbon. It was originally built as a residential building, the Coruchéus' Palace (*Palácio dos Coruchéus* in Portuguese), and it was turned into a library in 2013. The building is shown in its current form in Figure 3.5.

Figure 3.5 – Aerial view of the Coruchéus' library, from south-East, adapted from Google Earth.

According to Galante (1999), the building dates back to the beginning of the XIX cent. – end of the XVIII cent.

The palace passed through different owners during the decades, and it ended up being expropriated by the Municipality of Lisbon in 1945. At the time, the building was in such bad conditions that it was considered as an unsafe housing, thus it was adopted as a depot. Then, in the 1960s, the City Council of Lisbon decided to turn it into a multifunctional cultural space, which opened in 1971. Figures 3.6a, 3.6b and 3.7 show the state of the construction before, during and after the refurbishing performed to prepare the building for its re-opening of 1971. The building ended up hosting the Department of Cultural Heritage of the Municipality from 1989 to 2011 (Galante, 1999). Then, in April 2013, the Coruchéus' Library was inaugurated (Público, 2014).

a.  b. 

Figure 3.6 – From left to right:(a) a picture of the Coruchéus' Palace in 1965 (Arquivio Municipal de Lisboa), before being refurbished, and (b) during the refurbishing (Arquivio Municipal de Lisboa).

Figure 3.7 – A picture of the Coruchéus' Palace in 1972, after the re-opening as a multifunctional cultural space (Arquivo Municipal de Lisboa).

The building envelope is made of thick masonry walls, as typical of Lisbon, where traditional constructions are largely characterized by massive envelopes in limestone masonry (Pina dos Santos and Rodrigues, 2009). The walls are plastered and painted both at the indoor and outdoor facing sides, as shown in Figures 3.8a and 3.8b. The outdoor-facing side of the walls is enriched with details in stonework, such as in the corner's detail shown in Figure 3.8c. Doors are made of wood, while glass doors and windows are made of wooden frames and single glazing, as shown in Figures 3.8b and 3.8d.

Figure 3.8 – Views of the Coruchéus' library. From left to right, top to bottom: (a) view on the exterior of the building, (b) view on the interior, (c) stonework detail, and (d) some of the openings.

Most spaces are adopted as reading rooms, one is adopted as a computers room and two are of exclusive use of the library staff (Figure 3.9). Most rooms are equipped with fan coils that are used for heating and cooling. The systems are managed by the library staff from a centralized control device. The use of the systems is generally intermittent, meaning that the staff turns on the systems when needed, during the opening hours, while they rarely let it work when the library is closed. The set-point usually adopted is 18-20°C in winter and 23°C in summer.

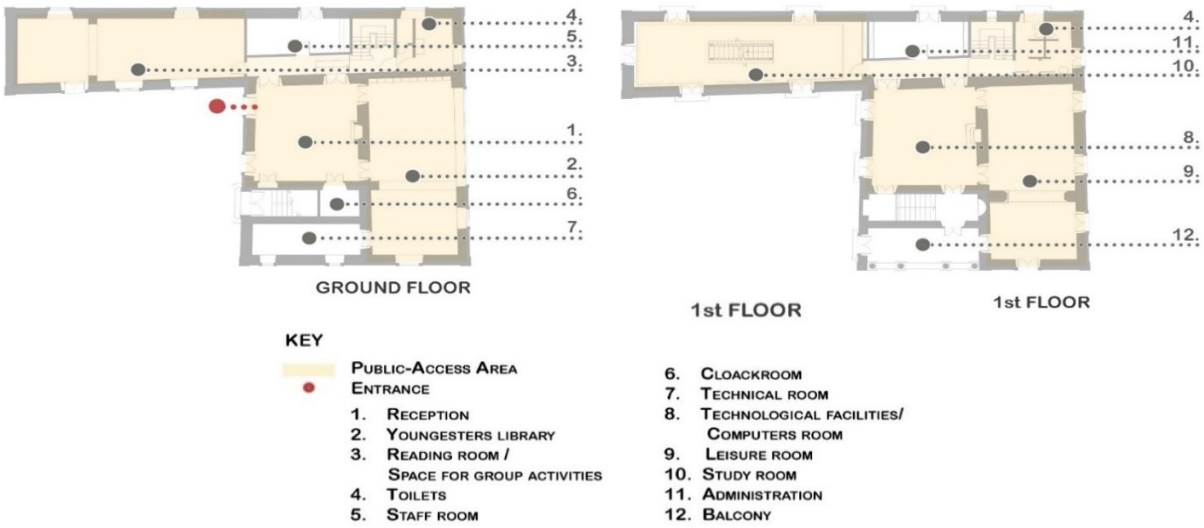

Figure 3.9 – Plans of the Coruchéus' library with the usage of the main rooms.

The library is open 10 AM - 6 PM from Tuesday to Friday. During summer, namely 15th July-15th September, the library is open also on Mondays, 10 AM - 6 PM.

3.2.3. LIBRARY OF SAN GIORGIO IN POGGIALE, BOLOGNA (IT)

The ex-church of San Giorgio in Poggiale is nowadays serving as the Art and History Library of Bologna, a city located in northern Italy. The construction dates back to the XVI Century and it is shown in Figure 3.10.

Figure 3.10 – Aerial view of the Library of San Giorgio in Poggiale, from North-East, adapted from Google Earth.

The building was constructed in the XVI century as a Baroque-style church, a fact that is still readable in its current façade, displayed in Figure 3.11a.

The construction was severely damaged by a bomb explosion in 1943: the vaulted ceiling was destroyed, and windows, floor and roof were damaged. The decorative features were almost completely lost. After this occurrence, the building was left in a state of neglect for several years, as shown in Figure 3.11b.

A first rehabilitation was then performed in the 1970s: a new floor and ceiling were constructed, new windows were added, and the remaining structures were restored. The construction was then used for public functions until 2005. It was further renovated in 2007-2009, to prepare the building for its re-opening as a library. The interior of the building, in its current form, is sown in Figure 3.11c.

a.  b. 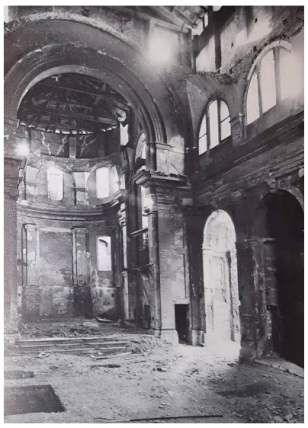 c. 

Figure 3.11 – Library of San Giorgio in Poggiale. From left to right: (a) the façade in its current state, (b) an indoor view of the building left in a state of neglection after the damages suffered in the 1940s (from Bergonzoni and Branchesi, 1979) and (c) an indoor view of the building nowadays.

The building envelope is made of massive masonry walls in solid bricks, as typical of the area of Bologna. The façade is in exposed bricks, as Figure 3.12a displays, whereas the other walls are rendered. At the indoor-facing side, all walls and ceilings are plastered, as shown in Figures 3.12b and 3.12c.

a.  b. 

c. 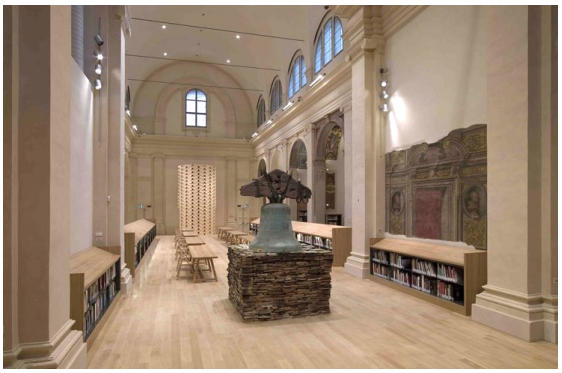 d. 

Figure 3.12 – Library of San Giorgio in Poggiale. From left to right, top to bottom: (a) a detail of the façade, (b, c) views on the interior, (d) a detail of the roof structure, picture taken during the last renovation works (2007-2009).

The floor structure dates back to the works performed in the 70s and it is reported by the technicians of the library to be made of mixed hollow bricks and concrete slab structure finished with a flooring made of oak wood. The roof is made of a simple wooden structure, covered with wooden battens and finished with ceramic tiles, as readable in Figure 3.12d. The ceiling was re-constructed in the same period, following the traditional technique of the "reed-false vault" (Bergonzoni and Branchesi, 1979). This type of structure consists of a vaulted wooden frame covered with a mat of reed and finished with gypsum plaster. The building has wooden doors and windows made of single glasses and timber frames. Insulation was not part of the original design, nor was added to any of the main building components in the refurbishment works.

The building is vertically divided into three parts: an underground space that is currently adopted as a deposit for books and pieces of art, the main space that hosts the library and an unheated attic, as shown in the section in Figure 3.13.

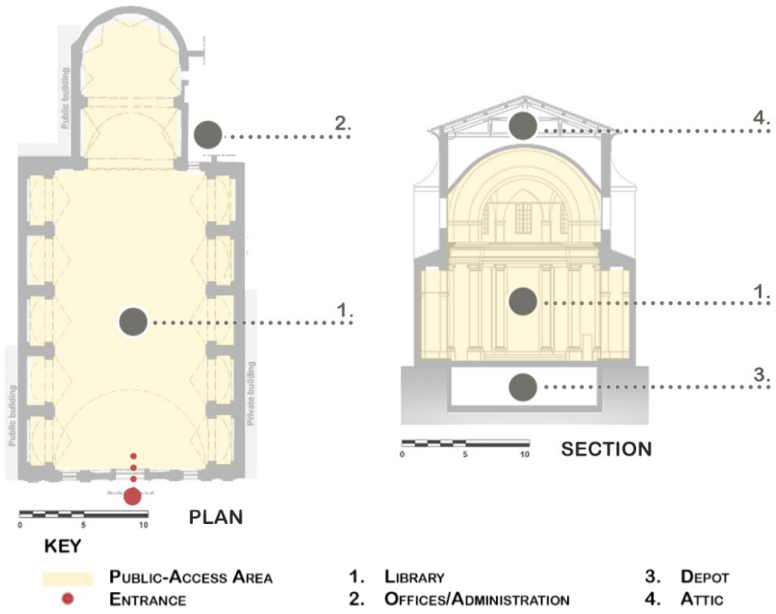

Figure 3.13 – Plans of the Library of San Giorgio in Poggiale with the usage of the main spaces.

The construction is organized around a single nave hall, with five self-contained chapels at each side, and, at the end of the nave, a triumphal arch marks the transition to the presbyterium area, which ends in a semi-circular apse. To guarantee indoor comfort for the users, the main volume of the church is served by two different heating and cooling systems, a ventilation system and a humidifier.

The library is open 9 AM - 1 PM from Monday to Friday, and also on Tuesday afternoon until 5 PM.

3.3. EXPERIMENTAL MONITORING – METHODS

In this section, the equipment and methods adopted in the experimental monitoring campaign are presented. Indoor air temperature, relative humidity, and superficial temperatures are the parameters investigated. Additional tests are performed using infrared thermography, to characterize the vertical thermal stratification in one of the case studies.

3.3.1. INDOOR AIR TEMPERATURE AND RELATIVE HUMIDITY

Indoor air Temperature (T) and Relative Humidity (RH) were measured for at least one year in each case study, during regular usage of the buildings. In the case studies located in Lisbon and Bologna, a period of prolonged free fluctuation was observed in winter and summer, respectively, during holiday-closure periods. Since the case study of Porto did not close for prolonged holiday periods, an additional 2-week-long-monitoring was performed during the forced closure determined by the COVID-19 emergency in 2020. Thus, periods of regular operations and complete closure were observed in each case study.

The indoor microclimate monitoring was performed using 2 types of data-loggers produced by HOBO®: HOBO UX100-003(accuracy: ±0.21°C, and ±3.5% in the range 25- 85% RH, 5% out of this range) and HOBO U12-013(accuracy: ±0.35°C, and ±2.5% in the range 10- 90% RH, 5% out of this range). The two sensors are shown in Figure 3.14. The data were recorded with a sampling interval of 10-minutes and the final results were obtained from the hourly average values.

Figure 3.14 – Dataloggers: HOBO UX100-003 and HOBO U12-013.

Before starting the measurements, the equipment performance was checked using the climatic chamber of the Laboratory of Building Physics (LFC) of the Faculty of Engineering of the University of Porto (FEUP), as reported in ANNEX I.

The sensors were installed in the case studies at specific locations, aiming at protecting them from interaction with users and from the influence of drafts, lights and HVAC systems.

In the Municipal Library of Porto, the sensors were located at about 1.5m heigh, inside shelves that were not accessible to the library users: some of them were inside locked metal cages (used to protect historic books) and others were put in the archives, which are not accessible to the public. The spatial distribution of HOBO dataloggers is presented in Figure 3.15.

In the Coruchéus' Library, the sensors were located at the top of bookshelves, at about 2m height, to avoid interactions with the library users. The distribution in the building is shown in Figure 3.16.

In the Library of San Giorgio in Poggiale, 3 sensors were located on the top of bookshelves, at about 2.5m height, and one was located near the floor, in the apse, at about 0.5 m height. The underground space was not accessible because of the precious artefacts, and the attic was inaccessible as well, thus no measurements were performed in these two spaces. The positions of the sensors are shown in Figure 3.17.

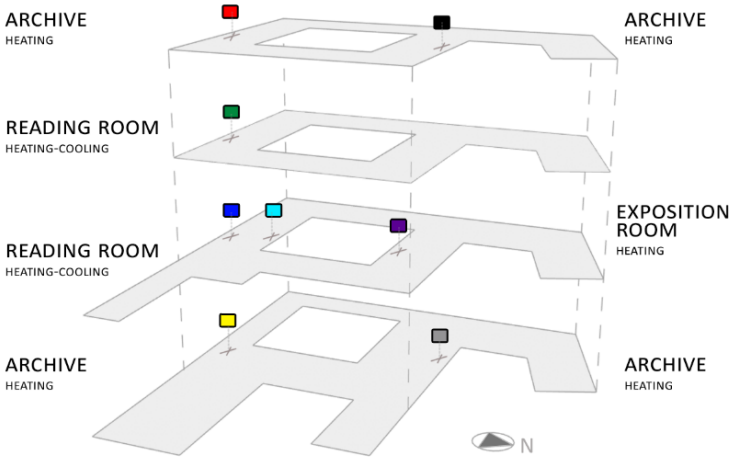

Figure 3.15 – Municipal Library of Porto: Positions of HOBO data-loggers.

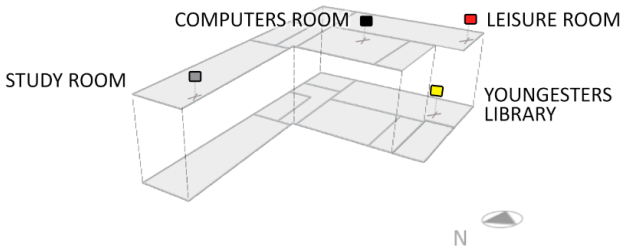

Figure 3.16 – Coruchéus' Library: Positions of HOBO data-loggers.

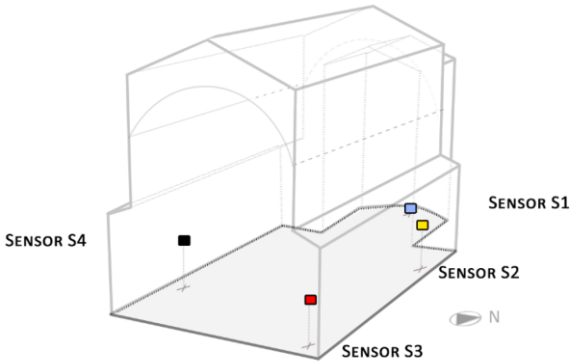

Figure 3.17– Library of San Giorgio in Poggiale: Positions of HOBO dataloggers.

3.3.2. INFRARED THERMOGRAPHY

Infrared thermography represents a non-destructive tool that can be applied for inspections in-situ (Nikzad, Kari, and Tahmasebi, 2011).

In this work, it was adopted to confirm the presence of a vertical temperature stratification in the indoor air of the main space of the library of San Giorgio in Poggiale, where it was expected because of the monumental vertical extension of the room and the presence of different HVAC systems located at different heights. The measurements were performed by adopting a vertical paper strip, hanging on helium balloons, as shown in Figure 3.18. The method consists in taking an infrared picture of the strip in thermal equilibrium with environmental air. Thus, the distribution of temperature observed along the strip is considered representative of the one of indoor air, as shown by Camuffo, Bertolin and Fassina (2009) when evaluating the thermal layering in a heated church.

On 6th November, 2019, when the heating system was working, the survey was conducted using a thermal camera (FLIR, ThermaCAM B360). The camera measures transmitted infrared radiation in wavelength between 7.5-13 μm, converts the measured radiation into surface temperatures and displays them through a colour gradient in a picture.

Figure 3.18 – Paper strip adopted for the measurements of the vertical distribution of air temperature in a lateral chapel (left) and in the main room (right) of the Library of San Giorgio in Poggiale.

3.3.3. SUPERFICIAL TEMPERATURES OF WALLS, AND AIR TEMPERATURE NEAR THE SURFACES

Superficial temperatures appear useful to evaluate the reliability of the models adopted for mono-dimensional simulations.

For this sake, the internal and external superficial temperatures of one wall were measured for at least three weeks, in each case study. The air temperature in the close proximity of the interior wall surface and the exterior temperature near the building envelope were measured too, to help discuss the representativeness of the boundary conditions adopted for the simulations in Chapter 5.

The equipment adopted is produced by Eltek and it is composed of sensors for the measurement of air temperature (accuracy of ±0.4°C) and superficial temperatures (accuracy of ±0.3°C). An Eltek RX250AL data logger was used to collect and store data with a sampling interval of 10 minutes. The results were defined using the hourly averages obtained from the data collected.

Figure 3.19a shows one device equipped with the two sensors, while Figure 3.19b and 3.19c show an example of the installation at the interior and exterior side of the walls, respectively. The sensor for the measurement of air temperature was located in the proximity of the wall surface, while the surface sensors were applied on the wall surface by means of adhesive tape. Between the surface sensor and the wall, a thermal paste (high thermal conductivity) was applied to guarantee continuous contact between the sensor and the support.

a. 

b. 
c. 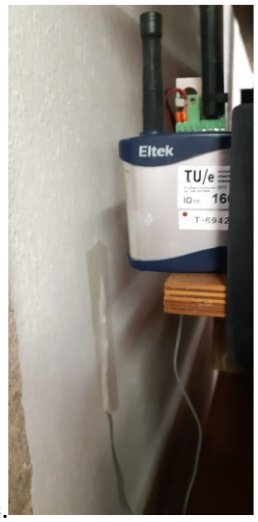

Figure 3.19– Eltek equipment: (a) a sensor for air and superficial temperature and an example of the installation of the sensors for measuring (b)exterior and (c) interior superficial temperature of a wall.

At the end of the monitoring campaign, Eltek sensors were kept for more than 24hours in a closed container with the HOBO data-loggers, which were previously checked in the climate chamber of FEUP. The data thus obtained with HOBO and Eltek equipment were compared to evaluate the performance of the latter. This qualitative assessment of the calibration of the equipment is based on the suggestions

provided by Eibl and Kilian (2011) in the European project “Climate for Culture”. Results are provided in ANNEX I.

The location of the sensors for superficial temperatures is shown in Figure 3.20.

Eltek equipment was provided by TU/e (Eindhoven University of Technology) in the context of an exchange period organized during the PhD research. For this reason, the measurements performed with ELTEK equipment regard a period that is much more reduced than the one considered for the measurements with HOBO equipment.

External and internal air temperatures were measured close to the walls whose superficial temperature was monitored. The only exception is the external air temperature measured for the case study in Lisbon, where, for practical reasons, the sensor was located next to a north-oriented wall while the superficial temperature was measured for a S-W oriented one.

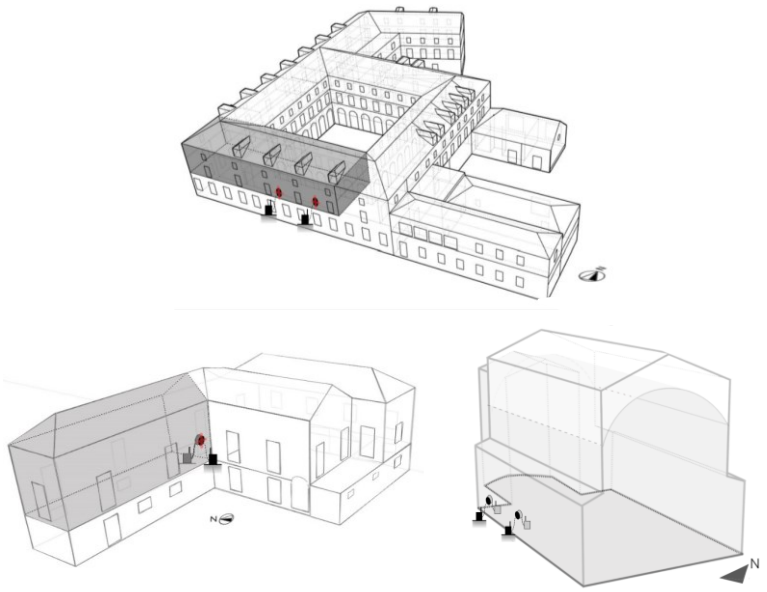

Figure 3.20 – From top to bottom, left to right: the location of the equipment adopted in the case studies of Porto, Lisbon and Bologna. In grey are highlighted the rooms where the air temperature nearby the envelope was measured.

3.4. EXPERIMENTAL MONITORING – RESULTS AND DISCUSSION

In this section of the study, the results obtained in the experimental monitoring are presented and commented.

3.4.1. INDOOR AIR T AND RH

3.4.1.1. MUNICIPAL LIBRARY OF PORTO

Figure 3.21 presents the results obtained in the indoor monitoring of the Municipal Library of Porto in the period March 2019 - February 2020, and in about 2 weeks of monitoring during a forced closure (31 March – 15 April 2020). For each parameter two graphics are provided: the first one shows the results obtained in archives and the second presents the data obtained in spaces open to the public.

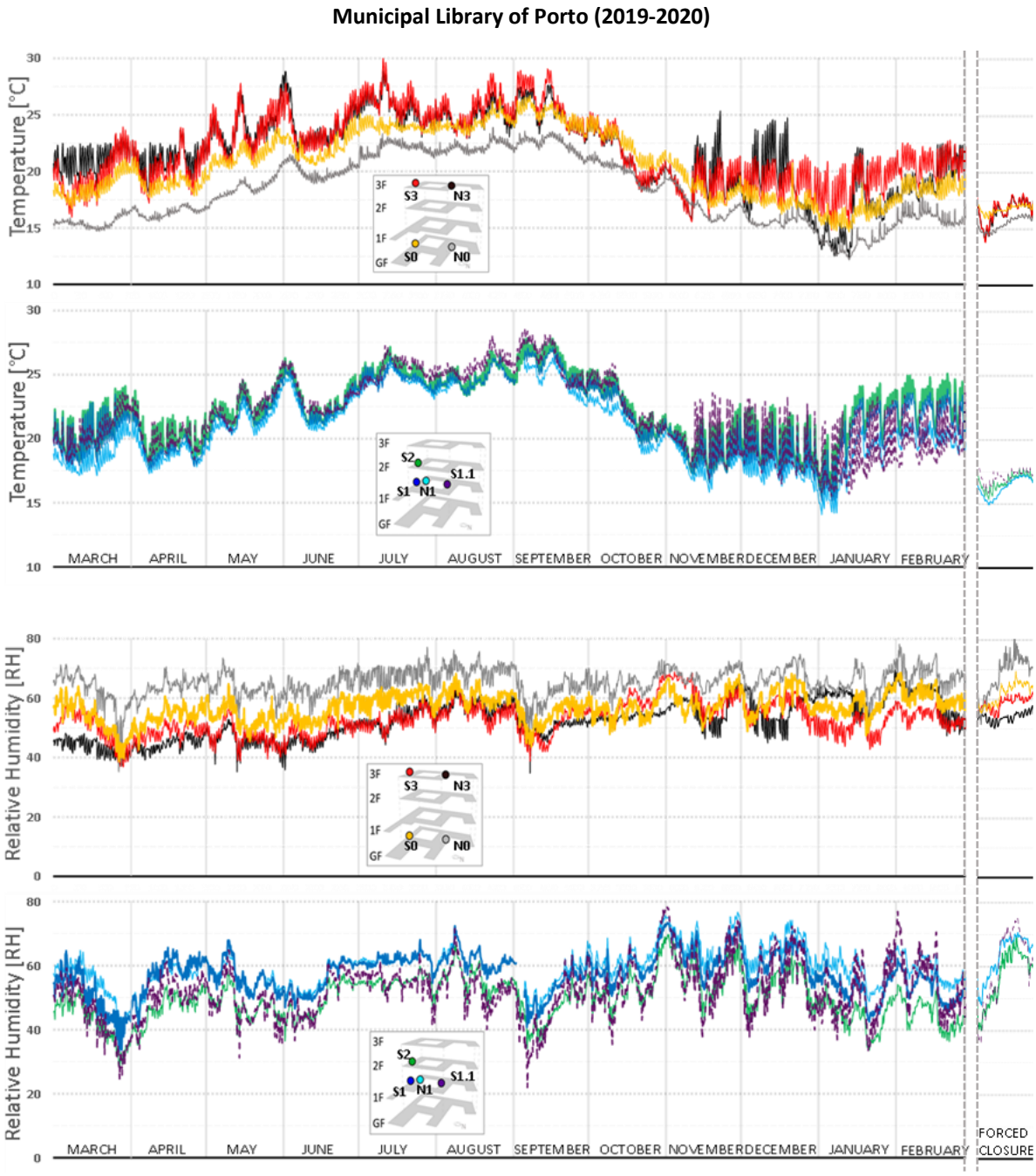

Figure 3.21 – Municipal Library of Porto: T-RH for one year (March 2019-February 2020) and during a period of forced closure (31 March – 15 April 2020). For each parameter two graphics are provided, the top one represents the results in the archives, the lower one gives the results in the spaces open to the public.

In the first graphic, the temperature in the archives is shown. It appears that the sensor located at the ground floor, near a North-oriented wall (sensor N0, grey in Figure 3.21), has lower temperatures than the others for a large part of the year. This outcome may be the result of the north-facing exposure and the location on the ground floor. The other sensor located on the ground floor, but near a South oriented wall (sensor S0), is represented in yellow in Figure 3.21. Temperatures collected by S0 show a similar trend to the ones measured by sensor N0, but a few degrees higher throughout the whole year. This similarity can be observed in detail in the weekly results reported in Figure 3.22. In winter and middle seasons, the difference between the two temperatures may be further increased by the different use of heating. The peaks of temperatures of S0 observable from September on suggest that the use of heating systems starts in the archive of S0 much earlier than in the room of N0, where similar peaks cannot be detected until December. Furthermore, the days of heating in the two spaces are also likely to be different. For example, the results reported for one week during the heating season in Figure 3.22 show that the room of S0 is heated on Saturday while the one of N0 is not.

Archives located in the attic, show stronger fluctuations of air temperature, which is coherent with their stronger exposition to the influence of outdoor climate, indeed the archives are located on the last floor (exposed walls and roof). These peaks can be observed more in detail in the results provided for one week during the cooling season and in free fluctuation in Figure 3.22 (results shown in red and black).

The results obtained for relative humidity appear to be directly dependent on indoor air temperature, showing lower relative humidity for spaces with higher temperatures. Results obtained for spaces open to the public show similar behaviour of temperatures, with lower results for the sensor located near a north-oriented wall (N1, light-blue in the Figures), during summer and middle seasons. Looking at the results of relative humidity, they appear to be quite in agreement with the temperature trends, giving lower relative humidity when the temperature rises and the other way round. It is interesting to notice that spaces open to the public do show a higher variability of relative humidity than archives, with the latter rarely going under 40% RH. This result may be the effect of several causes like the different use of heating in the spaces, the use of humification devices in the archives and the moisture buffering ability of books (Kompatscher et al., 2019), which can help to reduce RH fluctuations.

Looking at the winter weekly graphic in Figure 3.22, it is interesting to notice that all spaces open to the public are heated throughout the whole week except for Sunday. Furthermore, it is worth observing that while the temperature results shown in light blue (sensor N1) are about 1°C higher than violet ones (sensor S1.1) on Friday, Saturday and Sunday, the corresponding relative humidity of N1 is lower than S1.1 only on Sunday, when the rooms have no occupancy. This outcome suggests that on Friday and Sunday the reading room where N1 is located had higher occupancy than the exposition room where sensor S1.1 is located, which is consistent with the general occupancy patterns observed in situ.

The peaks observed in the annual graphics of temperatures suggest that the heating systems are turned on in March and April, as well as from November to February. Thus, the heating season seems to be in November-April while the specific periods of use of heating appear to depend on the room considered. This outcome is coherent with the fact that the heating devices adopted in the library rely on manual control operated by the library staff according to the perceived needs, room by room.

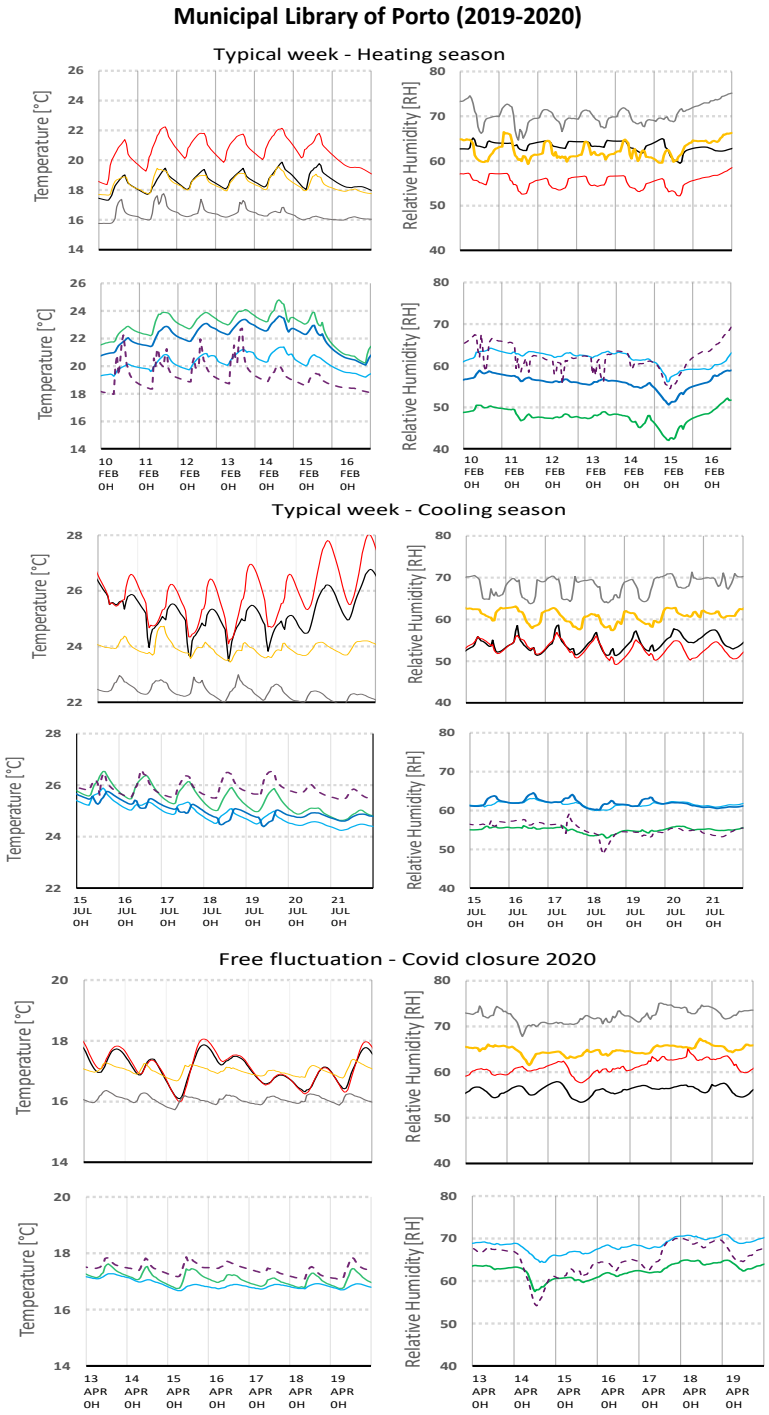

Figure 3.22 – Municipal library of Porto: T-RH during one week in the heating season, cooling season and during closure. For each parameter two graphics are provided, the top one represents the results in the archives, the lower one gives the results in the spaces open to the public.

3.4.1.2. CORUCHÉUS' LIBRARY

The results obtained in terms of indoor air temperature and relative humidity in the Coruchéus' Library, from March 2019 to February 2020, are shown in Figure 3.23.

From May to September, the temperatures detected in the 4 spaces show very similar behaviours, with the results in black (sensor NW1) being generally higher than the others. This outcome is likely to be the result of the sensor position itself: close to an internal wall, whereas all the others are nearby outdoor facing ones. The temperature fluctuations observable from the end of October suggest an intermittent use of heating. It is also interesting to notice that at the beginning of January and February there are periods where all spaces seem to be heated except for the room whose results are presented in grey (Sensor SW1).

The data of relative humidity show high variability, ranging about 20% to 90%, which can be related to the intermittent use of heating, together with occupancy and ventilation patterns, and air infiltration.

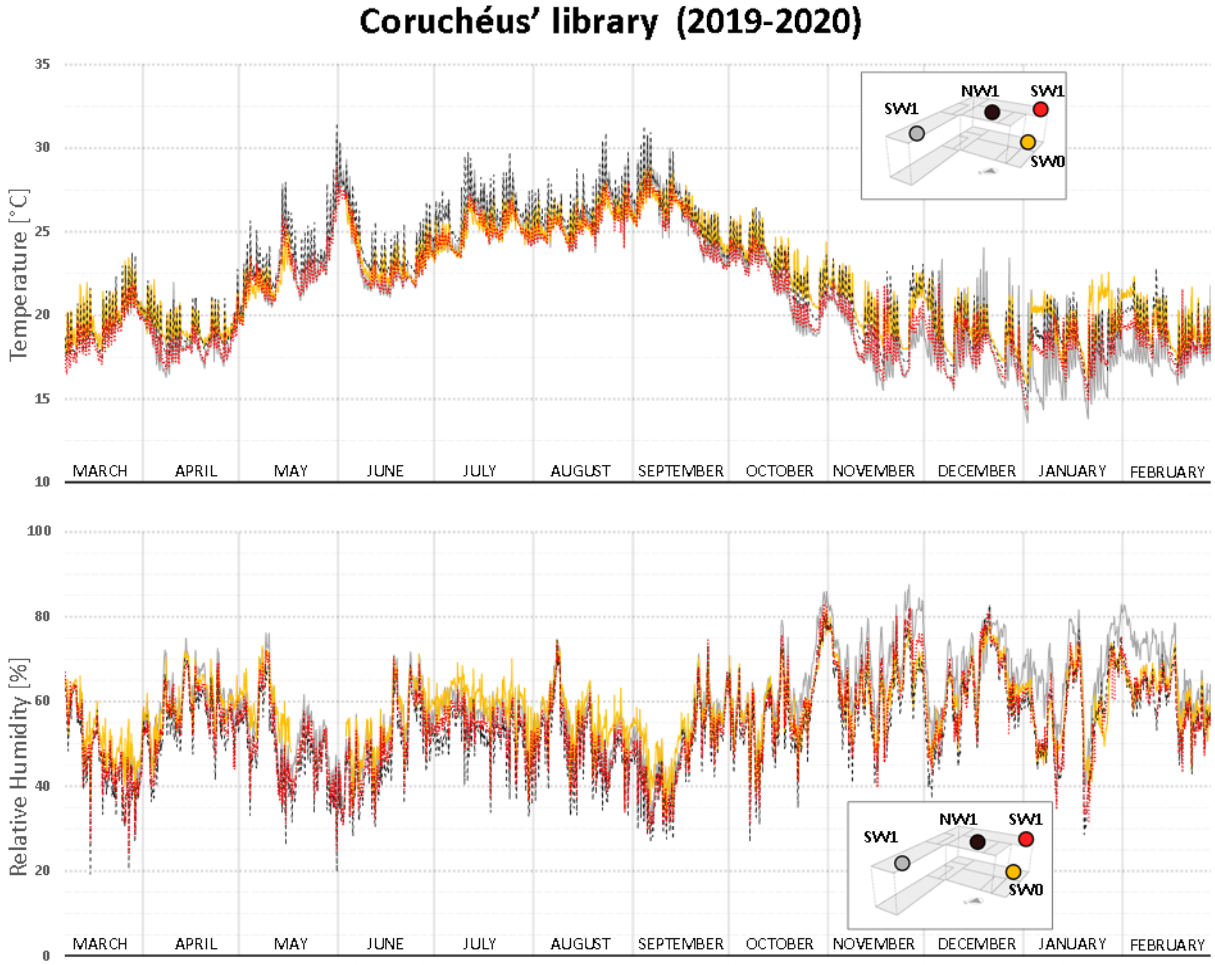

Figure 3.23 – Coruchéus' Library: T-RH along one year (March, 2019-February, 2020).

Weekly results shown in Figure 3.24, indicate that heating systems are used in all rooms during weekdays and not in the weekend. Considering the results in free fluctuation, it seems that temperatures shown in grey decrease at a much faster rate than all the others. This result is probably related to the fact

that sensor SW1 is located in the only room that does not have an attic above the ceiling, thus the room is directly covered with the roof structure, determining more heat losses for this space than the others.

In Figure 3.24, RH fluctuations seem to depend directly on temperature variation. An exception can be observed in the weekly results during the heating season, where the temperatures decrease at a fairly constant rate during the weekend while relative humidity registers a peak. This result is probably the effect of the air infiltration rate and a variation in outdoor humidity, which was high on Saturday Afternoon (10th November 2019) due to rain.

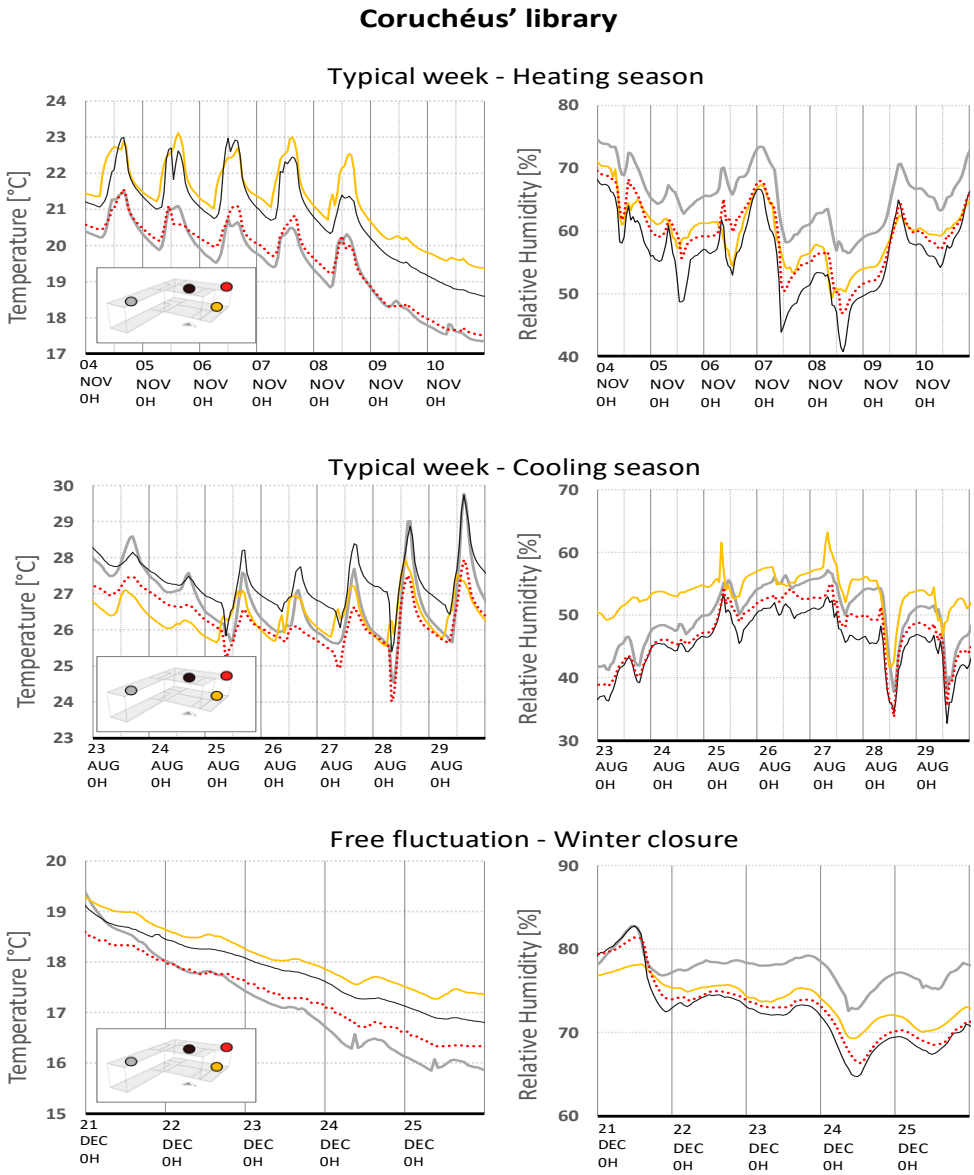

Figure 3.24 – Coruchéus' Library: T-RH during one week in the heating season, cooling season and during closure.

3.4.1.3. LIBRARY OF SAN GIORGIO IN POGGIALE

The results obtained in the Library of San Giorgio in Poggiale, for the year 2019, are presented in Figure 3.25. Temperature fluctuation during the heating season reflects the specific use of heating systems adopted: from January to May, heating devices were kept working continuously with a higher set point during daytime and a lower one at night and weekends. Furthermore, the setpoints adopted were dynamically changing based on outdoor temperatures, according to an algorithm defined by the technicians of the library.

Between the end of April and the beginning of May, the fall of temperatures corresponds to the shout-down of one of the two heating systems (due to technical problems), which was then repristinated from 10th May to the end of the month. In November and December, the picks of temperatures show a different strategy of heating, based on intermittent use of it (adopted only during opening hours).

From middle June to 8th of August, temperature results indicate an intermittent use of cooling systems. The two following weeks are in free fluctuation (summer closure of the library).

Relative humidity appears to be low from January to April, when the continuous heating strategy is adopted. During the intermittent heating period, November-December, it appears to be higher.

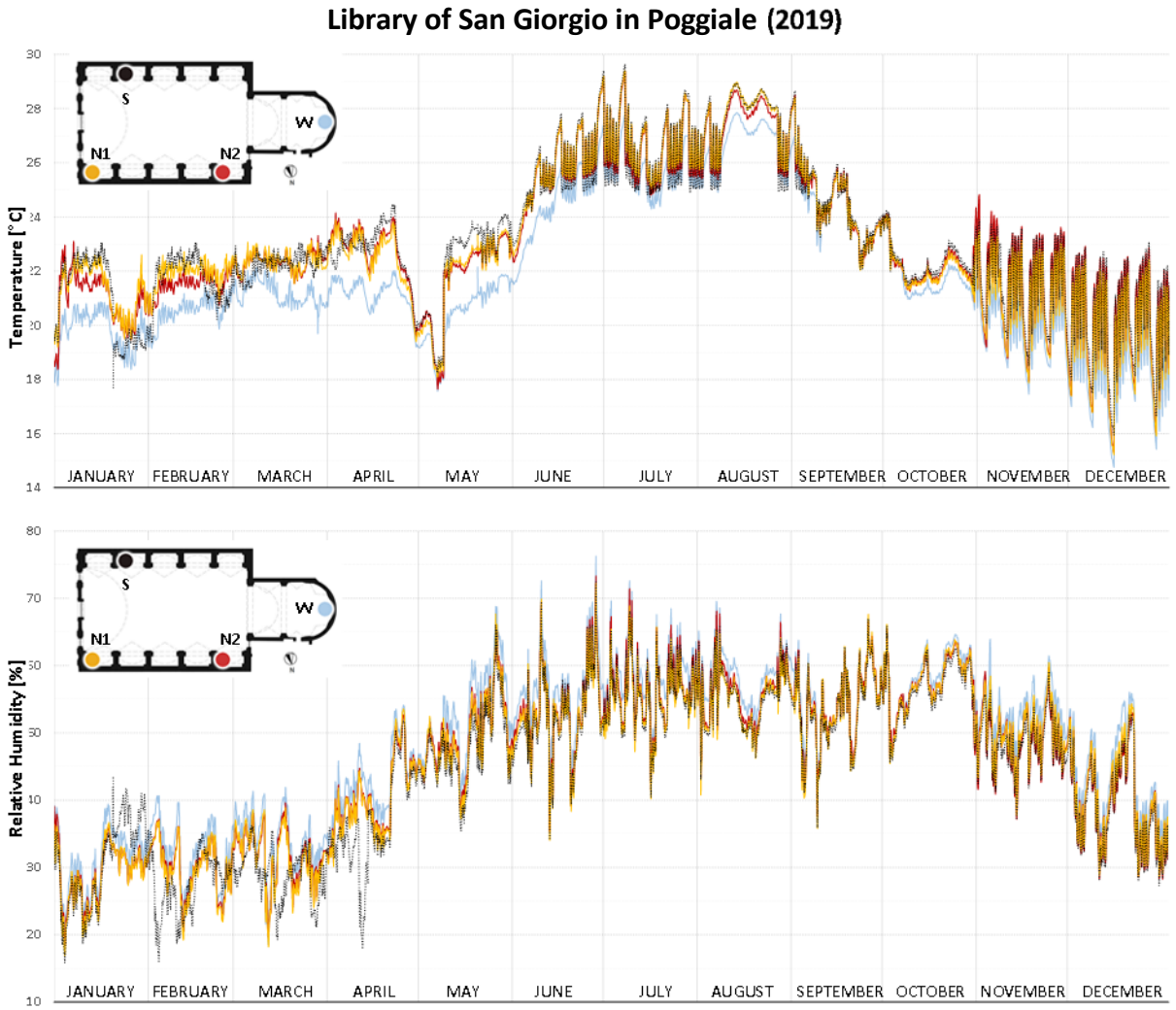

Figure 3.25 – Library of San Giorgio in Poggiale: T-RH along one year (January, 2019-December, 2019).

The weekly results presented in Figure 3.26 for the heating and cooling season show that relative humidity varies according to temperature fluctuations, suggesting that occupancy does not have a strong effect on indoor RH. This outcome is coherent with the low occupancy observed in-situ.

It is evident that for most time of the year, especially during the period of continuous heating and in the free-fluctuation of August, the temperatures represented in light-blue (sensor W, located at about 0.5m height) are few degrees lower than all the other ones (located at about 2.5m height). This difference is readable also in the weekly measurements presented in Figure 3.26. This difference suggests a vertical stratification of temperature in the indoor air, which is not an unexpected phenomenon for a monumental room like the one analysed (about 15m high).

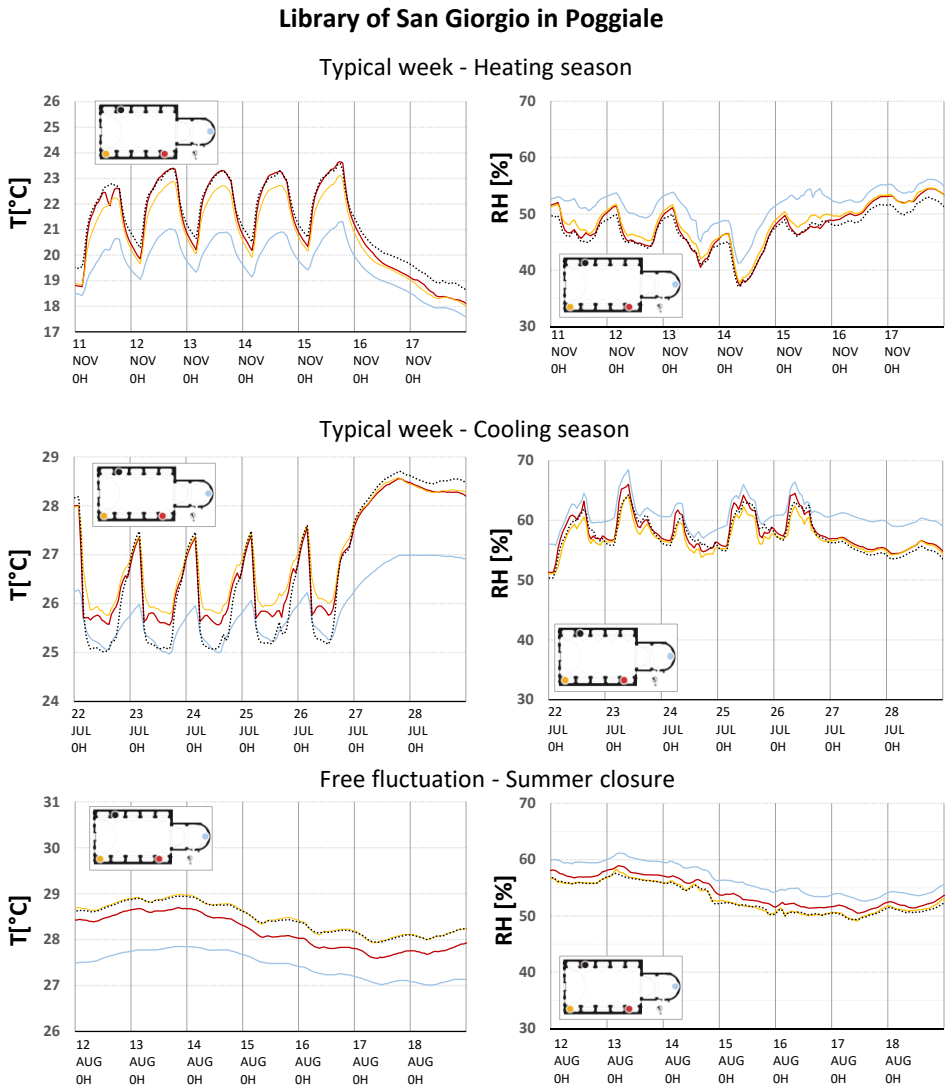

Figure 3.26 – Library of San Giorgio in Poggiale: T-RH during one week in the heating season, cooling season and closure.

3.4.2. INFRARED THERMOGRAPHY

Figure 3.27 shows the results obtained with infrared thermography, during opening hours in the heating season.

The results obtained show a difference of about 1°C between the floor level and the air at 3m-height. Furthermore, a difference of about 1.5 °C is detected between the ground level and the top of the chapels, as well as between the floor and the top of the central nave. Thus, the stratification is stronger in the chapel, as it has the same temperature difference of the nave but in a much smaller vertical extension. This outcome is consistent with the fact that most heating units are located inside the chapels, at about 3.5m in height, thus creating a stronger temperature gradient in the chapels rather than in the nave space.

Given the vertical extension of the monumental room, a much stronger vertical stratification was expected, while the one obtained (1.5°C) is very moderate. Anyway, this result can be useful for numerical modelling purposes, as shown in some preliminary simulations performed to represent the hygrothermal behaviour of this building (Posani et al., 2020).

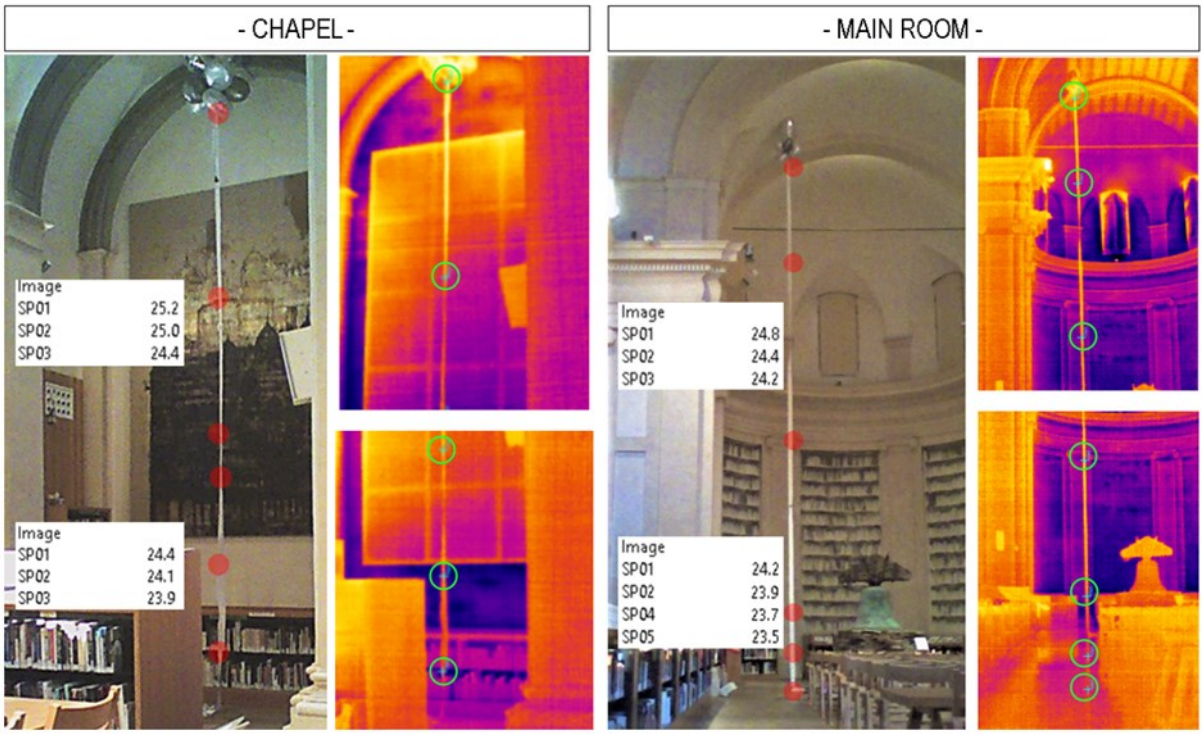

Figure 3.27 – Library of San Giorgio in Poggiale: temperature stratification observed with a vertical strip and infrared thermography.

3.4.3. SUPERFICIAL TEMPERATURES, INTERIOR AND EXTERIOR AIR TEMPERATURE NEAR BUILDINGS ENVELOPE

3.4.3.1. MUNICIPAL LIBRARY OF PORTO

The superficial temperatures of a wall of the Municipal Library of Porto were obtained as the average results from two sensors located on the interior surface of the wall, and two located on the exterior surface. The results are displayed in red in Figure 3.28, while the temperatures obtained for interior (average of 2 sensors) and exterior air temperature (1 sensor) are reported in black. In the same graph, the results obtained for indoor temperature from the indoor monitoring campaign (average of the 3 HOBO sensors located in the room, near its envelope, S1, S2, N1) and external air temperature from a meteorological station (data provided by the *Portuguese Institute of Sea and Atmosphere*, from a station located at about 11.5 km from the case study) are presented in grey.

It clearly emerges that the outdoor temperature measured by the meteorological station tends to be few degrees lower than the one measured near the building envelope. This outcome is probably the result of the position of the meteorological station, which is outside the city of Porto, where the microclimate can

be slightly different from the one of the neighbourhood of the case study. On the contrary, the indoor temperature measured nearby the wall is very similar to the average obtained from the three HOBO sensors located in the room.

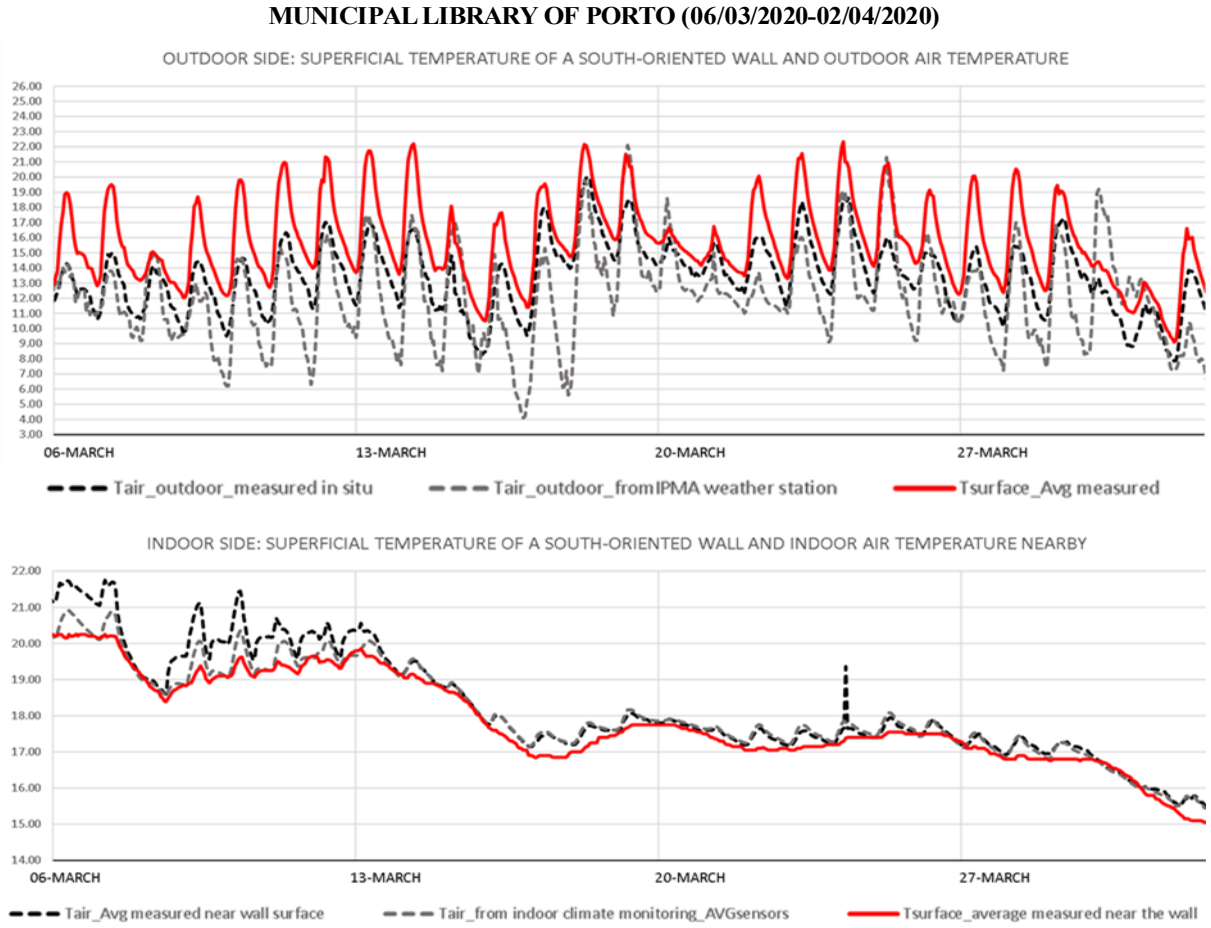

Figure 3.28 – From top to bottom: results at the outdoor and indoor side for the case study located in Porto.

The first graph shows the outdoor air temperature measured near the building envelope (black line), the one obtained from the meteorological station near the city of Porto (grey line) and the external superficial temperature measured for one wall. The second graph shows the indoor air temperature measured near the wall surface (black), the air temperature obtained in the indoor monitoring of the room (grey) and the measured interior superficial temperature of the wall (red).

3.4.3.2. CORUCHÉUS' LIBRARY

The results of internal and external superficial temperature monitoring of a wall of the Coruchéus' library, and the indoor and outdoor air temperature near the envelope are obtained each one from one sensor. The results are reported in red and black in Figure 3.29 for, respectively, superficial and air temperatures. In grey, for comparison, are also reported the indoor air temperature obtained via indoor

microclimate monitoring in the room (HOBO sensor SW1) and the exterior temperature obtained by a meteorological station (data provided by the *Portuguese Institute of Sea and Atmosphere*, from a station located at about 2.5 km from the case study).

The temperature obtained from the sensor located in the room (SW1) and the one located near the wall interior surface are in very good agreement. In this case, the outdoor temperatures measured by the meteorological station and the sensor located near the envelope are very similar, which is probably the result of the close proximity of the station to the case study.

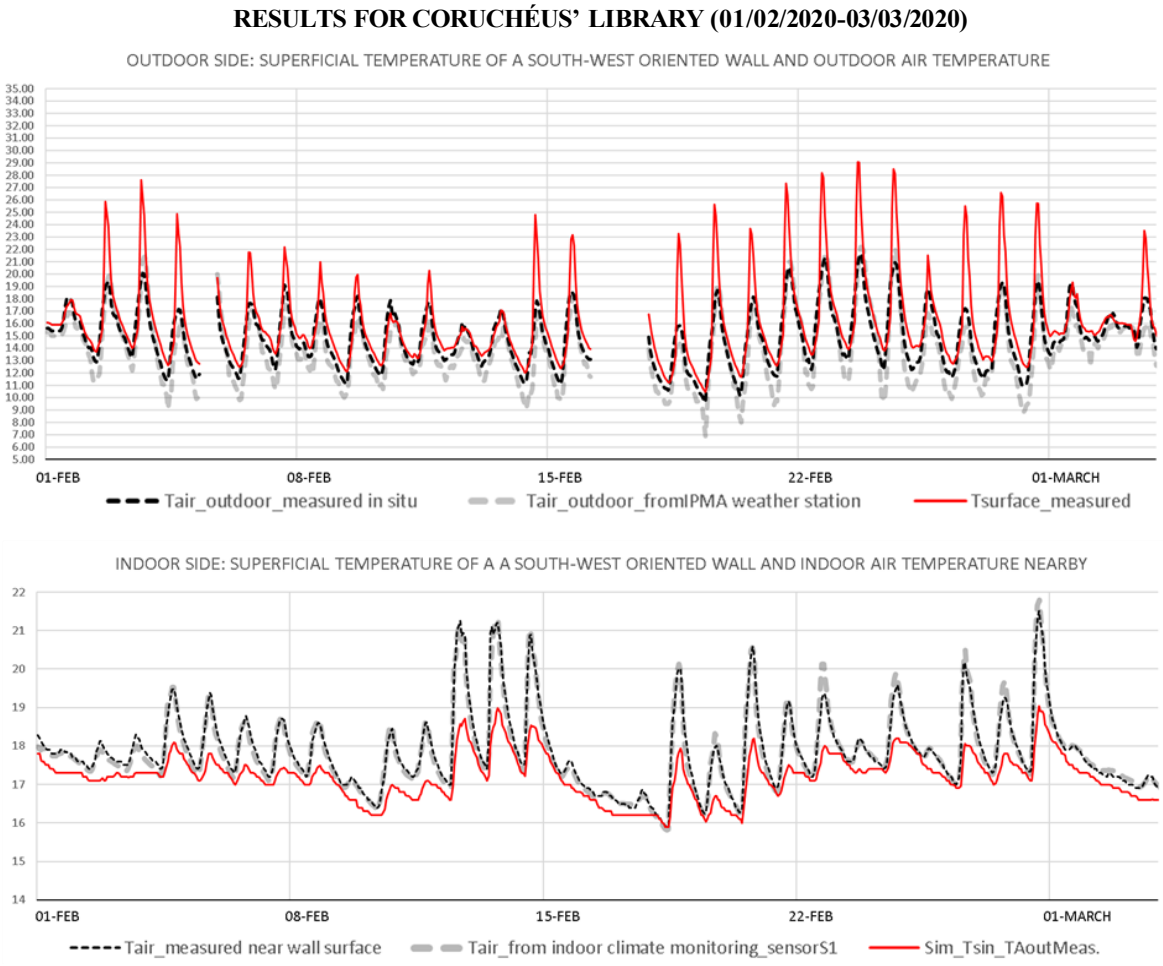

Figure 3.29 – From top to bottom: results at the outdoor an indoor side for the case study located in Lisbon.

The first graph shows the outdoor air temperature measured near the building envelope (black line), the one obtained from the meteorological meteorological station near the city of Lisbon (grey line) and the external superficial temperature measured for one wall. The second graph shows the indoor air temperature measured near the wall surface (black), the air temperature obtained in the indoor monitoring of the room (grey) and the measured interior superficial temperature of the wall (red).

3.4.3.3. LIBRARY OF SAN GIORGIO IN POGGIALE

Each parameter resulted from the measurements performed in the case study located in Bologna was obtained as the average of the data from two sensors. The outcomes are reported in red and black in Figure 3.30 for, respectively, superficial and air temperatures. In grey, for comparison, are reported also the indoor air temperature obtained via indoor microclimate monitoring from a sensor located near the building envelope (HOBO sensor W) and the exterior temperature obtained from a meteorological station (data provided by the by the public entity ARPAE, from a station located at about 3 km from the case study).

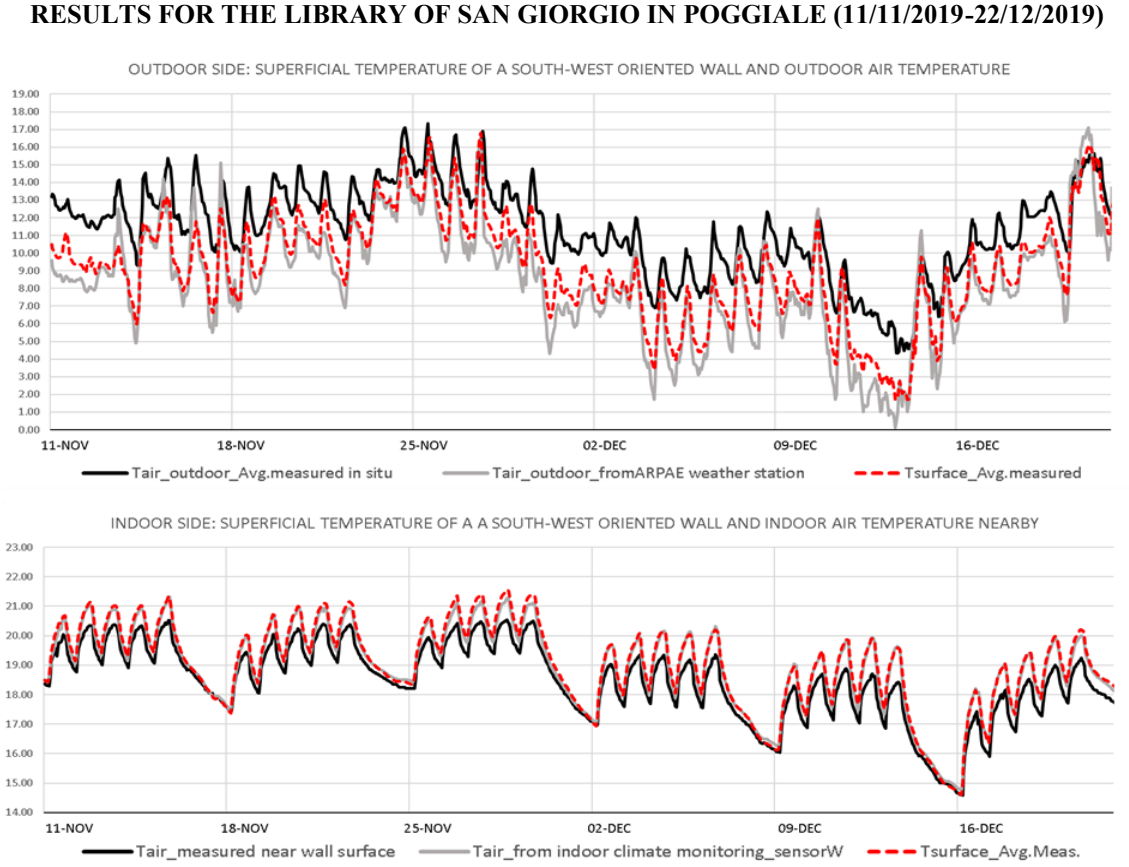

Figure 3.30 – From top to bottom: results at the outdoor an indoor side for the case study located in Bologna.

Indoor air temperature obtained from a sensor located very close to the building envelope is very similar to the ones obtained via indoor monitoring (HOBO sensor W), while outdoor air temperatures measured and obtained from the meteorological station have more relevant differences. The differences in outdoor temperature are probably related to the fact that the local meteorological station is located close to the city, but out of the very urbanized context where the building is situated, resulting in slightly different microclimates.

The first graph shows the outdoor air temperature measured near the building envelope (black line), the one obtained from the meteorological station near the city of Bologna (grey line) and the external superficial temperature measured for one wall. The second graph shows the indoor air temperature

measured near the wall surface (black), the air temperature obtained in the indoor monitoring of the room (grey) and the measured interior superficial temperature of the wall (red).

3.5. OUTDOOR AIR T AND RH – DATA FROM LOCAL METEOROLOGICAL STATIONS

The outdoor climate data, namely air temperature and relative humidity, of the cities of Porto and Lisbon, were provided by the *Portuguese Institute of Sea and Atmosphere* (IPMA), from weather stations located respectively at about 11.5 km and 2.5 km from the case studies. For the city of Bologna, the hourly data were provided by the public entity ARPAE, which has a meteorological station at about 3 km from the Library of San Giorgio in Poggiale. The periods considered are April 2019 – April 2020 for Porto and Lisbon, and the whole 2019 for Bologna. Thus, the dataset of each climate consists of one year, and they are reported in Figure 3.31, where data are re-organized into a timeline 1st January-31st march.

According to Köppen–Geiger system (Peel, Finlayson, and McMahon, 2007), all cities are characterized by temperate climates, with moderate temperatures during winter and hot (Lisbon and Bologna) or warm (Porto) summers. From Figure 3.31, it is possible to observe that Bologna is the only city whose temperature fell below zero in the period considered, furthermore it is the climate with the highest share of temperatures above 30 °C. On the contrary, the temperature of Porto rarely reaches levels above 30°C.

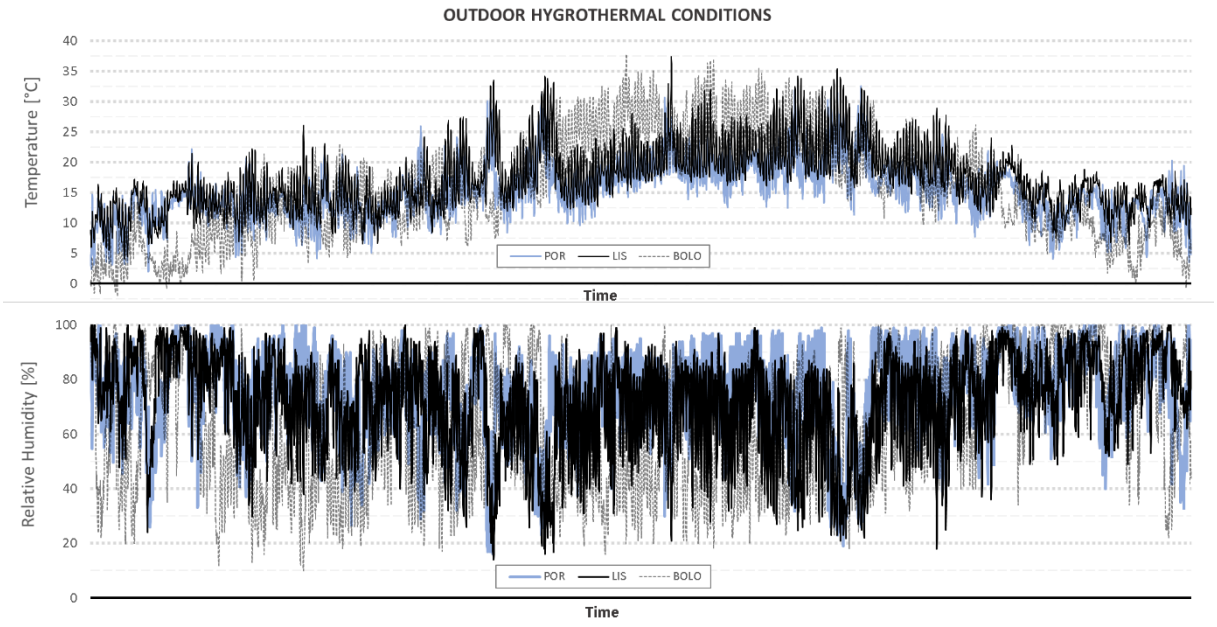

Figure 3.31 – Outdoor temperature and Relative Humidity, registered b local meteorological stations in Porto, Lisbon and Bologna. The timeline indicates the time from 1st January-31st December.

3.6. EXPERIMENTAL MONITORING – ANALYSIS OF RESULTS

3.6.1. STATISTICAL ANALYSIS OF OUTDOOR HYGROTHERMAL CONDITIONS

Considering the cumulated frequency of temperatures reported in Figure 3.32, the distribution of temperatures in Porto and Lisbon is very similar, with Porto showing colder temperatures than Lisbon.

During winter, Porto and Bologna show colder conditions than Lisbon, having temperatures below 15°C for 50% of the year, while in Lisbon temperatures are lower than 15°C for less than 40% of the year. Lisbon and Bologna have hotter summer conditions than Porto, being the temperature above 25°C for 10-20% of the year.

Thus, Bologna shows more extreme thermal conditions than the Portuguese climates, being colder in winter and hotter in summer. Bologna also appears to have lower levels of relative humidity than the two Portuguese climates.

Finally, Porto emerges as the climate with the mildest thermal conditions in summer, with outdoor temperature rarely going above 25°C.

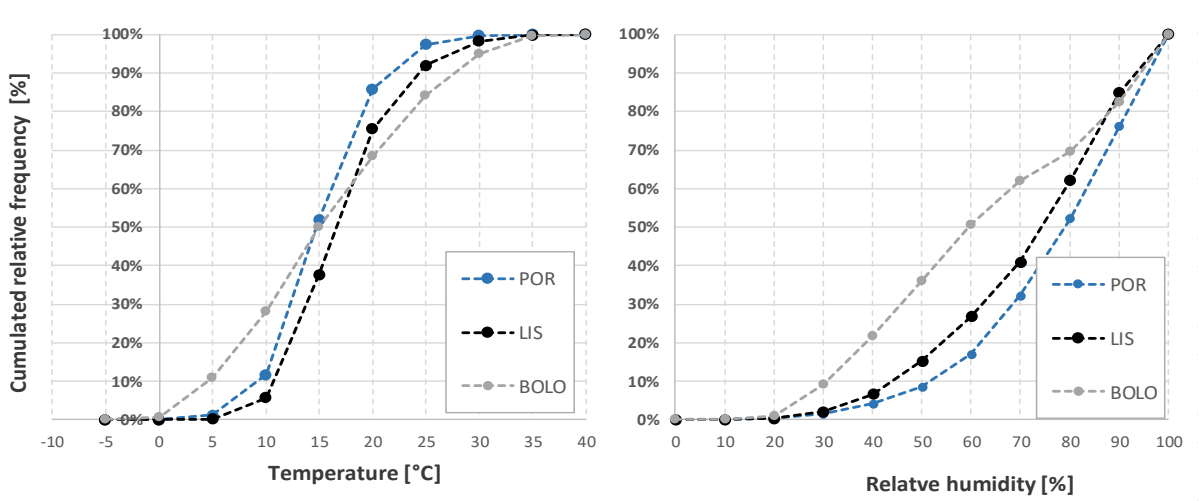

Figure 3.32 – Outdoor Temperature and Relative Humidity: Cumulated relative frequency.

3.6.2. STATISTICAL ANALYSIS OF INDOOR HYGROTHERMAL CONDITIONS AND COMPARISON WITH OUTDOOR CLIMATE DATA

The cumulative relative frequency of air temperature and relative humidity in the interior space of the case study located in Porto is presented in Figure 3.33.

The distribution of temperatures is very similar in the archives located in the attic of the building (red and black lines), as well as the RH distribution. The two spaces appear warmer and with lower levels of relative humidity than the archives located on the ground floor (yellow and grey lines). Furthermore, they experience temperatures higher than 26°C for a relevant share of time. The same high temperatures are observed for a significant time, 5-10% of the year, in the reading rooms, near south-oriented walls, while the sensor located near a north-oriented wall (light blue line) does not appear to register temperatures above 26°C.

In the case studies located in Lisbon and Bologna, a relevant share of data is found above 26°C.

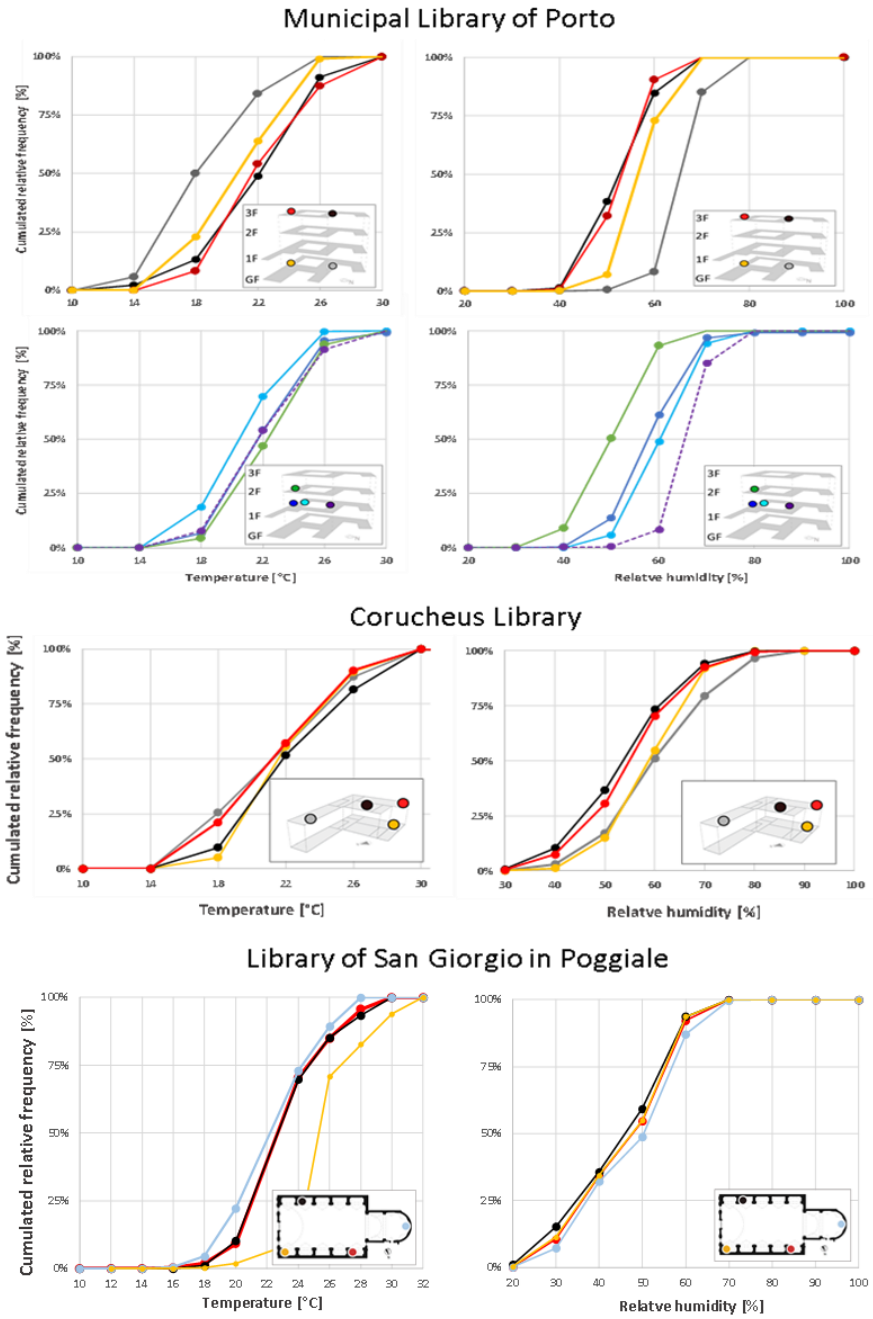

Figure 3.33 – Indoor Temperature and Relative Humidity: Cumulated relative frequency in the case studies. From top to bottom, the results obtained in the Municipal Library of Porto (archives, study rooms), the Coruchéus Library, and the Library of San Giorgio in Poggiale.

The relative humidity observed in the case study located in Bologna is much lower than in the Portuguese case studies, being below 60% for most of the year, and below 30% for a relevant share of time. On the contrary, the Portuguese case studies never have environmental RH below 30%. This result seems related to the higher use of heating adopted in Bologna. For the same reason, Bologna case study shows warmer indoor conditions, with the environmental temperature never going below 18 °C, while the Portuguese case studies have temperatures falling below 18°C for a relevant share of the year.

Except for the archives located at the ground floor of the Municipal Library of Porto, most of the spaces monitored appear to have a relevant share of temperatures above 26°C.

3.6.3. SEASONAL EVALUATION OF HYGROTHERMAL DATA

In order to provide for a synthesis of the distribution of the data recorded, a seasonal boxplot of temperature and relative humidity is provided for each outdoor and indoor climate. The results are respectively displayed in blue and black in Figure 3.34. The indoor temperatures considered in the Figure regard only spaces open to the public, thus the archives of the Municipal Library of Porto are not considered.

In the box plot adopted, the upper and lower quartiles of the data are portrayed as the top and bottom of a rectangle, while the median is represented by a horizontal line in-between. The medium, maximum and minimum values are represented as points and the vertical lines indicate the distance of the minimum and maximum from the lowest and highest quartiles, respectively. When minimum and maximum values were found to be outliers (further than 1.5 interquartile distance from the quartiles, according to Chambers et al., 1983) the vertical lines represent 1.5 interquartile distance. Other outliers are not represented.

As already observed, Lisbon and Bologna have higher outdoor temperatures than Porto during summer, with Bologna having more extreme conditions than Lisbon since the average summer temperature is above 25°C while in Lisbon it is around 20°C. Furthermore, Bologna has colder winter conditions, with an average winter temperature below 10°C, whereas it is above 10 °C in the two Portuguese climates. In terms of humidity, Bologna shows generally lower relative humidity levels than the two Portuguese climates, having seasonal averages in the range 50%-80%, while seasonal averages are between 65% and 85% in Porto and Lisbon.

Indoor climate appears to be warmer in the case study located in Porto rather than in the one sited in Lisbon, during winter. Despite the colder outdoor conditions of Bologna, the Library of San Giorgio in Poggiale appears to have warmer indoor conditions than the Portuguese case studies, having the former an average winter temperature above 20°C, while the case studies in Lisbon and Porto have an average winter temperature below 20°C, with Lisbon case study having even the upper quartile below this level. This result suggests a higher use of heating in the Italian case study.
In summer, the Portuguese case studies show average temperatures around 25°C, while the Library of San Giorgio in Poggiale has higher temperatures, with the lower quartile being above 25°C during summertime.
The higher use of heating, together with the observed reduced outdoor RH, leads to extremely low RH conditions in the Library of San Giorgio in Poggiale, with an average winter RH being around 30%, while in the Portuguese case studies it is between 50% and 65%.

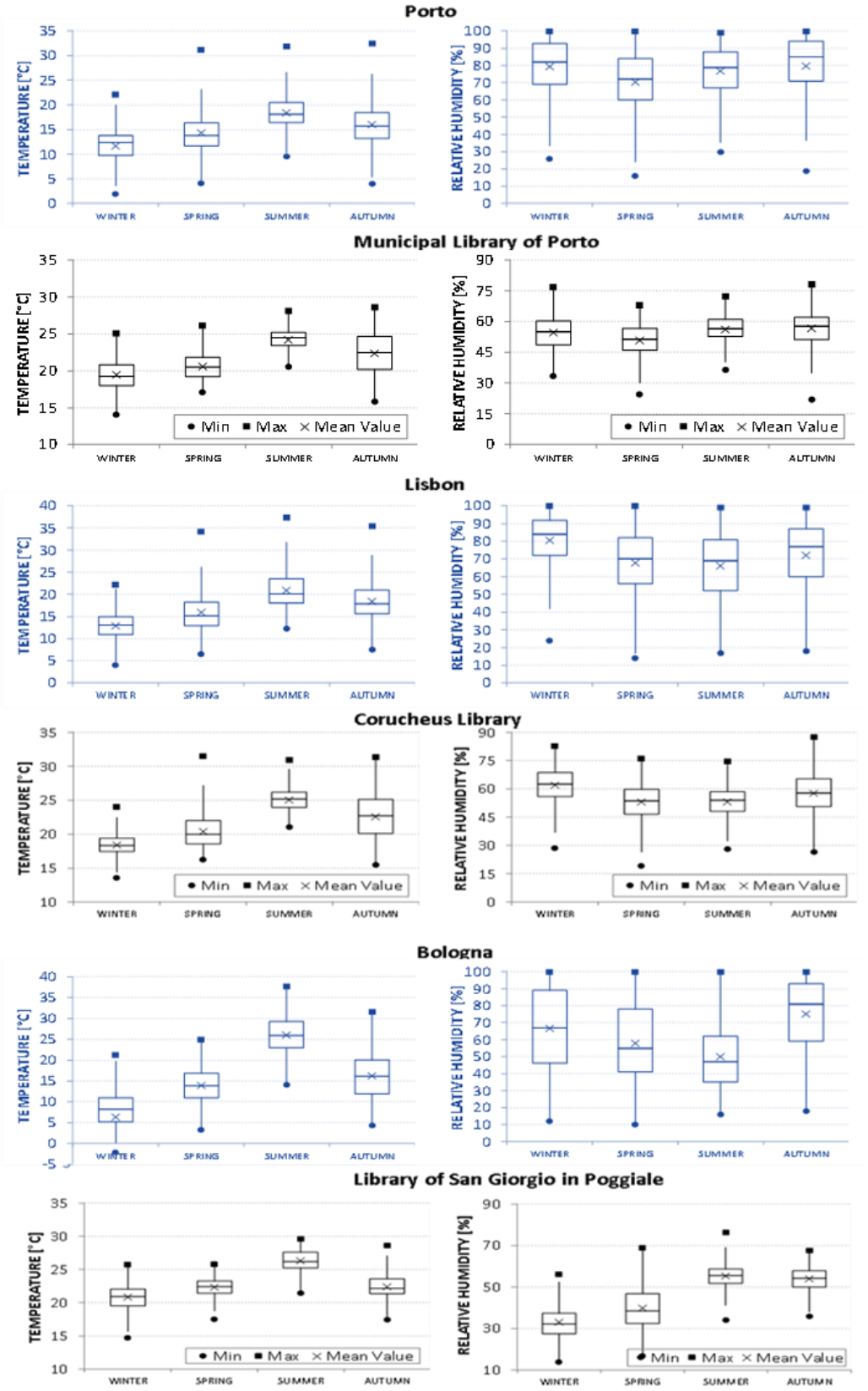

Figure 3.34 – Seasonal distribution of temperature and relative humidity in the outdoor climate and in the interior climate of the case studies (only rooms with users occupancy).

3.6.4. HYGROTHERMAL COMFORT INDOOR – DURING OPENING HOURS

It is well known that indoor comfort depends on several parameters (e.g., radiant temperature, airspeed, metabolic rate, …) and, among them, air temperature and relative humidity are of major relevance. As a rule of thumb, 18-24°C (WHO, 1984) and 40-60% (Sung, Hsiao and Shih, 2019) can be used to define a range of comfortable indoor air temperatures and relative humidity.

Figure 3.35 displays the data obtained in the rooms open to the public, during opening hours, in the three case studies and their cumulated frequency. Those data are compared to the comfort conditions previously mentioned (highlighted with a yellow area).

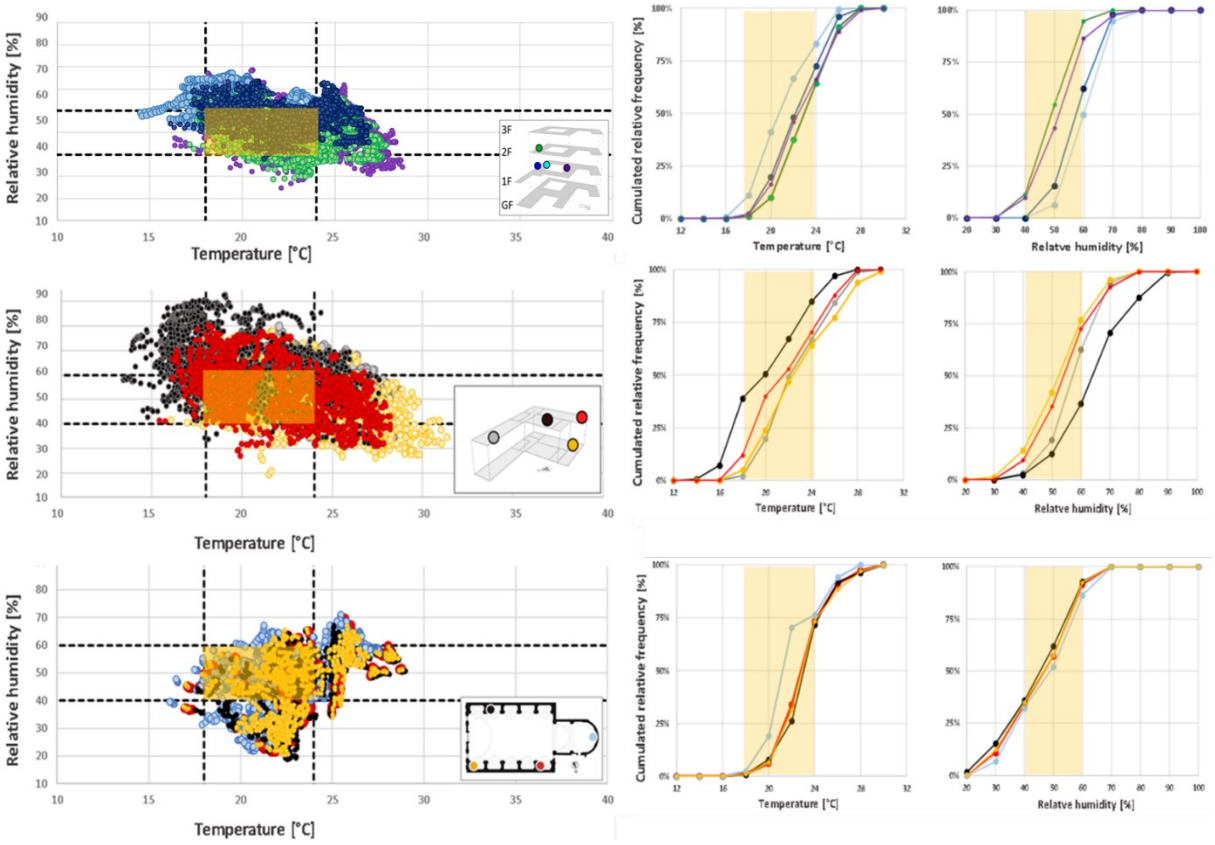

Figure 3.35 – Hygrothermal data recorded in the rooms open to the public, during opening hours, in the three case studies and their cumulated frequency. From top to bottom: the Municipal library of Porto, the Coruchéus' Library and the Library of San Giorgio in Poggiale.

It is evident that the graphics of the Portuguese cases studies have much more data than the one of the Italian case study, because of the very short opening hours the latter has.

All buildings appear to offer uncomfortable indoor air temperatures for a relevant part of the year. Results show that in winter the two Portuguese case studies have uncomfortable temperatures more often than the case study located in Bologna. In the Italian case study temperature almost never goes below 18°C, while a noticeable quantity of data are below this level in the Coruchéus' Library. All case studies have a noticeable share of temperatures above 24°C, with worse results (highest number of hours of discomfort) found in the case study located in Lisbon. Despite the high external temperatures during

summer, the case study located in Bologna appears to provide for milder indoor temperatures than the one in Lisbon, thanks to the high use of cooling systems.

In the Italian case study the discomfort is mainly caused by the low RH, being it below 40% for about 40% of the year and below 30% for about 10-20% of the time. Also in the Portuguese case studies relevant humidity-related discomfort is observed, and it is related to the high humidity levels, being RH above 60% for a relevant share of time.

3.7. CONCLUSION

The results obtained via indoor monitoring allowed having a first, rough perception of the use of heating and cooling systems in the case studies. What is more, they gave an indication concerning indoor comfort conditions.

The results obtained appear to be realistic and consistent, and they constitute the database necessary for defining the boundary conditions and the qualitative validation of the mono-dimensional numerical simulations presented in chapter 5. Furthermore, the information collected in this chapter provides the data necessary for the calibration and validation of the whole building hygrothermal simulations introduced in chapter 6.

To simulate the hygrothermal behaviour of historic walls, retrofitted with thermal mortars, the hygrothermal properties of the materials adopted in the thermal insulation systems should be known. Thus, the next chapter presents the experimental campaign performed on a selection of materials and thermal insulation systems, for the sake of determining the parameters needed as input in the numerical simulations.

3.8. REFERENCES

Arquivio Municipal de Lisboa, 1965. Palácio Dos Coruchéus - PT/AMLSB/CMLSBAH/PCSP/004/SER/004871.

Arquivio Municipal de Lisboa. 1968. Visita Do Presidente Da Câmara Municipal de Lisboa, França Borges Ao Palácio Dos Coruchéus - PT/AMLSB/CMLSBAH/PCSP/004/SER/010224.

Arquivo Municipal de Lisboa, 1972. Palácio Dos Coruchéus - PT/AMLSB/CMLSBAH/PCSP/004/VGF/001813.

Bergonzoni, Franco, and Pacifico M Branchesi, 1979. La Chiesa Di San Giorgio in Poggiale. Cassa di Risparmio in Bologna: Bologna, Italy.

Camuffo, Dario, Chiara Bertolin, and Vasco Fassina, 2009. "Microclimate Monitoring in a Church." In *Basic Environmental Mechanisms Affecting Cultural Heritage*. Nardini Editore: Florence, Italy. ISBN: 978-88-404-4334-8

Chambers, J M, W S Cleveland, B Kleiner, and P A Tukey, 1983. Graphical Methods for Data Analysis. In *The Wadsworth & Brooks/Cole Statistics/Probability Series*. Springer Bookserie: Switzerland. ISBN 10: 053498052X

Direção Geral do Património Cultural DGPC, 2020. "Edifício Onde Se Encontra Instalada a Biblioteca Pública Municipal Do Porto." Available online: http://www.patrimoniocultural.gov.pt/pt/patrimonio/patrimonio-imovel/pesquisa-do-patrimonio/classificado-ou-em-vias-de-classificacao/geral/view/73483/. (Accessed 26/10/2020)

Eibl, Melanie, and Ralf Kilian, 2011. EU Project - Climate for Culture – "Deliverable D2.2: Collection of Indoor and Outdoor Climate Data from Historic Buildings throughout Europe for the Determination of the Overall Range of Indoor Climate Climate Modeling Building Simulation Mitigation and Adaptation".

Filipe, Isabel ;, and Ana Sereno, 2012. "Sistema de Informação Para o Património Arquitectónico - Direção Geral Do Património Cultural." Available online: http://www.monumentos.gov.pt/Site/APP_PagesUser/SIPA.aspx?id=5418. (Accessed 26/10/2020)

Galante, Zaida. 1999. "Os Palácios de Lisboa – Da Propriedade Privada Ao Edifício Municipal." In Cadernos Do Arquivo Municipal, 198–199. Arquivo Municipal de Lisboa. Available online: http://arquivomunicipal.cm-lisboa.pt/fotos/editor2/Cadernos/cad3/39.pdf. (Accessed 26/10/2020)

JPN-Jornalismo PortoNet - University of Porto, 2008. "Biblioteca Municipal Do Porto: Uma História Com 1 Milhão e 300 Mil Documentos." Available online: https://jpn.up.pt/2008/07/09/biblioteca-municipal-do-porto-uma-historia-com-1-milhao-e-300-mil-documentos/.(Accessed 26/10/2020)

Kompatscher, K, R. P. Kramer, B. Ankersmit, and H. L. Schellen, 2019. "Intermittent Conditioning of Library Archives: Microclimate Analysis and Energy Impact." Building and Environment, 147, 50-66. doi:10.1016/j.buildenv.2018.10.013.

Nikzad, Samira, Behrouz M Kari, and Farhang Tahmasebi, 2011. "The Application of Thermal Imaging as a Nondestructive Test in Historic Buildings." In *XII DBMC : 12th International Conference on Durability of Building Materials and Components, Porto, Portugal, 12th-15th April 2011.*

Oliveira, Mariana Inês Lopes, 2015. "Do Convento de Santo António Da Cidade à Actual Biblioteca Pública Municipal Do Porto. Projectos de Intervenção de Eduardo Souto de Moura." Master Thesis,Faculty of Architecture , University of Porto.

Peel, M. C, B. L. Finlayson, and T. A. McMahon, 2007. "Updated World Map of the Köppen-Geiger Climate Classification." Hydrology and Earth System Sciences, 11(5), 1633-1644. doi:10.5194/hess-11-1633-2007.

Pina dos Santos, Carlos A, and Rodrigo Rodrigues, 2009. "ITE54—Coeficientes de Transmissão Térmica de Elementos Opacos Da Envolvente Dos Edificios." Laboratório Nacional de Engenharia Civil/National Laboratory of Civil Engineering: Lisboa, Portugal.

Posani, Magda, Maria Do Rosario Veiga, Vasco Peixoto de Freitas, Karin Kompatscher, and Henk Schellen, 2020. "Dynamic Hygrothermal Models for Monumental, Historic Buildings with HVAC Systems: Complexity Shown through a Case Study." In E3S Web of Conferences, 172, 15007.

Público (Portuguese news journal), 2014. "Obras Para Trazer Bibliotecas Municipais de Lisboa Para o Século XXI Estão Atrasadas." Available online: https://www.publico.pt/2014/03/15/local/noticia/obras-para-trazer-bibliotecas-municipais-de-lisboa-para-o-seculo-xxi-estao-atrasadas-1628338. (Accessed 26/10/2020)

Rebelo da Costa, Agostinho. 1788. "Descrição Topográfica e Histórica Da Cidade Do Porto." In , 117. 3ª edição. Editora Frenesi: Lisboa, Portugal.

Sung, Wen Tsai, Sung Jung Hsiao, and Jing An Shih, 2019. "Construction of Indoor Thermal Comfort Environmental Monitoring System Based on the IoT Architecture." Journal of Sensors. doi:10.1155/2019/2639787.

UNESCO, 2012. "International Memory of the World Register - Roteiro da primeira viagem de Vasco da Gama à Índia, 1497-1499 (Journal of the first voyage of Vasco da Gama to India, 1497-1499)". Available online: http://www.unesco.org/new/fileadmin/MULTIMEDIA/HQ/CI/CI/pdf/mow/nomination_forms/portugal_first_voyage_vasco_da_gama_to_india.pdf. (Accessed: 05-Jun-2020).

WHO - World Health Organization. 1984. "The Effects of the Indoor Housing Climate on the Health of the Elderly: Report on a WHO Working Group." World Health Organization: Copenhagen, Denmark.

4

EXPERIMENTAL CHARACTERISATION OF THERMAL MORTAR-BASED INSULATION SOLUTIONS.

4.1. INTRODUCTION

Within the aim of evaluating the impact of thermal plasters and renders on historic massive walls, five thermal insulation systems based on thermal mortars are considered in this chapter.

The experimental campaign hereby presented aims to provide a full database of hygrothermal properties to be used in numerical simulations. The properties analysed are open porosity, dry bulk density, thermal conductivity (dry and moisture-dependent), specific heat capacity, sorption isotherm, resistance to water vapour diffusion (via dry and wet-cup) and capillary water absorption coefficient. Although not necessary for numerical simulations, a complementary test of drying is also considered, to have a more complete view of moisture transport in the materials and systems analised.

Testing procedures and samples characteristics are mainly defined following two regulations: the European specifications for mortars for masonry – EN 998-1:2017 and the European Assessment Document for External Thermal Insulation Composite Systems (ETICS) with renderings ” – EAD 040083-00-0404:2020 (EOTA - European Organisation for Technical Approvals, 2020). Standard EN 998-1 sets the requirements for commercial mortars in Europe, and it is the one adopted by manufacturers to certify and classify thermal mortar-based insulation systems. This standard accounts for tests on samples of single or painted materials. The EAD provides the procedures for certifying (CE marking) ETICS, since they are not covered by harmonized European standards. This document accounts for samples of complete multi-layered systems. The results obtained with standard samples of single or painted materials are compared to the ones of multi-layered samples and complete systems. The outcomes are used to evaluate whether and how the layered structure and the presence of inter-layer interfaces affect the performance of multi-layered systems. Consequently, the appropriateness of standard EN 998-1:2017 for the characterization of insulation solutions based on thermal mortars is discussed, considering that it neglects the behaviour of complete insulation systems as whole units.

The main outcomes of this chapter were presented in:

- Posani, M., Veiga, M. R., and Freitas, V.P. (2021). Thermal mortar-based insulation solutions for historic walls: An extensive hygrothermal characterization of materials and systems. *Construction and Building Materials*, 304, 124595. Doi: 10.1016/j.conbuildmat.2021.125640.

4.2. MATERIALS

4.2.1. THERMAL MORTARS, THERMAL PLASTERING AND RENDERING SYSTEMS.

The nomenclature “thermal insulating mortar” or, simplifying, “thermal mortar”, indicates a mortar with thermal insulation properties, namely a thermal conductivity lower than 0.2 W/(m.K) at 10°C, according to standard EN 998-1:2017.

Thermal mortars can be applied on the external or internal side of building components, and they may be referred to as thermal renders (Henry and Stewart, 2011) or thermal plasters (Ranesi, Veiga, and Faria, 2021), respectively in the former and latter cases. Generally, thermal mortars are designed to be covered with a regularization layer and/or a finishing layer. The composite solutions can be referred to as thermal plastering /rendering systems or as thermal mortar-based systems.

Thermal mortars are generally obtained using lightweight aggregates in the mix design. For instance, several studies have considered mortars with Expanded Polystyrene (EPS) and/or cork aggregates (Maia, Ramos, and Veiga, 2018; Gomes et al., 2019; Brás, Gonçalves, and Faustino, 2014), while other investigations have analysed the thermal benefits provided by the addition of hemp (Mazhoud et al., 2016), expanded clay (Arizzi and Cultrone, 2012), silica aerogel (Nosrati and Berardi, 2018; Maia et al., 2021), expanded glass and perlite (Torres and García-Ruiz, 2009). Additionally, some authors have accounted for the environmentally-friendly nature of reusing waste in building materials by incorporating olive stones (Barreca and Fichera, 2013) and plastic waste (Corinaldesi, Donnini, and Nardinocchi, 2015) in energy-efficient mortars. In the context of heritage buildings, Walker and Pavia (2015) adopted lime plasters containing cork and hemp in a field investigation on historic walls, while other authors have analysed the use of mortars containing aerogel (Ganobjak, Brunner, and Wernery, 2019), expanded glass (Coppola et al., 2019) and perlite (Vyšvařil et al., 2020; Govaerts et al., 2018).

4.2.2. MATERIALS AND SYSTEMS

This study investigates thermal insulation systems based on thermal mortars that are commercially available and designed for application on historic or traditional masonry walls. The three thermal mortars considered can be described as having low water absorption coefficients and high vapour permeability, according to the classification proposed in Chapter 2 (considering manufacturers’ declared properties: A_w<0.11 kg $m^{-2}s^{-1/2}$, $\delta_p \geq 17.9\ 10^{-12}$ kg m^{-1} s^{-1} Pa^{-1}). Their declared values of thermal conductivity are in the range of 0.045-0.08 W/(m.K), and they are developed by two different manufacturers.

From the first manufacturer, two lime-cork mortars (A1, A2) are analysed. These materials are designed to be covered with a regularization mortar (B1) and a final layer of paint: a lime-based one (C1) for indoor-exposed systems and one with potassium silicate (C2) for external solutions, both of which are declared to be “breathable” finishings. Hence, 4 systems (S1, S2, S3, S4) are considered from the first manufacturer: two based on the first thermal mortar (S1: A1+B1+C1, S2: A1+B1+C2) and two on the second one (S3: A2+B1+C1, S4: A2+B1+C2).

From the second producer, a mortar based on mixed binders and Expanded Polystyrene (EPS) aggregates is considered (A3). This material is used in combination with a regularization mortar that also works as a finishing layer (B2) and the system (S5) is suitable for both interior and exterior interventions (S5: A3+B2). All in all, 7 materials and 5 systems are tested, as shown in Figure 4.1 and Table 4.1.

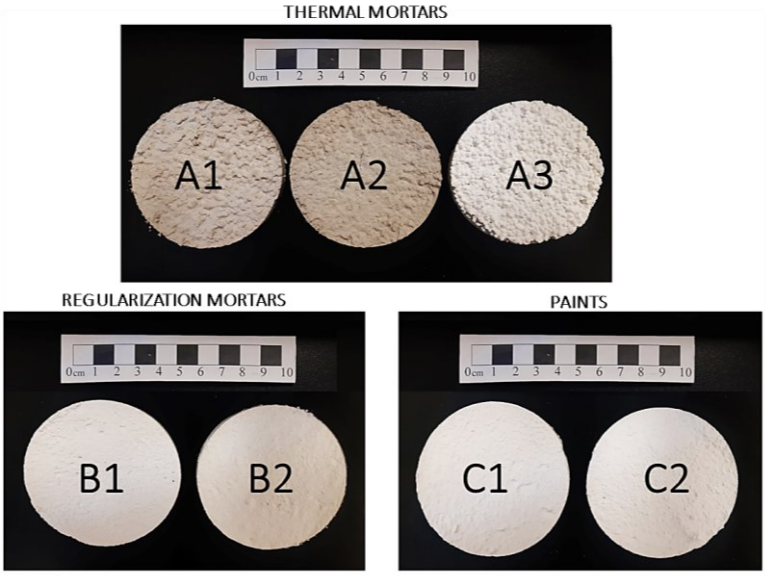

Figure 4.1 – Materials considered in the study. Two thermal mortars with hydraulic lime and cork-aggregates (A1, A2), and one with mixed binders and EPS-aggregates (A3). Two regularization mortars, one based on air lime (B1) and one based on mixed hydraulic binders (B2). A lime paint (C1) and a potassium silicate paint (C2).

Table 4.1 – Materials and systems considered in the study. Manufacturers' declared values of vapour resistance factor, capillary water absorption coefficients and thermal conductivity of single materials.

Manufacturer	**Identification**	**Code**	**μ* [-]**	**A_w* [kg/(m²min$^{0.5}$)]**	**λ* [W/(mK)]**
Materials (main binders and lightweight aggregates)					
1st	Thermal mortar 1 (Hydraulic lime and Cork aggregates)	A1	4	0.4	0.045
	Thermal mortar 2 (Hydraulic lime and Cork aggregates)	A2	4	0.63	0.08
	Regularization Mortar (Air lime)	B1	≤ 15	≥0.40	/
	Paint (Lime-based) – Indoor use	C1	*"breathable"*	/	/
	Paint (Potassium silicate-based) – Outdoor use	C2	*"breathable"*	*"Water-repellent"*	/
2nd	Thermal mortar 3 (Mixed binders and EPS aggregates)	A3	≤ 5	≤ 0.2	0.05
	Regularization and finishing Mortar (Mixed Hydraulic binders)	B2	≤ 5	≤ 0.2	/
Notation: μ- Declared vapour resistance factor, A_w- Declared capillary water absorption coefficient, λ -Declared Thermal conductivity **All properties reported in the technical sheets of thermal mortars were determined according to the indications of EN998-1 (i.e. test methods referred in standards EN 1015-19, EN 1015-18, and EN 1745, for μ, A_w and λ). For thermal mortar A3, the manufacturer further specifies the additional use of standard EN 12664, which is the one designated by EN1745 for tests involving guarded hot plates and heat flow meters.*					
Systems					
1st	S1: A1+B1+C1 (Indoor use) S2: A1+B1+C2 (Outdoor use)				S1 S2
	S3: A2+B1+C1 (Indoor use) S4: A2+B1+C2 (Outdoor use)				S3 S4
2nd	S5: A3+B2 (Indoor and outdoor use)				S5

4.2.3. PREPARATION OF FRESH MORTARS

Before preparing the samples for the experimental campaign, a few tests were performed considering powder mixes and fresh mortars. More in detail, their bulk density was determined and compared with the values declared in the technical sheets. The water ratio adopted for the fresh mortars was chosen within the range suggested by the manufacturers and the slump test was performed to evaluate the workability of fresh mortars. All mortars were prepared in a mixer, using the minimum speed available, and a mixing period of 3.5 minutes, as suggested in the technical sheets provided my the first manufacturer.

4.2.3.1 BULK DENSITY OF POWDER MIXES AND FRESH MORTARS

The test performed to measure the bulk density of powder mixes is based on the French certification standard CSTB n°2669 – "CSTB certification for one coat renders" (CSTB, 1993). The testing equipment consists of a V-shaped funnel and a measuring cup, as shown in Figure 4.2(a). First, the mass of the empty cup was defined with 3 measures while its volume was known from technical sheets. Then, the end of the funnel was closed, and the powder mix was poured in, one scoop at a time, paying attention to minimizing the vertical pressure on the powder. The funnel was then opened to let the powder fall into the measuring cup. The exceeding powder was removed from the top of the cup with a spatula, taking care not to exert pressure on the powder. The residues of powder were removed from the external surfaces of the cup with a cloth and the full cup was weighed three times. The bulk density was thus defined as the difference in mass between the full and empty cup, divided by its volume.

Bulk density of fresh mortars was defined according to European standard EN 1015-6:1998 - "Methods of test for mortar for masonry - Part 6: Determination of bulk density of fresh mortar" using one sample per mix type to contain the waste of material. Indeed, all the samples tested were considered unusable for any other scope after this test, since it involves "compacting phases" (tilts) that may reduce the content of air voids in the mortar, which is an important characteristic for the thermal mortars analysed (containing air-entraining admixtures). The test was performed with a metal vessel whose volume was known. The empty container was weighed three times when empty and it was then filled up to about half of its height with fresh mortar. The vessel was tilted of about 30 mm on alternate sides for a total of 10 times, on a rigid support. It was then filled with further material, more than needed to reach the edge of the container, and it was compacted with the same 10-tilts procedure. The excess of mortar was removed from the top of the vessel as shown in Figure 4.2(b). The full vessel was then weighed 3 times. The bulk density of the fresh mortar was indirectly measured as the difference in mass between the full and empty cup, divided by its volume.

a.  b. 

Figure 4.2 – Equipment for testing the bulk density of powder mixes (a) and fresh mortars (b).

4.2.3.2 WATER RATIO AND WORKABILITY

The water ratio chosen for preparing each mortar was selected within the interval suggested in the technical sheets. The mortars workability was analysed in terms of consistency by flow table test, as shown in Figure 4.3. The test is based on the European Norm EN 1015-3:2007 – "Methods of test for mortar for masonry. Determination of consistence of fresh mortar (by flow table)" and it was performed once for each mortar to contain the waste of material.

The test was performed by placing the fresh mortar into a truncated cone mould in two successive layers, and after each application 10 short strokes were used to compact the sample. The mould was then removed, and the flow table was jolted 15 times, at a rate of one stroke per second. Finally, the diameter of the mortar spread was measured, in two orthogonal directions, with a calliper. Test results were calculated as the average of the two measurements.

a.  b. 

Figure 4.3 –The mixer adopted to prepare the fresh mortars (a) and one sample at the end of the flow table test (b).

4.2.4. SAMPLES PREPARATION AND CURING

To assess the hygrothermal properties of hardened materials and systems, different types of specimens were considered. The characteristics of the samples and the properties tested are summarized in Table 4.2, while the moulds adopted are shown in Figure 4.4.

All samples were obtained through spatula application of mortars, while the paints were applied using paint-rollers.

The first three types (a, b, c in Figure 4.4) were used to prepare standard samples aligned with EN 998-1:2017 by pouring in fresh mortars, storing them in a conditioned room (23°C ± 5°C, 50% ± 5% RH), and demoulding after 5 days. The samples were left in the same conditions for a further 85 days, reaching a 90-day curing time. After that, some samples were finished with paint and left to dry under the same controlled conditions for 15 days more. The last type of mould, (d in Figure 4.4), was used to prepare thicker tile samples that better represent real applications, following the indications of the EAD. In these moulds, large tiles (550mm x 150mm x 40mm) of thermal mortars were prepared with two successive layers, each one 20mm thick, as required in the materials technical sheets. In further detail, the first layer of mortar was poured and left for 24 hours at "normal indoor conditions" (free-floating indoor microclimate, 13-20°C and 40-80% RH were registered). Then, the mortar surface was moistened, and a new layer of fresh material was applied. After 5 days of drying under "normal indoor

conditions", the hardened samples were demoulded, and they were put under controlled conditions (23°C ± 5°C; 50% ± 5% RH) until reaching a 90-day curing period. Thereafter, the tiles were cut into smaller specimens. Some of these smaller samples were covered with a layer of regularization mortar and left to cure at controlled conditions for a further month. Part of them were then finished with paint and put to dry under controlled conditions for 15 days more. The tile samples of thermal mortars created with this method have a thickness of about 40mm, while the ones to which also regularization mortar was applied, with or without paint, have an average thickness of 42 mm.

The timing adopted for curing and demoulding the samples was chosen for several reasons.

A period of 5 days was adopted for the demoulding to comply with the time prescribed by standard EN 1015-11:2019, i.e. 2 to 5 days depending on the binder. Thus, the maximum time was adopted for all mortars to homogenize demoulding schedules, while avoiding the risk of mortars with longer setting times breaking in the process. A 90-day curing time was chosen to allow the specimens of mortars to reach a high level of carbonation, while complying with the minimum reference time referred to in norm 1015-19:2008 (28days). Moreover, 90 days is a curing period often adopted for testing lime-based materials (Veiga et al., 2010; Veiga, 2017).

A curing period of 30 days was selected for the regularization layer applied on tiles of thermal mortars to comply with the minimum time period of standard 1015-19. It was considered sufficient for carbonation because of the very reduced thickness of this layer (about 2mm). A curing time of 15 days was defined for the paints applied on samples thus complying with the minimum time required in standard EN1062-3:2008 for finishings (7 days).

a.  b. 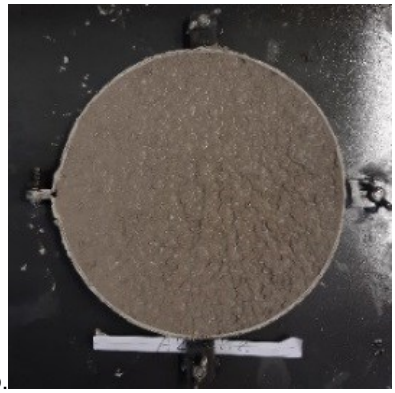

c. 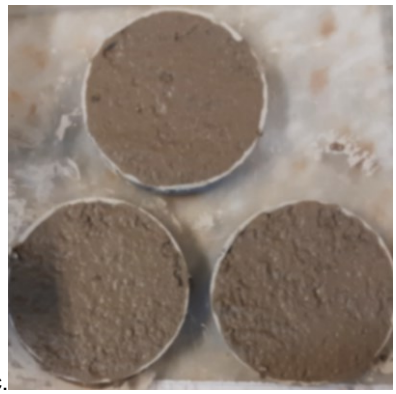 d. 

Figure 4.4– Moulds used for (a) prism, (b) disk, (c) small disk and (d) tile samples.

Table 4.2 – Summary of the specimens adopted.

Samples	Size	Material	Properties tested
Standard samples: single materials and applied paints. Based on EN 998-1:2017			
Prism	160mm x 40mm x 40mm (cut in half: 80mm x 40mm x 40mm)	A1-Thermal mortar A2 - Thermal mortar B1- Regularization mortar A3 - Thermal mortar B2- Regularization mortar	Dry bulk density and open porosity Capillary water absorption Drying
Disk	ϕ, 200mm x, 20mm	A1 - Thermal mortar A2 - Thermal mortar B1- Regularization mortar B1+C1- Reg. m and finishing B1+C2- Reg. m.and finishing A3 - Thermal mortar B2- Regularization mortar	Resistance to water vapour diffusion
Small disk	ϕ 70mm x 10mm	A1 - Thermal mortar A2 - Thermal mortar B1- Regularization mortar B1+C1- Reg. m. and finishing B1+C2- Reg. m. and finishing A3 - Thermal mortar B2- Regularization mortar	Sorption isotherm
Tile samples: thermal mortars, addition of regularization layer, and complete systems. Samples prepared by layers to better represent real applications. Based on the EAD for ETICS.			
Tile*	150mm x 150mm x *40mm	A1 A1+B1 S1 (=A1+B1+C1) S2 (=A1+B1+C2) A2 A2+B1 S3 (=A2+B1+C1) S4 (=A2+B1+C2) A3 S5 (=A3+B2)	Capillary water absorption Drying
Tile*	110mm x 150mm x *40mm	A1 A1+B1 S1 (=A1+B1+C1) S2 (=A1+B1+C2) A2 A2+B1 S3 (=A2+B1+C1) S4 (=A2+B1+C2) A3 S5 (=A3+B2)	Resistance to water vapour diffusion
Tile*	90mm x 50mm x *40mm	S1 (=A1+B1+C1) S2 (=A1+B1+C2) S3 (=A2+B1+C1) S4 (=A2+B1+C2) S5 (=A3+B2)	Sorption isotherm
Tile	150mm x 150mm x 40mm	A1, A2, A3	Thermal conductivity Specific heat capacity

*In these samples, 40mm thickness refers to the layer of thermal mortar. The average thickness of samples where regularization mortars B1 or B2 were applied, with and without paint, is on average 42mm.

4.3. TEST METHODS

The methods adopted for the experimental campaign are described in detail in this section.

The tested properties were selected according to the inputs needed for numerical simulations with the software WUFI Pro and WUFI Plus (IBP, 2018). Thermal properties were determined only for thermal mortars, i.e. the only insulating materials adopted in the systems, whereas hygric properties were tested for all single and painted materials (standard samples).

Additional tests were performed, although not necessary for the sake of numerical simulations. These were all the tests performed on tile samples, which were used to investigate the influence of layered structure and interface phenomena on the hygric properties of composite samples. Similarly, additional tests of drying were performed on all types of samples to have a more complete understanding of moisture transport in the studied materials and systems. The standards and methods adopted for the tests are synthesized in Table 4.3.

The main European standard for product qualification of thermal mortars, and all mortars in general, is EN 998-1:2017. It provides some indications concerning the classification of the materials, based on their physical, mechanical and hygrothermal properties, as well as other characteristics such as fire resistance and durability. Moreover, it indicates minimum performance requirements and reference standards for testing procedures. In terms of hygrothermal properties, standard EN 998-1 accounts for capillary water absorption, resistance to water vapour diffusion and thermal conductivity, recommending standards EN1015-18:2002, EN1015-19:2008 and EN1745:2020 for the corresponding test methods. Commercial thermal mortar-based systems are required to comply with the indications of standard EN 998-1 for single materials. On the contrary, External Thermal Insulation Composite Systems (ETICS) must comply with the requirements defined by the European Assessment Document EAD 040083-00-0404:2020. This last standard accounts for tests performed on samples of complete insulation solutions, thus considering the behaviour of each system as a whole unit.

In this work, both regulations are accounted for in the test procedures. Standard samples of single and painted materials are tested with consideration of the European specifications EN 998-1, while tile samples of single and combined materials, as well as complete systems, are evaluated accounting for the indications of EAD 040083-00-0404.

For the reason of synthesis, in this research thesis the European Assessment Document for External Thermal Insulation Composite Systems (ETICS) with renderings - EAD 040083-00-0404:2020, is also referred to as the EAD for ETICS, or simply as the EAD.

In regards to capillary water absorption and resistance to water vapour diffusion, the European Committee for Standardization (CEN) also provides some specifications for testing materials for interventions on heritage buildings: standards EN15801:2009 and EN15803:2009. These two regulations are thus taken into account in the testing procedures and in the analysis of results.

Concerning dry bulk density, even though standard EN 998-1 recommends adopting a test of full immersion in water as in EN1015-10:1999, the testing procedure FE Pa 44 (LNEC, 2015) is hereby preferred because it defines the measurement of both dry bulk density and open porosity, by means of the same test of immersion in water under vacuum conditions. Standard 998-1 and the EAD for ETICS

do not consider properties related to the hygroscopic behaviour of materials and systems, such as the sorption isotherm. For this reason, the international standard ISO 12571:2013 is adopted. Thermal properties are measured with a Modified Transient Plane Source (MTPS). Hence, in addition to standard EN1745, also ASTM D7984:2016 is considered since it specifically addresses the use of MTPS equipment. The first standard is considered for defining the test conditions, such as environmental T and RH, while the second one is used to determine the minimum dimensions of samples.

Finally, EN 998:1 and the EAD for ETICS do not consider tests on the drying properties of materials and systems, thus standard EN16322:2016 – "Conservation of Cultural Heritage - Test methods - Determination of drying properties" is the one followed for the additional tests on drying" is adopted.

Table 4.3 – Summary of the test methods and standards adopted in the experimental campaign.

Samples	**Property**	**Standards / Test procedures**	**Method**
Tests on physical properties			
Standard samples	- Open porosity - Dry bulk density	FE Pa 44 (LNEC, 2015)	Water saturation under vacuum conditions
Tests on hygric properties			
Standard samples	- Sorption isotherm	ISO 12571:2013 (ISO, 2013)	Climatic chamber
	- Resistance to water vapour diffusion	EN 1015-19 (CEN, 2008) EN 15803:2009 (CEN, 2009)	Dry-cup Wet-cup
	- Capillary water absorption	EN 1015-18:2002 (CEN, 2002) EN 15801:2009 (CEN, 2009)	One-direction absorption by partial immersion
Tile samples	- Sorption isotherm	ISO 12571:2013 (ISO, 2013)	Climatic chamber
	- Resistance to water vapour diffusion	EAD 040083-00-0404:2020 (EOTA, 2020)	Dry-cup Wet-cup
	- Capillary water absorption	EAD 040083-00-0404:2020 (EOTA, 2020)	One-direction absorption by partial immersion
Tests on thermal properties			
Tile samples of Thermal mortars	- Thermal conductivity ($\lambda_{10°C,dry}$) - Specific heat capacity (c_{dry})	EN 1745:2020 (CEN, 2020) ASTM D7984:2016 (ASTMInternational, 2016)	MTPS (Modified transient plane source)
	- Thermal conductivity, moisture dependent (at 23°C)	Test procedure explained in the text	
Complementary test on moisture transport			
Standard and Tile samples	- Drying curve	EN16322:2016 (CEN, 2016)	Drying under controlled conditions (23°C $\pm$ 5°C; 50% $\pm$ 5% RH)

4.3.1. OPEN POROSITY AND DRY BULK DENSITY

The dry bulk density and open porosity of hardened mortars were determined according to the testing procedure FE Pa 44 – "Determination of open porosity and bulk and real densities" (LNEC, 2015). For each material, 3 prism specimens (160x40x40mm) were taken into analysis. Each one was cut into two halves and only one of these halves was tested.

The samples were first dried in a ventilated oven (40 ± 5ºC) until constant mass was reached (M_{dry}). Then, the samples were put under vacuum conditions for 24 hours (± 2h) by using a desiccator (400mbar, Figure 4.5), for the sake of eliminating the air from open pores. Then, a pipe was used to introduce a flow of distilled water in the desiccator. The samples were kept in this condition of full immersion under vacuum for 24 hours (± 2h). The desiccator was then opened and, after 30 minutes, the mass of the samples was measured by hydrostatic weighing (M_h). The excess of water was then removed with a damp cloth, and the saturated mass of the samples (M_{sat}) was measured. Open porosity, dry bulk density and saturation water content (w_{sat}) were defined according to equations 1, 2 and 3:

$$P_O = \frac{M_{max}-M_{dry}}{\rho_w} \cdot \frac{1}{V} \cdot 100\% = \frac{M_{max}-M_{dry}}{M_{max}-M_h} \cdot 100\% \quad (4.1); \qquad \rho_{dry} = \frac{M_{dry}}{V} \quad (4.2);$$

$$w_{sat} = \frac{M_{max}-M_{dry}}{V} = \frac{M_{max}-M_{dry}}{M_{max}-M_h} \cdot \rho_w = P_O \cdot \rho_w \quad (4.3).$$

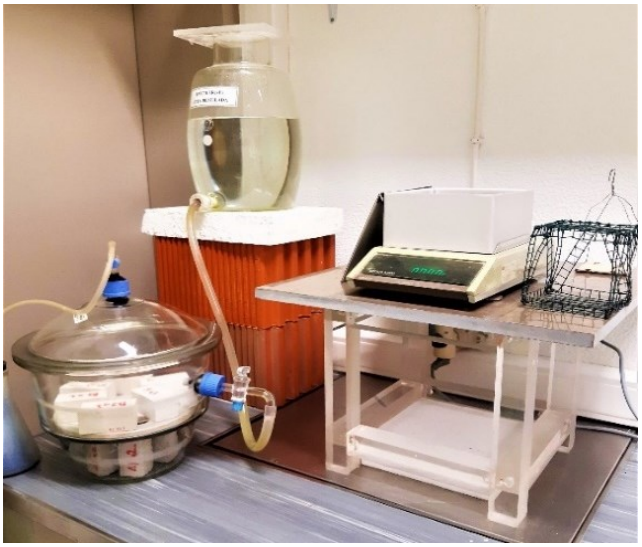

Figure 4. 5– Equipment adopted for determining open porosity.

4.3.2. THERMAL CONDUCTIVITY AND SPECIFIC HEAT CAPACITY

Measurements of thermal conductivity in building materials may be performed through a variety of methods, which are broadly classified into two categories: steady-state methods and transient methods (Yüksel, 2016).

Steady-state methods are based on establishing a steady temperature gradient over a known thickness of the sample and on controlling the heat flow from one side to the other, thus thermal conductivity can be defined by applying Fourier's law (Franco, 2007). Whereas, transient techniques consider samples that

are in equilibrium with the environment and that are then exposed to a short heating pulse. The feedback response is recorded along time. This response depends on the thermal transport properties of the material, thus it allows the equipment to define the thermal conductivity, thermal diffusivity and specific heat capacity of the material through mathematical analyses (Yüksel, 2016).

Within this experimental campaign, the goal of testing thermal properties was primarily to determine thermal conductivity and specific heat capacity of samples in dry conditions. Secondly, the analysis of thermal conductivity of moist samples, with different water contents, was considered to provide the basic information for discussing the efficacy of thermal insulations at real in-situ conditions. Indeed, porous materials located in outdoor-exposed components may experience wide changes in moisture content during the year, with a consequent variation of thermal conductivity that can strongly impact their thermal performances (Gomes et al., 2017; Amorim et al., 2020).

A transient method was chosen to perform the test, because of the several benefits it offers. First of all, transient methods measure both thermal conductivity and specific heat capacity within the same test. In addition, transient tests require smaller samples, their results depend less on the operator and they are easier to perform than the steady-state tests, as observed by Gomes et al. (2018). What is more, transient methods are reported to be more appropriate than steady-state ones for measurements on moist materials. Indeed, they induce a very limited water migration through the sample during the test (Mazhoud et al., 2016) and they require a shorter testing-time, thus limiting the exchange of moisture between the specimens and the environment (Delgado, Azevedo, and Guimarães, 2019).

The test is performed using an ISOMET 2114 device (Modified Transient Plane Source, MTPS). The equipment offers a measuring range of 0.04-0.3 W/(m.K), which appeared suitable for the mortars analysed in this study (declared thermal conductivities ranging 0.045-0.08 W/(m.K)). For each thermal mortar, 3 specimens 150x150x40 mm were adopted and each measurement was performed by putting the sample on two lateral supports to avoid any contact between the sample and the table, as shown in Figure 4.6.

First, the thermal properties were determined at standard conditions, 10°C, dry (EN 1745:2020). Then, the thermal conductivity at different moisture contents, 23°C, was determined. The samples were conditioned at 23°C, 50% RH and tested (ISO 10456:2007). After that, they were soaked with liquid water and left to dry under controlled conditions (23°C ± 5°C, 50% ± 5% RH). During the drying process, their thermal conductivity was determined at different moisture states, similarly as in Parracha *et al.* (2021).

More in detail, three moisture states were considered (apart from the stable condition at 23°C, 50% RH). The water content of each state was determined by considering the wet mass of the specimen as the average between the mass at the beginning and at the end of the MTPS measurement, disregarding inhomogeneities in moisture distribution through the sample.

It is worth underlining that the MTPS is not the standard equipment considered in the European standard EN 1745:2020, the Heat Flow Meter (HFM) is. Nonetheless, according to the literature, the MTPS emerged to offer several advantages and it seems the best solution for meeting the purpose of this investigation, since it is particularly suitable for measurements on moist samples. In addition, although providing for less accurate results, the MTPS seems suitable for the scope because it was found to provide moderately different results than the HFM when applied on thermal mortars, namely ranging 10-30% (Gomes et al., 2018).

Figure 4.6 – Set-up for measurements with the Modified Transient Plane Source method.

4.3.3. SORPTION ISOTHERMS

Porous materials exposed to constant conditions of temperature and relative humidity tend to exchange moisture with the environment until reaching a state of equilibrium, i.e when the partial pressure and temperature of the water vapour in the pores of the material is quite the same as in the environment (Hansen 1986). The sorption isotherm, describes the relationship between relative humidity and equilibrium moisture content of a material in the hygroscopic range (Zhao et al., 2017), at a constant temperature. Sorption isotherms are necessary in analysing the moisture condition of structures (Hansen 1986), especially when multi-layered systems with no capillary-breaking separations are analysed, which is the case of mortars applied on masonry components (Künzel 1995).

The determination of moisture content in the hygroscopic range is based on the climate chamber method defined in ISO 12571:2013 - "Hygrothermal performance of building materials and products - Determination of hygroscopic sorption properties". All thermal mortars were tested, as well as the regularization mortars with and without the finishing paints (disk-shaped samples in Figure 4.7). Samples of complete systems were analysed too (tile-shaped samples in Figure 4.7). All samples were sealed on their lateral surface and base with aluminium tape, thus exposing only the upwards-facing area to exchanges of moisture with the environment.

Figure 4.7 – Samples adopted for testing moisture storage functions.

The samples were dried in a ventilated oven (40 ± 5ºC) until a constant mass was reached (M_{dry}). Then, they were put in the climate chamber where the environment was kept at a constant temperature of 23°C, while RH was periodically increased. The steps adopted for defining the sorption isotherm were RH of 30%; 50%; 70%; 80% and 95%. The mass of the samples was weighed every 24 hours until reaching the equilibrium with each RH condition (M_{RH_i}) and the correspondent moisture content (w_{RH_i}) was obtained as:

$$w_{RH\_i} = \frac{M_{RH\_i} - M_{dry}}{V} \quad (4.4),$$

where V indicates the volume of the samples, which was geometrically determined. The sorption isotherms were finally obtained by plotting equilibrium water contents against relative humidity.

4.3.4. RESISTANCE TO VAPOUR DIFFUSION

The water vapour permeability test was based on ISO 12572:2016 – "Hygrothermal performance of building materials and products. Determination of water vapour transmission properties", EN 15803:2009 - Conservation of cultural property - Test methods - Determination of water vapour permeability (δp) and the EAD for ETICS - "European Assessment Document. External Thermal Insulation Composite Systems (ETICS) with renderings"(EOTA, 2020). The test was performed in a climate chamber, at (23 ± 2) °C, (50 ± 5) %, with the (dry and wet) cup method, as shown in Figure 4.8.

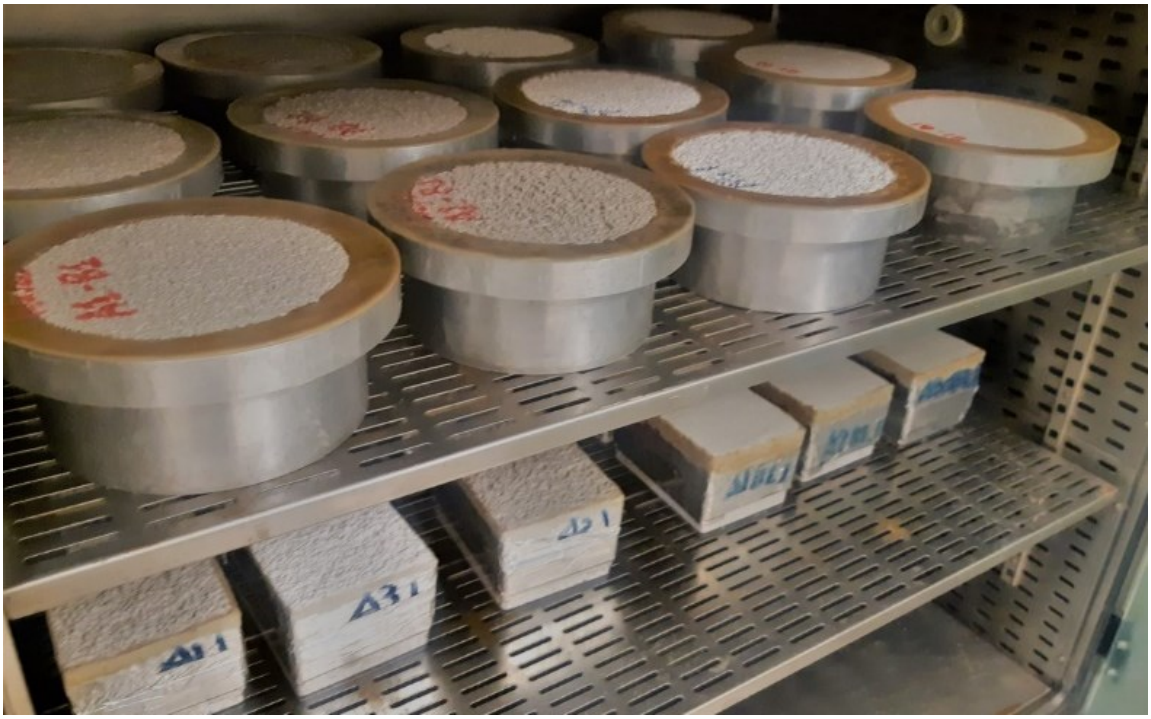

Figure 4. 8– Sealed disk and tile samples, located in the climate chamber to test their resistance to water vapour diffusion.

As vapour permeability depends on the conditions of humidity taken into account (Ramos, Delgado, and Freitas, 2010), two types of tests were performed, with the dry-cup and wet-cup settings. The dry-cup test was performed by using a desiccant (aqueous solution saturated with calcium chloride, $CaCl_2$)

to create a 0% RH environment inside the cup. In the wet cup, the indoor environment was kept at 100% RH by using liquid water (Slavík, Bruthans, Weiss, and Schweigstillová, 2020). In order to ensure that vapour flux would pass only through the horizontal surface of the samples, their lateral areas were sealed (wax for rounded metal cups, aluminium tape and additional wax for tile samples in plastic cups).

Once the experimental setup was ready, periodic weights were performed until constant vapour flux was reached in 5 successive measurements. At that point, the water vapour permeability of the sample was quantified according to Fick's law as suggested in ISO 12572:2016:

$$\delta = d \cdot \left(\frac{G}{A \cdot \Delta p_v}\right) \quad [\text{kg/ (m s Pa)}] \qquad (4.5),$$

where:
- d is the thickness of the specimen, measured in m;
- G is the vapour flux, in Kg/s, defined as the average of the vapour flux obtained in the last 5 measurements;
- A is the exposed area of the sample, in m^2;
- Δp_v is the difference of vapour pressure applied at the sample faces, in Pa, calculated from the mean measured temperature and relative humidity throughout the test, with

$$p_v = \text{RH} \cdot p_{sat} \qquad (4.6) \qquad\qquad p_{sat}\,[\text{Pa}] = 610.5 \cdot e^{\frac{17.269\,\theta}{237.3+\theta}} \qquad (4.7)$$

being θ the temperature in °C.

Given that the experiment was carried out at 23°C, the vapour saturation pressure was 2807.81 Pa (equation 5), determining a vapour pressure of:

- Pv_0 = 0.00 Pa, at RH= 0% (inside the dry cup);
- Pv_{50} = 1403.91 Pa, at RH=50% (in the climatic chamber);
- Pv_{100} = 2807.81 Pa, at RH= 100% (inside the wet cup).

Finally, the water vapour resistance factor was defined as the ratio between the vapour permeability of still air and the permeability of the sample:

$$\mu = \frac{\delta_a}{\delta} \qquad (4.8).$$

Where δ_a is the vapour permeability of still air, in kg/(m s Pa), which can be determined by:

$$\delta_a \left[\frac{\text{kg}}{\text{m h Pa}}\right] = \frac{0.083 \cdot p_0}{R_v \cdot T \cdot p} \cdot \left(\frac{T}{273}\right)^{1.81} \qquad (4.9),$$

with R_v= 462 being the gas constant of water vapour, p being the barometric pressure in hPa, and p_0=1013.25 hPa being the standard barometric pressure, while T is the temperature in K. Thus, the permeability of still air, at 23°C and atmospheric pressure was defined as δ_a = 7.03 10^{-7} kg/(m h Pa) ≈ 195 10^{-12} kg/(m s Pa).

For systems and paints, guidelines and standards consider vapour diffusion equivalent air thickness, s_d, thus this parameter was also adopted in this study:

$$s_d = \mu \cdot d \tag{4.10}.$$

The equivalent air thickness (and consequent vapour resistance factor) of paints and single layers of regularization mortars were calculated by difference, applying Fick's law to a multi-layered system, as shown in Maia (2019):

$$s_{d,S} = s_{d\_air\_i} + s_{d,support} + s_{d\_paint} + s_{d\_air\_e} \tag{4.11},$$

where $s_{d,S}$, $s_{d_{air_i}}$, $s_{d,support}$, $s_{d_{paint}}$, $s_{d_{air_e}}$ are the vapour diffusion equivalent air thicknesses of the whole system, of the interior surface of the sample, of the base support for the paint, and of the exterior surface of the sample. The resistance of the surfaces are evaluated following the indication of Worch (2004):

$$s_{d_{air}} \ [m] = \frac{1}{67+90\,v} \tag{4.12},$$

with v[m/s] indicating air velocity at the surface, which is accounted to be negligible inside the cup ($v_i \approx$ 0 m/s, $s_{d\_air\_i} \approx 0.015$ m) and equal to the air velocity in the chamber at the exterior surface, ($v_e \approx 0.3$ m/s, $s_{d\_air\_e} \approx 0.011$ m). The air velocity in the chamber was estimated by means of a hot-film anemometer (CaTec-air velocity transmitters EE65, working range:0–10 m/s, accuracy: ±0.2 m/s).

4.3.5. CAPILLARY WATER ABSORPTION

4.3.5.1 TEST ON PRISMS SAMPLES: SINGLE MATERIALS

The testing process adopted for single materials accounts for the European standards:
- EN 1015-18:2002 - "Methods of test for mortar for masonry - Part 18: Determination of water absorption coefficient due to capillary action of hardened mortar";
- EN 15801:2009 - "Conservation of cultural property - Test methods - Determination of water absorption by capillarity".

For each material, 3 prism specimens (160x40x40mm) were cut into two halves and only one of them was considered in the test. The face resulting from the cut was regularized with sandpaper and its area was geometrically determined (A), as shown in Figure 4.9. The lateral surface of the specimens was sealed (paraffin) and, after that, the samples were left for 24h at controlled conditions (23°C ± 5°C, 50% ± 5% RH). The mass of the samples was then measured (M_0) and the test was performed, at the same environmental conditions, by keeping the regularized surface of the samples in direct contact with liquid water. The water content was periodically measured by weighting. More in detail, the process adopted was the following.

Each sample was positioned inside a tray, on two supports, and the tray was then filled with water until its level was 5-10 mm above the surface of the samples, as shown in Figure 4.10a. After that, the mass of the specimens (M_i) was periodically determined, until reaching constant mass in all samples.

Before each weighing, the surface of the sample was slightly wiped off with a damp cloth to remove the excess of liquid water. The drying curves were then obtained by plotting the change of water content per unit area, $(M_i-M_0)/A$, versus the square root of time, $t^{1/2}$.

a.  b.  c. 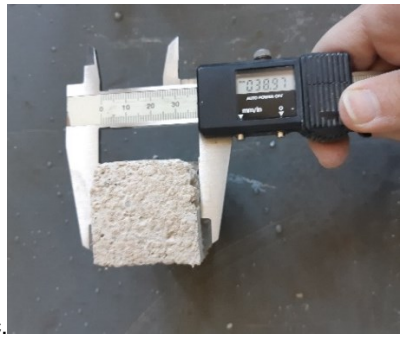

Figure 4.9 – Cut (a), regularization (b), measurement (c) of the specimens for capillary water absorption test.

4.3.5.2 TESTS ON TILE SAMPLES: WHOLE-SYSTEMS, COMBINED MATERIALS AND SINGLE MATERIALS

The testing methodology is based on the EAD for ETICS - "European Assessment Document. External Thermal Insulation Composite Systems (ETICS) with renderings"(EOTA, 2020).

Tile samples (150x150x40 mm) were used and the test procedure followed was very similar to the one adopted for single materials: samples were sealed (paraffin) along their lateral surface and they were left for 24h at 23°C ± 5°C, 50% ± 5% RH. Then, their testing surface (external face, opposite to the one in contact with the base mould) was kept in contact with water, as shown in Fig 3.10b, and the specimens were periodically weighed. Water absorption curves were determined in the same way as for prisms-specimens.

a.  b. 

Figure 4.10 –Capillary water absorption test on prism samples (a) and some of the tile specimens(b).

4.3.5.3 CAPILLARY WATER ABSORPTION COEFFICIENT

The water absorption curves can be separated into two parts. The first part describes the capillary-dominated part and can be approximated by a straight line (Plagge, Scheffler, and Nicolai, 2007). The

capillary water absorption coefficient represents the rate of capillarity action (Sicakova, Draganovska, and Kovac, 2017) in this first part.

Standard EN 1015-18:2002 simplifies this coefficient by considering the absorption rate between 10 minutes (wight M1) and 1.5 hours (weight M2). Instead, standard EN 15801:2009 accounts for the slope of the regression line through the first 5 measurements. Another type of approximation, indicated in the EAD for ETICS, considers the rate between the starting point and the absorption at 24h.

The three coefficients are compared and discussed according to the capillary absorption curves obtained from the tests and one of the definitions is chosen, over the others, to define the value to adopt as input in the numerical simulations.

4.3.6. DRYING

Even though the drying test is not necessary to evaluate materials' properties for numerical simulations, it provides for a better understanding of moisture transport in the studied materials and systems. Indeed, the test covers a large range of moisture transport, from the material saturated with liquid water to the final drying phase, based on vapor transport only (Scheffler and Plagge, 2010). Thus it provides indirect information on both liquid transport and vapour permeability in the overhygroscopic range and in the transition from overhygroscopic to hygroscopic (Carmeliet and Roels, 2001).

The test was performed on samples saturated by capillary absorption, which were left to dry following the standard EN16322:2016 – "Conservation of cultural heritage - Test methods - Determination of drying properties".

More in detail, the damp samples obtained from the capillary absorption test, were located on a vapour proof base, with the surface exposed upwards to allow the drying, as shown in Figure 4.11. The test was performed in a controlled environment, 23±5°C, 50±5% RH. During the process, the mass of the samples was periodically measured. The drying curve was plotted as the change in water content per unit area $(M_i-M_{dry})/A$ in time.

The drying curve was also defined in terms of saturation degree (Govaerts et al., 2018), by plotting the measured mass as a ratio of the saturated mass, against time. This curve provides a relative indication that accounts for both the speed of drying and the initial water content. Indeed, a good drying behaviour can be obtained:

- with a material that absorbs a high quantity of water, at saturation level, and then dries fast in absolute terms (water content in time);
- with a material that has a lower capillary absorption and dries out slower.

This curve is used to evaluate and compare those types of behaviours.

The drying curve is typically composed of two distinct phases.
The first phase is characterized by an almost linear weight loss in time. During this phase, the material transports liquid water to the evaporation surface fast enough to compensate for the losses due to evaporation, thus the surface remains wet, allowing for evaporation at a constant rate (EN16322:2016). During the first drying phase, the drying is limited by the boundary conditions (temperature, relative humidity, air flow velocity), thus the first part of the curve reflects these conditions.
In the second drying phase, this physical phenomenon reverses. Moisture transport becomes slower and it is not sufficient to keep the exposed surface moist, thus the rate of evaporation decreases. In this case,

the drying process is dominated by the vapour diffusion mechanism (EN16322:2016). Hence, during the second drying phase, the drying is limited by the material properties (Scheffler and Plagge, 2010).

Figure 4.11 –Some of the samples during the drying test and, on the top-left corner, the datalogger used to record air temperature and relative humidity.

According to standard EN16322:2016, the drying rate corresponding to the first drying phase is obtained as the negative slope of the curve: residual water content (kg/m^2) in time (h), by accounting for the linear regression through, at least, 5 successive measurements. Whereas, the drying rate of the second phase is the negative slope of the linear section of the curve: residual water content (kg/m^2) against the square root of time ($h^{1/2}$), obtained as the linear regression through, at least, 5 successive measurements.

4.4. POWDER MIXES AND FRESH STATE RESULTS

The Bulk densities obtained with the pre-mixed powders of the five mortars are shown in Table 4.4. The results obtained for mortars A1, A2 and B1 are compatible with the ones reported in their technical sheets (360 ± 20 kg/m^3, 450 ± 45 kg/m^3, 1120 ± 110 kg/m^3). The second manufacturer does not provide the bulk density of A3 and B2 mixes, but he gives the values for the fresh mortars of A3 (455 ± 50 kg/m^3), which is compatible with the one experimentally obtained.

Thermal mortars resulted to have lower bulk densities than regularization ones, which was expected because of the lightweight aggregates. What is more, the powder mix of EPS-based mortar (A3) has a noticeably lower bulk density than cork-based ones, a fact that can be related to the difference of bulk density between the two aggregates (EPS: ρ_{dry} =10-50 kg/m3 and Expanded cork: ρ_{dry} =90-140 kg/m3, according to EN ISO 10456:2007). Furthermore, there is a noteworthy difference among cork-based mortars, with A2 powder mix being about 40% heavier than A1, thus suggesting a larger presence of lightweight aggregates in the latter.

The quantity of mixing water was defined for each material in accordance with the manufacturers' indication and it is reported in Table 4.4, together with the consistency obtained as the mean value of two orthogonal measurements with the Slump-test. Thermal mortars showed slumps ranging from 101mm to 122mm, whereas regularization mortars had larger slumps, i.e. 146mm and 166mm. If these results are compared with the bulk densities of the powders, it emerges that the lighter the mortar the

smaller the slump. This outcome is coherent with the indications provided in EN 1015-2:2007, where reduced values of slumps are suggested for lighter mortars.

Table 4.4 – Bulk density (ρ) of powder mixes and bulk density, water ratio and consistency of fresh mortars.

Producer	Material	Bulk density: ρ[kg/m^3]		Water ratio	Consistency (slump)
		powder mixes	fresh mortars		
1st	A1 – Thermal mortar	360	753	0.80	115mm
	A2 – Thermal mortar	499	890	0.60	122 mm
	B1 – Regularization mortar	1055	1754	0.28	166 mm
2nd	A3 – Thermal mortar	238	407	0.90	101mm
	B2 – Regularization mortar	1140	1398	0.22	146mm

All in all, the consistency obtained for the studied mortars was smaller than indicated in standard EN 1015-2:2007, except for mortar B1. Nonetheless, the results were considered acceptable because all mortars appeared workable. What is more, the consistencies obtained for thermal mortars were similar to the ones adopted in other studies on mortars with light-weight aggregates: 100-120 mm in Contrafatto et al. (2020) and 125-175mm in Kramar and Bindiganavile (2011).

4.5. HARDENED STATE RESULTS

For each type of sample, three specimens were prepared and tested for the sake of taking potential irregularities into account (Govaerts et al. 2018). Test results are expressed as the average of the measurements performed on the three specimens, and an estimation of the error is provided by using the Standard Error of the Mean (SEM, with 2 significative digits), i.e. the standard deviation (σ) divided by the square root of the number of measurements (SEM= $\sigma/\sqrt[2]{3}$).

4.5.1. OPEN POROSITY AND DRY BULK DENSITY

The results obtained for open porosity (P_0) and dry bulk density (ρ_{dry}) of hardened mortars are reported in Table 4.5, together with the values declared by the manufacturers.

All mortars have similar values of porosity, around 29% - 34% for thermal mortars and about 31% for regularization mortars. The values obtained with regularization mortars are in line with the P_0 experimentally observed by other authors, (Govaerts et al., 2018; Maia, Ramos, and Veiga, 2018; Gomes et al., 2019), i.e. 26%-38% for plastering/rendering mortars made with cement, hydraulic lime and mixed binders. On the other hand, the open porosity observed in thermal mortars appears quite low for industrial mixes containing air-entraining admixtures, considering that other authors obtained about 70% for a lime-perlite thermal render (Govaerts et al., 2018b) and 46-47% for commercial lime-cork mortars (Gomes et al., 2019). Similar results were instead obtained in an experimental study on cement-

cork mortars where no admixtures were considered (P_0=38%, in Gomes et al., 2019). These outcomes suggest a lack of efficacy of the air-entraining admixtures adopted in the thermal mortars analysed. This concern is further confirmed, in the case of mortars A1 and A2, by the fact that the P_0 experimentally obtained is less than half the declared value.

The dry bulk densities measured are very similar to the design values for mortars A3 and B2, and comparable for mortar B1 (with a difference of about 20%). On the contrary, the results obtained for cork-based mortars (A1, A2) are 65% higher than declared. This outcome is coherent with the reduced open porosity obtained for the two cork-mortars in comparison with the value declared in their technical sheets, which indicates a limited presence of voids in the materials and higher compactness than originally designed for. The three thermal mortars have a dry bulk density lower than 1300 kg/m^3, which is the maximum value admitted for lightweight mortars in standard EN 998-1.

The discrepancy observed in the measured and declared dry bulk density for lime-cork mortars A1 and A2 appears very relevant. For this reason, the accuracy of the measurements was investigated by repeating the test with another method and different samples. Three tile specimens of thermal mortars A1 and A2, stabilized at 23°C ± 5°C and 50% ± 5% RH, were considered. Their volumes were geometrically determined, and their mass was measured by gravimetric weighing. The results obtained, $\rho_{dry\_A1\_tile}$ = (567.4 ± 2.2) kg/m^3 and $\rho_{dry\_A2\_tile}$ = (695.6± 3.9) kg/m^3, are in the same order of magnitude as those observed with prism samples, thus indicating that the dry bulk densities presented in Table 4 are in fact representative of the samples of hardened mortars A1 and A2 obtained in the laboratory.

Table 4.5– Open porosity, dry bulk density and thermal conductivity of hardened mortars (measured and declared). Specific heat capacity measured for thermal mortars.

	Properties declared by the manufacturers.			Experimental Results (Average ± SEM)			
	P_0 [%]	ρ_{dry} [kg/m^3]	λ [10^{-3} W/ m K]	P_0 [%]	ρ_{dry} [kg/m3]	$\lambda_{10°C, dry}$ [10^{-3} W/ m K]	C_{dry} [J/ kg K]
A1	71.64	370 ± 10%	45	34.16 ± 0.18	612.8 ± 5.4	97.83 ± 0.72	843 ± 50
A2	71.64	440 ± 10%	80	30.72 ± 0.26	724.2 ± 6.2	126.90 ± 0.84	848 ± 60
A3	---	350 ± 50	50	28.83 ± 0.46	342.3 ± 6.1	65.4 ± 2.8	919 ± 146
B1	---	1350 ± 10%	/	30.654 ± 0.074	1616.5 ± 1.8	/	/
B2	---	1450 ± 100	/	31.11 ± 0.25	1315.5 ± 7.5	/	/

--- : not declared; / : disregarded; P_0.: Open Porosity, ρ_{dry}: Dry bulk density, λ : Thermal Conductivity, C: Specific Heat Capacity

4.5.2. THERMAL CONDUCTIVITY AND SPECIFIC HEAT CAPACITY

The thermal properties of dry thermal mortars, at 10°C, are reported in Table 4.5. The measured specific heat capacity is around 850 J/(kg K) and 920 J/(kg K) for the two cork-based mortars and the one with EPS, respectively: a difference that does not seem significant, given the high variability in the C_{dry} of the EPS-mortar (high SEM). These results are in line with the value observed by Walker and Pavía

(2015) for a lime-cork mortar (866.50 W/kg.K) and with the ones measured by Horma et Al. (2020) for EPS-cement plaster composites (1000-1150 W/kg.K).

Also the results obtained for thermal conductivity are similar to the ones observed in previous studies on thermal mortars. The thermal conductivity of A3 is in line with the results obtained by Maia, Ramos, and Veiga (2018) for lime and mixed-binders mortars containing EPS, which were in the range of 0.049-0.078 W/(m.K). The results of lime-cork mortars A1 and A2 are similar to those presented by Gomes et Al. (2017) for lime and cement mortars containing cork aggregates, i.e. values between 0.07 and 0.10 W/(m.K). These values are also aligned with the ones observed by authors studying thermal mortars for adoption in historic buildings, such as lime-based solutions with hemp, cork and perlite, i.e. 0.07 – 0.10 W/m.K (Walker and Pavía, 2015; Govaerts et al., 2018). Furthermore, the thermal conductivities detected are more promising than those obtained in studies considering plasters based on gypsum and EPS (Bouzit et al., 2021: λ= 0.12–0.22 W/(m.K)) or lime and expanded glass (Coppola et al., 2019: λ= 0.35 W/(m.K)), while they offer lower performance than solutions based on lime and advanced insulation materials such as aerogel (Nosrati and Berardi, 2018: thermal conductivity as low as 0.025 W/(m.K)).

All mortars showed higher thermal conductivities than the ones declared by manufacturers. Mortar A3 was found to have a $\lambda_{10°C,\ dry}$ 30% higher than declared, A2 more than 60% higher, and A1 had more than twice the declared value. For A3, the discrepancy may be related to differences in preparation and conditioning of the samples, or to a difference in the application method adopted, as observed by Govaerts et Al. (2018) who obtained a 50% higher thermal conductivity than declared when studying lime-perlite thermal mortars. In addition, it might be related to the use of the MTPS equipment, which is less accurate than the standard equipment recommended in the European standards. On the contrary, for thermal mortars A1 and A2, the results are probably affected by the reduced open porosity experimentally obtained.

According to the European standard EN 998-1, thermal mortars A1 and A3 can be classified as T1, i.e. thermal conductivity (λ) ≤ 0.10 W/(m.K), whereas A2 belongs to thermal class T2 (λ≤ 0.20 W/(m.K)). Nevertheless, considering the values declared by the manufacturers, they would all be classified as T1. The EAD for ETICS set stricter requirements, defining a maximum threshold value of λ_{max}=0.065 W/(m.K) for the insulation layer. Thus, the thermal mortars considered only offer moderate thermal insulation capacity in comparison to typical ETICS solutions (such as EPS and mineral wool), since they exceed the λ_{max} defined by the EAD for ETICS. However, they still seem to be of interest for adoption in climates with moderately cold winters because they comply with the requirements set by EN 998-1 for thermal mortars, and they offer much better thermal performance than traditional renders and plasters based on gypsum, lime and cement, whose thermal conductivities are typically in the range of 0.4 – 1.0 W/(m.K) (EN 12524:2000).

The results obtained with thermal mortars at different moisture contents are shown in Figure 4.12. As expected, thermal conductivity relevantly increases when moving from lower to higher water contents. Furthermore, a strong exponential correlation ($R^2 \geq 0.97$) is found between the moisture content (mass by mass) and the thermal conductivity, normalized by its value at 23°C, 50% RH, as suggested in standard EN 10456:2007.

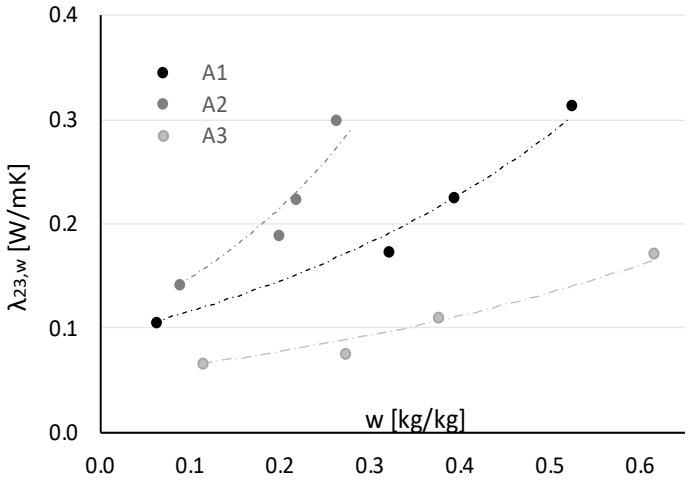

Exponential correlation curves

A1 $\lambda_{23,w}=\lambda_{23,50}*e^{(2.2448*(w-w_{23,50})}$ $R^2=0.995$
A2 $\lambda_{23,w}=\lambda_{23,50}*e^{(3.7322*(w-w_{23,50})}$ $R^2=0.971$
A3 $\lambda_{23,w}=\lambda_{23,50}*e^{(1.8171*(w-w_{23,50})}$ $R^2=0.977$

with
$\lambda_{23,w}$: Thermal conductivity [W/mK], at 23°C, moisture content- dependent
$\lambda_{23,50}$: Thermal conductivity [W/mK], at 23°C, 50% RH
w : moisture content [kg/kg]
$w_{23,50}$: moisture content [kg/kg] at reference conditions 23°C, 50% RH.

Figure 4.12 – Thermal conductivity of thermal mortars at different water contents and 23°C. On the left, the graphic presents the measured data (grey and black points) and the exponential regression curves correlating thermal conductivity and water content for each thermal mortar (dashed lines). On the right, the expression and coefficient of determination of the curves are reported.

4.5.3. SORPTION ISOTHERM

4.5.3.1 STANDARD SAMPLES: SMALL DISK SAMPLES OF SINGLE MATERIALS AND APPLIED PAINTS

Figures 3.13a and 3.13b show the Sorption isotherms obtained via laboratory testing, in comparison with some results found in the literature. Cork-based mortars (A1, A2) show very similar curves while EPS-based mortar (A3) has a lower moisture absorption at all steps of relative humidity. This difference is probably due to the difference in open porosity between the first two mortars and A3, and to the hydrophobic nature of EPS. The literature indeed indicates that EPS has a lower moisture content than cork along the whole sorption curve (Figure 4.13a). Regularization mortars B1 and B2 have similar moisture absorption at all steps of RH, with small but noticeable differences at 70% and 80% RH. The effect of paint C1 on regularization mortar B1 is to lower its moisture content to a very small extent, which appears to be relevant only at 95% RH. On the contrary, silicate paint C2 noticeably reduces the moisture absorbed by the sample, from 70% RH on. The results obtained for cork-based mortars are in agreement with the water content measured for a lime-cork mortar at 23°C, 80% RH by Walker and Pavía (2015). Similarly, the moisture contents obtained for thermal mortar A3 and regularization mortars B1 and B2 are close to the values observed at 80% and 90% RH by Maia, Ramos, and Veiga (2018) for a mixed binder mortar with and without EPS aggregates, respectively. Detailed results obtained with single materials and regularization mortars finished with paints are reported in Table 4.6 and they are the ones adopted for the database for numerical simulations.

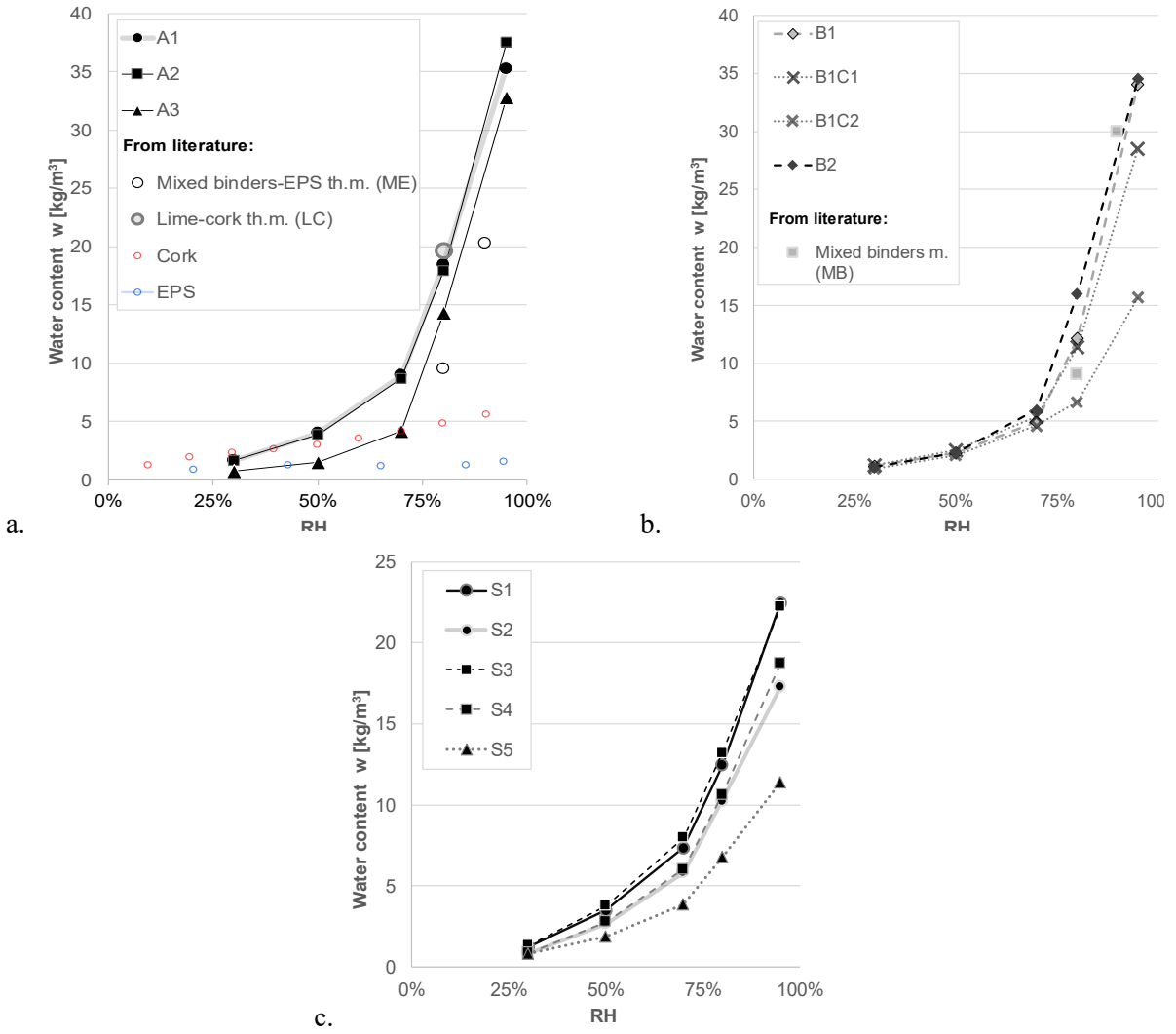

Figure 4.13 – Sorption isotherms of (a) thermal mortars, (b) regularization mortars with and without paints and (c) whole systems, compared to other results from the literature: cork and EPS (Hansen 1986), ME, MB (Maia, Ramos, and Veiga, 2018) and LC (Walker and Pavía, 2015).

4.5.3.2 TILE SAMPLES: SAMPLES OF COMPLETE SYSTEMS.

Sorption isotherms of complete systems are reported in Figure 4.13c.

Systems S1 (A1+B1+C1) and S3 (A2+B1+C1) show very similar behaviour, which was expected since they are regularized and finished with the same materials, and their base thermal mortars also have very similar sorption isotherms. Likewise, systems S2 (A1+B1+C2) and S4 (A2+B1+C2) present comparable moisture contents along all their sorption curves, as readable in Table 5. Furthermore, systems finished with paint C1 have higher sorption isotherms than the ones painted with C2, and S5 has the lowest equilibrium moisture content throughout the whole test.

Table 4.6 – Sorption isotherms, experimental results.

	Volumetric water content, w [kg/m^3]					
At RH :	***30%***	***50%***	***70%***	***80%***	***95%***	
A1	1.643 ± 0.0060	3.98 ± 0.041	9.0 ± 0.1	18.4 ± 0.25	35.3 ± 0.56	
A2	1.66 ± 0.034	3.87 ± 0.038	8.7 ± 0.16	17.9 ± 0.35	37.5 ± 0.91	
A3	0.74 ± 0.031	1.53 ± 0.033	4.16 ± 0.075	14.3 ± 0.22	33 ± 1.1	
B1	1.11 ± 0.015	2.29 ± 0.018	4.92 ± 0.082	12.2 ± 0.21	34.1 ± 0.92	
B1C1	1.20 ± 0.058	2.49 ± 0.079	5.4 ± 0.21	11.4 ± 0.46	29 ± 1.4	
B1C2	0.92 ± 0.018	2.09 ± 0.018	4.64 ± 0.051	6.7 ± 0.13	15.7 ± 0.38	
B2	1.06 ± 0.037	2.29 ± 0.031	5.99 ± 0.034	16.0 ± 0.25	34.6 ± 0.75	
S1	1.23 ± 0.038	3.5 ± 0.10	7.3 ± 0.22	12.4 ± 0.32	22 ± 1.8	
S2	0.85 ± 0.045	2.7 ± 0.12	5.8 ± 0.22	10.2 ± 0.30	17.3 ± 0.48	
S3	1.31 ± 0.019	3.76 ± 0.048	7.96 ± 0.090	13.2 ± 0.15	22.3 ± 0.32	
S4	0.87 ± 0.051	2.79 ± 0.091	6.0 ± 0.15	10.6 ± 0.12	18.8 ± 0.15	
S5	0.80 ± 0.015	1.86 ± 0.023	3.87 ± 0.039	6.75 ± 0.091	11.4 ± 0.18	

4.5.4. RESISTANCE TO WATER VAPOUR DIFFUSION

4.5.4.1 STANDARD SAMPLES: DISK SAMPLES OF SINGLE MATERIALS AND APPLIED PAINTS.

The vapour resistance factors obtained with standard disk samples are shown in Figure 4.14 and Table 4.7. The results obtained with the wet-cup method are lower than with the dry-cup. This outcome is characteristic of hygroscopic materials, as they experience an increase in moisture transport at high relative humidity, because of the contribution of liquid transport effects (Künzel,1995; Trechsel, 1994). With each method, thermal and regularization mortars show similar vapour resistance factors, all in the order of magnitude 10-20, which is coherent with the fact that they have comparable open porosities.

With the wet-cup settings, all thermal mortars (A1, A2, A3) comply with the restriction of EN 998-1:2017, which defines a maximum vapour resistance factor of 15 for thermal mortars. For other rendering and plastering mortars, the standard only requires that materials have a μ that is equal to or lower than the one declared by the manufacturer. In this regard, mortar B1 shows, at wet testing conditions, a resistance factor that agrees with the value declared by the manufacturer, i.e. $\mu \leq 15$. On the contrary, mortar B2 and all thermal mortars have resistance factors that are more than double the declared value ($\mu_{declared} \leq$ 4-5), at wet conditions.

Even though paints C1 and C2 are both declared to be “breathable”, they give very different results when applied on samples of regularization mortar. C1 has a negligible effect (a maximum of 5% increase in μ of the finished sample) while C2 causes a strong increase of the resistance factor of the samples, especially at dry conditions (5 times higher μ than in the unfinished specimens). Hence, silicate-paint C2 shows much higher resistance to vapour diffusion than lime-paint C1.

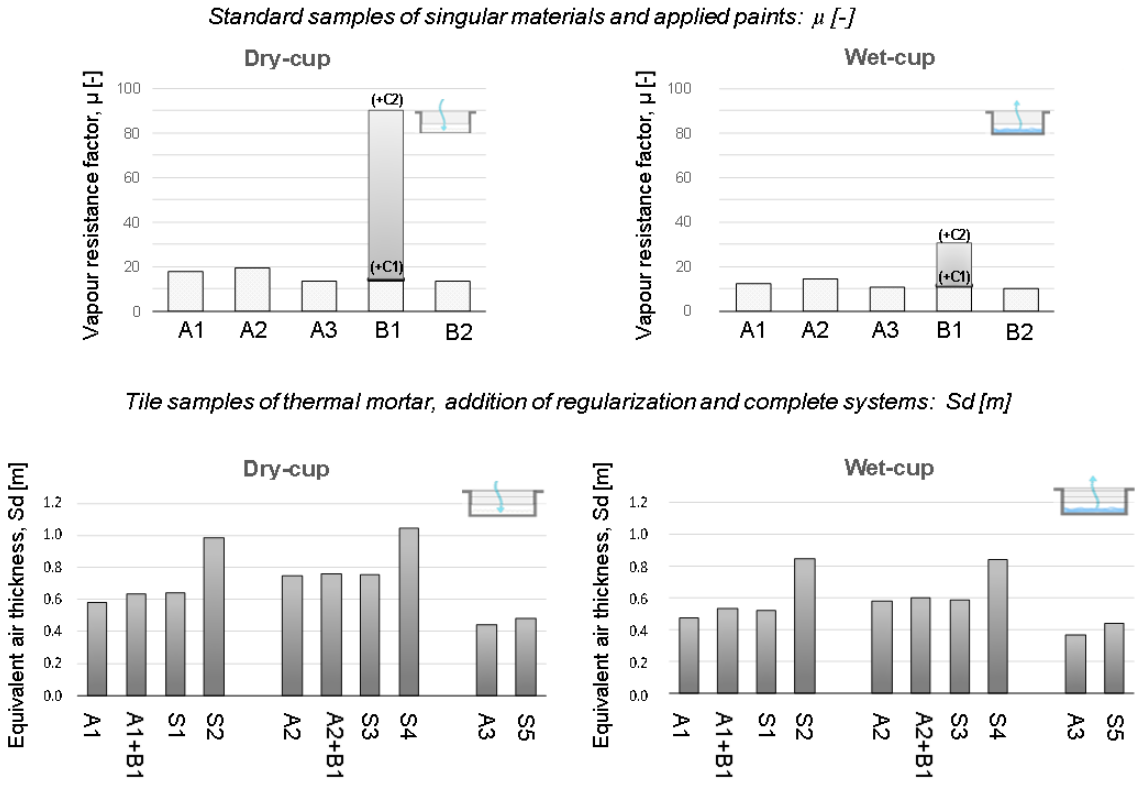

Figure 4.14 - Resistance to water vapour diffusion, experimental results.

The results obtained for regularization mortars are aligned with a previous study on cement-based mortars, where industrial and traditionally prepared mixes gave μ-values of about 8.2-14 and 18, at wet testing conditions (Flores-Colen et al., 2016). Furthermore, the results obtained have the same order of magnitude of the resistance factors observed by Veiga et al. (2010) with mortars based on cement and air lime, i.e. μ-values in the range of 4.6-6.0. The vapour resistance factors obtained with the specimens of thermal mortars are similar to those observed in previous studies, i.e. 7.5-13.5 for cork and EPS thermal renders (Maia, Ramos, and Veiga, 2018) and around 10-20 for hemp-lime plasters (Mazhoud et al., 2016), at dry testing conditions.

On the other hand, the experimentally observed results are worse (higher resistance to vapour diffusion) than the ones obtained in a study (Corinaldesi, Donnini, and Nardinocchi, 2015) on thermal mortars made of various binders, glass fibre reinforced polymer powder (GFRP) and air-entraining additives, i.e. μ-values in the range of 1.2-6.6. In this case, the authors inferred that the combined use of additives and GFRP powder improved the level of entrapped air in the mortars, which is probably why they obtained much better results than the ones hereby observed with thermal mortars which have a moderate open porosity.

The s_d measured for paints (applied on regularization mortar B1, as showed in Table 4.7) is in agreement with the results obtained in other studies where various silicate-paints were tested at wet conditions (s_d around 0.4-0.6m) (Šadauskiene, Monstvilas, and Stankevičius, 2007) and lime-paints were analysed with the dry-cup method (s_d of about 0.01-0.03m) (Brito, Gonçalves, and Faria, 2011).

4.5.4.2 TILE SAMPLES: SAMPLES OF THERMAL MORTAR, ADDITION OF REGULARIZATION, AND COMPLETE SYSTEMS.

The water-vapour diffusion-equivalent air layer thickness (s_d) measured with tile samples is reported in Figure 4.14.

The results obtained with both the dry and wet-cup show that the addition of regularization mortars (B1, B2) and lime-paint C1 leads to very small increases of s_d, with a maximum difference of about 10% between the samples of thermal mortars and the ones completed with B1 and C1. By contrast, the use of silicate-paint C2 causes a high increase of s_d: systems S2 and S4 have about 40% to 50% higher s_d-values than unfinished samples. Nonetheless, all systems do comply with the threshold value indicated by the EAD for ETICS (EOTA, 2020), i.e. $s_d \leq 1.0$m at wet conditions (wet-cup with 93% RH in the EAD).

It is worth highlighting that the EAD for ETICS does not set a requirement on the vapour permeability of complete systems, but it does for the s_d of the rendering applied on the insulation. Thus, this is the threshold value hereby adopted as a reference. Furthermore, the maximum s_d recommended by the EAD depends on the type of insulation material adopted, namely cellular plastic or mineral wool. In this study, the value considered is the one set for mineral wool-based insulation as it is a vapour-permeable material, similarly to the thermal mortars hereby considered.

The detailed results obtained for tile samples, as well as the resistance of the paints indirectly measured, are reported in Table 4.7.

The s_d obtained for paints confirms that C2 is much less permeable than C1: according to EN 1062-1:2004 , the vapour permeability of the two paints can be respectively classified as medium (V_2: $0.14 \leq s_d < 1.4$) and high (V_1: $s_d \leq 0.14$). The magnitude of the results is consistent with the outcomes of previous studies: s_d values in the range of 0.4-0.6m were measured for various silicate-paints by Šadauskiene, Monstvilas, and Stankevičius (2007) and increases of 0.01-0.03m in the s_d of samples were detected when two types of lime-paints were applied to them, by Brito, Gonçalves, and Faria (2011).

Similar but not completely compatible results are observed with paints applied in different systems. On one hand, the results obtained for the s_d of paint C1 from samples of system S1 and S2 are compatible. On the other hand, the results obtained for C2 from samples of S2 and S4 are compatible only at dry conditions. This fact can be related to the higher uncertainties that are involved in the wet-cup method, which is considered less reliable than the dry-cup because of the sensitivity of the results to changes in relative humidity and surface resistance at the inside-exposed surface of the samples (Trechsel 1994).

The results obtained for the systems are similar to those observed in a previous study on insulation solutions based on thermal mortars with EPS and cork aggregates (Maia, Ramos, and Veiga, 2018). In this study, the authors obtained s_d of about 0.4-1.2m and 0.4-1.0m, at dry and wet test conditions, respectively (results approximatively converted from the original values referring to 20mm-thick samples, by adopting a conversion factor of 2). Comparable results were also obtained in a study on an aerogel render-based solution (Pedroso et al., 2020), where the equivalent air thickness of the whole system, finished with impermeable epoxy paint, was about 1.0m at dry conditions (value roughly converted from the original result referring to 25mm-thick samples). Finally, it is worth highlighting the scarcity of literature considering the vapour permeability test on complete insulation systems based on thermal mortars, which is probably a consequence of the standard requirements of EN 998-1, which does not account for the behaviour of complete systems, but only single mortars.

Table 4.7 - Resistance to water vapour diffusion, experimental results

Standard samples of single materials and applied paints												
Direct measures						*Indirect measures (difference with substrate)*						
Vapour resistance factor, μ [-]						*Equivalent air thickness of paints, Sd [m]*						
	Dry - cup			*Wet - cup*				*Dry - cup*			*Wet - cup*	
A1	**17.8**	±	0.97	**12.1**	±	0.19						
A2	**19.1**	±	0.68	**14.3**	±	0.06						
A3	**13.3**	±	0.82	**10.7**	±	0.98						
B1	**13.6**	±	0.36	**11.1**	±	0.07						
B1+C1	**14.3**	±	0.46	**11.2**	±	0.91	→ **Sd_C1**	**0.020**	±	0.0090	**0.01**	± 0.010
B1+C2	**90**	±	14	**30.4**	±	2.2	→ **Sd_C2**	**1.5**	±	0.26	**0.38**	± 0.041
B2	**13.2**	±	0.18	**10.1**	±	0.18						
Tile samples - thermal mortar, addition of regularization and complete systems.												
Direct measures						*Direct* and Indirect measures (difference with substrate)*						
Equivalent air thickness, Sd [m]						*Vapour resistance factor of mortars, μ [-]* *Equivalent air thickness of paints, Sd [m]*						
	Dry - cup			*Wet - cup*				*Dry - cup*			*Wet - cup*	
A1	**0.58**	±	0.014	**0.47**	±	0.016	→ **μ_A1***	**14.6**	±	0.29	**12.0**	± 0.49
A1+B1	**0.633**	±	0.0092	**0.533**	±	0.0044	→ **μ_B1**	**20**	±	2.4	**12**	± 1.8
S1	**0.642**	±	0.0013	**0.519**	±	0.0008	→ **Sd_C1**	**0.058**	±	0.0042	**0.035**	± 0.0016
S2	**0.98**	±	0.037	**0.84**	±	0.019	→ **Sd_C2**	**0.41**	±	0.039	**0.37**	± 0.022
A2	**0.747**	±	0.0090	**0.584**	±	0.0080	→ **μ_A2***	**18.8**	±	0.26	**14.7**	± 0.22
A2+B1	**0.759**	±	0.0080	**0.60**	±	0.013	→ **μ_B1**	**16**	±	1.8	**15**	± 2.7
S3	**0.75**	±	0.017	**0.59**	±	0.026	→ **Sd_C1**	**0.048**	±	0.0071	**0.04**	± 0.019
S4	**1.04**	±	0.058	**0.84**	±	0.018	→ **Sd_C2**	**0.33**	±	0.062	**0.28**	± 0.024
A3	**0.44**	±	0.020	**0.37**	±	0.016	→ **μ_A3***	**11.0**	±	0.52	**9.2**	± 0.44
S5	**0.48**	±	0.010	**0.40**	±	0.014	→ **μ_B2**	**16**	±	3.0	**14**	± 3.5

*For A1, A2, and A3, the vapour resistance factor is directly measured from the results obtained with tile samples made of thermal mortars. For regularization mortars (B1, B2) and paints (C1, C2) the results are obtained indirectly.

4.5.4.3 STANDARD AND TILE SAMPLES: COMPARISON OF RESULTS AND VALUES SELECTED FOR THE DATABASE FOR NUMERICAL SIMULATIONS.

The vapour resistance factors of mortars, obtained from tile and standard samples, are provided in Table 4.7. Results show that the resistance factors have some variability according to the type of samples adopted. In particular, the results obtained with tile specimens of thermal mortars were very similar to

the ones resulting from testing disk samples (2%-18% differences at dry conditions). Thus, the difference in geometry and construction of samples via double layering does not appear to have affected the results to a relevant extent. For regularization mortars, the differences are more important, with tile samples giving, 20-30% higher s_d than standard ones. In this case, the application of the mortars on a porous substrate and the definition of the results by indirect measurement had a more evident influence on the test outcomes; however, results are still comparable. A much more important difference is found between the results obtained for paints applied on disk and tile supports, especially for paint C2, whose s_d is about 4-times higher with disk samples than with tile ones.

In summary, the different samples adopted (standard disks and layered tiles) gave quite comparable results for the resistance to water vapour of mortars and very different results for paints, especially C2. This outcome appears coherent with the observations presented in previous studies which stated that:

- the permeability to water vapour of paints can noticeably depend on the substrate adopted (Ramos, Delgado, Freitas, 2010);

- the use of layered samples of mortars can affect the porosity of the specimen, because of the suction that the first hardened layer (porous support) may exert on the water contained in the fresh mortar applied on it (Torres, Veiga, and Freitas, 2018).

Thus, samples obtained from moulds (standard samples) and from the application of successive layers of mortars (composite tile samples) can show differences in their physical properties, potentially leading to different vapour permeability of the paint-layer applied on them. The geometry of the samples may have also played a role in leading to different results with different types of samples. However, given that specimens of the same material (thermal mortars) gave quite comparable results, regardless of the shape of the samples (disks and tiles), the influence of the geometry is considered of minor importance.

Even though the results obtained with standard disk samples offer higher accuracy, thanks to the direct measurements performed, the values obtained indirectly for single materials, from tile samples, are selected for the database for numerical simulations. Indeed, layered tile samples, and the results obtained with their use, are considered to be more representative of real applications. For B1, C1 and C2, the resistance to water vapour selected for the database for numerical simulations is the average of the results obtained from the application on different substrates (substrates A1 and A2 for application of B1, substrates A1+B1 and A2+B1 for paints C1 and C2).

4.5.5. CAPILLARY WATER ABSORPTION

4.5.5.1 STANDARD SAMPLES: PRISM SAMPLES OF SINGLE MATERIALS

The capillary water absorption curves obtained for single materials are presented in Figures 3.15a and 3.15b. Lime-cork mortars A1 and A2 have absorption rates that are in line with their open porosities, meaning that the higher the open porosity, the faster the water absorption. Concerning thermal mortar A3, it shows a different behaviour, having a higher water content than mortar A2 in the first hours of the test. This result suggests that even though A3 has a lower total volume of interconnected pores than A2, it has a higher share of them in the large capillary range (Thomson et al., 2004). This behaviour is clearly readable in the capillary water absorption coefficients reported in Figure 4.15c, where A3 has a higher absorption rate than A2 in the first 5 measurements and a lower one at 24 hours. From 24 hours on, A3 shows the lowest water content among the tested materials, which is probably the result of both

the reduced porosity of the material and the hydrophobic nature of EPS aggregates. In addition, this outcome is aligned with the results obtained by Gomes et Al. (2019), who observed a significantly higher reduction of water absorption in mortars containing EPS than in those containing cork aggregates.

Regularization mortars B1 and B2 have similar open porosities, i.e. around 31%, but they have very different absorption rates: at 24 hours, the water content of mortar B1 is almost four times higher than in mortar B2. The reduced water absorption of the latter material can be explained by the presence of hydrophobic agents, which is very likely since B2 is designed for direct exposure to outdoor climate.

The capillary water absorption coefficients determined with the three different methods specified in EN 15801, EN 1015-18 and the EAD for ETICS are presented in Figure 4.15c. In all cases, the value obtained with the first 5 measurements (A_{w_Reg5}) is the highest, and the value that accounts for the average absorption rate at 24hours is the smallest (A_{w24}). This result clearly shows that the absorption curves have slopes that flatten with time, meaning that the absorption rate decreases while passing from dry to saturated conditions. Furthermore, it emerges that the coefficient obtained at 24 hours is not representative of the materials analysed, as some of them (A3 and B1) reach saturation before this time.

The coefficients A_{w_Reg5} and the coefficient of determination of the regression lines are also reported in Figure 4.15c. According to these results, mortars A2, A3 and B2 have an absorption coefficient lower than 0.40 kg/(m^2.$min^{1/2}$), and thus they belong to the absorption class W1, while A1 and B1 belong to the class W0 of standard EN 998-1. Mortar A1 does not comply with standard requirements as the coefficients determined with the three methods are all above the reference threshold value recommended for thermal mortars (0.40 kg.m^{-2}.$min^{-1/2}$). This result is likely to be related to the low open porosity experimentally obtained, which suggested a lack of efficacy of the air-entraining admixtures, with consequent reductions of the macropores in the mortar, as well as of their effect on lowering the capillary water absorption coefficient of the material (Corinaldesi, Donnini, and Nardinocchi, 2015).

Standard EN 998-1 does not indicate restrictions on the water absorption of mortars for general renders and plasters, like B1 and B2, allowing all types of absorption coefficients for them. Regularization mortar B1 has the highest capillary absorption coefficient among the analysed materials, as expected. It is in fact declared to be above 0.4 kg/(m^2 $min^{1/2}$) in its technical sheets.

Mortars A3 and B2 have a declared capillary absorption coefficient of less than 0.2 kg/(m^2 $min^{1/2}$), which is not far from the A_{w_Reg5} obtained and, additionally, it is in strong agreement with the $A_{w\_10\_90}$ determined, which is the type of coefficient declared in technical sheets, according to standard EN998-1 and EN1015-18.

The absorption coefficient obtained for A1 is higher than the manufacturer's declared value, while the coefficient obtained for mortar A2 is lower. These discrepancies are imputable to a different method of preparation of the samples between this study and the one carried out by the manufacturers (e.g. spatula or spray application of mortars) with consequent differences in physical properties, as already observed when analysing the results of open porosity.

The results obtained for the mortars analysed are similar to the ones observed by Maia, Ramos and Veiga (2018). The authors reported coefficients of 0.1-0.23 kg/(m^2 $min^{1/2}$) for thermal renders with cork and EPS aggregates and 0.05-1.6 kg/(m^2 $min^{1/2}$) for regularization mortars. Other authors observed great variability in the results obtained with industrial thermal mortars with cork and EPS (Gomes et al., 2019), namely 0.2-1.0 kg/(m^2 $min^{1/2}$).

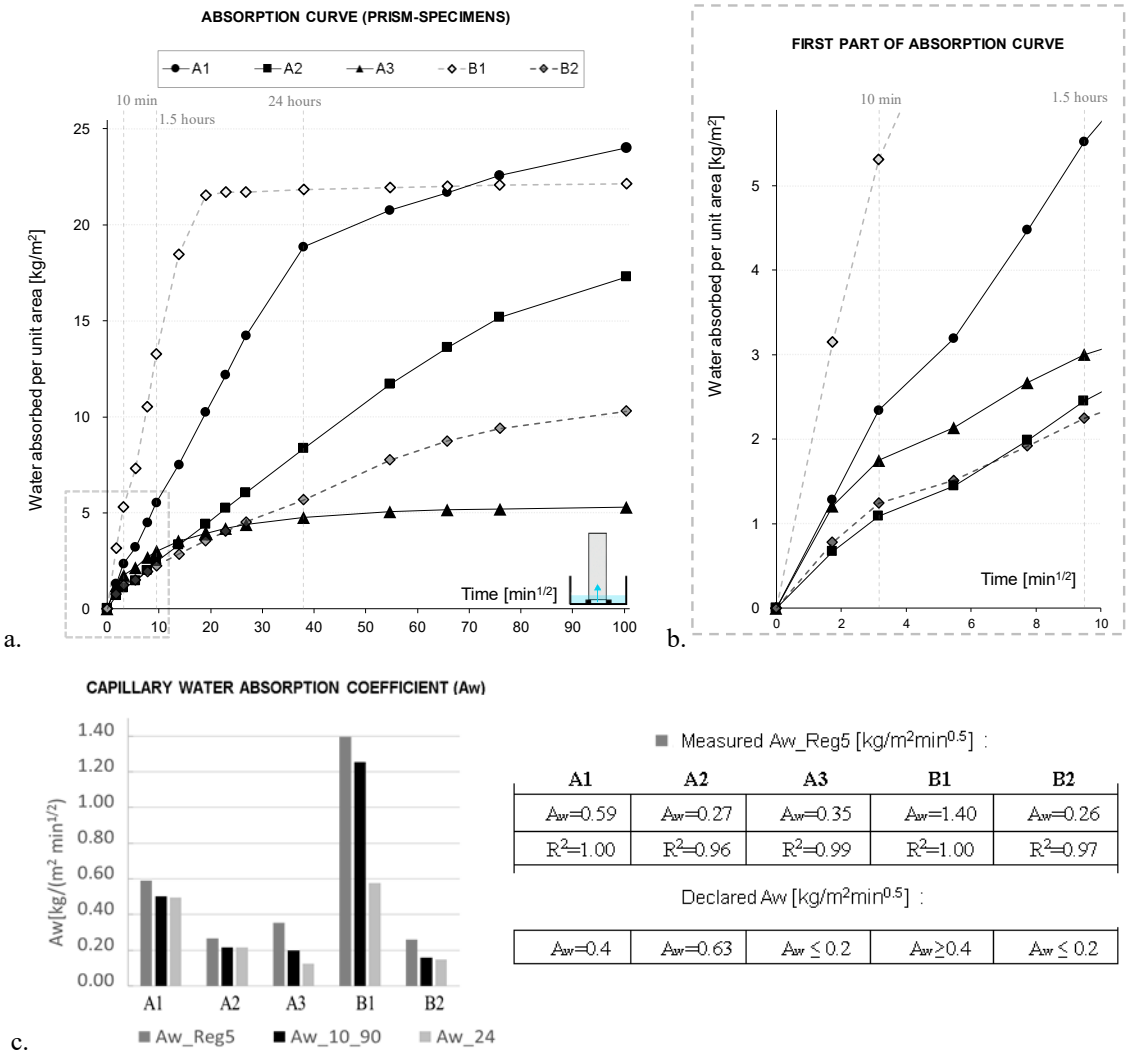

Measured Aw_Reg5 [kg/m²min^0.5] :

A1	A2	A3	B1	B2
A_w=0.59	A_w=0.27	A_w=0.35	A_w=1.40	A_w=0.26
R^2=1.00	R^2=0.96	R^2=0.99	R^2=1.00	R^2=0.97

Declared Aw [kg/m²min^0.5] :

A_w=0.4	A_w=0.63	$A_w \leq 0.2$	$A_w \geq 0.4$	$A_w \leq 0.2$

Figure 4.15 –Capillary absorption curves of single materials (prism specimens).

4.5.5.2 TILE SAMPLES: SAMPLES OF THERMAL MORTARS, ADDITION OF REGULARIZATION, AND COMPLETE SYSTEMS.

Water absorption curves obtained for tile specimens of whole systems are presented in Figures 3.16a and 3.16b. Results show that systems S2 and S4 have much smaller water content than S1 and S3, throughout the whole test. This difference is clearly related to the different use of paints: C2 in S2 and S4, C1 in S1 and S3. This outcome confirms the water-repellent nature of C2, which is indeed designed to finish outdoor-exposed components. Regarding S5, the system is designed for both indoor and outdoor exposure. It shows a high water content in the first 45 minutes of the test, which is similar to the moisture content in systems S1 and S3. From that point on, S5 has a lower water content than S1 and S4, and it reaches saturation before 24 hours, with the lowest saturation water content per unit area of all the systems. Hence, S5 shows very reduced moisture content in the long run, but not in the first hour of wetting. For this reason, it is a system that may experience high water absorption when subjected to short periods of rain.

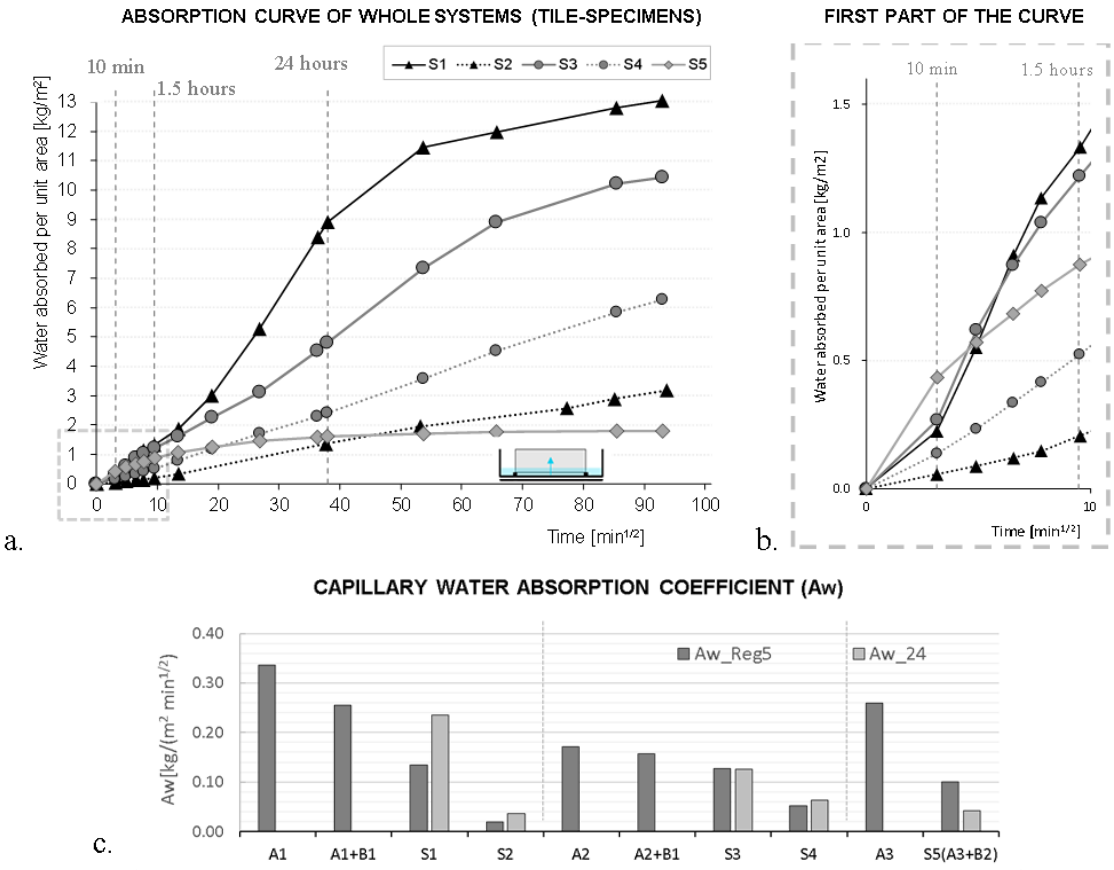

Figure 4.16– Capillary water absorption, results obtained with tile samples.

In Figure 4.16c, the coefficients obtained at 24 hours for whole systems are presented (A_{w_24}). All systems designed for outdoor exposure, i.e. S2, S4 and S5, exceed the limitations recommended by the EAD for ETICS, which is an A_{w_24} lower than 0.013 kg/(m^2 min$^{1/2}$), explicitly indicated in the EAD as a maximum water content of 0.5kg/m^2 at 24hours. The coefficients obtained at 24 hours for the systems indicate that C1 can be ranked as highly water permeable ($A_{w\_24} > 0.065$ kg.m^{-2}.min$^{-1/2}$) and C2 as mediumly permeable (0.065 kg.m^{-2}.min$^{-1/2} \geq A_{w_24} > 0.013$ kg.m^{-2}.min$^{-1/2}$), according to standards EN 1062-1:2004 and EN 1062-3:2008 for paints and varnishes.

The capillary absorption contents obtained with the regression line through the first 5 measurements (A_{w_Reg5}) with all tile samples (thermal mortars, thermal mortar and regularization, and whole systems) are reported in Figure 4.16c as well, and they are discussed in comparison with the results obtained for standard prism samples in the following section. It is worth highlighting that the A_{w_Reg5} reported in Figure 4.16c for mortar A3 was calculated considering only the first three points of the absorption curve, due to the fact that tile samples of A3 appeared to get close to saturation after the third measurement.

Results obtained with complete systems designed for outdoor exposure (S2, S4 and S5) appear to perform worse than the solutions considered in previous studies on thermal rendering systems, where much lower capillary absorption coefficients were measured. Indeed, Maia, Ramos and Veiga (2018) observed water absorption coefficients as low as 0.012 kg/(m^2 min$^{1/2}$) with solutions based on industrial

thermal renders with cork and EPS, while a coefficient of 0.010 kg/(m^2 min$^{1/2}$) was measured by Pedroso et Al. (2020) with an aerogel render-based solution finished with impermeable epoxy paint.

Finally, it is worth highlighting the scarcity of literature considering the capillary water absorption test on complete insulation systems based on thermal mortars. Also in this case, the lack of literature is considered to be a consequence of the standard requirements of EN 998-1, which does not account for the behaviour of complete systems, but only single mortars.

4.5.5.3 STANDARD AND TILE SAMPLES: COMPARISON OF RESULTS AND VALUES SELECTED FOR THE DATABASE FOR NUMERICAL SIMULATIONS.

The coefficients obtained for thermal mortars with tile samples (A_{w_Reg5}) are noticeably smaller than the ones obtained with prism specimens (35% to 75% reductions). This result reflects the differences in the geometry of the samples and their construction, as the tile-shaped ones are prepared with two successive layers of thermal mortar, a construction that tends to reduce water absorption according to a study from Silveira et Al. (2020) on cement mortars. With this type of preparation, each layer (from the second one on) is applied on a previously hardened one, which acts as a porous substrate. As explained by different authors (Silveira et al., 2020; Torres, Veiga, and Freitas, 2018), the suction exerted by a porous substrate on the water contained in the layer of fresh mortar causes a pore tightening in this material, which has an effect on its water absorption capabilities. The authors also indicate that the higher the porosity of the substrate, the stronger it affects the applied mortar, which is consistent with the result hereby presented. Indeed, A1 has the highest open porosity and the strongest decrease of absorption coefficient from prism to tile samples, i.e. about 75%, followed by A2 and A3 with reductions of around 55% and 35%. Furthermore, the construction by successive layers gives rise to the presence of interfacial hygric resistances in-between, which can further reduce liquid water transport (Delgado, Freitas, and Guimarães, 2016, Guimarães et al., 2018).

A similar reduction of capillary absorption is likely to affect also the performance of regularization mortars. Indeed, although a high absorption coefficient is observed with prism samples of B1, the application of this mortar on samples of thermal mortars A1 and A2 do not imply an increase in the water absorption coefficient of the samples, but quite the opposite. This result suggests a reduction in the absorption capabilities of B1, due to the application on a porous support, together with the presence of interfacial hygric resistances between successive layers in the assembly.

The capillary water absorption coefficients considered for the database for numerical simulations are those obtained from the regression line through the first five measurements. This choice is taken to avoid underestimating the absorption of liquid water during short periods of rain. This aspect is indeed very relevant as moisture is the most important in-service degradation agent (Flores-Colen et al., 2016), and it can lead to serious damage in the walls (Stigl Freitas et al., 2020). For thermal mortars, the results obtained with tile samples are the ones selected, as they appear more representative of real applications. For regularization mortars, the A_w can not be extrapolated from the results obtained with tile-layered samples, thus the value adopted is the A_{w_Reg5} of standard specimens. For paints, the results obtained with the application of the two finishings on tile samples (complete systems) are adopted. In particular: for C1 the value is obtained from the average A_{w_Reg5} of systems S1 and S3, and C2 is taken as the average of systems S2 and S4.

4.5.6. DRYING

4.5.6.1 TEST ON PRISM SAMPLES: SINGLE MATERIALS

The drying curves obtained with prism samples are displayed in Figure 4.17. In the same picture, a histogram shows their drying rates in the first and second phases of the process, which were calculated, respectively, with the results of the first 5 hours and between 280 and 360 hours.

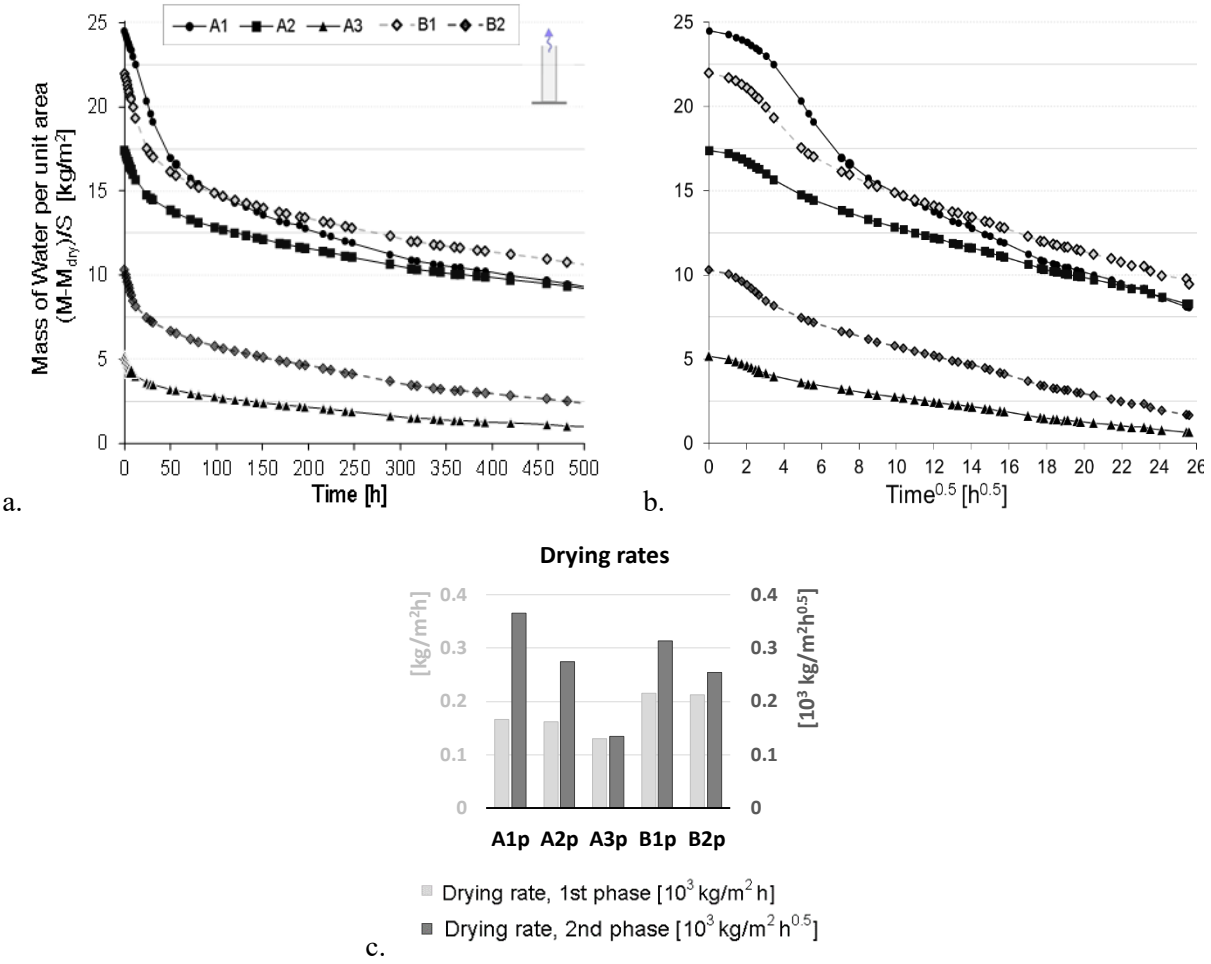

Figure 4.17 – Drying curves (with time, a, and square root of time, b, on the x-axis) and rates obtained with prism samples (c).

All materials appear to have similar drying curves, except for thermal mortar A1, which has an evidently steeper decrease of water content, during the second drying phase, as confirmed by the drying rates.

During the first phase of drying, regularization mortars B1 and B2 have the highest drying rates, followed by thermal mortars A1 and A2. Thermal mortar A3 has the lowest one. In the second drying phase, the highest rate is the one of thermal mortar A1, and A3 has the smallest.

Despite having the worst drying rates, A3 is the material with the lowest final water content, thanks to its small initial moisture. On the contrary, B1 and A1, which are the materials with the better drying rates, in the first and second phases respectively, end up having the highest water contents at the end of the test, because of their high initial water content.

In order to take into account both the saturation water content and the drying behaviour, the saturation degree decrease of the specimens during the drying test is reported in Figure 4.18. Since the beginning of the drying test, mortars A3 and B2 have a faster decrease of saturation degree than mortars A1, A2 and B1: after 1 day the first two materials are under 75%, while the latter mortars are still at 80-85%. This difference increases with the drying time, with B2 and A3 having a saturation degree lower than 25% after 20 days of drying, while A1, B1 and B2 stay at about twice as much, with saturation degrees ranging 40-54%.

Among thermal mortars, A1 shows the best drying rates while A3 has the best behaviour in terms of saturation degree decrease: meaning that A1 is the material that dries out faster but mortar A3 is the one that is best able to stay at low saturation degrees thanks to its low free saturation water content. Similarly, taking into account regularization mortars, B1 has the best drying rates, while B2 shows the fastest saturation degree decrease, thanks to its small initial water content. This outcome suggests that A1 and B1 may perform better than the other materials when applied at the interior side of walls, where moderate water contents are expected, so that the material stays at low saturation degrees and dries out fast. Similarly, A3 and B2 are expected to perform better than the other materials when applied at the exterior side of walls, where high water contents may arise.

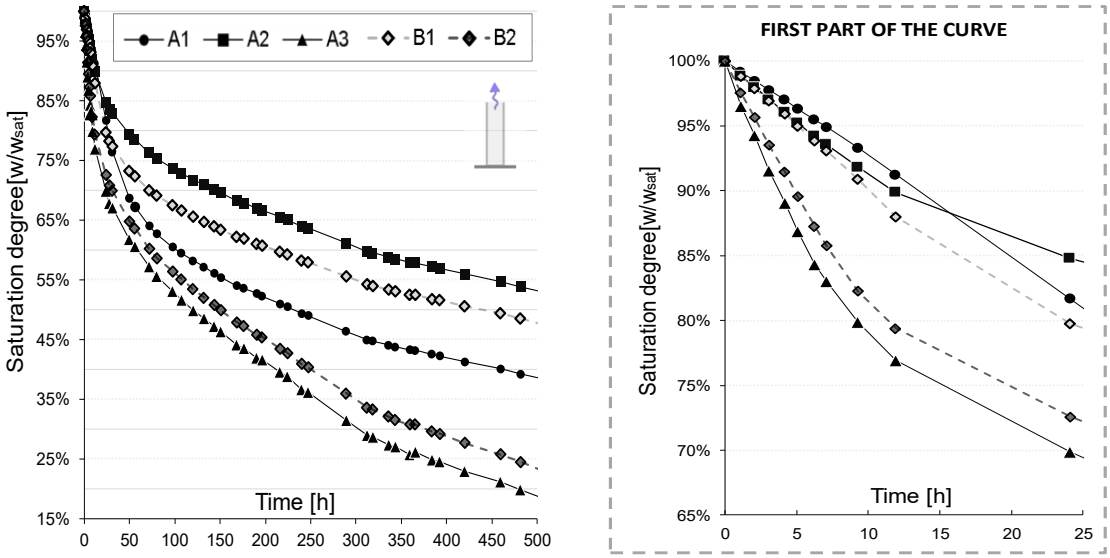

Figure 4.18 – Saturation degree during drying - prism samples.

4.5.6.2 TESTS ON TILE SAMPLES: WHOLE-SYSTEMS, COMBINED MATERIALS AND SINGLE MATERIALS

The drying curves of whole systems and the drying rates obtained with all tile samples (thermal mortars, combined materials, whole systems) are reported in Figure 4.19.
Systems S2 and S4, which are designed for outdoor exposure, show lower drying rates than systems S1 and S3, as well as higher saturation degrees through the whole test. This result is coherent with the lower capillary absorption and higher resistance to vapour diffusion of the first two systems, which entails reduced moisture-transport capabilities during drying. System S5, which is designed for indoor and outdoor applications, shows low drying rates, especially in the second phase of drying but it has the best behaviour in terms of saturation degree (Figure 4.20), thanks to its low free saturation water content.

This result is coherent with the outcomes obtained for the single mortars that compose this system, A3 and B2, which were found to have a good drying in terms of saturation degree decrease.

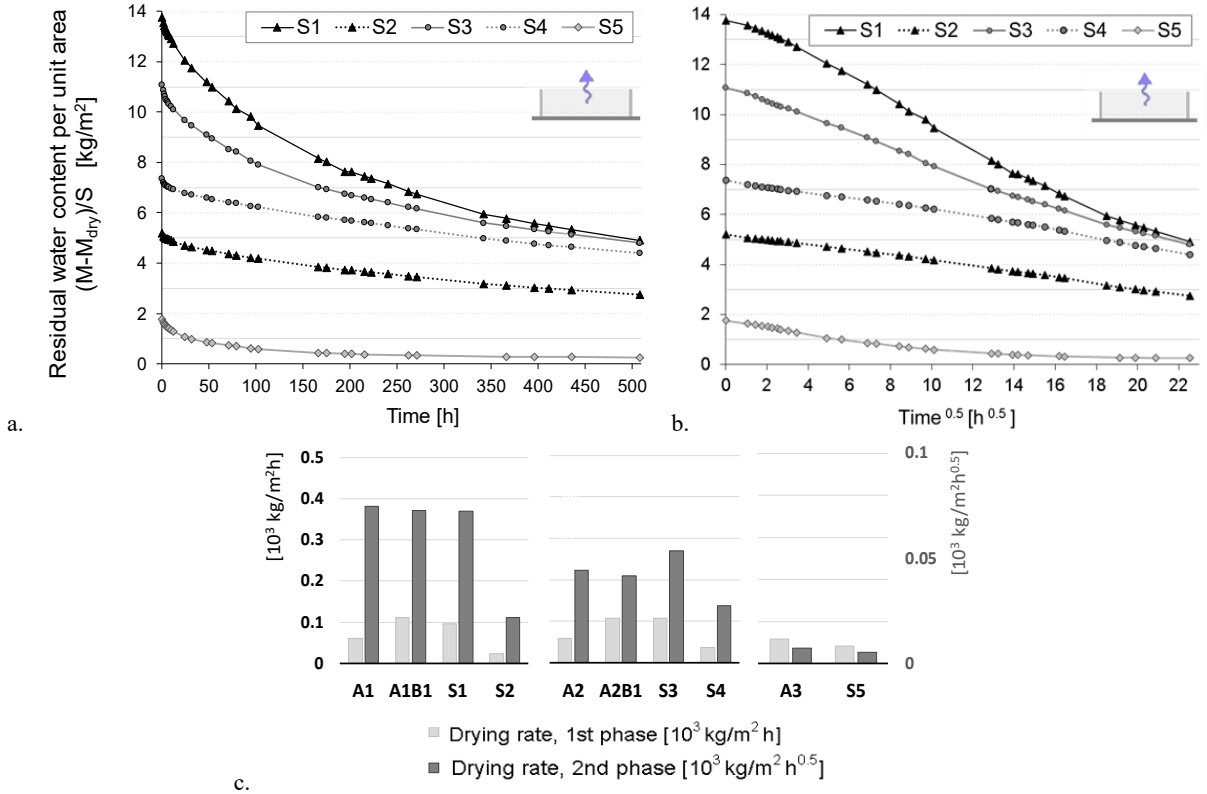

Figure 4.19 – Drying curves (with time, a, and square root of time, b, on the x-axis) and rates obtained wit prism samples (c).

The drying rates reported in Figure 4.19 suggest that the use of finishing C2 slows down the drying of the samples considerably in both drying phases, indeed systems S2 an S3 have much smaller drying rates than the correspondent samples finished with paint C1 and unfinished ones. The results obtained for tile samples of thermal mortars in the first drying phase are lower than the ones obtained with prisms samples, which is likely to be the result of their lower capillary absorption coefficient and the presence of interfacial hygric resistances, which both slow down water movement in the samples. Finally, the addition of regularization mortar B1, as well as paint C1, does not appear to relevantly affect the drying behaviour of the samples.

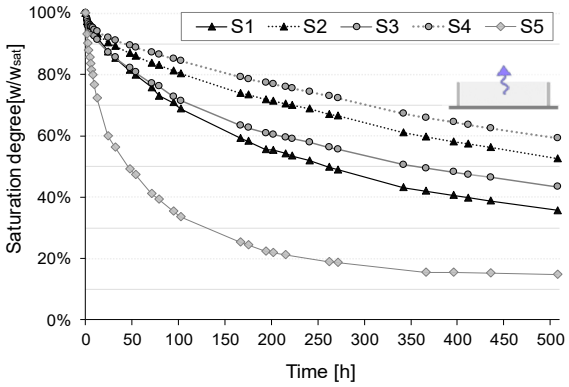

Figure 4.20 – Saturation degree during drying - tile samples.

4.6. DISCUSSION AND SYNTHESIS OF RESULTS

4.6.1. DISCUSSION OF RESULTS

4.6.1.1 RESULTS OBTAINED WITH DIFFERENT TYPES OF SAMPLES

Different types of specimens were adopted for the experimental campaign: standard samples of single and painted materials and tile samples, prepared by layers, which better represent real applications and complete systems. The first typology is based on the European specifications for mortars for masonry EN 998-1 and the second one is aligned with the requirements of the European Assessment Document for ETICS (EAD 040083-00-0404). The results obtained led to the following observations:

- the use of layered-tile and standard samples did not result in relevant differences in terms of vapour permeability of mortars, but it did for paints, especially for C2 at dry conditions. In the latter case, the sd obtained with standard samples was 4-times higher than the one obtained with tiles. This outcome is coherent with a previous study (Ramos, Delgado, and Freitas 2010) which observed that the resistance of paints to vapour diffusion can noticeably depend on the substrate adopted;
- relevant reductions of capillary water absorption were obtained with tile layered samples of thermal mortars, with A_w coefficients 75%-35% lower than in standard samples. Similar differences have been observed also in previous studies (Silveira et al., 2020, Torres, Veiga, and Freitas, 2018) which indicate that sample preparation can affect the physical properties of mortars, especially when they are applied on porous supports (for example the previously hardened layer) that can absorb water from the fresh mortar applied. Furthermore, in samples prepared by successive layers, the effect of hygric resistances at the interfaces (Guimarães et al. 2018) between layers may have further contributed to reducing the capillary water absorption coefficient of the specimens.

These outcomes show that complete insulation systems may have very different moisture transport properties than expected from the characterization of single materials. Thus, it would be beneficial to add some information concerning the behaviour of complete systems, as whole units, in the technical sheets of thermal mortar-based insulation solutions: namely the s_d for all systems, and also the A_w for those designed for outdoor exposure. This additional information would allow designers to make a much more informed choice and to better forecast the realistic impact of the system on the moisture dynamics of the wall, potentially leading to reduced degradation risks and improved durability of the retrofitted components.

4.6.1.2 PROPERTIES OF COMPLETE SYSTEMS

In terms of the properties of complete insulation systems, the following information was obtained:

- systems intended for external application showed a lower capillary water absorption than those designed for interior exposure (S1, S3), due to the reduction of water intake provided by the finishing layer: paint C2 (in system S2, S4) or mortar B2 (in system S5). Nonetheless, the three systems (S2, S4, S5) did not comply with the maximum capillary water absorption defined by the European Assessment Document for ETICS with renderings (EAD 040083-00-0404:2020);
- regularization and finishing may strongly impact the hygric performance of the systems, resulting in characteristics that are very different from those of the insulation layer. For instance, systems

that differ only in the finishing layer (S1-S2 and S3-S4) resulted in having 40%-60% higher sd (at wet conditions) when paint C2 was used instead of C1, even though they were both declared to be "breathable" finishings. This outcome is clearly observable in Figure 4.21, where the capillary absorption coefficient and resistance to vapour diffusion of the complete systems are synthesized;

- the drying rates obtained with tile samples showed that the use of paint can strongly affect the drying of complete systems, indeed systems finished with paint C2 have much lower drying rates than the ones painted with C1 in both the first and second phase of drying.

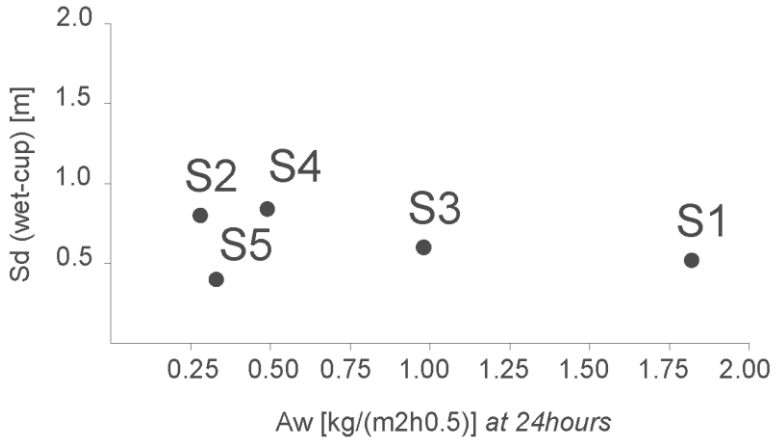

Figure 4.21 – A_w (at 24 hours) and s_d (wet cup) obtained for the complete systems.

4.6.1.3 THERMAL PERFORMANCE AND DEPENDENCY ON WATER CONTENT

The thermal mortars analysed complied with the restrictions set by EN 998-1 for the thermal conductivity of thermal mortars, while they exceeded the maximum value allowed by the EAD for ETICS. Thus, while they have lower thermal insulation capacity than typical ETICS, they still offer much better performance than traditional plasters and renders based on gypsum, lime and cement, and so they appear to be promising for application in climates with moderately cold winters.

Experimental results showed that the influence of water content on thermal conductivity was very significant. This aspect appears to be relevant, and it should be indicated and quantified in the technical sheets of thermal mortars, especially if they are designed for external insulation systems, as they may experience relatively high water content during some periods of the year, which could lead to poor thermal performance. However, the moisture content of exterior systems may be controlled by the use of an adequately water protective paint or coating (Coppola et al. 2019), and this could also be stated in the technical sheets.

4.6.1.4 DIFFERENCES BETWEEN DECLARED AND MEASURED PROPERTIES:

Relevant differences were found between declared and measured properties of lime-cork mortars (A1, A2), especially in terms of thermal conductivity, which ranged from 60% higher to more than twice the declared value. The increase observed is considered to be the result of the following circumstances:

- the lack of efficacy of the air-entraining admixtures, which resulted in reduced porosity in the tested materials. Indeed, thermal mortars A1 and A2 were found to have less than half of the declared open porosity. This reduction is concerning because the materials were carefully prepared following the manufacturer's instructions. Thus, if this low porosity was obtained in the laboratory, it is very likely to re-present itself when the materials are prepared in-situ, with presumably much less attention and time given to the preparation;
- the application of mortars by spatula. Thermal mortars are sensitive to manipulation, and it is expected that they provide better performance when applied by mechanical spraying. It is indeed expected that spray application does improve the entrance of air into the fresh mortar, resulting in higher porosity and, consequently, lower thermal conductivity of the hardened materials. A high amount of entrained air may also reduce the capillary water absorption (Corinaldesi, Donnini, and Nardinocchi 2015), as large voids (above capillary range) work as water barriers. If strong differences are systematically found between the properties of thermal mortars applied by mechanical spraying and by spatula, it would be useful to provide some correlated indications in the technical sheets of the materials, when they are designed to be applied with both techniques.

4.6.2. PERFORMANCE OF MATERIALS AND SYSTEMS IN COMPARISON WITH STANDARD REQUIREMENTS

The results experimentally obtained are summarized in Table 4.8, in comparison with the standard threshold values set in the standard EN 998-1:2017 and the European Assessment Document EAD 040083-00-0404:2020. In the table, "V" and "X" are adopted to indicate if the requirements were fulfilled or not, respectively.

Table 4.8 – Compliance of mortars and insulation systems with standard requirements (EN 998-1 and EAD).

Standard requirements	materials					systems				
	A1	A2	A3	B1	B2	S1	S2	S3	S4	S5
- Resistance to water vapour diffusion										
EN 998-1: μ-value (wet-cup) ≤15 for TM	V	V	V	-	-	-	-	-	-	-
EAD: s_d (wet-cup) ≤ 1.0m	-	-	-	-	-	V	V	V	V	V
- Capillary water absorption										
EN 998-1: Aw ≤0.40 kg.m^{-2}.min$^{-1/2}$ for TM	X	V	V	-	-	-	-	-	-	-
EAD: $Aw_{\_24}$ ≤0.013 kg.m^{-2}.min$^{-1/2}$	-	-	-	-	-	-*	X	-*	X	X
- Thermal conductivity										
EN 998-1: λ ≤ 0.20 W/(m K) for TM	V	V	V	-	-	-	-	-	-	-
EAD: λ ≤ 0.065 W/(m K)	-	-	-	-	-	X	X	X	X	X

TM: thermal mortars, V : verified, X: failed, - : not applicable, -: not considered for internal insulation systems*

4.6.3. SYNTHESIS OF RESULTS: DATABASE FOR NUMERICAL SIMULATIONS

The extensive experimental campaign presented in this study allowed the definition of a complete hygrothermal characterization of materials and systems to be used in numerical simulations. The data obtained is synthesized in Table 4.9.

Table 4.9 – Characteristic of thermal insulation systems and properties of the materials for numerical simulations.

THERMAL INSULATION SYSTEMS:

SYSTEMS		Side of insulation	Composition of the system
S1	based on cork-mortar A1	INTERIOR	th.m. A1 (4cm) + reg.m. B1 (2mm) + paint C1 (0.5mm)
S2	based on cork-mortar A1	EXTERIOR	th.m. A1 (4cm) + reg.m. B1 (2mm) + paint C2 (0.5mm)
S3	based on cork-mortar A2	INTERIOR	th.m. A2 (4cm) + reg.m. B1 (2mm) + paint C1 (0.5mm)
S4	based on cork-mortar A2	EXTERIOR	th.m. A2 (4cm) + reg.m. B1 (2mm) + paint C2 (0.5mm)
S5	based on EPS-mortar A3	INTERIOR/EXTERIOR	th.m. A3 (4cm) + reg.-finishing m. B2 (2mm)

th.=thermal, m.=mortar, reg.=regularization

MATERIALS ADOPTED IN THE INSULATION SYSTEMS:

	A1	**A2**	**A3**	**B1**	**B2**	**C1**	**C2**
DRY BULK DENSITY [Kg/m^3]	612.8	724.2	342.3	1617	1316	1617	1617
OPEN POROSITY [m^3/m^3]	0.342	0.307	0.288	0.307	0.311	0.307	0.307
VAPOUR RESISTANCE FACTOR [-]						*For layers of paint 0.5mm thick:*	
dry conditions	14.6	18.8	11.0	18.3	15.6	106	737
wet conditions	12.0	14.7	9.17	13.4	13.7	72.5	648
CAPILLARY WATER ABSORPTION COEFFICIENT [Kg/ (m^2 s$^{0.5}$)]	0.044	0.022	0.034	0.181	0.034	0.017	0.005
FREE WATER SATURATION wsat[Kg/m^3]	300.0	215.9	66.2	276.7	128.6	276.7	276.7
MOISTURE STORAGE FUNCTION / SORPTION ISOTHERM (w[Kg/m^3])							
at RH 30%	1.64	1.66	0.74	1.11	1.06	1.20	0.92
at RH 50%	3.98	3.87	1.53	2.29	2.29	2.49	2.09
at RH 70%	8.97	8.71	4.16	4.92	5.99	5.40	4.64
at RH 80%	18.42	17.91	14.30	12.18	16.02	11.42	6.69
at RH 95%	35.27	37.52	32.84	34.07	34.58	28.57	15.71
at RH 100%	300.0	215.9	66.2	276.7	128.6	276.7	276.7
REFERENCE WATER CONTENT w_{80} [Kg/m^3]	18.42	17.91	14.30	12.18	16.02	11.42	6.69
SPECIFIC HEAT CAPACITY [J/kg K]	843	848	920	*850	*850	*850	*850
THERMAL CONDUCTIVITY Dry [W/mK]	0.098	0.128	0.065	*0.7	*0.7	*0.7	*0.7
THERMAL CONDUCTIVITY	**A1**		**A2**		**A3**		
moisture dependent λ(w)	**w**	**λ**	**w**	**λ**	**w**	**λ**	
at w0 (50% RH)	33.0	0.107	59.7	0.142	31.7	0.067	
at w1	171	0.175	133	0.190	75.9	0.076	
at w2	210	0.226	148	0.224	105	0.111	
at w3	280	0.315	181	0.300	171	0.171	
****at saturation**	342	0.325	307	0.498	288	0.249	
	with λ [W/mK] and w [Kg/m3]						

*assumed from typical values found in lime-mortars from WUFI database (IBP, 2018). **extrapolated from the exponential correlations λ-w.

4.7. CONCLUSIONS

The outcomes of the experimental campaign on materials and systems led to observing that the thermal conductivity of the analysed thermal mortars was higher than designed by the manufacturers, which is probably due to the variability introduced by the application conditions. Nonetheless, all solutions appeared to be potentially beneficial for application in moderately cold climates (measured $\lambda \leq 0.20$

W/m.K). Furthermore, a strong dependency was observed in the thermal conductivity of thermal mortars on water content, $\lambda(w)$.

Experimental results showed that the use of standard samples of thermal mortars can lead to much higher water absorption coefficients than layered samples, as up to 75% higher A_w coefficients were observed. Moreover, the permeability to water vapour of the paints was found to vary noticeably depending on whether samples of single materials or complete systems were adopted. In particular, the s_d of paint C2 was found to be 4-times higher in the latter scenario, at dry conditions. These outcomes showed that the effect of layered constructions and interfacial phenomena can have a relevant influence on the hygric behaviour of complete systems. Thus, testing single materials only, which is the standard requirement for thermal mortar-based systems (EN 998-1), is in fact not sufficient for understanding the behaviour of composite insulation solutions based on thermal mortars. For this reason, it would be beneficial to introduce some information concerning the hygric behaviour of complete systems into the technical documentation of thermal mortar-based insulation solutions. This additional data would help designers to better forecast the impact of thermal plastering and rendering systems on the moisture dynamics of walls, which is extremely important when dealing with historic constructions.

The experimental campaign presented in this chapter allowed to obtain a complete hygrothermal characterization of a selection of thermal mortars and thermal mortar-based insulation systems, useful as a numerical database for numerical hygrothermal simulations. The database defined is adopted in the next chapter, where monodimensional simulations are used to investigate the impact of thermal insulation on the hygrothermal behaviour of massive historic walls.

4.8. REFERENCES

Amorim, Mafalda, Vasco Peixoto de Freitas, Isabel Torres, Tomasz Kisilewicz, and Umberto Berardi. 2020. "The Influence of Moisture on the Energy Performance of Retrofitted Walls." In *MATEC Web of Conferences*, 322:1035. EDP Sciences.

Arizzi, A., and G. Cultrone. 2012. "Aerial Lime-Based Mortars Blended with a Pozzolanic Additive and Different Admixtures: A Mineralogical, Textural and Physical-Mechanical Study." *Construction and Building Materials* 31. doi:10.1016/j.conbuildmat.2011.12.069.

ASTMInternational. 2016. "ASTM. D7984-16:2016 - 'Standard Test Method for Measurement of Thermal Effusivity of Fabrics Using a Modified Transient Plane Source (MTPS) Instrument.'"

Barreca, F., and C. R. Fichera. 2013. "Use of Olive Stone as an Additive in Cement Lime Mortar to Improve Thermal Insulation." *Energy and Buildings* 62. doi:10.1016/j.enbuild.2013.03.040.

Bouzit, S., F. Merli, M. Sonebi, C. Buratti, and M. Taha. 2021. "Gypsum-Plasters Mixed with Polystyrene Balls for Building Insulation: Experimental Characterization and Energy Performance." *Construction and Building Materials* 283. doi:10.1016/j.conbuildmat.2021.122625.

Brás, Ana, Fábio Gonçalves, and Pedro Faustino. 2014. "Cork-Based Mortars for Thermal Bridges Correction in a Dwelling: Thermal Performance and Cost Evaluation." *Energy and Buildings* 72. doi:10.1016/j.enbuild.2013.12.022.

Brito, Vânia, Teresa Diaz Gonçalves, and Paulina Faria. 2011. "Coatings Applied on Damp Building Substrates: Performance and Influence on Moisture Transport." *Journal of Coatings Technology and Research* 8 (4). Springer: 513–525.

Carmeliet, Jan, and Staf Roels. 2001. "Determination of the Isothermal Moisture Transport Properties of Porous Building Materials." *Journal of Building Physics*. doi:10.1106/Y6T2-9LLP-04Y5-AN6T.

CEN. 1998. "EN 1015-6:1998 - 'Methods of Test for Mortar for Masonry - Part 6: Determination of Bulk Density of Fresh Mortar.'"

CEN. 1999. "EN 1015-10:1999 - 'Methods of Test for Mortar for Masonry. Determination of Dry Bulk Density of Hardened Mortar.'"

CEN. 2000. "EN 12524:2000 - 'Building Materials and Products. Hygrothermal Properties. Tabulated Design Values.'"

CEN. 2002. "EN 1015-18:2002 - 'Methods of Test for Mortar for Masonry - Part 18: Determination of Water Absorption Coefficient Due to Capillary Action of Hardened Mortar.'"

CEN. 2004. "EN 1062-1:2004 - 'Paints and Varnishes - Coating Materials and Coating Systems for Exterior Masonry and Concrete - Part 1.'"

CEN. 2007a. "EN 1015-3:2007 - 'Methods of Test for Mortar for Masonry. Determination of Consistence of Fresh Mortar (by Flow Table).'"

CEN. 2007b. "EN 1015-2:2007 - 'Methods of Test for Mortar for Masonry - Part 2: Bulk Sampling of Mortars and Preparation of Test Mortars.'"

CEN. 2008a. "EN 1015-19:2008 - 'Methods of Test for Mortar for Masonry - Part 19: Determination of Water Vapour Permeability of Hardened Rendering and Plastering Mortars.'"

CEN. 2008b. "EN 1062-3:2008 - 'Paints and Varnishes - Coating Materials and Coating Systems for Exterior Masonry and Concrete - Part 3.'"

CEN. 2009a. "EN 15801:2009 - 'Conservation of Cultural Property - Test Methods - Determination of Water Absorption by Capillarity.'"

CEN. 2009b. “EN 15803:2009 - ‘Conservation of Cultural Property. Test Methods. Determination of Water Vapour Permeability (Δp).’”

CEN. 2016. “EN16322:2016. Conservation of cultural heritage - test methods - determination of drying properties.”

CEN. 2017. “EN 998-1:2017 - ‘Specification for Mortar for Masonry - Part 1: Rendering and Plastering Mortar.’”

CEN. 2019. “EN 1015-11:2019 - ‘Methods of Test for Mortar for Masonry - Part 11: Determination of Flexural and Compressive Strength of Hardened Mortar.’”

CEN. 2020. “EN 1745:2020 - ‘Masonry and Masonry Products. Methods for Determining Thermal Properties.’”

Contrafatto, Loredana, Carmelo Lazzaro Danzuso, Salvatore Gazzo, and Leopoldo Greco. 2020. “Physical, Mechanical and Thermal Properties of Lightweight Insulating Mortar with Recycled Etna Volcanic Aggregates.” *Construction and Building Materials*. doi:10.1016/j.conbuildmat.2019.117917.

Coppola, L., D. Coffetti, E. Crotti, A. Marini, C. Passoni, and T. Pastore. 2019. “Lightweight Cement-Free Alkali-Activated Slag Plaster for the Structural Retrofit and Energy Upgrading of Poor Quality Masonry Walls.” *Cement and Concrete Composites* 104. doi:10.1016/j.cemconcomp.2019.103341.

Corinaldesi, Valeria, Jacopo Donnini, and Alessandro Nardinocchi. 2015. “Lightweight Plasters Containing Plastic Waste for Sustainable and Energy-Efficient Building.” *Construction and Building Materials* 94. doi:10.1016/j.conbuildmat.2015.07.069.

CSTB. 1993. “Certification CSTB Des Enduits Monocouches d’imperméabilisation, Cahiers Du CSTB N°2669. Juillet-Aout, Paris. (in French).” CSTB.

Delgado, J. M.P.Q., V. P. de Freitas, and A. S. Guimarães. 2016. “Water Movement in Building Walls: Interfaces Influence on the Moisture Flux.” *Heat and Mass Transfer/Waerme- Und Stoffuebertragung*. doi:10.1007/s00231-016-1755-z.

Delgado, João M P Q, António C Azevedo, and Ana S Guimarães. 2019. “Chapter 2. Hygrothermal Properties f the Tested Materials.” In *Drying Kinetics in Building Materials and Components: The Interface Influence*. Springer.

EOTA - European Organisation for Technical Approvals. 2020. "EAD 040083-00-0404:2020 - 'European Assessment Document. External Thermal Insulation Composite Systems (ETICS) with renderings'".

Flores-Colen, I., L. Silva, J. De Brito, and V. P. De Freitas. 2016. “Drying Index for In-Service Physical Performance Assessment of Renders.” *Construction and Building Materials*. doi:10.1016/j.conbuildmat.2016.03.034.

Franco, Alessandro. 2007. “An Apparatus for the Routine Measurement of Thermal Conductivity of Materials for Building Application Based on a Transient Hot-Wire Method.” *Applied Thermal Engineering*. doi:10.1016/j.applthermaleng.2007.02.008.

Freitas, Teresa Stingl, Ana Sofia Guimarães, Staf Roels, Vasco Peixoto de Freitas, and Andrea Cataldo. 2020. “Is the Time-Domain Reflectometry (TDR) Technique Suitable for Moisture Content Measurement in Low-Porosity Building Materials?” *Sustainability (Switzerland)* 12 (19). doi:10.3390/SU12197855.

Ganobjak, Michal, Samuel Brunner, and Jannis Wernery. 2019. “Aerogel Materials for Heritage Buildings: Materials, Properties and Case Studies.” *Journal of Cultural Heritage*. Elsevier.

Gomes, M. Glória, I. Flores-Colen, F. da Silva, and M. Pedroso. 2018. “Thermal Conductivity Measurement of Thermal Insulating Mortars with EPS and Silica Aerogel by Steady-State and Transient Methods.” *Construction and Building Materials*. doi:10.1016/j.conbuildmat.2018.03.162.

Gomes, M. Glória, I. Flores-Colen, L. M. Manga, A. Soares, and J. de Brito. 2017. “The Influence of Moisture Content on the Thermal Conductivity of External Thermal Mortars.” *Construction and Building Materials*.

doi:10.1016/j.conbuildmat.2016.12.166.

Gomes, M. Glória, Inês Flores-Colen, Humberto Melo, and António Soares. 2019. "Physical Performance of Industrial and EPS and Cork Experimental Thermal Insulation Renders." *Construction and Building Materials* 198: 786–795. doi:10.1016/j.conbuildmat.2018.11.151.

Govaerts, Yves, Roald Hayen, Michael de Bouw, Ann Verdonck, Wendy Meulebroeck, Stijn Mertens, and Yves Grégoire. 2018. "Performance of a Lime-Based Insulating Render for Heritage Buildings." *Construction and Building Materials*. doi:10.1016/j.conbuildmat.2017.10.115.

Guimarães, A. S., J. M.P.Q. Delgado, A. C. Azevedo, and V. P. de Freitas. 2018. "Interface Influence on Moisture Transport in Buildings." *Construction and Building Materials*. doi:10.1016/j.conbuildmat.2017.12.040.

Hansen, Kurt. 1986. *Sorption Isotherms: A Catalogue. Technical Report 162/86.*

Henry, Alison, and John Stewart. 2011. "Practical Building Conservation: Mortars, Renders & Plasters." In *English Heritage*.

Horma, Othmane, Mouatassim Charai, Ahmed Mezrhab, and Mustapha Karkri. 2020. "Thermal Characterization of Cement-Plaster-Expanded Polystyrene Composites." In *2020 5th International Conference on Renewable Energies for Developing Countries (REDEC)*, 1–6. IEEE.

IBP, Fraunhofer Institute for Building Physics. 2018. "WUFI (En), Home." Accessed March 29, 2018. https://wufi.de/en/.

ISO. 2007. "ISO 10456:2007 - 'Building Materials and Products — Hygrothermal Properties — Tabulated Design Values and Procedures for Determining Declared and Design Thermal Values.'"

ISO. 2013. "ISO 12571:2013 - Hygrothermal Performance of Building Materials and Products — Determination of Hygroscopic Sorption Properties."

ISO. 2016. "ISO 12572:2016 - Hygrothermal Performance of Building Materials and Products - Determination of Water Vapour Transmission Properties." doi:10.1007/978-94-009-6175-3_3.

Kramar, Derek, and Vivek Bindiganavile. 2011. "Mechanical Properties and Size Effects in Lightweight Mortars Containing Expanded Perlite Aggregate." *Materials and Structures/Materiaux et Constructions*. doi:10.1617/s11527-010-9662-0.

Künzel, Hartwig M. 1995. *Simultaneous Heat and Moisture Transport in Building Components One- and Two-Dimensional Calculation Using Simple Parameters . Physics*. Vol. 1995. doi:ISBN v.3-8167-4103-7.

LNEC. 2015. *FE Pa 44 - " Ficha de Ensaio - Revestimentos de Paredes - Determinação Da Porosidade Aberta e Das Massas Volúmica Aparente e Real" . Lisbon. (in Portuguese)*.

Maia, J., M. Pedroso, N. M.M. Ramos, P. F. Pereira, I. Flores-Colen, M. Glória Gomes, and L. Silva. 2021. "Hygrothermal Performance of a New Thermal Aerogel-Based Render under Distinct Climatic Conditions." *Energy and Buildings* 243. doi:10.1016/j.enbuild.2021.111001.

Maia, J., Nuno M.M. Ramos, and R. Veiga. 2018. "Evaluation of the Hygrothermal Properties of Thermal Rendering Systems." *Building and Environment*. doi:10.1016/j.buildenv.2018.08.055.

Maia, Joana. 2019. "Durability of Thermal Rendering and Plastering Systems." PhD thesis. FEUP- University of Porto, Portugal.

Mazhoud, Brahim, Florence Collet, Sylvie Pretot, and Julien Chamoin. 2016. "Hygric and Thermal Properties of Hemp-Lime Plasters." *Building and Environment* 96. Elsevier: 206–216.

Nosrati, Roya Hamideh, and Umberto Berardi. 2018. "Hygrothermal Characteristics of Aerogel-Enhanced Insulating Materials under Different Humidity and Temperature Conditions." *Energy and Buildings*. doi:10.1016/j.enbuild.2017.09.079.

Parracha, J. L., G. Borsoi, I. Flores-Colen, R. Veiga, L. Nunes, A. Dionísio, M. Glória Gomes, and P. Faria. 2021. "Performance Parameters of ETICS: Correlating Water Resistance, Bio-Susceptibility and Surface Properties." *Construction and Building Materials*. doi:10.1016/j.conbuildmat.2020.121956.

Pedroso, Marco, Inês Flores-Colen, José Dinis Silvestre, M. Glória Gomes, Luis Silva, Pedro Sequeira, and Jorge de Brito. 2020. "Characterisation of a Multilayer External Wall Thermal Insulation System. Application in a Mediterranean Climate." *Journal of Building Engineering* 30. doi:10.1016/j.jobe.2020.101265.

Plagge, Rudolf, Gregor Scheffler, and Andreas Nicolai. 2007. "Experimental Methods to Derive Hygrothermal Material Functions for Numerical Simulation Tools." *Thermal Performance of Exterior Envelopes of Whole Buildings X International Conference*.

Posani, Magda, Maria Do Rosário Veiga, and Vasco Peixoto De Freitas. 2018. *Historic Buildings Resilience: A View over Envelope Energy Retrofit Possibilities. . 8th International Conference on Building Resilience. November 14-16, 2018. Lisbon, Portugal*.

Ramos, N. M.M., J. M.P.Q. Delgado, and V. P. De Freitas. 2010. "Influence of Finishing Coatings on Hygroscopic Moisture Buffering in Building Elements." *Construction and Building Materials*. doi:10.1016/j.conbuildmat.2010.05.017.

Ranesi, Alessandra, M Rosário Veiga, and Paulina Faria. 2021. "Laboratory Characterization of Relative Humidity Dependent Properties for Plasters: A Systematic Review." *Construction and Building Materials* 304. Elsevier: 124595.

Šadauskiene, Jolanta, Edmundas Monstvilas, and Vytautas Stankevičius. 2007. "The Impact of Exterior Finish Vapour Resistance on the Moisture State of Building Walls." *Technological and Economic Development of Economy* 13 (1). Taylor & Francis: 73–82.

Scheffler, Gregor A., and Rudolf Plagge. 2010. "Introduction of a Drying Coefficient for Building Materials." In *Thermal Performance of the Exterior Envelopes of Whole Buildings - 11th International Conference*.

Sicakova, Alena, Martina Draganovska, and Marek Kovac. 2017. "Water Absorption Coefficient as a Performance Characteristic of Building Mixes Containing Fine Particles of Selected Recycled Materials." In *Procedia Engineering*. doi:10.1016/j.proeng.2017.04.287.

Silveira, Dora, Ana Gonçalves, Inês Flores-Colen, M Rosário Veiga, Isabel Torres, and Rafael Travincas. 2020. "Evaluation of In-Service Performance Factors of Renders Based on in-Situ Testing Techniques." *Journal of Building Engineering*. Elsevier, 101806.

Thomson, M, J E Lindqvist, J Elsen, and CJWP Groot. 2004. "2.5 Porosity of Mortars." *Characterisation of Old Mortars with Respect to Their Repair-Final Report of RILEM TC 167-COM*. Rilem Publications Sarl, 77–106.

Torres, Isabel, Rosário Veiga, and Vasco Freitas. 2018. "Influence of Substrate Characteristics on Behavior of Applied Mortar." *Journal of Materials in Civil Engineering*. doi:10.1061/(asce)mt.1943-5533.0002339.

Torres, Marcos Lanzón, and P. A. García-Ruiz. 2009. "Lightweight Pozzolanic Materials Used in Mortars: Evaluation of Their Influence on Density, Mechanical Strength and Water Absorption." *Cement and Concrete Composites* 31 (2). doi:10.1016/j.cemconcomp.2008.11.003.

Trechsel, Heinz R. 1994. *Moisture Control in Buildings*. ASTM Philadelphia.

Veiga, Rosário, M., Ana Fragata, Ana Luisa Velosa, Ana Cristian Magalhães, and Goreti Margalha. 2010. "Lime-Based Mortars: Viability for Use as Substitution Renders in Historical Buildings." *International Journal of Architectural Heritage* 4 (2): 177–195. doi:10.1080/15583050902914678.

Veiga, Rosário. 2017. "Air Lime Mortars: What Else Do We Need to Know to Apply Them in Conservation and Rehabilitation Interventions? A Review." *Construction and Building Materials*. doi:10.1016/j.conbuildmat.2017.09.080.

Vyšvařil, Martin, Milena Pavlíková, Martina Záleská, Adam Pivák, Tomáš Žižlavský, Pavla Rovnaníková, Patrik Bayer, and Zbyšek Pavlík. 2020. "Non-Hydrophobized Perlite Renders for Repair and Thermal Insulation Purposes: Influence of Different Binders on Their Properties and Durability." *Construction and Building Materials* 263. doi:10.1016/j.conbuildmat.2020.120617.

Walker, R., and S. Pavía. 2015. "Hermal and Hygric Properties of Insulation Materials Suitable for Historic Fabrics." In *Proceedings of III International Congress on Construction and Building Research.* https://pdfs.semanticscholar.org/2288/22c8daff6bb97b5bdf7aee883d91e78e2884.pdf.

Walker, Rosanne, and Sara Pavía. 2015. "Thermal Performance of a Selection of Insulation Materials Suitable for Historic Buildings." *Building and Environment* 94 (P1): 155–165. doi:10.1016/j.buildenv.2015.07.033.

Worch, Anatol. 2004. "The Behaviour of Vapour Transfer on Building Material Surfaces: The Vapour Transfer Resistance." *Journal of Thermal Envelope and Building Science* 28 (2). Sage Publications Sage CA: Thousand Oaks, CA: 187–200.

Yüksel, Numan. 2016. "The Review of Some Commonly Used Methods and Techniques to Measure the Thermal Conductivity of Insulation Materials." In *Insulation Materials in Context of Sustainability*. doi:10.5772/64157.

Zhao, Jianhua, John Grunewald, Ulrich Ruisinger, and Shuo Feng. 2017. "Evaluation of Capillary-Active Mineral Insulation Systems for Interior Retrofit Solution." *Building and Environment* 115. Elsevier Ltd: 215–227. doi:10.1016/j.buildenv.2017.01.004.

5

HYGROTHERMAL BEHAVIOUR OF RETROFITTED WALLS: The impact of thermal insulation.

5.1. INTRODUCTION

Dynamic hygrothermal simulations are a very useful tool when studying possible retrofit interventions for historic buildings. Indeed, they allow understanding the hygrothermal behaviour of components exposed to outdoor climate, thus helping to avoid damages or undue heat losses, while predicting the consequences of constructive modifications. Furthermore, they offer an effective alternative to experimental investigations, which are rather expensive, time-consuming and very limitedly feasible in historic constructions.

In this chapter, the hygrothermal behaviour of the walls of three case studies is considered. The assessment is performed through mono-dimensional hygrothermal simulations, which are qualitatively validated with the data from the monitoring campaign presented in Chapter 3. The models are adopted to investigate the effect of different types of internal or external thermal insulation solutions on the hygrothermal behaviour of the walls. Thermal mortar-based systems, namely those characterized in Chapter 4, are compared to more commonly adopted insulation solutions based on expanded polystyrene (EPS) and hydrophobic mineral wool (MW). In addition, one of the thermal mortars is also used for a parametric study aimed to investigate the effect of hygric transport properties of the insulation layer on the performance of the system.

Results are analyzed in terms of moisture-related risks and thermal performance. Specifically, the evaluation concerns moisture content in the wall substrate, reduction of drying, high relative humidity between the wall and internal insulation, and heat losses during winter. The assessment criteria adopted are used to define indexes of risk and performance. Those indexes are collected in matrixes, which are adopted to synthesize the result and derive overall recommendations, as well as evaluate whether thermal mortars are competitive with more current solutions.

The overall consideration defined in this chapter specifically refer to thick masonry walls of historic buildings, located in areas with temperate climates with warm or hot summers and mild winters, where heating systems are adopted.

5.2. NUMERICAL MODELS

The Software adopted for mono-dimensional hygrothermal simulations, its main characteristics and limitations are introduced in this section. Then, the input data adopted to simulate the behaviour of the walls of the three case studies are presented.

The software selected for the study is WUFI Pro 5 (Fraunhofer Institute for Building Physics IBP, 2013), which allows performing mono-dimensional hygrothermal simulations of multi-layered walls cross-section under realistic climatic conditions.

This choice was made for several reasons. First, It is largely recognised that simplified steady-state methods, like Glaser's, are not suitable to represent moisture dynamics in porous walls exposed to wind-driven rain (Little, Ferraro and Aregi, 2015). Additional factors should be considered, such as dynamic boundary conditions and liquid transport, according to standard EN 15026:2007 (Browne, 2012). WUFI Pro complies with the aforementioned standard (Fraunhofer IBP, 2007) and it offers a detailed calculation model of combined heat and moisture transport, which includes liquid transport, vapour diffusion, hygroscopic behaviour of porous materials and the dependency of thermal conductivity on moisture content. Furthermore, WUFI Pro has been validated through several years of field and laboratory testing (Hägerstedt and Arfvidsson, 2010; Mundt-Petersen and Harderup, 2013; Alev *et al.*, 2014; Stöckl, Zirkelbach and Künzel, 2014; Villmann, 2014), and it is widely adopted to investigate the hygrothermal behaviour of historic and traditionally-constructed building components, as well as their retrofits (e.g. Finken, Bjarløv and Peuhkuri, 2016; Abdul Hamid and Wallentén, 2017; Stahl *et al.*, 2017; Kaczorek, 2018; Lisitano *et al.*, 2018; Vacek and Kostelník, 2019; Amorim, Freitas, *et al.*, 2020).

The software allows introducing materials properties as input data, thus insulation systems can be modelled according to the information obtained in the experimental characterization shown in Chapter 4. At the same time, the software offers a large and complete database, with reliable materials properties, which appears useful for modelling historic walls, whose materials properties were not experimentally measured.

Finally, the software is commonly adopted by the research group LFC-FEUP, which has a direct collaboration protocol with the Fraunhofer Institute of Building Physics (IBP), i.e. the developer of the software.

5.2.1. BASICS OF THE NUMERICAL MODEL

The software relies on Künzel's (1995) differential equations for the simultaneous transport of heat and moisture. These equations are discretised by means of an implicit finite volume method and iteratively solved in the software calculations (Martin and Klaus, 2009). A more detailed description of the software and its limitations is provided in Annex II.

The inputs required by the software are materials properties, the geometry of the assembly and climatic boundary conditions, as schematically represented in Figure 5.1.

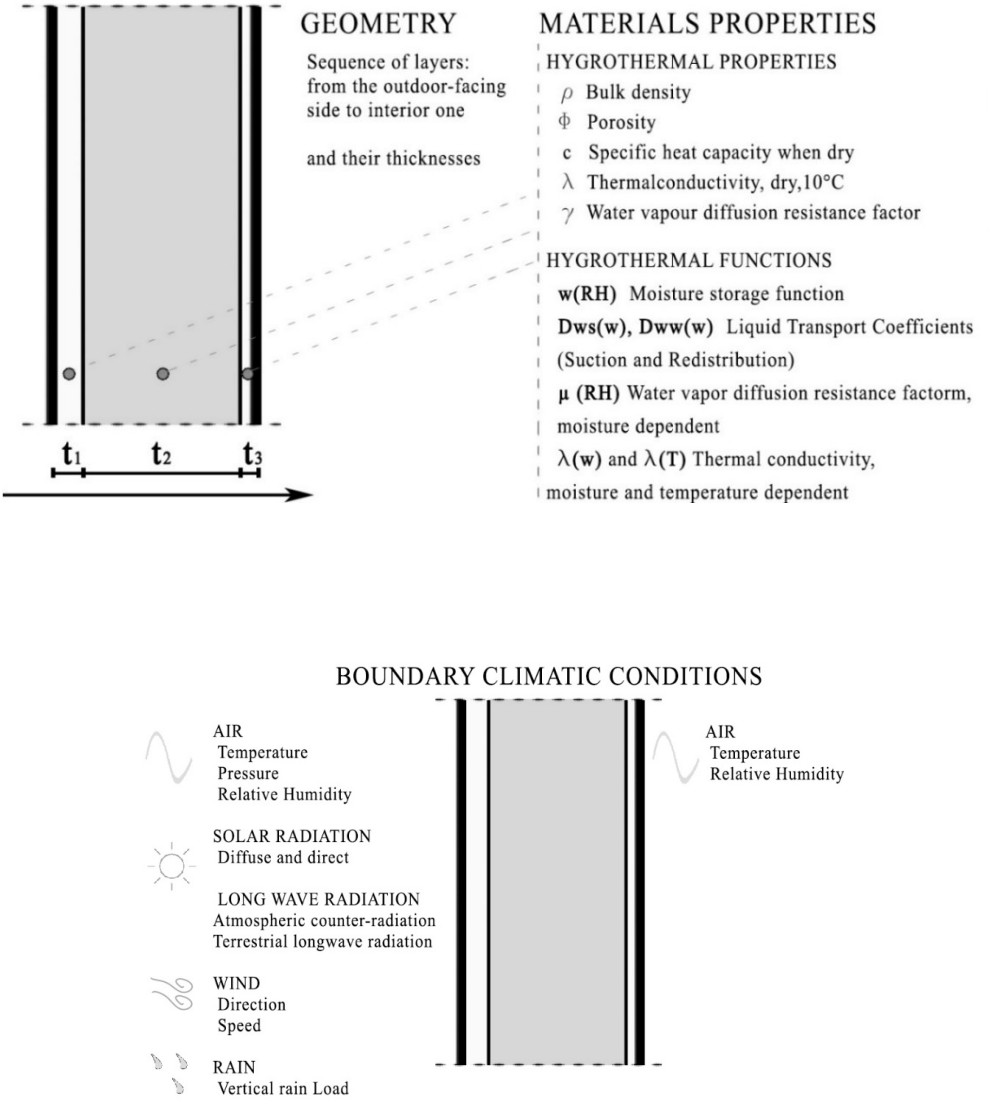

Figure 5.1 – Main input parameters for defining the simulation model in WUFI Pro.

Indoor climate conditions are simplified with hourly data of air temperature and relative humidity. The outdoor climate is defined through hourly data of air temperature, pressure and relative humidity, solar radiation (two parameters among diffuse, direct and global radiation), rain, wind speed and direction. Furthermore, terrestrial longwave radiation and atmospheric counter-radiation can be considered.

The last two parameters are disregarded in this study because of a lack of data. Thus, the heat transfer by longwave radiation is simplified in the software by considering an increase of the heat transfer coefficient of walls external surface. For most hygrothermal simulations this simplified treatment is

sufficient, even though it does not account for the effect of night-time overcooling on the external surface temperature (Kunzel, Schmidt and Holm, 2002). Night-time overcooling can be very important for condensation and deterioration at the external surface when external insulation systems like ETICS are adopted, because of their high thermal resistance and low specific heat capacity (Barreira and Freitas, 2013) but it is likely to be less relevant for interventions based on thermal mortars. Indeed, thermal mortars typically have relevant specific heat capacities (in the order of magnitude of traditional bricks) and more moderate thermal resistances. Night-time overcooling may be a source of degradation in mineral wool and EPS-based systems, but this fact is disregarded since the focus of the study lies in the hygrothermal risks entailed by thermal mortar-based systems.

5.2.2. INPUT DATA ADOPTED IN THE SIMULATIONS

5.2.2.1. BOUNDARY CLIMATIC CONDITIONS - OUTDOOR

The outdoor climate datasets (air pressure, temperature, relative humidity, global and diffuse solar radiation, rain, wind speed and direction) were obtained as follows.

For the cities of Porto and Lisbon, the weather data were provided by the *Portuguese Institute of Sea and Atmosphere* (IPMA), from weather stations located respectively at about 11.5 km and 2.5 km from the case studies. For the city of Bologna, the hourly weather data were provided by the public entity ARPAE, which has a meteorological station about 3 km far from the Library of San Giorgio in Poggiale. The data concerning solar radiation were incomplete, for this reason, the global and direct solar radiation were taken from the Test Reference Years (TRYs). The TRY adopted for Porto is the one defined by the Faculty of Engineering of Porto (Barreira *et al.*, 2017). For Lisbon and Bologna, the TRY was created with the software Meteonorm (METEOTEST - Meteonorm 6.0).

In Figures 5.2 and 5.3, the main climatic parameters of the outdoor climates considered are synthesized: air temperature and relative humidity in the former, wind-driven rain and solar radiation in the latter. Bologna has the coldest temperature in winter and the highest in summer, among the three cities considered. Porto and Lisbon have similar temperatures, with the former showing qualitatively lower temperatures both in winter and summer.

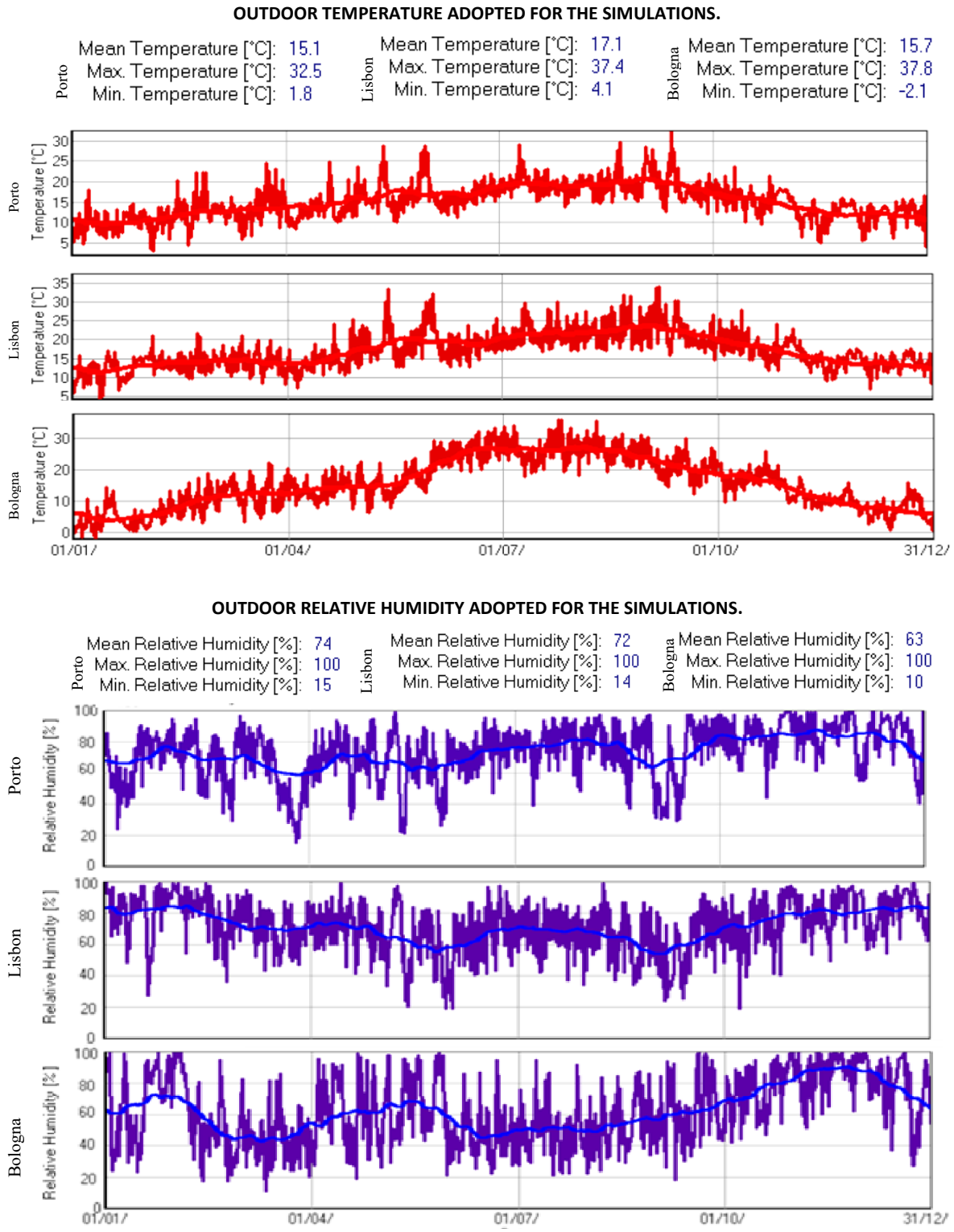

Figure 5.2 – Temperature and relative humidity in the Cities of Porto, Lisbon and Bologna, according to the data obtained from local meteorological stations. The lighter red and light blue lines represent the centred moving monthly means.

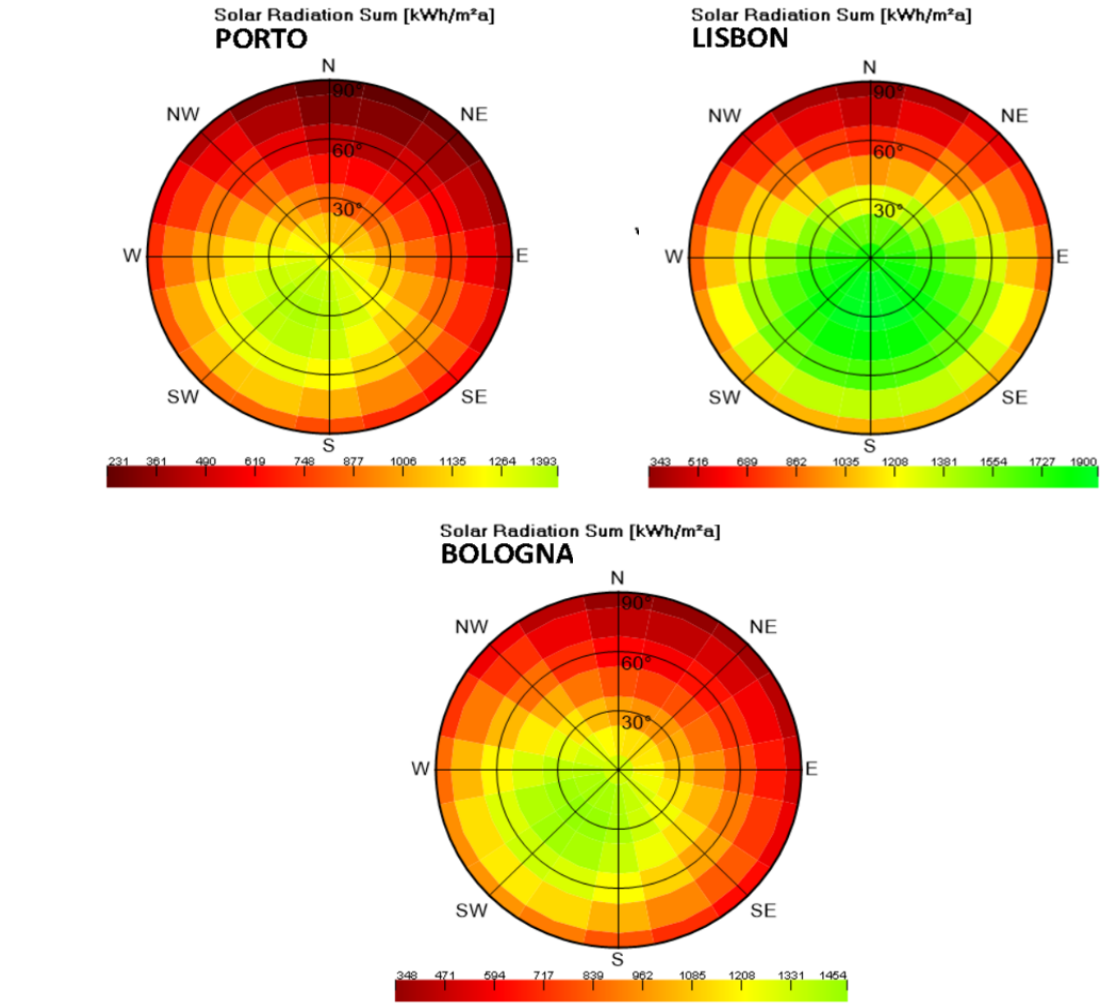

a.

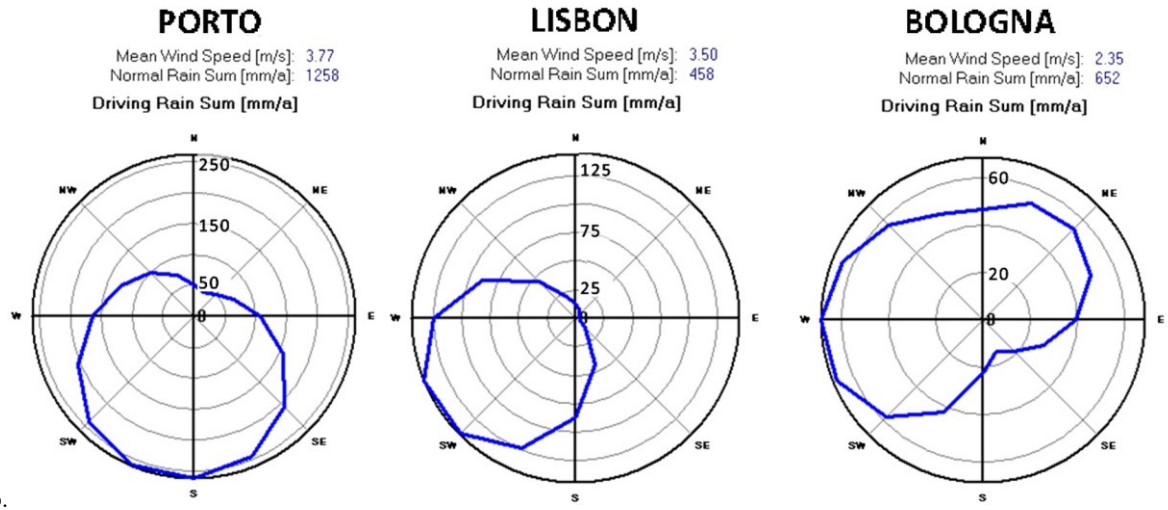

b.

Figure 5.3 – Wind-driven rain and solar radiation. From top to bottom: (a) annual sum of solar radiation, where the values reported for an inclination of 90° refer to vertical components, and 0° refer to horizontal ones; (b) mean wind speed, normal rain sum and annual sum of wind-driven rain for various orientations of walls in Porto, Lisbon and Bologna.

In terms of annual sum of solar radiation, Lisbon has the highest values, with a maximum of 1200 kWh/(m^{2}a) for south-oriented vertical components. Whereas, the maximum values for walls located in Porto and Bologna are found for South-west oriented vertical components, with values around 980 and 1100 kWh/(m^{2}a), respectively.

Wind-driven rain (WDR) is recognized to be the most important moisture source affecting hygrothermal performance and durability of building facades (Blocken and Carmeliet, 2004). Given the importance of WDR for the moisture content of exposed walls, a more detailed evaluation is provided for two wall orientations in each climate, for some specific walls orientations, in Figure 5.4. The orientations were chosen to be representative of a higher and lower WDR load in each location (according to a sensitivity study presented in ANNEX II).

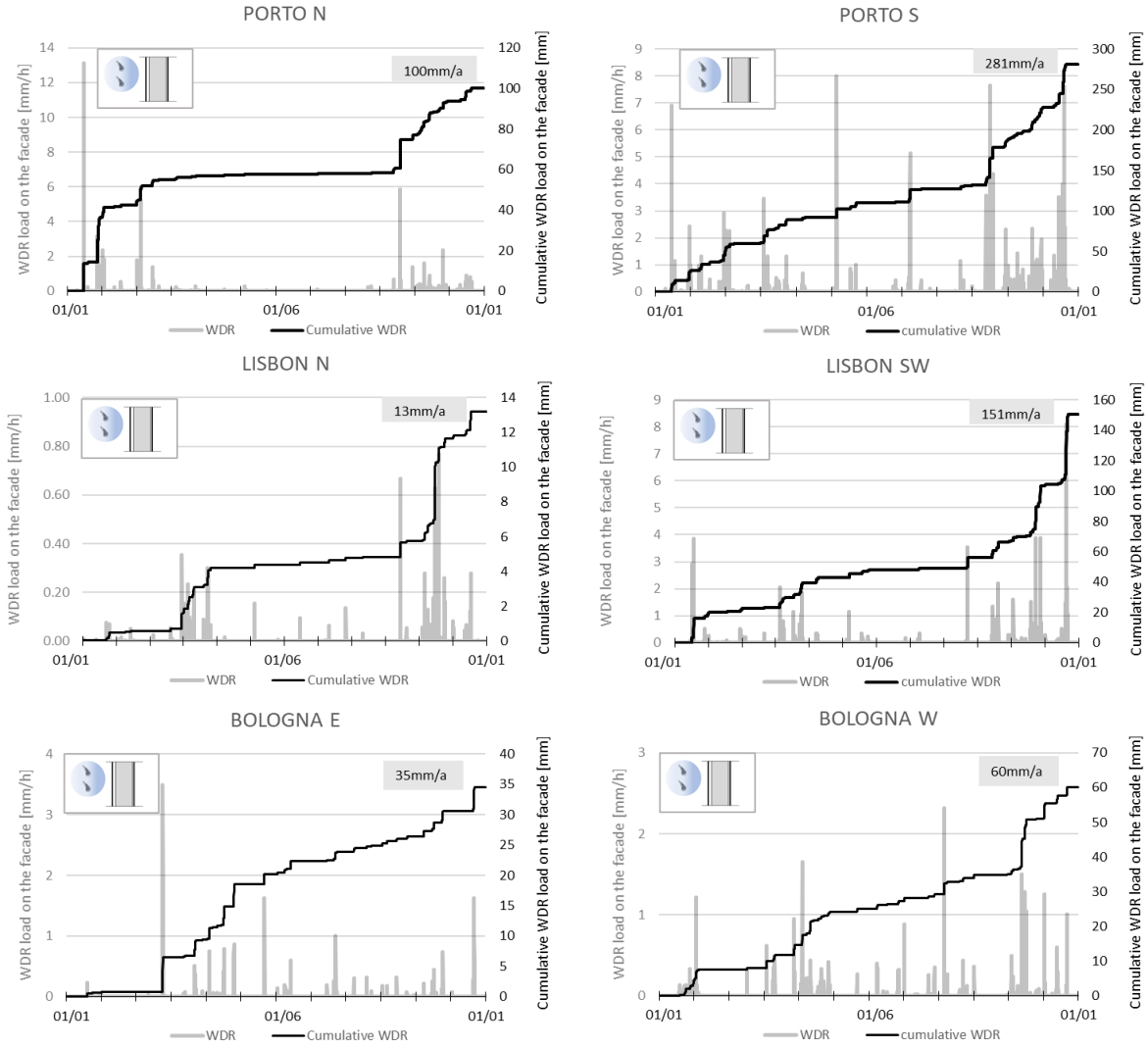

Figure 5.4 –Annual sum of wind-driven rain in Porto, Lisbon and Bologna, for the chosen walls orientations, according to equation WDR = R_h (0 + 0.07 V cos ψ), as explained in ANNEX II. The hourly load of WDR is shown in grey, and the cumulative load is displayed in black.

Considering the general data on WDR provided in Figure 5.3b, it emerges that Porto has a much higher annual amount of normal rain than Lisbon and Bologna, and also the highest mean wind speed. Coherently, Porto also has the highest annual WDR-load among the cases considered, namely about 280 mm/a on a South-oriented vertical surface. The distribution of WDR load appears extremely uneven in the two Portuguese climates, with South and South-West orientated walls having a much higher WDR load than N-oriented ones. In Bologna, the distribution of WDR loads is more evenly spread.

Moving to the detailed analysis presented in Figure 5.4, it is possible to notice that in Porto and Lisbon a relevant part of WDR is concentrated in the winter season, when a relevant increase in the cumulative WDR is observable. On the contrary, WDR in Bologna appears to be more evenly spread, having a significant increase of cumulative WDR also during summer. For reasons of synthesis, in this chapter the walls located in Porto and the SW-oriented one in Lisbon are referred to as affected by a high WDR load (namely an annual sum above 100 mm/a). West-oriented walls in Bologna are considered as exposed to relevant WDR, which is about 60mm/a. North-oriented walls located in Lisbon and East-oriented ones in Bologna are referred to as affected by low or not-relevant WDR.

5.2.2.2. BOUNDARY CLIMATIC CONDITIONS - INDOOR

Indoor air temperature and relative humidity were defined according to the data measured on-site, to represent realistic conditions and to account for the fluctuations determined by occupancy and use of HVAC appliances. The dataset is presented in Figure 5.5, and it covers one entire year for each case study.

The data used as indoor boundary conditions were selected from the ones obtained in the indoor monitoring campaign provided in chapter 4, as follows:

1. For the case study in Porto, the average of the measurements of sensors S1, S2 and N1, which are sensors located nearby the building envelope, in one of the monitored rooms;
2. For the case study in Lisbon, the data obtained from sensor SW1, which is the sensor located near a SW-oriented wall, and it is the only sensor positioned in the room whose walls are considered in this analysis;
3. For the case study in Bologna, the data obtained from sensor W, which is located near a W-oriented wall, and it is the only sensor in the room that is positioned near the building envelope of the case study.

The main difference between the indoor climates seems to be the drier and warmer indoor climate that characterizes the case study of Bologna. Indoor RH conditions appear quite anomalous, being very dry, which is a result that was already commented in Chapter 3.

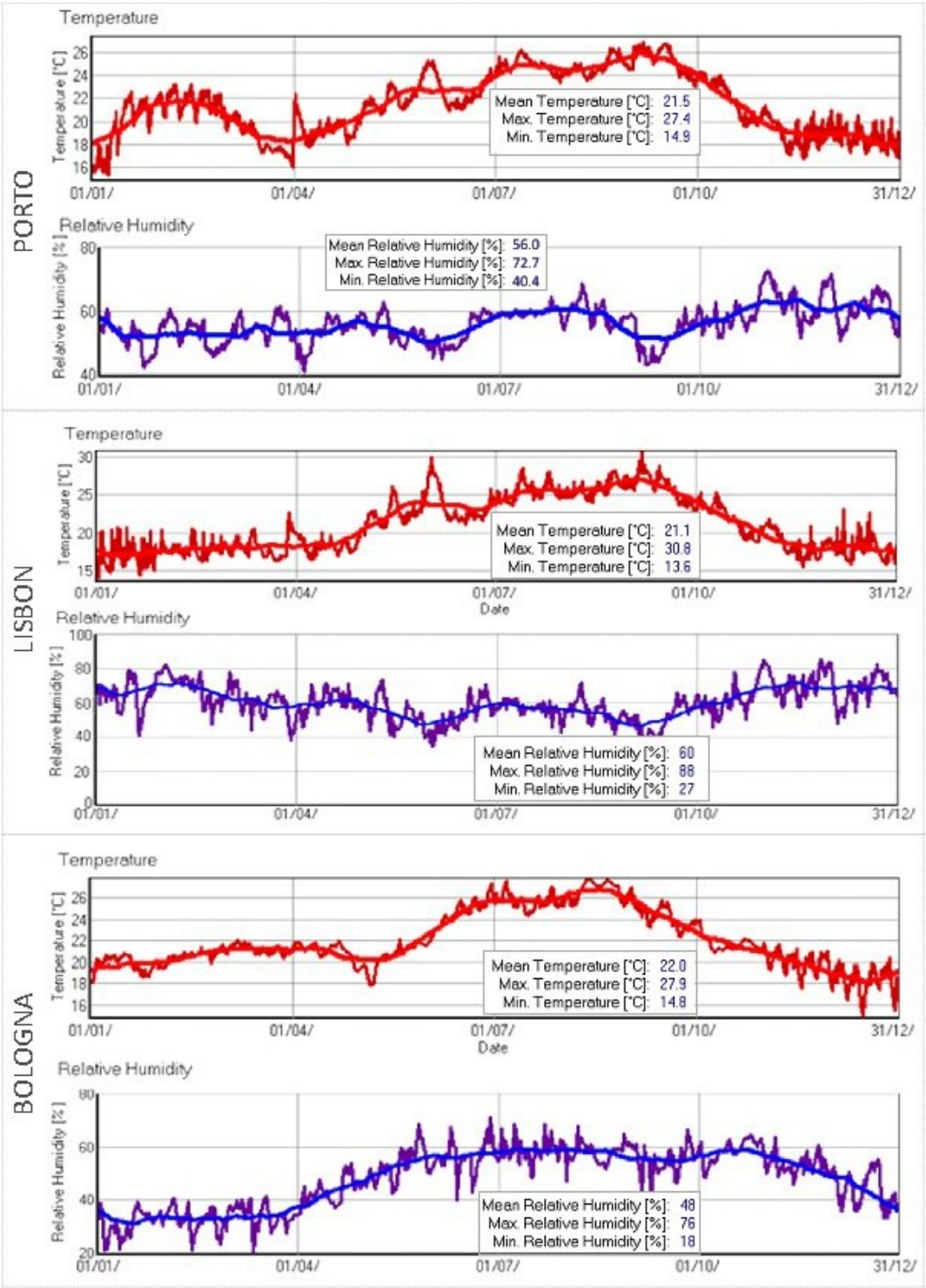

Figure 5.5 – Temperature and relative humidity: data set adopted as indoor climate for simulations, based on the indoor monitoring campaign. The lighter red and light blue lines represent the 30-day moving average values.

5.2.2.3. INITIAL CONDITIONS, TIME OF SIMULATION AND DYNAMIC EQUILIBRIUM OF THE UN-RETROFITTED WALLS

As previously outlined, the boundary conditions of the model, i.e., the indoor and outdoor climate, are defined for a 1-year-period. Nonetheless, simulations are run for longer times in this study, assuming that boundary conditions recur every year unchanged.

The initial conditions of the wall assembly, in terms of temperature and moisture content, are defined by the user as input data. Because of the repetition of the same yearly boundary conditions, after a certain period of time, the simulations reach dynamic equilibrium conditions (Künzel, 1998), meaning that the course of physical properties such as temperature and relative humidity does not change from one year to the next. After this steady annual performance is reached, simulation results do not depend on the initial conditions anymore, but only on the boundary climates (Grunewald, Ruisinger, & Häupl, 2006). For this reason, un-retrofitted walls are simulated for a 10-year-period of time, and the results considered for un-retrofitted walls are the ones of the last year of simulations. The retrofitted scenarios are simulated considering the application of insulation on the original moist wall, starting from a realist high moisture content. The initial water content is approximated considering a high water content found in winter, in the results of the un-retrofitted wall at dynamic equilibrium. On the contrary, the simulations of drying consider an initial moisture content equal to free water saturation in the wall substrate.

All simulations of retrofitted walls start from the 1st of January and are run for a 10-year-period.

5.2.2.4. WALLS ASSEMBLY

According to documental research, technical drawings and inspection in-situ, the actual configuration of the massive walls of the three case studies is reconstructed as: 90cm-thick granite wall for Porto, 70cm-thick rubble limestone wall for Lisbon, and 60cm-thick solid brick wall for Bologna, with interior surfaces plastered and external surfaces rendered. The materials adopted for the simulations are selected from WUFI Pro database. The only exception is Limestone, whose properties are taken from an experimental study of Torres and Freitas (2007) on a typical Portuguese limestone. The characteristics of the *original configuration of walls* are reported in Table 5.1.

Interior plasters and exterior renders are simplified using 3cm of lime mortar, as assumed in Ferreira (2015) for historic Portuguese buildings. The same lime mortar is adopted both at the interior and exterior side of walls because various studies on historic renders and plasters in Portugal showed that the characteristics and compositions of the two are generally similar (Veiga *et al.*, 2010; Damas, Veiga and Faria, 2016; Velosa and Veiga, 2016). According to these studies, the capillary absorption of traditional lime mortars is quite variable but a good representation is given by a capillary absorption between 1 and 1.5 $kg/m^2min^{0.5}$ (Veiga *et al.*, 2010), i.e. 0.1-0.2 $kg/m^2s^{0.5}$. For this reason, this study considers a lime mortar, selected from WUFI database, that has a capillary absorption coefficient of about 0.17 $Kg/m^2s^{0.5}$.

Table 5.1 – Characteristics adopted for the simulations of original walls configuration.

External layer (WUFI database)	Wall (WUFI database and Torres and Freitas, 2007)	Internal layer (WUFI database)	Indoor climate (measured on-site)	Outdoor climate (meteo-stations)
Lime plaster - 3cm	Granite-90cm (μ=70, λ= 2.3 W/mK, *A_w= 0.002 Kg/m^{2}s$^{0.5}$)	Lime plaster - 3cm	Municipal Library of Porto	Porto
Lime plaster-3cm (μ=12, λ=0.7 W/mK, A_w=0.17 Kg/m^{2}s$^{0.5}$)	Limestone-70cm (μ=41, λ=1.3 W/mK, A_w=0.02 Kg/m^{2}s$^{0.5}$)	Lime plaster-3cm	Coruchéus Library in Lisbon	Lisbon
Lime plaster - 3cm	Solid Brick-60cm (μ=15, λ=0.6 W/mK, *A_w=0.2 Kg/m^{2}s$^{0.5}$)	Lime plaster - 3cm	San Giorgio in Poggiale Library in Bologna	Bologna

*Aw approximated from D_{ws} at free saturation (w_f) according to the formula $D_{ws}(w_f)=3.8*(A/w_f)^2$ (Künzel, 1995).

The materials adopted to represent the stone walls of the case studies in Porto and Lisbon have thermal conductivities that are in good agreement with the indications given by LNEC technical report "ITE 54 – Thermal transmission coefficients of building envelope elements" (Pina Dos Santos and Rodrigues, 2010) for traditional Portuguese granite and limestone walls, i.e. respectively around 2.1 and 1.7 W/(m.K). In addition, the stone selected from WUFI database to represent granite was chosen because of the similarity of its hygrothermal characteristics to the data offered in the literature for granite specimens extracted from historic walls (Banfill, 2021). Similarly, the solid-brick masonry adopted for wall for the case study in Bologna has a thermal conductivity that is consistent with the values observed by Lucchi (2017) in an extensive study on historic walls in Italy, which resulted in the range 0.48-0.81 W/(m.K) for massive brick-walls.

An important difference between the three masonry walls lies in their capillary absorption coefficients, which indicate that brick-masonry wall absorbs liquid water faster than limestone and granite walls. Furthermore, the three materials have also very different free saturation water contents, namely about 370 kg/m^3, 190 kg/m^3 and 40 kg/m^3, respectively for bricks, limestone and granite, meaning that bricks can store a much higher quantity of liquid water than the other two materials. These differences can be very important during rainy periods, especially for walls exposed to WDR and not protected by a water-resistant coating system or hydrophobic treatment, which is the scenario considered.

5.3. QUALITATIVE VALIDATION

In each case study, the internal and external superficial temperatures of one wall were monitored for at least three weeks, as shown in chapter 4. In the same period, the temperature of the indoor and outdoor air, very close to the building envelope, was recorded.

The behaviour of the monitored walls was simulated, and the results obtained numerically for the superficial temperatures of the walls were compared to the ones measured in situ. This comparison was used to qualitatively validate the simulations defined in this chapter. This comparison is performed graphically and through a statistical quantification of the error that accounts for the three indexes that are suggested by ASHRAE Guidelines 14: 2014. Those indexes are (Ruiz and Bandera, 2017):

-the Normalized Mean Bias Error - NMBE, that quantifies the global difference between the real values and the predicted ones (recommended to be within -5%, +5%);

- the Coefficient of Variation of the Root Mean Square Error - CV(RMSE), which indicates the model ability to predict the overall load shape that is reflected in the data (suggested ≤ 30%);

- the coefficient of determination - R^2, which indicates how close simulated values are to the regression line of the measured values (recommended ≥ 0.75 for calibrated models).

5.3.1. METHOD

The results obtained via numerical simulations, in terms of superficial temperature at the interior and exterior surface of the walls, were compared to the ones experimentally measured on-site. The walls monitored were a South-oriented wall for Porto and a South-west-oriented wall for Lisbon and Bologna. Thus, the simulated walls were oriented accordingly.

The external surface-temperature-sensors located in the wall of the case study in Bologna were in a part of the wall that was found to be in the shadow for most of the time, for this reason, the wall was simulated as not exposed to direct sun radiation (constant shadow), for the sake of model validation. The sensor located on the external surface of the wall in Lisbon case study was found to be in the shadow for part of the day-time, for this reason, the simulations adopted for the validations were performed considering the wall in the shadow (no direct sun radiation) after 2 PM.

First, the simulations were run considering the boundary conditions provided by the meteorological stations and the indoor monitoring campaign, as previously outlined. Additionally, the simulations are also performed by accounting for the indoor and outdoor air temperature measured very close to the buildings envelope, for comparison purposes.

5.3.2. RESULTS AND DISCUSSION

A graphical comparison is provided in Figures 5.6, 5.7, 5.8 and the statistical evaluation of the errors is reported in Table 5.2.

As long as the interior superficial temperatures are concerned, all the simulations comply with the indication of ASHRAE guidelines for statistical errors. For external superficial temperatures, the results of the simulations performed with the air temperatures measured near the envelope (represented with a black line) fit very well with the measured superficial temperatures, which is confirmed by the statistical indexes for error evaluation. The results obtained using the weather data from the meteorological stations have a worse fit. This outcome is the result of the position of the meteorological stations out of the cities, where the local climate can be slightly different from the urban microclimate in which the buildings are located. Nonetheless, for Lisbon case study the indexes comply with ASHRAE indications in all cases, and thus the simulation model for Lisbon walls is considered qualitatively validated. For the other two case studies, the simulations are evaluated as qualitatively validated and reliable for the scope of the study, for the following reasons:

- the CV complies with the indication of ASHRAE Guidelines, showing that the overall load-shape of the data is correctly predicted;

- the NMBE is positive, meaning that the simulations underestimate the external superficial temperatures, thus safely increasing the predicted risks related to moisture accumulation.

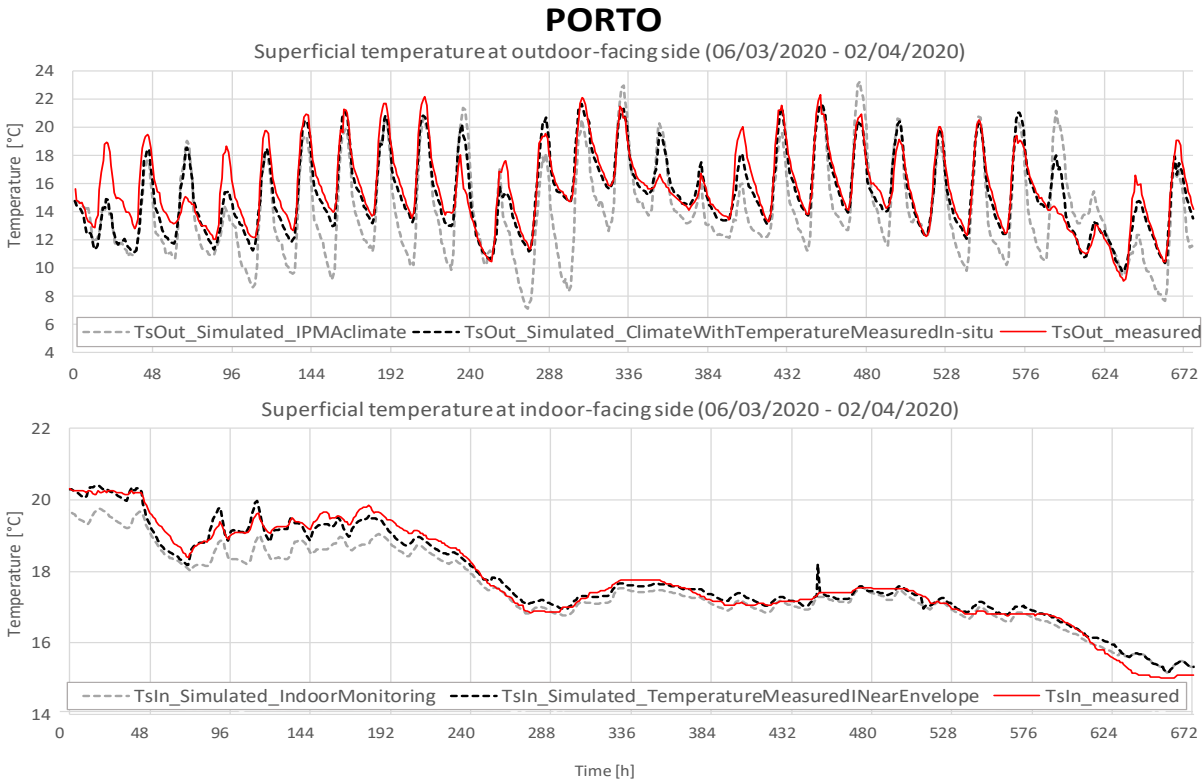

Figure 5.6– External and Internal superficial temperature of walls: Simulated and measured, Porto case study.

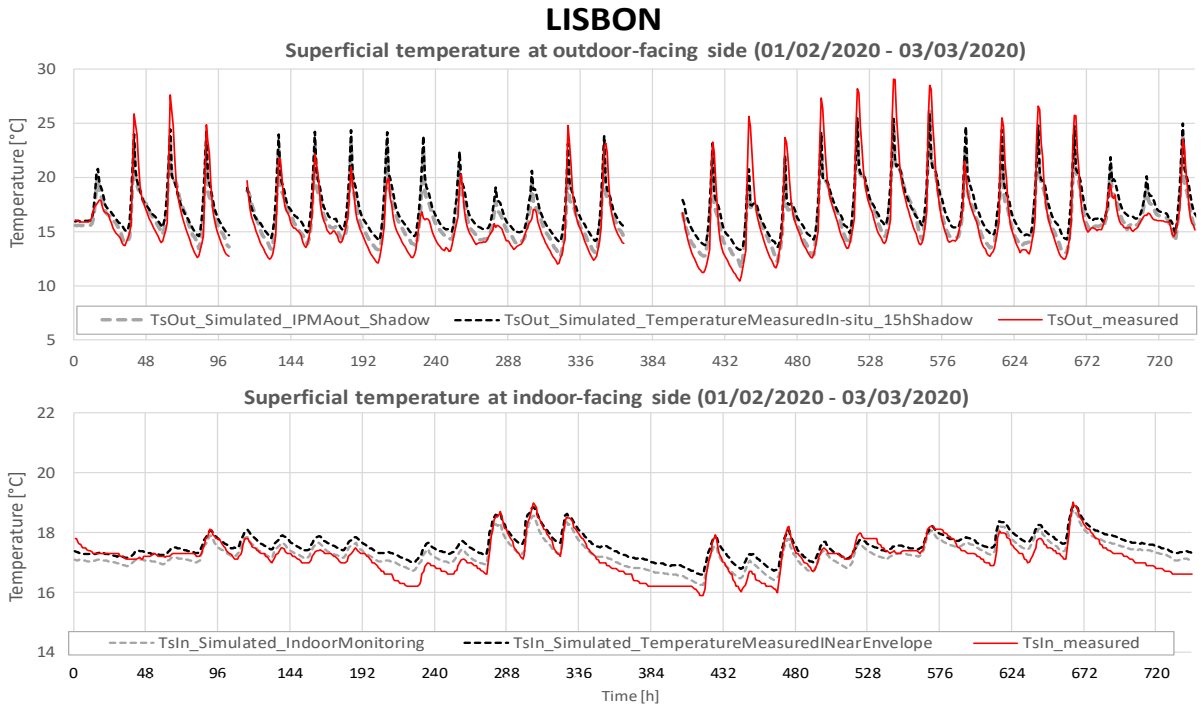

Figure 5.7 – External and Internal superficial temperature of walls: Simulated and measured, Lisbon case study.

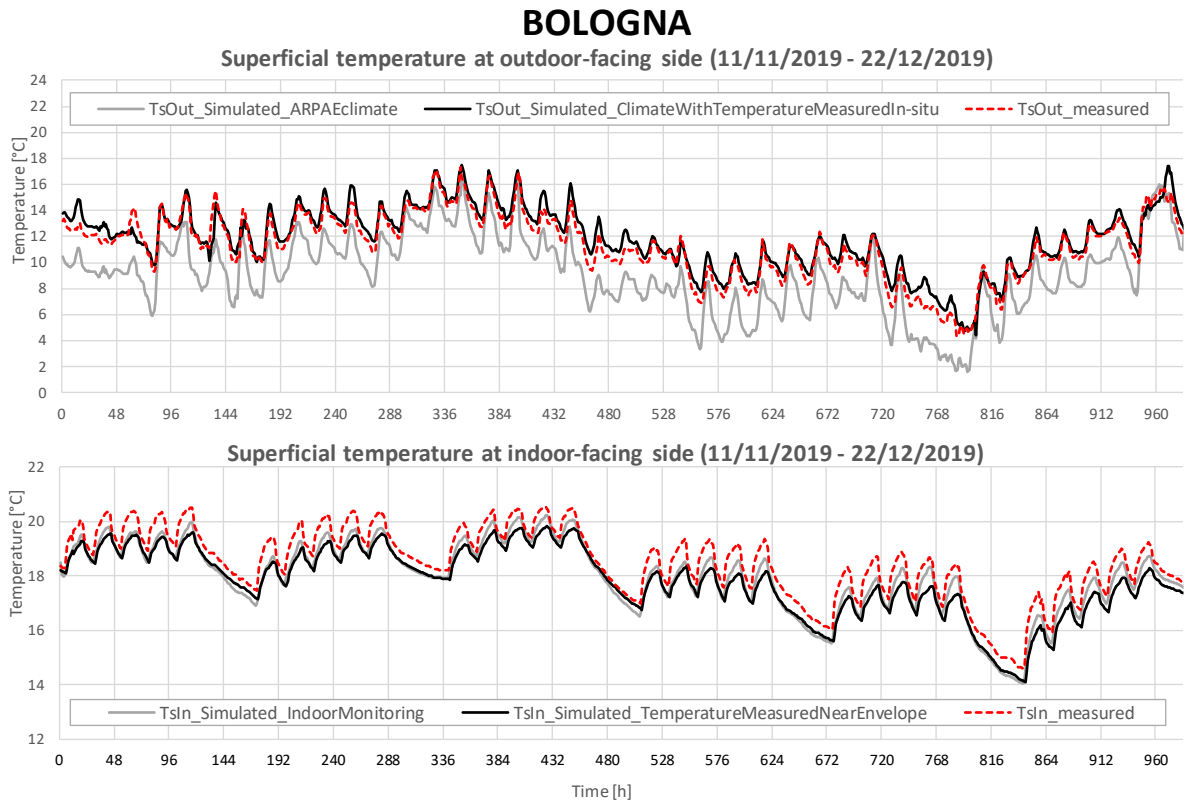

Figure 5.8 – External and Internal superficial temperature of walls: Simulated and measured, Bologna case study.

Table 5.2 – Statistical quantification of the error int the simulated superficial temperatures, where: Sim_GenericMeas indicates the simulations that used the temperatures from meteorological stations and indoor monitoring campaigns as boundary conditions; Sim_SpecificMeas. Indicates the simulations performed using the indoor and outdoor air temperatures recorded near the envelope.

	EXT.SURFACE				INT.SURFACE			
	OUT_Sim_SpecificMeas.		OUT_Sim_GenericMeas.		IN_Sim_SpecificMeas.		IN_Sim_GenericMeas.	
PORTO	NMBE		NMBE		NMBE		NMBE	
	3%	**≤10%**	**11%**		**0%**	**≤10%**	**2%**	**≤10%**
	CV=		CV=		CV=		CV=	
	8%	**≤30%**	**19%**	**≤30%**	**1%**	**≤30%**	**3%**	**≤30%**
	R^2=		R^2=		R^2=		R^2=	
	0.84	**≥0.75**	**0.60**		**0.98**	**≥0.75**	**0.98**	**≥0.75**
	OUT_Sim_SpecificMeas.		OUT_Sim_GenericMeas.		IN_Sim_SpecificMeas.		IN_Sim_GenericMeas.	
LISBON	NMBE		NMBE		NMBE		NMBE	
	-6%	**≤10%**	**-2%**	**≤10%**	**-2%**	**≤10%**	**0%**	**≤10%**
	CV=		CV=		CV=		CV=	
	12%	**≤30%**	**10%**	**≤30%**	**3%**	**≤30%**	**2%**	**≤30%**
	R2=		R2=		R2=		R2=	
	0.80	**≥0.75**	**0.82**	**≥0.75**	**0.80**	**≥0.75**	**0.79**	**≥0.75**
	OUT_Sim_SpecificMeas.		OUT_Sim_GenericMeas.		IN_Sim_SpecificMeas.		IN_Sim_GenericMeas.	
BOLOGNA	NMBE		NMBE		NMBE		NMBE	
	-4%	**≤10%**	**24%**		**4%**	**≤10%**	**3%**	**≤10%**
	CV=		CV=		CV=		CV=	
	6%	**≤30%**	**26%**	**≤30%**	**4%**	**≤30%**	**3%**	**≤30%**
	R^2=		R^2=		R^2=		R^2=	
	0.95	**≥0.75**	**0.92**	**≥0.75**	**0.94**	**≥0.75**	**0.98**	**≥0.75**

5.4. EVALUATION OF THE HYGROTHERMAL BEHAVIOUR OF WALLS RETROFITTED WITH DIFFERENT INTERNAL AND EXTERNAL INSULATION SOLUTIONS.

The numerical models of the walls are used to evaluate the performance of the envelopes after the adoption of thermal insulation. The study takes into account different insulation solutions, applied at the internal or external side of the walls, and based on thermal mortars. These solutions are compared to others based on more common insulation materials, such as hydrophobic mineral wool and EPS.

In this section, the thermal insulation solutions adopted are described and the properties of the materials are presented. The configurations studied are then schematically introduced, to synthesize which combinations of walls, climates, orientations, and insulation solutions are considered. Then, the criteria adopted for the evaluation of moisture-related risks and thermal performances are discussed. The analysis takes into consideration moisture accumulation in the wall substrate, reduction of drying, high humidity between the wall and the internal insulation, and the reduction of winter heat losses through the walls.

5.4.1. THERMAL INSULATION SOLUTIONS CONSIDERED

The thermal mortar-based systems considered are the ones characterized in Chapter 4 (S1-S5) and the properties of the materials adopted in the simulations are based on the results experimentally obtained.

These systems are compared with others made of hydrophobic mineral wool (MW) and expanded polystyrene (EPS), both of them finished with mortar B2, introduced in Chapter 4, which is designed for adoption in both indoor and outdoor exposed systems. These two materials, EPS and MW, are chosen because they are very commonly adopted (as seen in Chapter 2). They are non-hygroscopic materials with very low capillary absorption coefficients, which respectively have low (EPS) and high (MW) vapour permeability. It is worth underlying that hydrophobic mineral wool and EPS have such low A_w, less than 0.008 $Kg/m^2s^{0.5}$ according to the tests of Jerman and Černý (2012), that their suction and redistribution coefficients, which govern liquid transport in the materials, are simplified as null in WUFI database of insulation materials.

In order to evaluate how capillary transport coefficient and vapour permeability of the insulation layer affect moisture-related risks, one of the thermal mortars (A3) is also adopted with reduced liquid and vapour transport properties. Thus, three auxiliary systems are considered to have a small parametric evaluation on the importance of the hygric properties of insulation materials:

- **S5_mu:** where thermal mortar A3 is assigned with a μ=50, i.e., the same high vapour resistance factor of EPS;
- **S5_A_w.:** where thermal mortar A3 is assigned with an A_w=0 and a null sorption isotherm (non-hygroscopic), i.e. the same properties of EPS and hydrophobic mineral wool;
- **S5_A_w_mu:** where thermal mortar A5 is assigned with a μ=50, A_w=0 and a null sorption isotherm, like EPS.

The s_d and A_w of the three systems based on S5, are reported in Figure 5.9, together with system S5, to

schematically show the idea behind the parametric study.

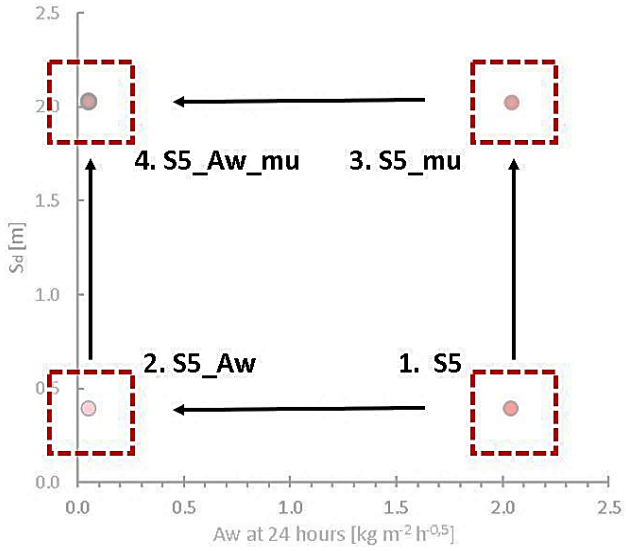

Figure 5.9 – Equivalent air layer thickness (s_d) and capillary absorption coefficient (Aw) of insulation solutions based on S5, adopted for the parametric study.

For practical reasons, systems having a neglectable A_w and sorption isotherm, which are simplified as null in the numerical simulations, are referred to as non-hygroscopic and hydrophobic or non-capillary-active materials in this work. On the contrary, systems with higher A_w and sorption isotherm are indicated as capillary-active and hygroscopic. In literature "capillary-active" and "hygroscopic" are terms that are adopted, at times, to indicate materials with high A_w and high hygroscopicity. In this work this assumption is not taken, thus materials with moderate or high Aw and hygroscopicity are all defined as hygroscopic and capillary active, as opposed to hydrophobic and non-hygroscopic materials such as EPS and MW.

The assembly considered for each insulation system is presented in Table 5.3 and the characteristics of the materials are provided in Table 5.4. All systems are in direct contact with the wall substrate, thus the intervention simulated consists of the removal of the original plaster or render, and successive application of the thermal insulation systems. For thermal mortars, it is common practice to apply the material on the wall directly. For EPS and MW, various types of application can be considered, for instance, the use of a glue mortar or mechanical application. In this study the second one is considered, to make the comparison with thermal mortars more direct.

The simulations are run under the hypothesis of perfect contact between the insulation layer and the surface of the wall.

Table 5.3 – Composition of the insulation systems.

SYSTEMS	Type	Adoption	Assembly
S1	based on cork-mortar A1	Indoor exposed	thermal m. A1(4cm) +regularization m. B1 (2mm) + paint C1 (0.5mm)
S2	based on cork-mortar A1	Outdoor exposed	thermal m. A1(4cm) +regularization m. B1 (2mm) + paint C2 (0.5mm)
S3	based on cork-mortar A2	Indoor exposed	thermal m. A2(4cm) +regularization m. B1 (2mm) + paint C1 (0.5mm)
S4	based on cork-mortar A2	Outdoor exposed	thermal m. A2(4cm) +regularization m. B1 (2mm) + paint C2 (0.5mm)
S5	based on cork-mortar A3	Indoor and outdoor exposed	thermal m. A3(4cm) +regularization/finishing m. B2 (2mm)
S_MW	based on mineral wool	Indoor and outdoor exposed	mineral wool MW(4cm)+regularization/finishing m. B2 (2mm)
S_EPS	based on EPS	Indoor and outdoor exposed	EPS(4cm)+regularization/finishing m. B2 (2mm)
S5_mu	*Same type and adoption of S5 It is the same system but with adapted properties (μ, Aw) in the insulation layer*		thermal m. **A3 with μ=50** (4cm) +regularization/finishing m. B2 (2mm)
S5_Aw			thermal m. **A3 with Aw=0 and null sorption isotherm** (4cm) +regularization/finishing m. B2 (2mm)
S5_Aw_mu			thermal m. **A3 with μ=50,Aw=0 and null sorption isotherm** (4cm) +regularization/finishing m. B2 (2mm)

5.4.2. HYGRIC PROPERTIES OF COMPLETE THERMAL INSULATION SYSTEMS

Hygric properties of complete insulation systems are important for evaluating their impact on the moisture dynamics of building components. The capillary absorption coefficient and resistance to vapour diffusion of complete systems are particularly relevant for external insulation solutions since these two properties regulate the wetting and drying of components exposed to outdoor weather.

The importance of these two parameters for outdoor-exposed building components emerges in two regulations. The European Assessment Document for External Thermal Insulation Composite Systems (ETICS) with renderings - EAD 040083-00-0404:2020 - (EOTA, 2020) and the German standard on rain-protective stuccos and coatings DIN 4108-3:2018-10 (Künzel, Künzel and Holm, 2004).

The first regulation set a maximum capillary absorption for complete insulation systems, namely 0.5 kg/m^2 of absorbed water at 24hours, corresponding to an A_w of 0.10 $kg.m^{-2}.h^{-0.5}$, and a maximum s_d of 1m for the coating of vapour permeable insulation materials. The second standard defines a hyperbola $A_w * s_d = 0.2$ $kg.m^{-1}.h^{-0.5}$, and all solutions having a lower $A_w * s_d$ are considered suitable to avoid moisture accumulation in walls, because of their good balance between rainwater intake and drying. The standard

also sets a maximum A_w and s_d, of 0.5 $kg.m^{-2}.h^{-0.5}$ and 2m respectively, to avoid too high rainwater intake and too low drying rates.

Table 5.4 – Hygrothermal characteristics of the materials composing the insulation systems.

	A1	A2	A3	B1	B2	C1	C2	MW	EPS
DRY BULK DENSITY [Kg/m³]	612.8	724.2	342.3	1617	1316	1617	1617	60	30
OPEN POROSITY [m³/m³]	0.342	0.307	0.288	0.307	0.311	0.307	0.307	0.950	0.950
VAPOUR RESISTANCE FACTOR [-]									
dry conditions	14.6	18.8	11.0	18.3	15.6	106	737	1.3	50
wet conditions	12.0	14.7	9.17	13.4	13.7	72.5	648	/	/
						(modelled 0.5mm thick)			
CAPILLARY WATER ABSORPTION COEFFICIENT [Kg/ (m² s$^{0.5}$)]	0.044	0.022	0.034	0.18	0.034	0.017	0.0046	***	***
FREE WATER SATURATION [Kg/m³]	300.0	215.9	66.2	276.7	128.6	276.7	276.7	0	0
MOISTURE STORAGE FUNCTION (w[Kg/m³])								0	0
at RH 30%	1.64	1.66	0.74	1.11	1.06	1.20	0.92		
at RH 50%	3.98	3.87	1.53	2.29	2.29	2.49	2.09		
at RH 70%	8.97	8.71	4.16	4.92	5.99	5.40	4.64		
at RH 80%	18.42	17.91	14.30	12.18	16.02	11.42	6.69		
at RH 95%	35.27	37.52	32.84	34.07	34.58	28.57	15.71		
at RH 100%	300.0	215.9	66.2	276.7	128.6	276.7	276.7		
REFERENCE WATER CONTENT w at 80%RH [Kg/m³]	18.42	17.91	14.30	12.18	16.02	11.42	6.69	0	0
SPECIFIC HEAT CAPACITY [J/kg K]	843	848	920	*850	*850	*850	*850	850	1500
THERMAL CONDUCTIVITY Dry [W/mK]	0.0978	0.128	0.0654	*0.7	*0.7	*0.7	*0.7	0.04	0.04

THERMAL CONDUCTIVITY [W/mK] moisture dependent	**A1**		**A2**		**A3**		
	w[Kg/m³]	**λ [W/mK]**	**w[Kg/m³]**	**λ [W/mK]**	**w[Kg/m³]**	**λ [W/mK]**	dependency on temperature and moisture is considered
at w0 (50% RH)	33.0	0.107	59.7	0.142	31.7	0.067	
at w1	171	0.175	133	0.190	75.9	0.076	
at w2	210	0.226	148	0.224	105	0.111	
at w3	280	0.315	181	0.300	171	0.171	
****at saturation**	342	0.325	307	0.498	288	0.249	

*assumed from typical values found in lime-mortars from Wufi database

**derived from exponential correlation λ -w

***very low capillary water absorption coefficient, which is simplified by WUFI Database as transport coefficients Dww, Dws=0 m2/s

The A_w and s_d of the original render and of the external insulation systems considered are displayed in Figure 5.10, together with the aforementioned standard recommendations for ETICS and rain-protective stucco/coatings. From Figure 5.10 it emerges that three systems comply with the limits set in the German standard: S5, S_MW and S5_A_mu. The latter two systems are also below the threshold values of the EAD for ETICS, thanks to their very low capillary absorption coefficient and high vapour permeability. Three systems fall out of the German-hyperbola, namely S2, S4 and S5_mu. Two systems exceed the recommendations of the German standard because of their high s_d value (S5_A_mu and S_EPS), although being below the hyperbola. The original plaster greatly exceeds the maximum absorption coefficient considered in the German standard, while having a very reduced s_d, meaning that it does not

provide relevant protection against rainwater intake, but it allows for the wall substrate to dry quite fast, thanks to its low resistance to vapour diffusion.

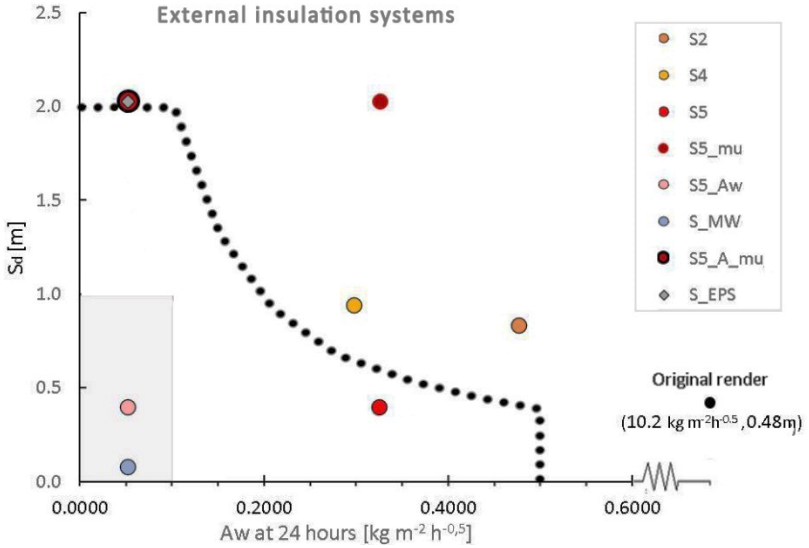

Figure 5.10 – Equivalent air layer thickness (s_d) and capillary absorption coefficient (A_w) of external insulation systems and original render. The black dotted line represents the recommendation of the german standard on rain-protecting stuccos and coatings and the grey area indicates the values below the maximum threshold references mentioned in the EAD for ETICS.

While both hygric properties appear very important for external insulation solutions, the A_w-coefficient of the system does not appear relevant for interior insulation. In fact, for indoor-exposed systems, no direct contact between liquid water and the surface of the system is expected (except for the unlikely case of superficial condensation problems). On the other hand, the capillary absorption coefficient of the insulation layer appears as an important characteristic, since it can help to avoid condensation and water accumulation behind the insulation, thanks to the ability of capillary active materials to buffer and redistribute liquid water (Vereecken and Roels, 2015). Thus, the properties considered important for the analysis of thermal insulation systems for interior application are the s_d of the entire system and A_w of the insulation layer. These properties are reported in Figure 5.11, together with the characteristics of the original plaster.

In the same figure, two dotted lines are adopted to indicate the sd-limits hereby assumed for defining very highly and highly vapour permeable insulation solutions, namely 0.5m and 0.7m respectively. Those reference values are obtained considering a layer of 4cm of insulation materials classified as having high or moderately high vapour permeability in the classification defined in Chapter 2. It follows that systems S_MW, S5_Aw and S5 can be ranked as very highly vapour permeable insulation solutions, while systems S1 and S3 emerge as having moderately high vapour permeability. Systems S_EPS, S5_aw_mu and S5_mu have much higher Sd than the other insulations, namely above 2m, and thus appear to rather vapour impermeable.

The properties presented in Figures 5.10 and 5.11 are, mostly, the ones determined experimentally in chapter 3. For systems based on EPS and MW, as well as S5_mu and S5_Aw_mu, the s_d of the complete systems was calculated according to the properties of single materials, because the s_d of these systems was not experimentally measured. Since there is no standardized calculation method for evaluating the

A_w of a composite system through the A_w of single materials, those of S_EPS, S_MW, S5_Aw and S5_Aw_mu were approximated using simulations of the wetting process.

The A_w of the paint adopted in the simulations is the average of the results experimentally obtained. Thus, the A_w of the systems modelled appears to be slightly different from the ones measured experimentally for systems S2 and S4. Even though these differences are small, it seems relevant to consider them because in the simulations systems S4 has a higher A_w than S2, whereas in the experimental results it was the other way round. The A_w of the modelled systems was approximated by accounting for the results obtained in a simulated wetting process.

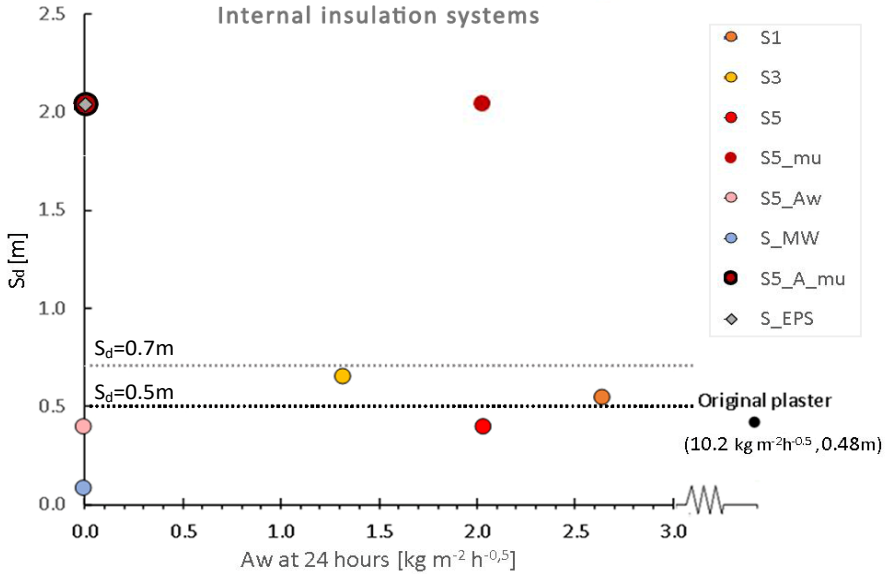

Figure 5.11 – Equivalent air layer thickness (Sd) of internal insulation systems and capillary absorption coefficient of the insulation layer (Aw). In black, also the hygric properties of the original plaster are reported. The black and grey dotted lines indicate the limits assumed for defining very high and high vapour permeable insulation solutions (0.5m and 0.7m), respectively.

5.4.3. SCHEMATIC SUMMARY OF THE SIMULATED SCENARIOS: COMBINATIONS OF WALLS, CLIMATES, ORIENTATION AND INSULATION SOLUTIONS.

In this analysis, three case studies (climate, wall material, wall thickness) are considered as well as two orientations and various insulation systems, applied on the interior or exterior sides of the walls.

The two orientations chosen for the study are the following: South and North for Porto, South-West and North for Lisbon, West and East for Bologna. They were selected to determine high and low water accumulation, according to a sensitivity analysis reported in Annex II.

The set of simulations defined is synthesized in Figures 5.12, 5.13 and 5.14. For each simulated scenario, moisture-related risks and thermal performance are analyzed.

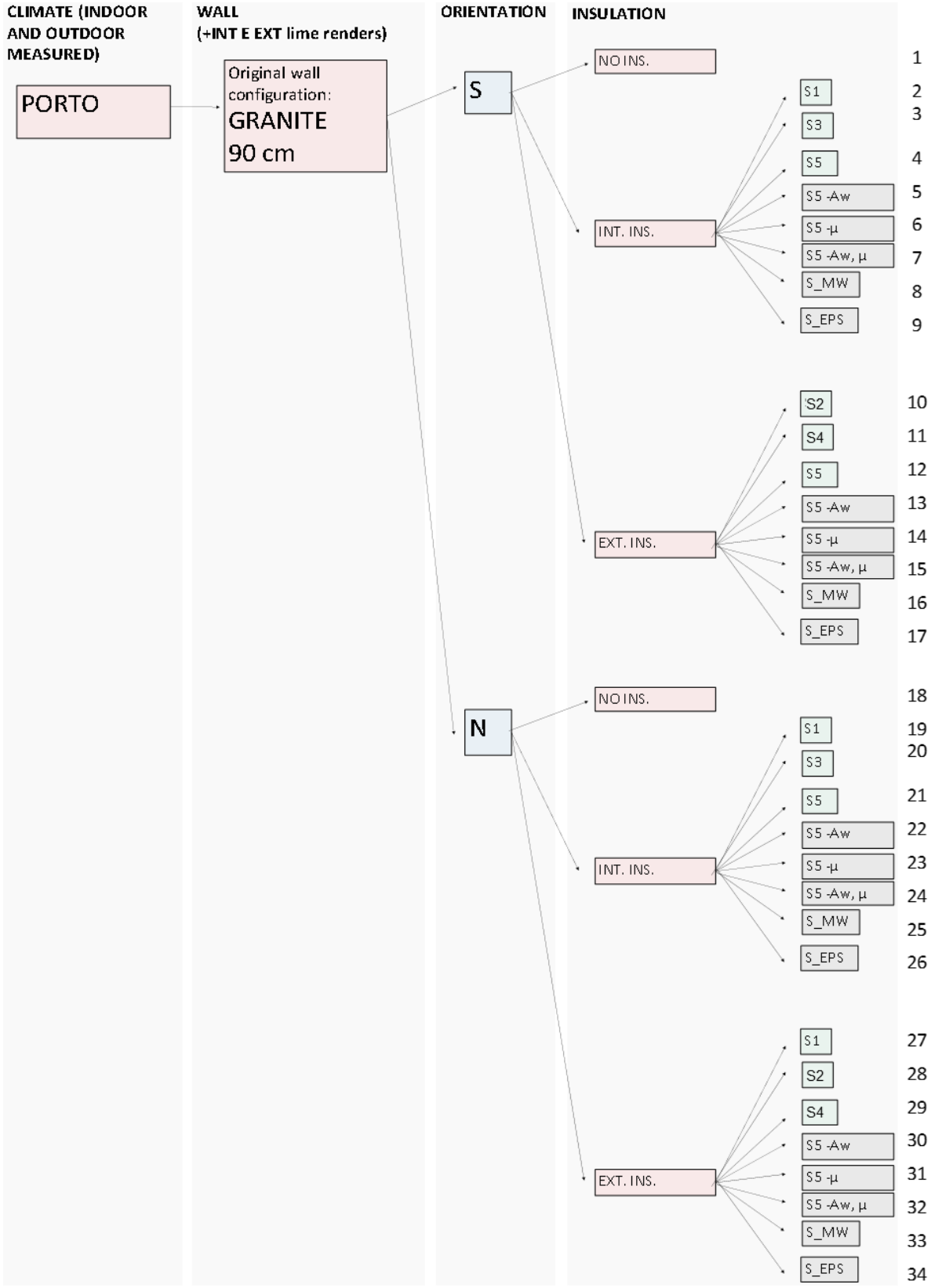

Figure 5.12– Simulation set for the case study in Porto.

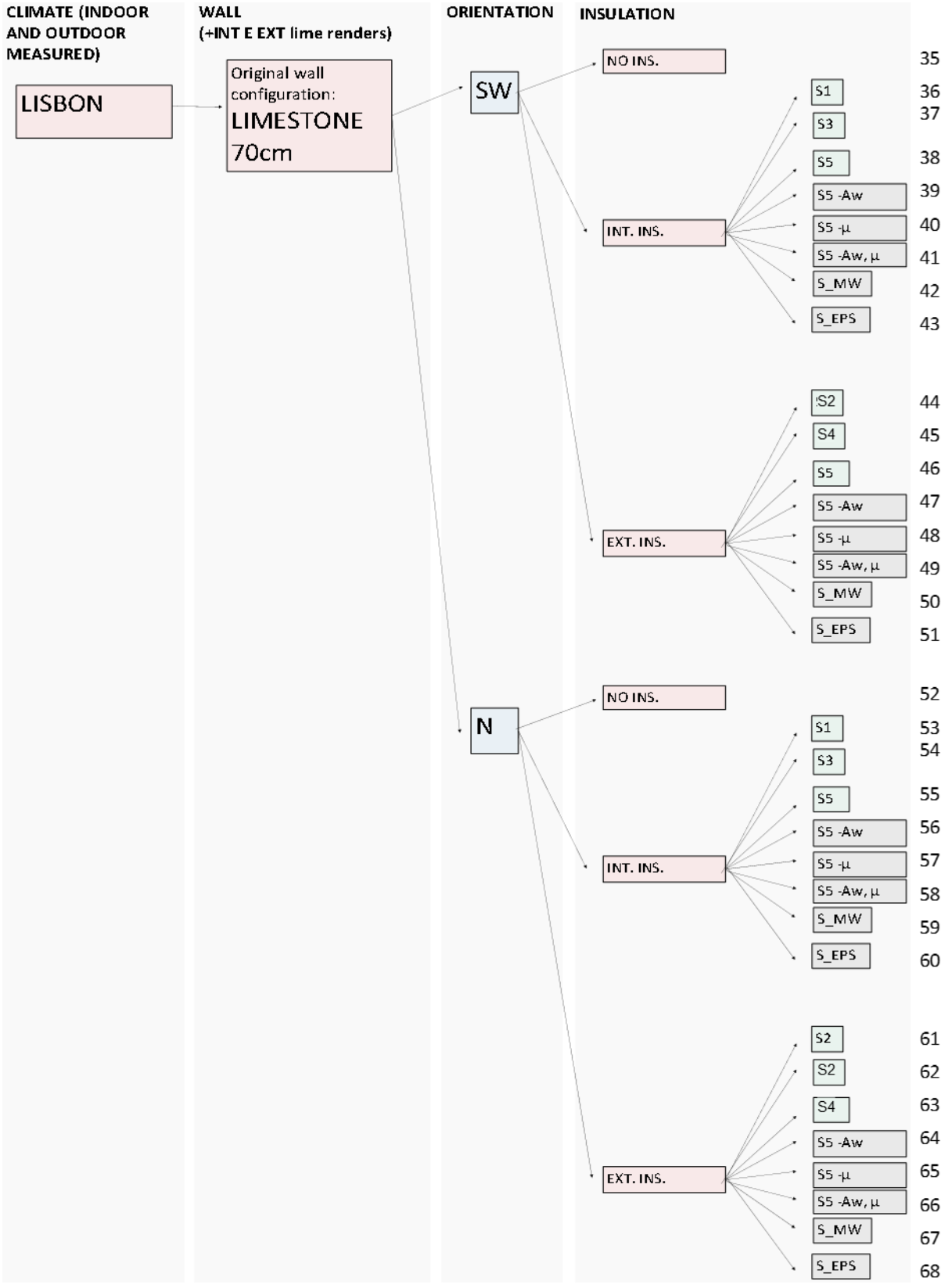

Figure 5.13 – Simulation-set for the case study in Lisbon.

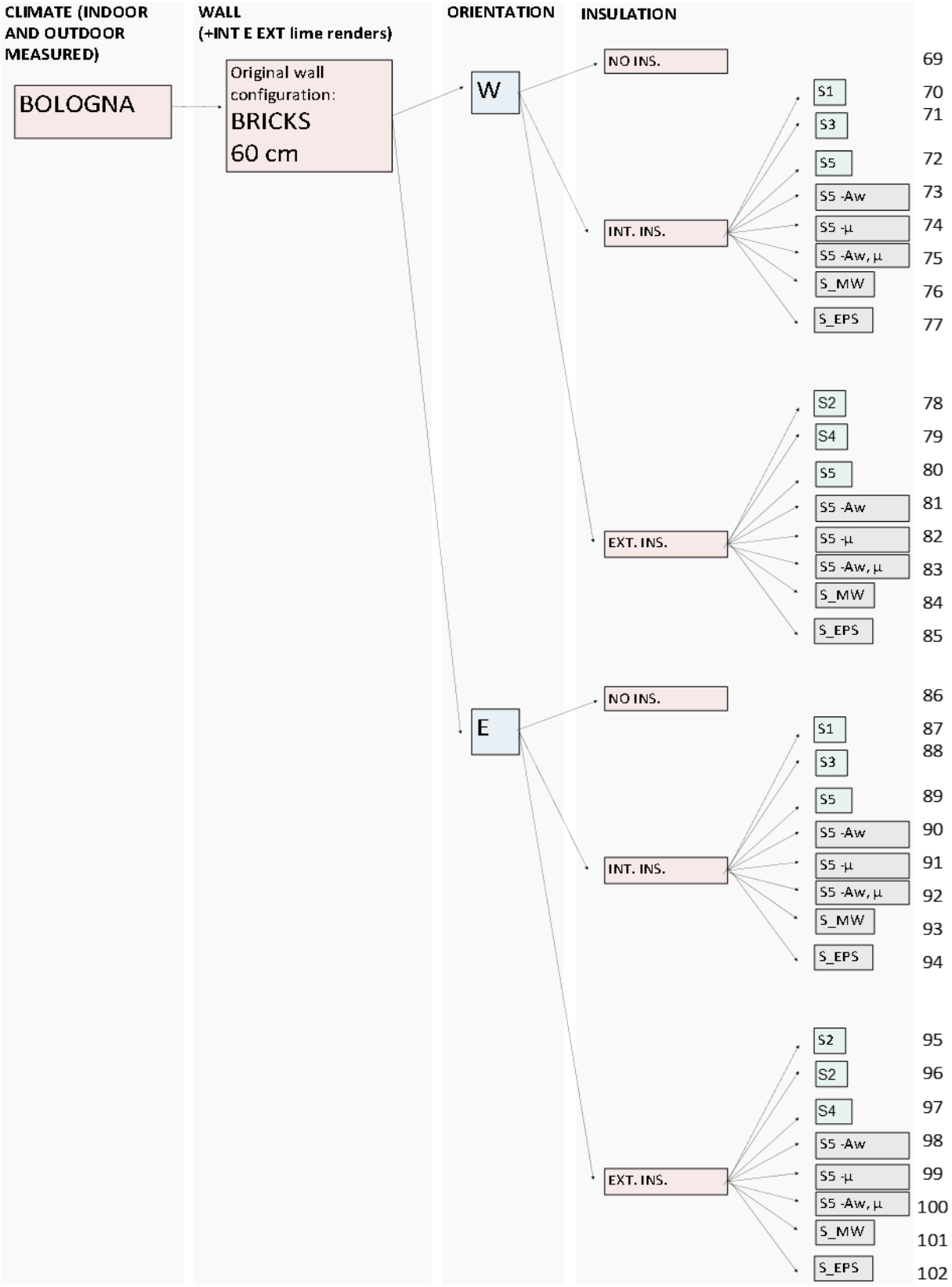

Figure 5.14 – Simulation-set for the case study in Bologna.

5.4.4. CRITERIA FOR THE EVALUATION OF MOISTURE-RELATED RISKS AND THERMAL PERFORMANCE

It is very well known that the best way of insulating a wall is to apply the insulation on its exterior surface (Künzel, 1998). Indeed, this intervention can help to reduce the intake of wind-driven rain while keeping the wall warmer during the heating season. On the other hand, external insulation can strongly reduce the drying of the component through its external surface because of the reduction of vapour permeability induced. Whereas, when internal insulation is adopted, the drying capacity of the wall through the external surface is reduced because of the lowering of the wall temperature. Furthermore, this intervention may increase the resistance to vapour diffusion of the assembly at the indoor facing surface, thus reducing its inward drying. Hence, in both cases, an increase in the moisture content of the wall can occur.
In order to assess whether the retrofit interventions entail moisture-related risks, the results of the simulations are analysed according to the criteria defined in this section. The risks considered are moisture accumulation in the wall substrate, reduction of drying, and high relative humidity between the wall and the internal insulation systems. In addition, thermal performance is evaluated by comparing the winter-heat losses through the wall, before and after the retrofit.

Other important risks that are not considered in this study are the degradation of embedded beam ends, and frost damages. The first risk is not discussed because mono-dimensional simulations do not allow for analyzing the connection between building components. Frost damages at the exterior side of walls are not considered because of the mild winter temperatures that characterize the climates of Porto, Lisbon and Bologna. Indeed, typical threshold values of temperature considered in the risk evaluation are as low as -2°C (Vereecken *et al.*, 2015), to account for salt dissolution and other occurrences. Such low temperatures occur only for one hour in Bologna's data set, and never in the two Portuguese climates.

Results related to the moisture content in the walls substrate are hereby presented and discussed in terms of saturation degree. Saturation degree is calculated as the ratio between the water content and the free saturation water content of the material [%], thus representing the fraction of open pores filled with moisture against those accessible for moisture (Zhao *et al.*, 2017). This parameter is adopted to make results more comparable, since the walls considered are made of different stones and bricks, with very different saturation water contents. The term water/moisture content (volumetric) is adopted to indicate the mass of water contained in the unit of volume of material.

5.4.4.1. MOISTURE ACCUMULATION

Post-insulating an existing wall entails a change in its heat and moisture transfer, which can result in an increase in moisture content.

This risk is qualitatively evaluated by comparing the water content in the wall substrate (granite, limestone, bricks) in the original configuration (at dynamic equilibrium) and during a 10-year-period for retrofitted configurations.

An index for evaluating the risk ($i_{m.a.}$) is hereby defined as the difference between the average annual water content in the substrate of the un-retrofitted and retrofitted wall, in the 2nd year of simulations, normalized by the average annual water content in the un-retrofitted wall. Thus, the greater the index

the higher the increase of water content in the wall, while negative results indicate that the retrofit leads to a reduction of average annual water content in walls.

Thus the index is evaluated according to the following equation:

$$i_{m.a.} = \frac{w_{avg\_retrofitted} - w_{avg\_un-retrofitted}}{w_{avg\_un-retrofitted}} [\%] \quad (5.1)$$

Where $w_{avg\_retrofitted}$ and $w_{avg\_un-retrofitted}$ respectively indicate the average water content in the substrate of the un-retrofitted wall at dynamic equilibrium, and in the retrofitted wall during the 2nd year of simulations.

5.4.4.2. REDUCTION OF DRYING

When adopting interior or exterior insulation systems for retrofitting exposed walls, the risk of determining a reduction in the drying ability of the wall should be considered (Künzel, 1998).

Safeguarding the original drying ability of traditionally constructed walls is always important, even for walls protected from wind-driven rain, since all walls may suffer from high-water content due to rising damp, damages in the envelope, pipes leakage or even floods, a concern that is growing with the worsening of climate change (Freitas *et al.*, 2020). What is more, interventions that reduce the drying ability of walls can determine an increased level of rising damp (Veiga, 2013).

The drying of walls is hereby studied by considering walls starting from saturation water content and drying under operational conditions. The drying abilities of the original and retrofitted walls are qualitatively compared by plotting the water content in the walls substrate during the first 10 years of drying, as shown in figure 5.15.

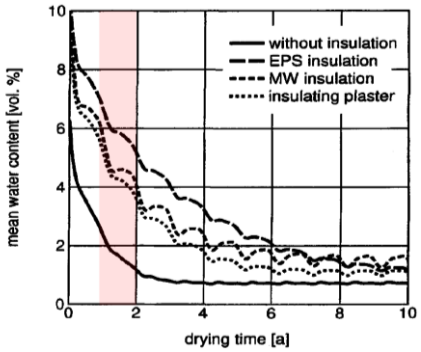

Figure 5.15– water content in different walls configurations during drying, adapted from Künzel (1998).

Then, a numerical index is adopted to compare the reduction of drying entailed by the different retrofit solutions. The index (i_{drying}) is hereby defined as the difference between the average annual water content in the substrate of the un-retrofitted and retrofitted wall, normalized by the average annual water content in the un-retrofitted wall, during the second year of drying, according to the following equation:

$$i_{drying} = \frac{w_{avg\_retrofitted} - w_{avg\_un-retrofitted}}{w_{avg\_un-retrofitted}} [\%]. \quad (5.2)$$

Hence, the higher the index the stronger the reduction of drying, whereas a negative index indicates that the retrofitted wall dries faster than the original configuration.

5.4.4.3. HIGH HUMIDITY BETWEEN THE WALL AND THE INTERIOR INSULATION SYSTEMS

When adopting internal insulation, condensation may occur at its cold side, during the heating season. It is thus important to evaluate for how long high humidity levels are found at this critical interface (Vereecken *et al.*, 2015), to assess if condensation gets relevant. For massive walls exposed to moderate outdoor temperatures like the ones considered, condensation between the wall and the interior insulation system is not expected. Nonetheless, it appears important to evaluate if the interventions lead to a persistent increase in the levels of RH at the critical interface since other problems may occur, such as mould growth when RH is above 80% RH, or even condensation when unfavourable and unpredicted conditions occur, for example, periods of high occupancy leading to high indoor humidity or interruption of heating due to problems with the heating devices, or around thermal bridges.

This risk is roughly evaluated by plotting the profile of relative humidity at the critical interface for the un-retrofitted and retrofitted walls, during the 10th year after the retrofit (when dynamic equilibrium conditions are observed in the RH at the interface).

The risk index ($i_{RH\_cr.int.}$) is elaborated as follows. First, the maximum RH behind the plaster in the original wall is identified. Then cumulated sum of the RH exceeding this limit, along the entire last year of simulations is calculated. The risk index is evaluated according to the following equation:

$$i_{RH\_cr.int.} = \left(\sum \Delta RH_{\ retrofitted} - \sum \Delta RH_{\ UNretrofitted}\right) 10^{-3} \quad [\%], \quad (5.3)$$

where $\sum \Delta RH$ is the sum of the hourly excess from the limit RH previously defined.

Thus, the higher the index the stronger the intensity of the increase in the RH levels at the critical interface, in the retrofitted configuration.

For the calculation of the index, a different threshold value for each wall, instead of a common high RH value, such as 80% or 95-100%, which are limits largely considered in the literature. This choice is taken because of the specific scenario considered. Indeed, in all case studies quite low RH levels are observed, which rarely go above 80%, or even 70% in the walls located in Bologna.

5.4.4.4. REDUCTION OF HEAT LOSSES DURING WINTER

The main benefit of adopting thermal insulation lies in the reduction of heat losses through the building envelope, namely from the warm indoor environment to the cold exterior one, during winter.

Simplified steady-state methods allow for evaluating the expected heat losses reduction obtained with thermal insulation, through the use of the U-value. The U-value, or thermal transmittance, of a building component, defines its ability to transmit heat under steady-state conditions, and it quantifies the heat that passes through one square meter of the wall when 1°C difference is applied at the boundary layers of air (Hegger *et al.*, 2013). Thus, the lower the U-value the larger reduction of heat losses is theoretically achieved. For most building materials, transmittance grows when relative humidity increases (Amorim *et al.*, 2020), therefore two U-values are calculated, one refers to dry conditions and the other accounts for a relative humidity of 80%. The details of the calculations adopted for calculating the static U-value are reported in ANNEX II.

The theoretical reduction of winter heat losses through the walls is then approximated with the following equation:

$$\Delta U_{\%}=(U_{retrofitted}-U_{original})\ /U_{original})\ [\%]. \quad (5.4)$$

On one hand, the U-value is very commonly referred to when analysing the reduction of heat losses through building components, on the other, it is more suitable to discuss lightweight elements than massive components. For the latters, the effect of thermal inertia can be very significant, and it must be considered to have a perception of the behaviour of walls under real climatic conditions, which are far from steady-state ones. Furthermore, components exposed to outdoor weather without rain protection may experience very high water contents and thus provide for unexpectedly high heat losses due to the presence of liquid water in the materials. In order to account for these occurrences, the heat losses in the original and retrofitted configurations are evaluated accounting for the hygrothermal behaviour of the walls after one year from the intervention, during winter months (December, January, February). The heat losses are quantified by calculating the net sum of the heat passing through the interior surface of walls, per unit of surface and time (W/m^2), while accounting as positive the heat directed from the interior space towards the wall and as negative the heat passing from the surface of the wall towards the indoor air. The percentual heat losses reductions ($\Delta Q_{loss,\%}$) obtained in the retrofitted scenarios are then calculated according to the following equation:

$$\Delta Q_{loss,\%} = \frac{Q_{loss\_insulated} - Q_{loss\_original}}{Q_{loss\_original}}\ [\%]. \quad (5.5)$$

The heat losses reductions expected according to steady-state calculations, based on the U-value only, are compared to the ones calculated with dynamic simulations. Finally, the potential effectiveness of thermal mortars, in comparison to EPS and MW, for reducing heat losses in massive walls exposed to outdoor climate is discussed.

5.4.4.5. MATRIXES OF RISKS AND PERFORMANCE

The results obtained in the study are synthesized by means of matrixes of indexes referring to moisture-related risks and thermal performance.

To help the reading of the matrixes, a colour scale is used, similarly to the assessment colour scale suggested in standard EN 16883:2017 - Guidelines for improving the energy performance of historic

buildings. The range found between the maximum and minimum risk index in each matrix will be divided in sub-ranges, corresponding to a colour from red to green accordingly to the sub-range of risk, were red indicates high risk/low thermal performance and green defines low risk/good thermal performance.

5.5. RESULTS AND DISCUSSION

For each simulated scenario, the moisture-related risks and thermal performance are analyzed in terms of moisture content in the wall substrate, reduction of drying, high relative humidity between the wall and the insulation (only for internal insulation systems), and heat losses during winter.

The results are discussed with a qualitative graphic comparison in this section, while in the next one they are synthesized in matrixes of indexes to facilitate deriving overall conclusions.

5.5.1. MOISTURE-RELATED RISKS WITH EXTERNAL INSULATION

5.5.1.1. MOISTURE CONTENT IN THE WALL SUBSTRATE – EXTERNAL INSULATION

In Figure 5.16, from top to bottom, the saturation degree in the walls located in Porto, Lisbon and Bologna is presented. On the left and right sides of the figure, the results obtained with walls exposed to higher and lower annual loads of WDR in each climate are reported, respectively.

The black line represents the saturation degree in the original wall.

In terms of moisture content in the original walls, it appears to grow during winter, when the outdoor temperature is low and rainfalls are significant, so the walls are both subjected to reduced drying and relevant wetting. Then the walls dry to a lower water content until the following winter, when the saturation degree rises again. In walls located in Bologna also during summer an increase in moisture content is observable, which is the result of the relevant WDR in summer (as shown in section 6.2.3.1). The lowest saturation degrees, namely below 5% for the whole simulation period, are found in the N-oriented wall in Lisbon and in the two walls located in Bologna. In Lisbon, the moderate water content is very likely to be the result of the extremely low annual load of WDR. In Bologna it is the combination of the moderate annual load of WDR and the fact that it is spread along the year, being relevant during summer, when walls can better evaporate because of the higher temperatures. Much higher moisture content is found in the walls of Porto and in the SW-oriented facade in Lisbon, where the load of WDR is much higher. Water content is especially high in the S-oriented wall in Porto, which is indeed affected by a very high WDR load, i.e. almost two to three times higher than in the other facades exposed to high WDR. Saturation degrees are roughly in the range 35-45% in the former wall and 20-30% in the latter ones. These values appear relevant since they are about one or two orders of magnitude higher than practical moisture content (i.e., content at 80% RH, which is about 2% and 0.7% for the substrate of Porto and Lisbon walls, respectively). In addition, a saturation degree of 30% corresponds to an increase of about 20% in thermal conductivity of these walls, in comparison to dry conditions. This result suggests that reducing their water content can be very beneficial for their thermal performance.

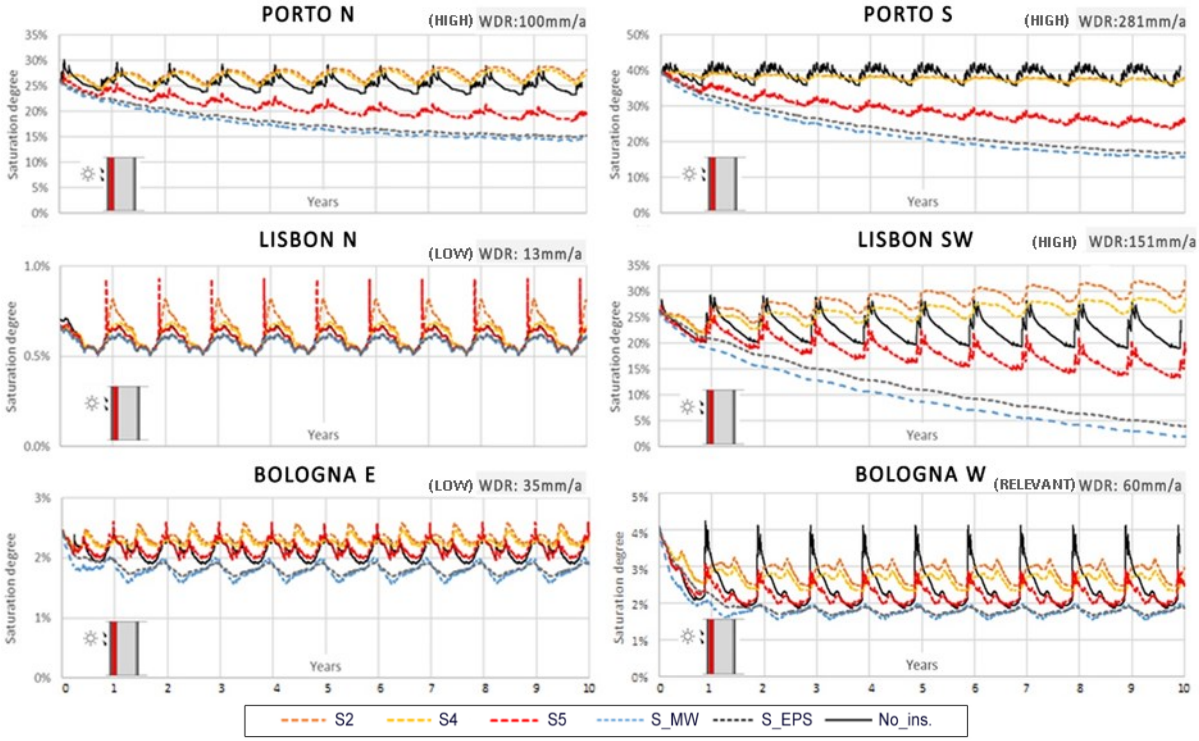

Figure 5.16 – Saturation degree in walls substrate in the original and retrofitted scenarios (external insulation).

Moving to the moisture content in retrofitted walls, it seems that adopting external thermal insulation in facades exposed to low WDR loads results in neglectable changes. Indeed, with all solutions, saturation degree stays around the practical value for the 10-year-period, namely 3% in the E-oriented facade of Bologna and 0.7% in the N-facing wall in Lisbon. On the contrary, for facades exposed to relevant or high WDR, the effect of the external insulation solutions on the moisture content of the wall is very significant.

The adoption of S_EPS and S_MW reduces moisture content, to a higher extent than any other insulation solution, in all walls. This seems the result of the very low A_w of these systems, which decreases rainwater intake in the facades. The effect is moderate in walls exposed to low WDR, and more relevant in walls exposed to higher WDR. The highest benefits are observed in walls exposed to high WDR, where the saturation degree falls to about 1/2 of the initial value in the walls located in Porto, and less than 1/5 in the SW-oriented facade in Lisbon, at the end of the 10-year-period. In the three walls exposed to high WDR, S_MW leads to a lower saturation degree than EPS. This result is likely to be related to the much lower s_d that MW has, which positively affects the drying ability of the wall through vapour diffusion.

Also with thermal mortar-based systems, the outcomes seem to depend on the WDR affecting the walls. The three systems S2, S4 and S5 do not result in relevant changes of saturation degree in walls exposed to low WDR. In the W-oriented wall in Bologna, which is subjected to relevant WDR, the reduction of rainwater intake provided by S5 is evident and the peak of saturation degree is reduced, but the minimum water content stays at the same level as in the un-retrofitted wall. This outcome shows that although reducing rainwater intake, S5 slightly slows down the drying of the wall. The effect of S2 and S4 on reducing the peak of saturation degree in the wall is very similar to S5, but they entail a much stronger

reduction in the drying ability of the wall. For this reason, they lead to noticeably higher water content than in the original wall, for most of the time. In walls exposed to high WDR, system S5 leads to a strong reduction of water content through the 10-year-period considered, which is the result of the protection from rain provided and the moderate impact on drying. On the contrary, systems S2 and S4, although reducing rainwater intake, seem to slow down the drying to a very relevant extent. Because of this effect, S2 and S4 lead to much higher water contents than S5, and even higher than in the un-retrofitted walls for the SW-oriented facade in Lisbon and the N-oriented one in Porto. In these two walls, water accumulation is observed when systems S2 and S4 are adopted, with saturation degree in the wall getting higher and higher through the 10-year-period. In the S-oriented wall in Porto, the systems do not lead to higher water contents than in the original wall. In this case, the balance between the reduced rainwater intake and the slower drying is more favourable than with the original render. This outcome seems the result of the very high WDR affecting the facade, which probably makes the reduction of rainwater intake provided by S2 and S4, more relevant than the reduction of drying entailed.

The results obtained for the parametric study on hygric properties are reported in Figure 5.17. In the picture, black lines represent the saturation degree in the walls substrate when the un-retrofitted configuration is considered.
In all cases, the best results are obtained when system S5 has a low water absorption coefficient (S5_A_w and S5_A_w_mu), even when it has a high s_d. Furthermore, lower water contents are observed with S5_A_w than S5_A_w_mu, in the S-oriented wall in Porto, and especially in the SW-oriented façade in Lisbon (where the wall substrate is more capillary active than in Porto), similarly to what was observed with systems S_EPS and S_MW. In the first year after the application, the walls in Bologna show higher water content with S5_A_w_mu than S5_A_w. These results suggest that even with a reduced intake of rainwater, the walls have a slower drying when the s_d of the system is high, which is consistent with the outcomes previously obtained with S_EPS and S_MW.
S5_mu determines higher water contents than S5, but to an extent that does not appear relevant, in most walls. The moderate impact of S5_mu on moisture content, despite its high sd, is probably because the reduction obtained in rainwater intake is more relevant than the reduction of drying entailed, under operational conditions with typical water contents. Overall, the impact of a low A_w seems more important than the impact of a high s_d in walls exposed to high wind-driven rain. In the walls of Bologna, S5_mu determines noticeably higher moisture content than S5 and the original render, but also in this case the saturation degree stays so low that the increase does not seem relevant.
Systems with a low A_w appeared to work well, independently from the s_d chosen (up to 2.05m), under typical operational conditions. Results show that the best performance is obtained with a system that has both low A_w and s_d (S5_A_w), exactly as observed with S_MW in the previous results. Furthermore, the system with low A_w and high s_d appears to work well under operational conditions and typical moisture content, coherently with what was previously observed with S_EPS.

In conclusion, the results obtained with external thermal insulation systems suggest that the impact of the systems on moisture content in the walls depends on their effect on rainwater intake and drying of the wall. Furthermore, the outcomes obtained are consistent with the recommendations provided in the German standard on rain-protective stuccos and coatings, and in the guidelines for ETICS (previously outlined in Section 6.4.2). Indeed, the only systems that determine a noticeable increase in the moisture

content in the wall substrate, after the retrofit, are S2, S4 and S5_mu (only in the wall exposed to low WDR), with the former two even leading to moisture accumulations in two walls. These three systems are the only ones that do not comply with the hyperbola defined in the German standard. The best results are obtained with S_MW and S5_Aw. Those are the only systems that comply with the stricter limits defined in guidelines for ETICS, thanks to their very reduced s_d and A_w. S_EPS and S5_A_w_mu are the only systems that exceed the maximum s_d allowed in the German standard, while complying with the recommended hyperbola. The high resistance to vapour diffusion of the systems does not appear problematic when operational conditions and typical moisture contents are considered. Nonetheless, it might be problematic during drying from high water content. This behaviour is evaluated in detail in the next section.

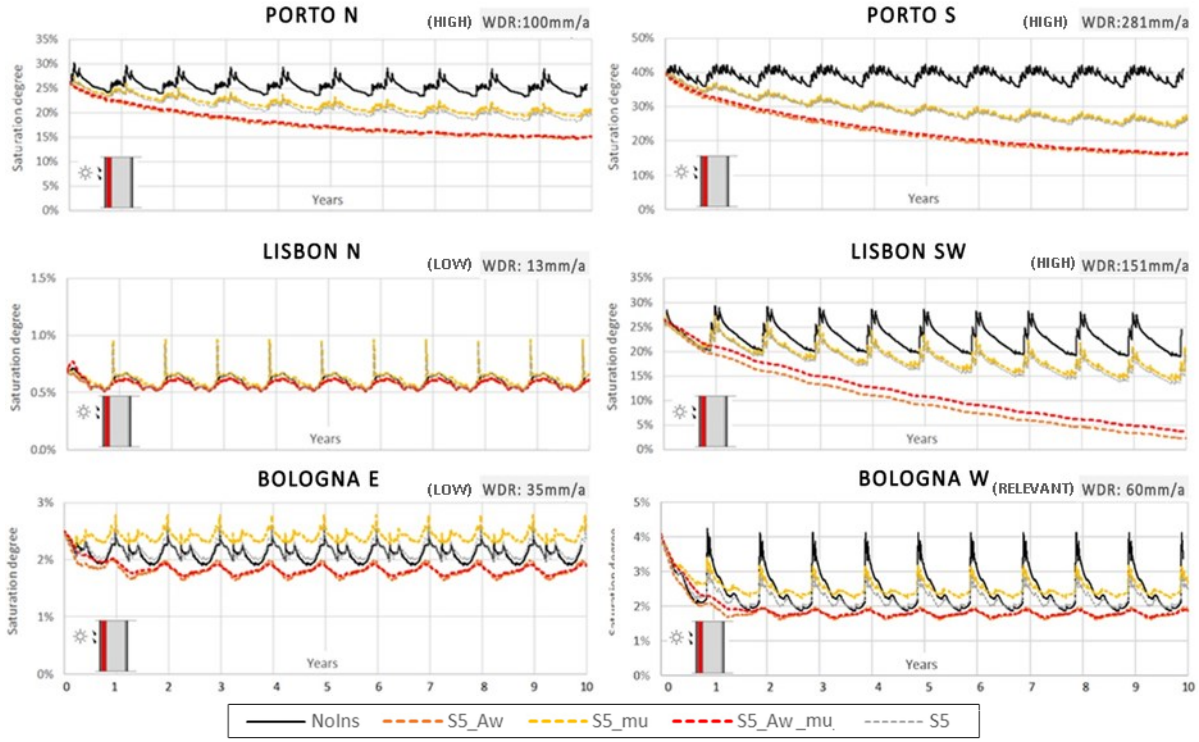

Figure 5.17 – Saturation degree in walls substrate in the original and retrofitted scenarios (parametric study on external insulation).

Finally, it is worth underlying that systems S2 and S4, which are the solutions with worse performance, are finished with a silicate paint that has relevant resistance to vapour diffusion. On the contrary, system S5 is covered with a mortar coating having higher vapour permeability. The different finishing is very likely to be responsible for the different hygric behaviour of the systems. For this reason, some complementary simulations are run while considering different finishings for the systems. The results obtained in the application on the walls of one case study are reported in ANNEX II. The study shows that the three thermal mortars considered provide for good performance when finished with the coating B2, while they do not when finished with B1+C2. Also in this case results are consistent with the recommendations of the German standard, since all systems finished with B2 comply with the hyperbola, while systems finished with the second coating do not.

5.5.1.2. DRYING – EXTERNAL INSULATION

The saturation water content observed during drying, in the retrofitted and un-retrofitted scenarios, are displayed in Figure 5.18. The black lines indicate the results obtained without insulation, and the different coloured ones represent the retrofitted scenarios.

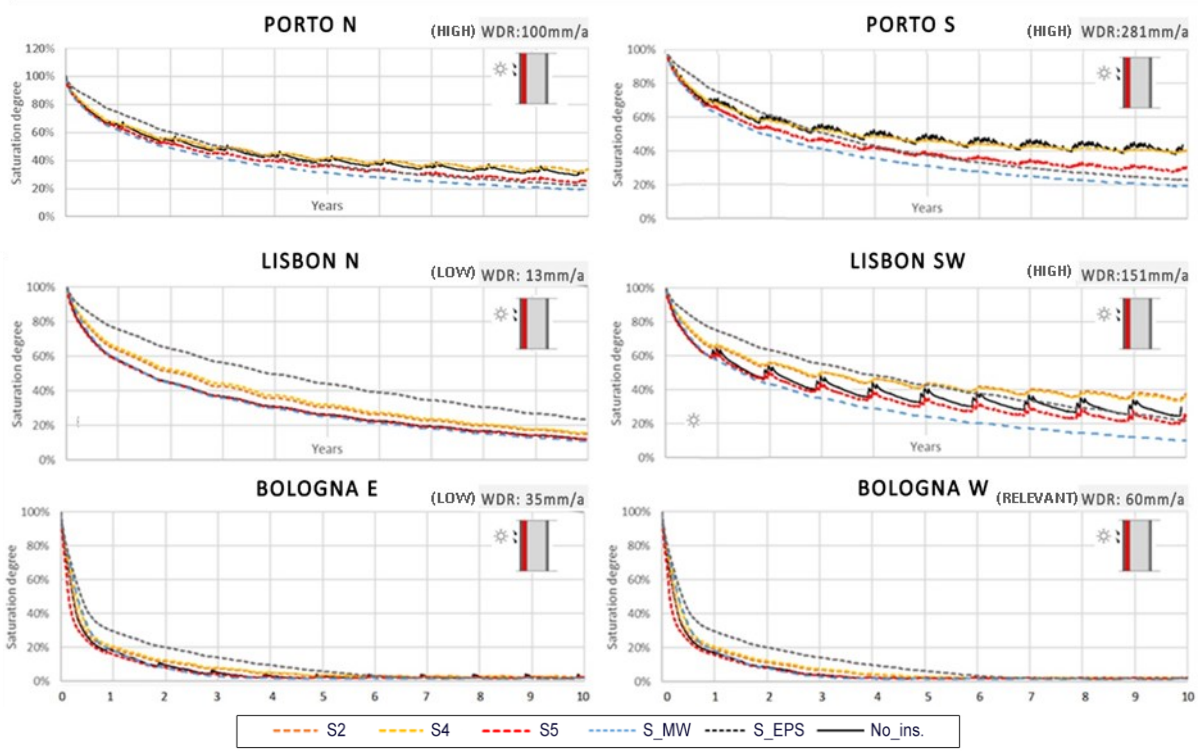

Figure 5.18 – Saturation degree in walls substrate during drying from saturation water content in the original and retrofitted scenarios (external insulation).

S_EPS determines higher water content than all other insulation systems and the un-retrofitted scenario, for at least the first two years in Porto walls, and for at least five years in Lisbon and Bologna walls. This result indicates that a system with a high s_d can relevantly reduce the drying of facades.
S_MW and S5 are the systems that work best for the drying of walls in Lisbon and Porto, at least in the first 4 years of drying. This result is coherent with the low s_d of the systems, which is below 0.5m, together with their good ability to reduce rainwater intake. In walls exposed to high WDR, S_MW starts working better than S5 in the second year, because of the stronger reduction of rainwater intake this system provides, during the drying. Also for the walls located in Bologna S5 and S_MW seem good solutions for letting the walls dry, because from the beginning of the second year the saturation degrees in the retrofitted and original walls are very similar and quite low. On the contrary, in the beginning of drying, S5 gives slightly better results than S_MW, namely in the first month in the N-oriented wall in Porto, 6 months for the S-oriented wall, and almost one year for walls in Lisbon. Even though the difference in saturation content obtained with the two systems is very small, it is an interesting result. Indeed, it suggests that in the first phase of drying, when liquid transport appears more relevant than the drying through vapour diffusion, capillary active insulation materials appear to perform better than

hydrophobic ones, for systems that have comparable s_d. This behaviour is clearly readable in the walls located in Bologna, where this first drying phase seems to last for the entire first year of drying.
Systems S2 and S4, noticeably reduce the drying of walls in Lisbon, and also in Bologna, between the second and fourth year of drying, in comparison with the original configuration. This seems the effect of the bad balance of the systems in terms of drying and rainwater intake. This behaviour appears to have a noticeable effect on walls having a quite capillary active substrate, such as in Lisbon and Bologna, while it does not appear significant in the granite walls of Porto.

In Figure 5.19 the saturation degree observed in the parametric study on hygric properties, during drying, is presented.

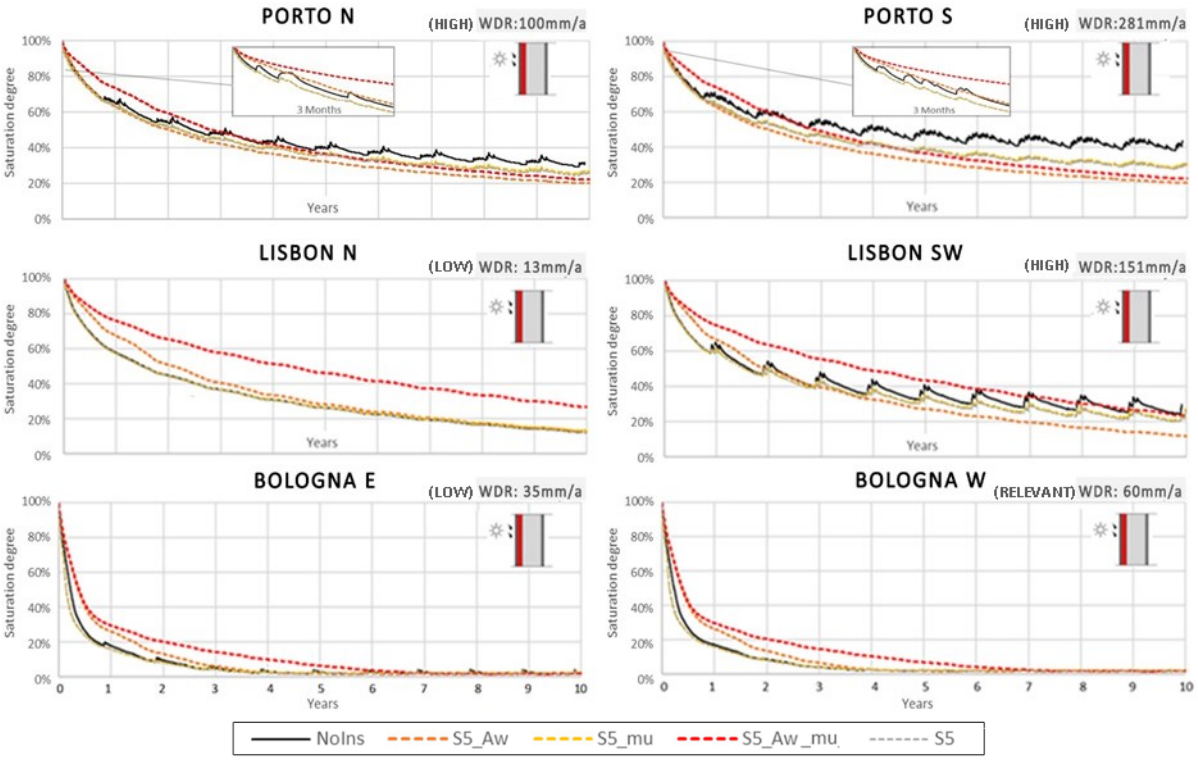

Figure 5.19 – Saturation degree in walls substrate during drying from saturation water content in the original and retrofitted scenarios (parametric study on external insulation).

The worst performance among retrofitted scenarios is obtained with the system that has both a high s_d and a low A_w, S5_A_w_mu, at least in the first 4 years of drying, similarly to what was previously observed with S_EPS. This result is consistent with the fact that a high s_d of the system diminishes vapour transport, while a reduced A_w in the insulation layer reduces the movement of liquid moisture towards the external surface, during drying. S5_A_w reduces the drying of the walls in Lisbon and Bologna, at least in the first 2 years, because of the reduced liquid transport to the external surface, which appears relevant for limestone and brick walls, because of their relevant capillary activity and high free water saturation. In Porto, where walls have a low capillary absorption coefficient and low free water saturation, this effect is observable for a much shorter period, namely for a few months after the intervention. In all cases, S5_mu does not appear to reduce the drying of the walls, in comparison to S5. This can be explained by the fact that the insulation layer considered is capillary active, so the water

is taken from the thermal mortar to the coating mortar by liquid transport, and from there liquid and vapour transport can occur thanks to the low s_d of the coating mortar. With a hydrophobic and vapour proof finishing the result might be quite different and the drying very reduced. By contrast, when the insulation has a high s_d in combination with a low A_w, the drying slows down relevantly more than with S5_Aw. This result indicates that when drying via liquid transport is reduced, the vapour permeability of the insulation gets very relevant, being then vapour diffusion the main moisture transport mechanism.

Overall, the worse drying is obtained with a system having low A_w ($A_w < 0.1$ kg.m^{-2}.h$^{-0.5}$) and high s_d ($s_d > 2$m), while the best results are obtained with systems having $s_d < 0.5$m, while being below the German curve for stuccos and coatings. One exception is observed, namely with S5_Aw. This system has low Aw and s_d, complying with the strict EAD requirements. Nonetheless, it appears to relevantly slow down the drying of walls. This outcome seems the result of the hydrophobic nature of the insulation layer, which reduces moisture transport in the first phase of drying, together with a vapour permeability that is not sufficiently low to compensate for this drawback (contrarily to S_MW). Anyway, this behaviour is relevant only in the first 2-3 years of drying, when saturation degree is very high, and it is not relevant in low capillary-active walls such as the ones made of granite in Porto.

According to the outcomes obtained with external thermal insulation, in terms of moisture content under operational conditions and drying from saturation, it emerges that good performance is provided by systems having low Aw and s_d, namely complying with the restriction of the EAD for ETICS. Furthermore, solutions exceeding the limit hyperbola of the German standard can lead to a strong increase of moisture content and moisture accumulation in historic walls. Systems that do not comply with the maximum s_d of 2m, recommended in the German standard, can have detrimental effects on the drying of the walls. Finally, it is interesting to underline those solutions that comply with the German hyperbola but not with the maximum s_d, such S_EPS, can show very good performance under operational conditions and very negative ones during drying.

5.5.2. MOISTURE-RELATED RISKS WITH INTERNAL INSULATION

5.5.2.1. MOISTURE CONTENT IN THE WALL SUBSTRATE – INTERNAL INSULATION

Figure 5.20 shows the saturation degree in walls retrofitted with internal insulation, for the 10 years following the intervention. In the same image, the saturation degree of un-retrofitted walls is reported in black.

In the walls located in Porto, all insulation systems determine a progressive increase of moisture content in the substrate along the whole period considered, with S_EPS and S_MW having the worst effect, and S1 and S3 the most moderate. Thus, despite the different hygric properties, systems with the highest and lowest U-values result in the highest and lowest water content in the wall substrate, respectively. This result suggests that the main reason behind the change in water content is the lower wall temperature, and the consequent reduction of drying entailed. In addition, S_EPS determines slightly higher water contents than S_MW, especially in the wall exposed to higher WDR. Given that the two systems have

the same U-value, this difference seems related to the higher reduction of the inward drying of the wall (due to the much higher s_d of S_EPS). The SW-oriented wall in Lisbon appears to not suffer any relevant change in moisture content with all systems except for S_EPS. Similarly, a noticeable reduction of drying is observed in the first two years after the application of S_EPS in the W-oriented wall in Bologna. In this last case, S_EPS does not lead to a noticeable change in the water content of the wall, in the long run.

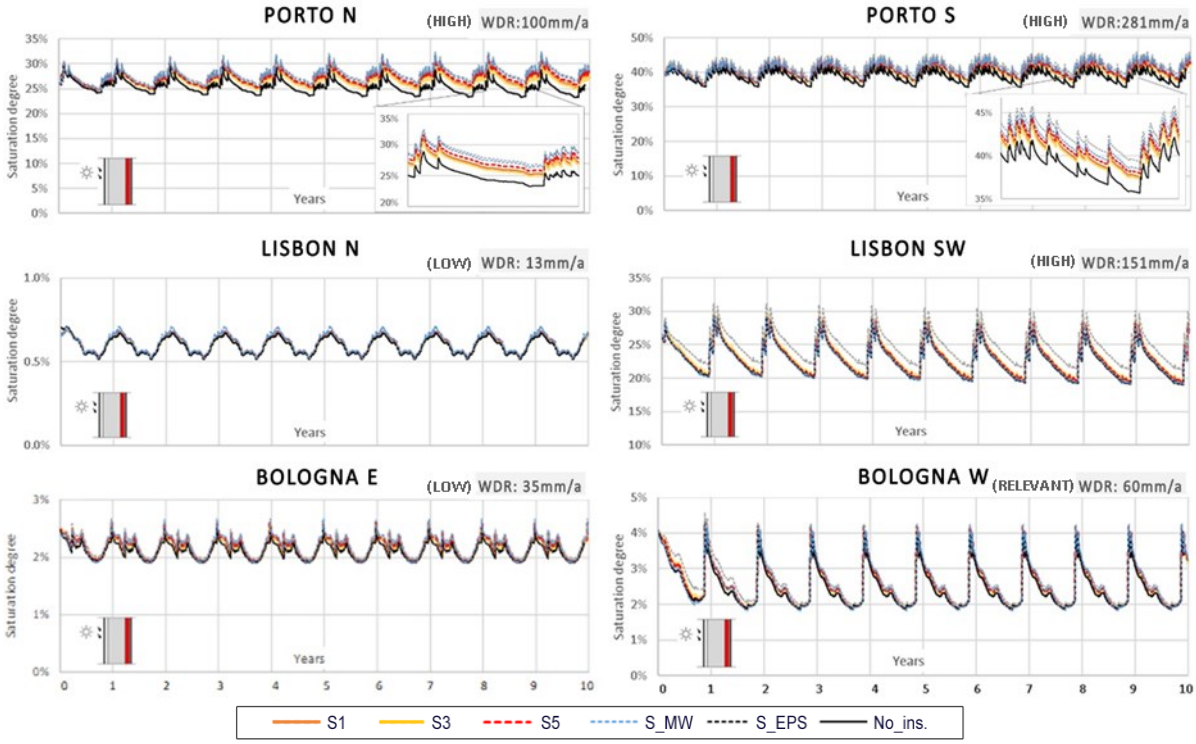

Figure 5.20 – Saturation degree in walls substrate in the original and retrofitted scenarios (internal insulation).

Hence, it emerges that in walls exposed to high or relevant WDR, S_EPS leads to worse performance than all the other insulation solutions. In walls exposed to low WDR, no significant variation of moisture content is observed with all the solutions considered.

Figure 5.21 shows the saturation degree in the walls substrate, when they are retrofitted with the interior insulation systems selected for the parametric study.

In the parametric study, all systems have the same thermal conductivity and different moisture transport properties. The results obtained with different systems applied on Porto walls, lead to quite similar moisture content, and they all lead to moisture accumulation. This outcome confirms that moisture accumulation in Porto walls is mainly related to a reduction of wall temperature. Whereas, the hygric properties of the systems adopted have less influence on the phenomenon.
In all walls exposed to relevant or high WDR, systems having a high resistance to vapour diffusion (S5_mu and S5_A_w_mu) determine the worse results. This outcome is similar to the one previously observed with S_EPS. In the walls located in Porto, the water contents with the two systems S5_mu and

S5_A_w_mu are higher than with the other solutions. In the SW-oriented wall in Lisbon, S5_A_w_mu determines much higher moisture content than S5 since the first year after the application. In the same wall, system S5_mu leads to water accumulation. With S5_mu, the increase of moisture content is not noticeable in the first years, but it becomes very relevant in the longer run. At the end of the 10-year-period, the moisture content in this wall, retrofitted with S5_A_w_mu and S5_mu, is similar and it is much higher than with S5. In the W-oriented wall in Bologna, S5_mu and S5_A_w_mu determine higher water contents in the first year after the intervention, because of the slower inward drying entailed by the system, but no relevant increase of moisture content is observed after this period.
On the contrary, no relevant changes in moisture content are observed for walls exposed to low WDR.

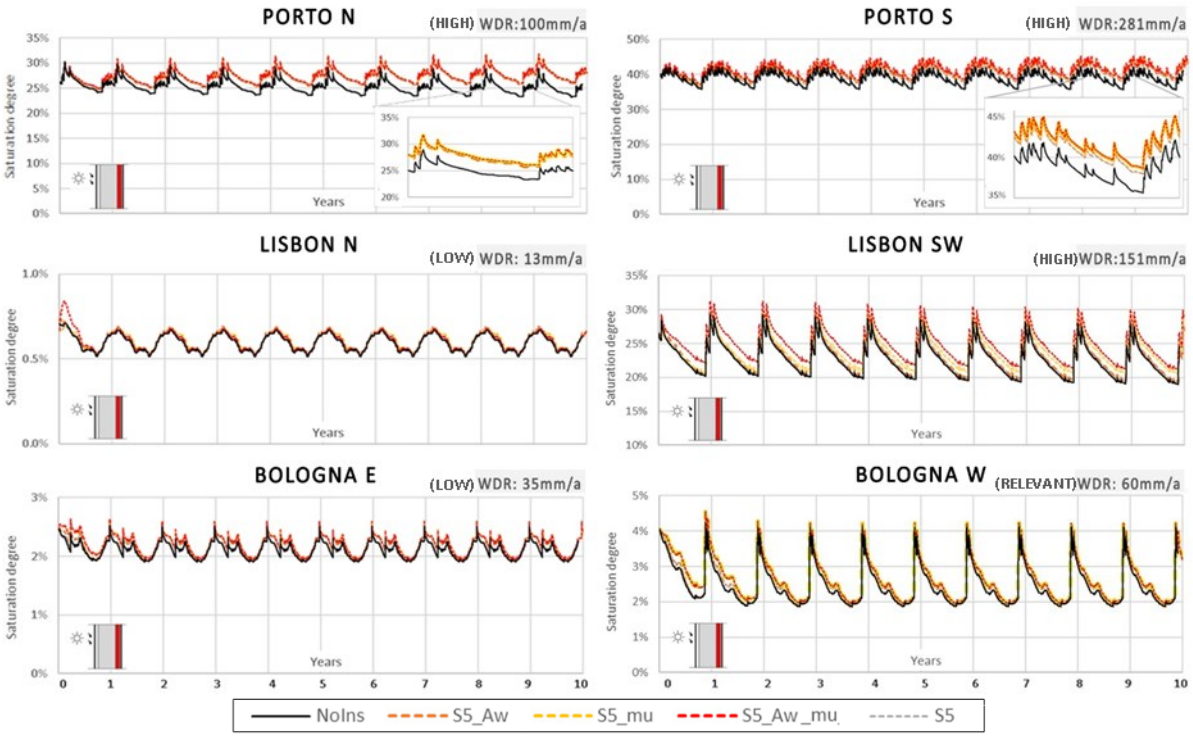

Figure 5.21 – Saturation degree in walls substrate in the original and retrofitted scenarios (parametric study on internal insulation).

Overall, the vapour permeability of the insulation systems emerged as the main parameter to influence moisture content in walls. Solutions having a high s_d gave the worse results, when applied on walls exposed to high or relevant WDR. This outcome seems very reasonable, given that the inward drying mainly happens through water vapour diffusion, under typical operational conditions. In walls exposed to low WDR, all insulation solutions appeared not to lead to relevant changes in moisture content. For the walls in Porto, all insulation solutions lead to moisture accumulation in the 10-year-period considered. This outcome appeared to be the consequence of the decrease in the wall temperature, rather than a result of the hygric properties of the insulation system adopted.

DRYING – INTERNAL INSULATION

Figure 5.22 shows the saturation degree in the substrate of the walls, through 10 years of drying from their free water saturation. The configurations considered are the original walls (black line) and the walls retrofitted with internal insulation systems.

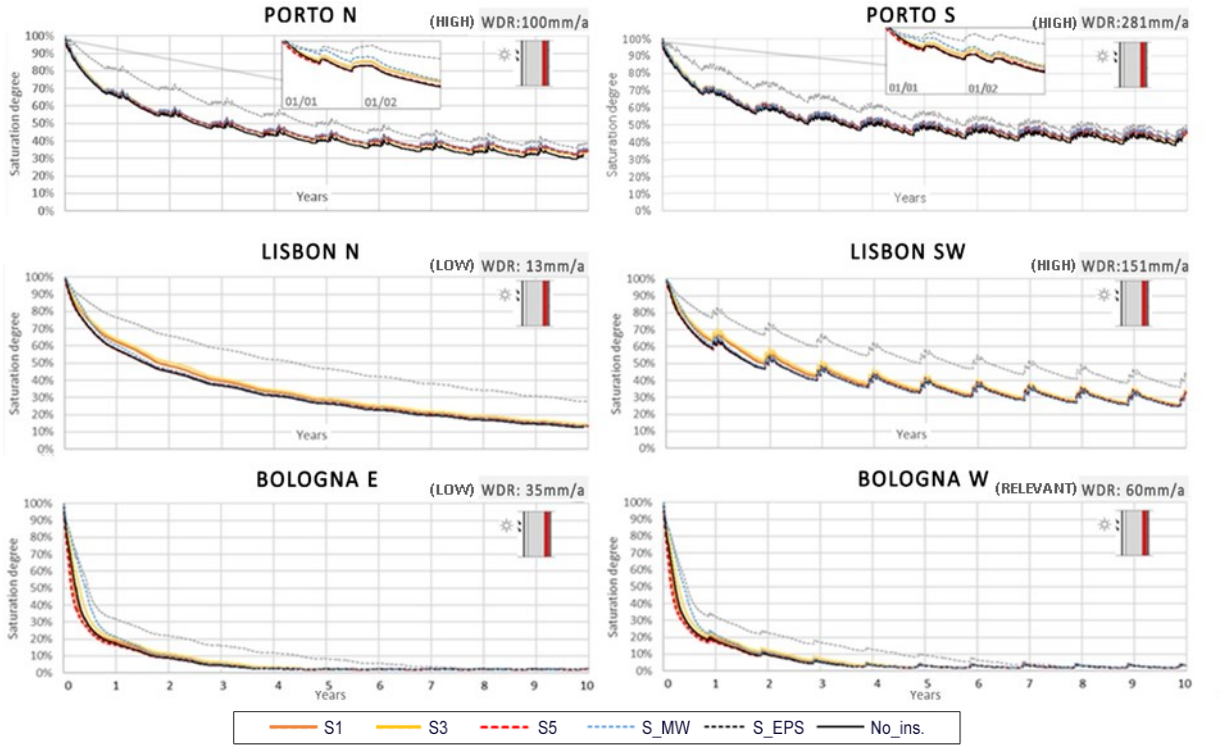

Figure 5.22 – Saturation degree in walls substrate during drying, in the original and retrofitted scenarios (internal insulation).

At the beginning of the drying process, S_MW leads to higher moisture contents than thermal-mortar based systems (S2, S4 and S5), in all walls. The time-extent of this phase is different for the different types of walls, being about 1 year for walls in Bologna, less than half a year for the walls in Lisbon, and about two days for walls in Porto. This difference is probably related to the different saturation water content and capillary absorption coefficient of the walls, which are very high for walls in Bologna, lower for walls in Lisbon, and the lowest in the walls in Porto. This outcome suggests that the non-capillary-active nature of mineral wool slows down the first phase of drying, namely when the moisture content near the wall surface is so high that liquid transport towards the indoor facing surface is very relevant for the drying process. Thermal mortar-based systems and S_MW, do not lead to a significant slowdown in the drying of the walls considered, from the second year on. On the contrary, S_EPS determines a relevant reduction of drying in all walls, for at least six years. This result appears coherent with the high s_d of the system and the low A_w of the insulation material, which both reduce the inward drying of the moist walls.

Figure 5.23 shows the results of the parametric study on internal thermal insulation solutions.

In all cases, S5_A_w_mu works worse than all the other solutions, which is the result of the combined reduction of liquid and vapour transfer towards the indoor-facing surface of the assembly. In addition, also system S5_Aw is found to perform worse than most of the other insulation systems, with reductions of drying that are very relevant for capillary active substrates (Lisbon and Bologna).
In walls with a capillary-active substrate, S5_Aw results in a strong reduction of drying during the first years after the adoption of the insulation, whereas S5_mu does not. This is clearly the result of the high initial water content considered, which makes liquid transport very relevant, at least during the initial phase of drying. For the walls in Porto, this effect is much reduced because of the low saturation water content of granite, because of which the first phase of drying is very short. The importance of vapour permeability emerges in the second phase of drying, when walls retrofitted with S5_Aw start to dry much faster than S5_mu_Aw.

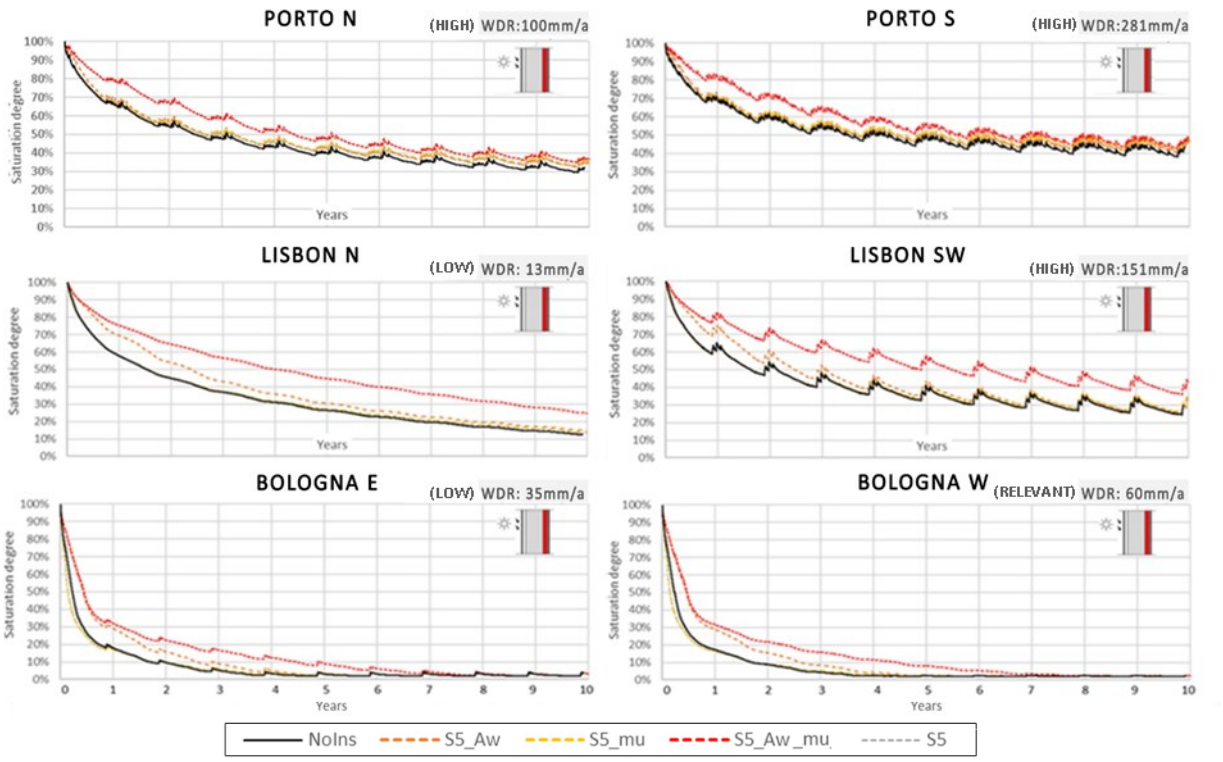

Figure 5.23 – Saturation degree in walls substrate, during drying,
in the original and retrofitted scenarios (parametric study on internal insulation).

Overall, the results show that systems with a capillary insulation layer can help the wall to dry, in comparison to insulations material with lower A_w. Furthermore, solutions that combine high s_d with an insulation layer having low A_w, such as S_EPS, should be avoided because of their detrimental effects on drying.

5.5.2.2. RH BEHIND INTERNAL INSULATION

Figure 5.24 shows the relative humidity at the interface between the wall and internal insulation. In the same graphic, the relative humidity behind the walls and the original plaster is also displayed, in black.

For each case study, the RH behind the original plaster appears to be almost independent of the orientation of the wall. It seems to depend mainly on indoor environmental conditions.

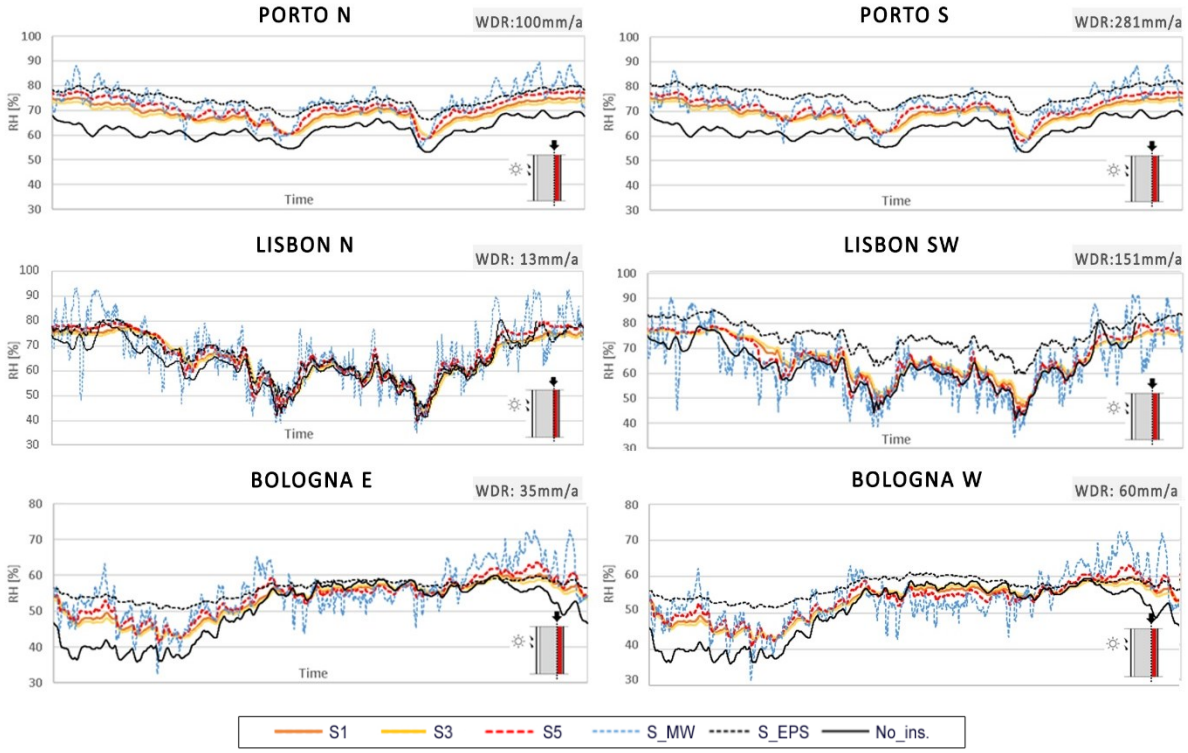

Figure 5.24 – Relative humidity at the interface between internal insulation and the wall and behind the original plaster and the wall, under dynamic equilibrium conditions.

Among all the insulation solutions considered, S_MW is the one that gives the strongest fluctuation of RH at the critical interface, in all walls. With this system, the RH level seems to predominantly depend on indoor climatic conditions. This outcome is probably the consequence of the high vapour permeability of the system. This feature allows a higher quantity of water vapour to pass through the insulation, which results in higher relative humidity peaks when vapour diffusion is directed towards the critical surface, and lower minimum levels when vapour is directed towards the interior environment. Thus, it seems that a system having low s_d, and a non-capillary-active, non-hygroscopic insulation layer, can be risky, because of the higher peaks of RH observed at the critical interface.

S_EPS is the only system that shows a relevant difference in RH levels at the critical interface, when applied in walls exposed to lower or higher WDR. In fact, it leads to higher RH levels in the latter scenarios. This result can be explained by the reduced vapour permeability of the system, which leads to a reduced vapour diffusion transport from the humid walls towards the indoor environment. Thus, with humid walls, S_EPS can result in a higher average RH level at the critical interface, than other insulation solutions.

All thermal mortars give similar results, with S5 leading to slightly higher maximum levels of RH than the other two systems.

The results obtained in the parametric study on the hygric properties of insulation materials applied at the interior side of walls, in terms of relative humidity behind the insulation, are displayed in Figure 5.25.

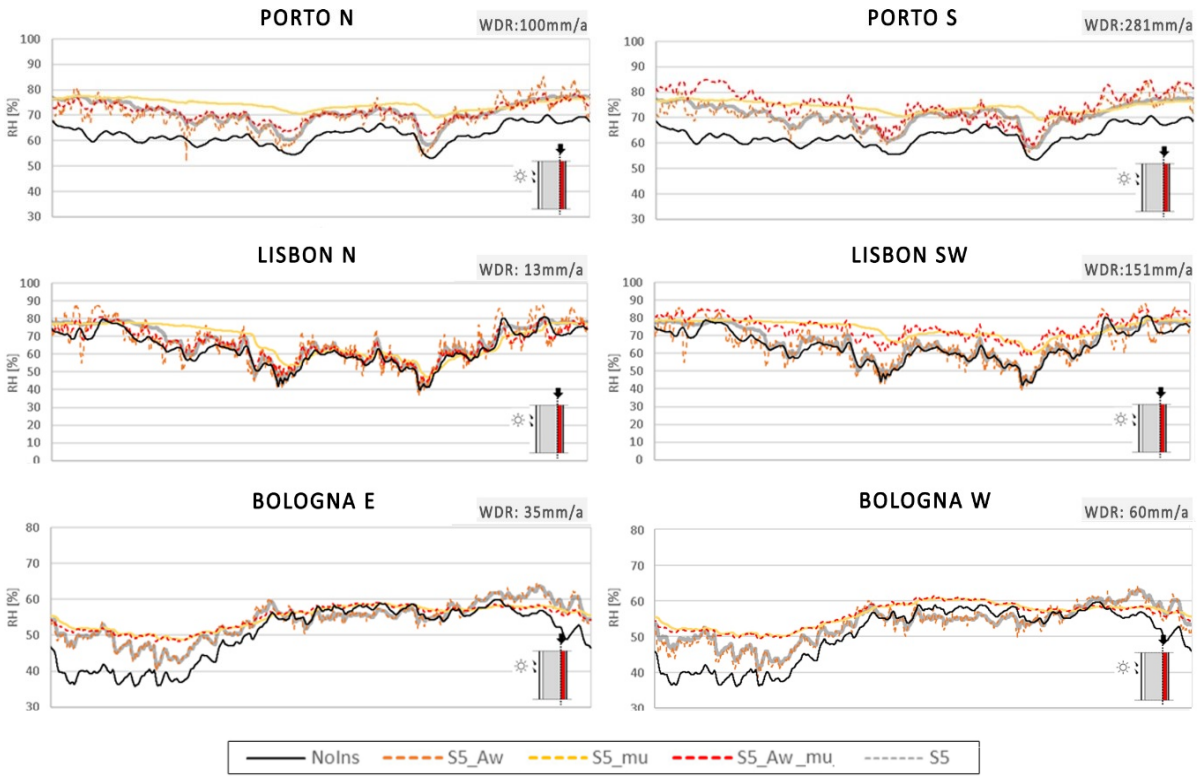

Figure 5.25 – Relative humidity at the interface between internal insulation (parametric study based on S5) and the wall and behind the original plaster and the wall, under dynamic equilibrium conditions.

In all walls, S5_mu leads to much smaller RH-fluctuations than S5, at the critical interface. This result shows that a reduced vapour permeability decreases the influence of the RH fluctuations of indoor air on the humidity at the critical surface. In walls exposed to relevant or high WDR, although leading to reduced peaks, S5_mu results in higher average RH conditions at the critical interface. This outcome seems the result of the decreased inward transport of vapour, when inward drying conditions occur. Thus, solutions with high s_d might be dangerous for parts of the walls subjected to elevated moisture contents, since they can lead to persistent conditions of high RH behind the insulation and result in condensation problems. For instance, it might have detrimental effects on areas experiencing high moisture content due to rising damp, pipe leakages or damages in the envelope.

In the walls located in Bologna, where WDR is moderate and indoor air has very low RH levels, systems S5_mu and S5_Aw_mu give very similar results. On the contrary, S5_Aw gives results that are very close to those obtained with S5. This outcome suggests that when RH at the critical interface is very low, because of the favourable indoor and outdoor climates, adopting a material that is hydrophobic and

non-capillary active, or one that has the opposite behaviour, does not relevantly affect the RH fluctuation at the critical interface. On the contrary, the s_d of the systems appeared to noticeably influence the RH at the critical interface.
For walls exposed to higher indoor RH conditions, such as the ones of Porto and Lisbon, different results are obtained. In these walls, S5_Aw leads to stronger fluctuations of RH than S5, showing that adopting non-hygroscopic and non-capillary-active insulation materials, in a vapour-permeable system, can lead to higher peaks of RH at the critical interface. This outcome is similar to what was already observed with S_MW. The effect of S5_mu_Aw on RH at the interface is similar, but fluctuations are more moderated since it has lower vapour permeability than S_MW. In walls exposed to higher WDR, namely S-oriented in Porto and SW-oriented in Lisbon, S5_mu_Aw leads to higher average levels of RH along the year than S5_Aw. This behaviour is very light in the N-oriented wall in Porto, and not noticeable in the N-oriented façade in Lisbon. This fact is probably the consequence of the more moderate moisture content in these walls, which entails a lower quantity of moisture passing through the inward-facing surface of the walls during drying.

In the case studies considered, RH at the critical interface appears to never get close to 100%, i.e. the level necessary for condensation to occur, and it is particularly low in the walls in Bologna. This seems the result of the specific indoor hygrothermal conditions analysed, which have very moderate indoor humidity. Nonetheless, in all walls, vapour permeable systems based on a hydrophobic and non-hygroscopic insulation material, such as S_MW and S5_Aw, lead to higher peaks of RH. Hence, these types of systems could lead to a higher risk of condensation in case of unfavourable conditions, e.g. thermal bridges-areas, periods of high indoor RH due to high occupation or anomalies in the heating systems. In addition, systems with reduced vapour permeability (such as S_EPS, S5_mu, and S5_Aw_mu), can lead to relevantly higher average RH levels at the critical interface, in walls exposed to high WDR. Although in the case studies this increase does not appear alarming, it might lead to prolonged periods of high RH and potential condensation, in parts of the walls experiencing high water content (e.g. due to rising damp).

Overall, it emerged that the adoption of interior insulation is quite a risky intervention, in comparison to the use of external insulation. Indeed, it can lead to moisture accumulation, independently from the type of insulation adopted, for walls exposed to high WDR. This type of behaviour was observed in the walls of Porto. For these walls, the adoption of interior insulation would require the introduction of a rain-protective layer or a hydrophobic impregnation treatment on the exterior surface. On the contrary, massive walls exposed to low WDR did not show any relevant increase of moisture content, after the adoption of interior insulation.
Solutions with low vapour permeability exhibited the worst consequences in terms of increased moisture content in walls exposed to high or relevant WDR. Furthermore, these solutions had detrimental effects on the drying from saturation, when based on a non-capillary-active and non-hygroscopic insulation layer. Finally, the aforementioned systems also appear risky for condensation when moist walls are considered. By extension, they can be problematic in areas subjected to high moisture contents due to rising damp, damages in the envelope, pipe leakages or thermal bridges. Vapour permeable insulation solutions, such as thermal mortars and mineral wool-based ones, appeared to lead to lower problems. Anyway, when highly vapour permeable solutions rely on a non-hygroscopic and non-capillary-active insulation material, such as mineral wool, they can lead to higher peaks of RH at the critical interface.

Consequently, this type of systems can lead to condensation in areas subjected to stronger thermal gradients due to thermal bridges or high moisture content.

5.5.3. THERMAL PERFORMANCE OF EXTERNAL AND INTERNAL INSULATION

5.5.3.1. HEAT LOSSES REDUCTION – STEADY-STATE CONDITIONS

Table 5.5 shows the U-values of the insulation systems and original walls, as single components, at dry conditions and at practical moisture content.

Table 5.5 – U-value of thermal insulation solutions and original wall, under stationary conditions.

	TH. INSULATION					ORIGINAL WALLS		
[W/(m²K)]	**S1-S2**	**S3-S4**	**S5**	**S_MW**	**S_EPS**	**PORTO**	**LISBON**	**BOLOGNA**
U-value, dry	2.01	1.69	1.26	0.84	0.84	1.38	1.74	0.84
U-value, 80%RH	2.06	1.75	1.27	0.84	0.84	1.41	1.77	0.89

Results show that S_EPS and S_MW do not suffer of reduced performances at 80% RH. System S5 has a negligible increase, and all other systems based on thermal mortars (S1-S4) have noticeable, but moderate, changes in their U-value. Also the original walls show noticeable increases of U-value at 80%RH.

The percentual reduction of U-value obtained with the retrofit is reported in Table 5.6. Outcomes at dry conditions and 80% RH are very similar, with maximum differences in the order of 1%. Thus, from this point on, the U-value obtained with dry materials will not be considered. The U-value calculated at RH 80% will be adopted as reference performance at stationary conditions.

Table 5.6 – Decrease of U-value of the wall with different insulation solutions, under stationary conditions. A scale from withe to grey is adopted to indicate the higher reductions of U-value.

Systems		**S1-S2**	**S3-S4**	**S5**	**S_MW**	**S_EPS**
λ_{dry} [W/(m.K)]		**0.10**	**0.13**	**0.07**	**0.04**	**0.04**
dry	POR WALL - Udecr.	-46%	-51%	-58%	-67%	-67%
	LIS WALL - Udecr.	-41%	-45%	-52%	-62%	-62%
	BOLO WALL - Udecr.	-30%	-33%	-40%	-50%	-50%
80% RH	POR WALL - Udecr.	-46%	-50%	-58%	-68%	-68%
	LIS WALL - Udecr.	-41%	-45%	-53%	-63%	-63%
	BOLO WALL - Udecr.	-30%	-34%	-41%	-51%	-51%

According to the results presented in the table, the theoretical reduction of winter heat losses obtained with S_MW and S_EPS are in the range 50-68%, from 40% to 58% with thermal mortar-based system S5, and between 30% and 51% with all other thermal rendering and plastering systems. Hence, they appear very promising for reducing winter heat losses in the case studies considered.

5.5.3.2. HEAT LOSSES REDUCTION DURING WINTERTIME - TRANSIENT CONDITIONS

The winter heat losses calculated through dynamic hygrothermal simulations are reported in Figure 5.26.

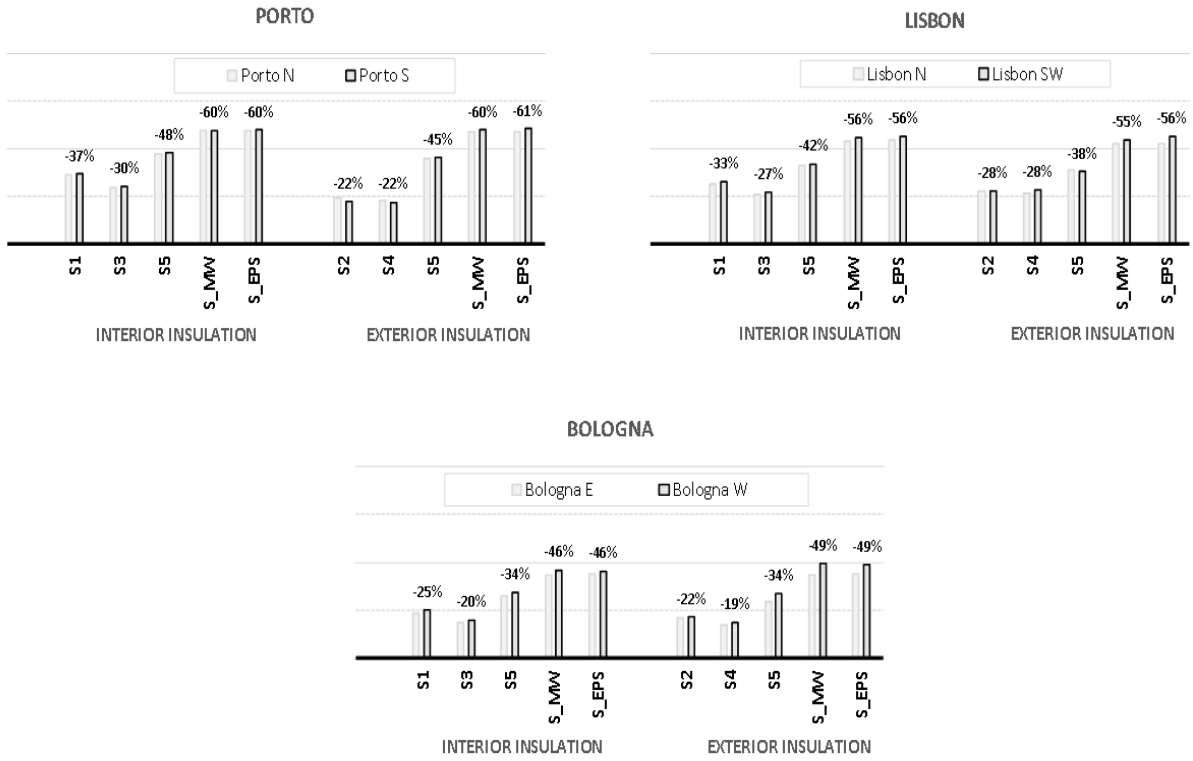

Figure 5.26 – Decrease of winter heat losses in the retrofitted walls, under dynamic conditions.

The difference in winter heat losses between walls affected by higher and lower WDR is moderate, in the range 1-15% in general, and below 6% when only internal insulation is considered. Both values are graphically reported in Figure 5.26, while the percentage label is displayed only for the walls exposed to higher WDR (i.e. results in darker grey), for reasons of synthesis.

Best performance is obtained with traditional insulation solutions, i.e., S_MW and S_EPS. These systems allow reaching reductions in the order of 40-60%. Competitive performance is provided by thermal mortar-based system S5, with reductions in the range 35-48%. The other systems based on thermal mortars, provide for a minimum reduction of 22% and a maximum of 34%.

The better performances obtained with S5 than other thermal mortar-based systems can be related to the lower thermal conductivity of the former system, together with its hygric properties. The better hygrothermal behaviour of S5, in comparison to S2 and S4, which are all the thermal mortar-based solutions adopted at the exterior side of walls, is readable in Figure 5.26. Indeed, S2 and S4 tend to show lower thermal performances than S1 and S3. The first and second solutions are based on the same thermal mortars, and respectively adopted on the exterior and interior sides of walls. The lower performance of external insulation systems S2 and S4 is particularly evident in the walls of Porto. On the contrary, S5 tends to show similar performance when adopted on the interior or exterior side of

walls. This outcome suggests that S5 has a better hygric behaviour than S2 and S4, a fact that was already observed when analysing moisture accumulation in section 6.5.1.

The differences between the reduction of heat losses observed with stationary and transient calculations, in absolute values, are reported in Table 5.7. The outcomes are highlighted with a color scale from white to grey, which is adopted to indicate the solutions that give the smaller and higher differences when compared to stationary calculations.
All values in Table 5.7 are positive, showing that the thermal performance estimated with the stationary U-value are always higher than those obtained under dynamic conditions. This outcome indicates that under realistic operational conditions lower performance than those calculated with the U-value$_{(80\%RH)}$ can be expected. Anyway, for traditional insulation solutions, such as the ones based on an EPS or MW insulation layer, the two performances are quite similar. The reductions of heat losses approximated with the stationary U-values and the ones calculated under transient conditions show differences in the range 2-10%. On the contrary, thermal mortar-based systems give higher differences, with systems adopted on the exterior side showing the most relevant discrepancies. This result is consistent with the exposure of exterior systems to outdoor weather, which makes moisture content variations stronger than indoor climate. The heat losses reduction calculated with the two methods, have differences up 16% with interior insulation systems, and reach almost 30% with exterior insulation solutions. Finally, system S5 shows smaller differences in the performance calculated with the two methods, than all the other thermal mortar-based systems.

The higher difference found with thermal mortars than with EPS and MW can be explained by the hydrophobicity and low saturation water content of the latter materials. These two features lead to moderate water contents in the insulation layer. Furthermore, the thermal conductivity of EPS and MW does not strongly depend on the moisture content in the material. On the contrary, the thermal conductivity of insulation mortars is much more sensitive to changes in the moisture content. In addition, thermal mortars are capillary active, hygroscopic and vapour permeable. Thus, they can experience large variations of water content along the year, depending on the climate they are exposed to and the composition of the insulation system (e.g. the finishing adopted).

Table 5.7 – Difference between the reduction of winter heat losses calculated with stationary and transient methods. A scale from white to grey is adopted to indicate the higher differences.

	$\lvert \Delta Q_{loss,stationary}\ [\%] \rvert - \lvert \Delta Q_{loss,\%,transient}\ [\%] \rvert$									
	S1	S2	S3	S4	$S5_{int}$	$S5_{ext}$	S_EPS_{int}	S_EPS_{ext}	S_MW_{int}	S_MW_{ext}
POR N	14%	26%	16%	23%	11%	14%	8%	10%	8%	9%
POR SW	14%	22%	16%	25%	10%	14%	8%	9%	8%	8%
LIS N	13%	16%	15%	15%	11%	13%	8%	9%	8%	9%
LIS SW	11%	29%	13%	11%	10%	12%	6%	4%	6%	3%
BOLO E	10%	13%	12%	13%	9%	12%	8%	8%	7%	8%
BOLO W	9%	20%	11%	12%	7%	9%	6%	4%	6%	4%

All considered, it emerges that a relatively-thin layer of insulation, such as 4cm, can lead to very interesting reductions of winter heat losses in massive historic walls having U-values above 0.8

W/(m^2.K). Under realistic dynamic conditions, EPS and MW show reductions in the range 40-60% and thermal mortar S5 showed competitive performance, such as reductions of about 35-50%. It was also observed that traditional calculations based on the U-value under stationary conditions provided for a very good approximation of the reduction of heat losses obtainable with hydrophobic insulation materials, namely EPS and MW. On the contrary, this method is less representative for thermal mortars, but it still gives an indication of the potential performance obtainable (differences observed were below 30%). Finally, under realistic operational conditions, all systems gave lower benefits than calculated under the hypothesis of stationary conditions and 80%RH.

5.6. SYNTHESIS OF RESULTS

The results shown and discussed in the previous section are hereby synthesized by means of matrixes of risks and thermal performance. First moisture related risks entailed by external and internal insulation are presented. Then thermal performance is synthetically shown, and a comprehensive assessment is finally provided.

5.6.1. MOISTURE RELATED RISKS WITH EXTERNAL INSULATION

The risk indexes related to moisture accumulation and reduction of drying are reported in Table 5.8.

The former index represents the change in water content in the wall substrate, during the second year of simulations, normalized by the average annual water content in the un-retrofitted wall. Negative results indicate that the retrofit decreased the average moisture content in the wall. The drying indexes represent the increase of average water content determined by the insulation during the second year of drying, normalized by the average annual water content in the un-retrofitted wall. The higher the index the stronger the reduction of drying, whereas a negative index indicates that the retrofitted wall dries faster than the original configuration.

At the top of the table, the walls considered are reported, which are organized according to a climate parameter, namely the ratio WDR/solar radiation. This parameter is adopted to account for the fact that a higher load of rain leads to higher moisture content while higher solar radiation theoretically reduces it because of the increased drying. Thus, from left to right are reported the walls exposed to stronger to milder outdoor climatic conditions. The first three walls are the ones exposed to high WDR, followed by those exposed to relevant and low WDR. In the same table, the thermal insulation systems are ordered according to their S_d*$A_{w,}$. This parameter is adopted because it was observed to be fundamental for moisture accumulations in the walls. To help synthesize the results, the s_d-values of the insulation systems are also reported in the table, and represented in bold when exceeding 2m. Similarly, the S_d*A_w>0.2 kg.m^{-1}.h$^{-0.5}$ are indicated in bold, and solutions that do not exceed these two limitations are underlined.

A scale from green to red is adopted to rank the indexes of risk, with red indicating the maximum level of risk and green the best decrease. The assessment scales are shown at the bottom of the table.

The matrix shows that the highest benefits can be obtained in walls exposed to high WDR. This outcome is clearly the result of the reduction of rainwater intake provided by some of the systems.

Best performances are observed with systems having a very low A_w*s_d, namely those complying with the EAD recommendations ($A_w \leq 0.10$ kg.m^{-2}.h$^{-0.5}$, $s_d \leq$ 1m), i.e. S5_A_w and S_MW. This outcome indicates that systems having low capillary water absorption and high vapour permeability appear more compatible than other solutions, for external interventions on traditionally constructed walls. It also emerged that these systems are particularly beneficial for walls exposed to high WDR. Thermal mortar-based system S5, which exceed EAD recommendations but complies with the German requirements on (A_w*s_d) and s_d, provides good performance. Indeed, it leads to benefits or very low risks in terms of moisture content in the wall. Additionally, it provides moderate benefits for the drying of the walls.

Systems that comply with the German hyperbola but exceed the maximum s_d, namely S_EPS and S5_Aw_mu, appear very risky. Indeed, although showing good performance under typical operational conditions, they have detrimental effects on drying. Finally, systems exceeding the hyperbola (A_w*s_d)=0.2 kg.m^{-1}.h$^{-0.5}$, namely S2, S4, and S5_mu, show bad performance. In fact, they are the only solutions leading to a high risk of moisture accumulation.

Table 5.8 – Indexes of risk with external insulation (moisture content in the wall substrate and drying from saturation).

EXTERNAL INSULATION								
Wall:			**PORTO S**	**PORTO N**	**LISBON SW**	**BOLOGNA W**	**BOLOGNA E**	**LISBON N**
Climatic parameter (WDR/solar r.):			0.31	0.28	0.13	0.06	0.06	0.03
s_d	(S_d*A_w)	SYSTEM	Moisture content in the wall substrate – risk indexes					
0.08	0.00	S_MW	-40%	-24%	-27%	-27%	-15%	-4%
0.39	0.02	S5_Aw	-39%	-23%	-25%	-26%	-14%	-4%
2.03	0.11	S5_A_mu	-29%	-14%	-18%	-19%	-12%	-4%
2.03	0.11	S_EPS	-30%	-16%	-18%	-20%	-13%	-4%
0.39	0.13	S5	-36%	-21%	-9%	-9%	2%	0%
0.94	**0.28**	S4	-34%	-19%	4%	14%	8%	3%
0.83	**0.40**	S2	-34%	-19%	10%	22%	11%	7%
2.03	**0.66**	S5_mu	-36%	-21%	-8%	4%	14%	3%
S_d	(S_d*A_w)	SYSTEM	Drying from saturation – risk indexes					
0.08	0.00	S_MW	-13%	-13%	-7%	-14%	-8%	-1%
0.39	0.02	S5_Aw	-11%	-11%	6%	47%	56%	14%
2.03	0.11	S5_A_mu	21%	21%	42%	140%	147%	44%
2.03	0.11	S_EPS	8%	8%	36%	121%	131%	44%
0.39	0.13	S5	-6%	-6%	-1%	-10%	-8%	-1%
0.94	**0.28**	S4	3%	3%	17%	38%	40%	17%
0.83	**0.40**	S2	3%	3%	15%	28%	30%	14%
2.03	**0.66**	S5_mu	-5%	-5%	-1%	-7%	-5%	-1%

*Risk assessment – ranking scales:

	High risk	Low risk	Neutral	Low benefit	High benefit
Moisture content in the wall substrate	22%	11%	0%	-20%	-40%
Drying from saturation	147%	74%	0%	-7%	-14%

Notation: Climatic parameter: ratio annual sum of WDR[mm/a] divided by the annual solar radiation [kWh/m^{2}a]; sd: equivalent-air-thickness [m], Aw: capillary water absorption coefficient [kg/ (m^2 h)].

*** Risk assessment – ranking scales:** the values reported in the scale represent the upper and lower limit of the intervals of risk and benefit, respectively. The class "neutral" is constituted by one value only, namely 0%.

5.6.2. MOISTURE RELATED RISKS WITH INTERNAL INSULATION

The risk indexes related to moisture accumulation, reduction of drying from saturation, and high humidity at the critical interface, with internal insulation, are reported in Table 5.9.

Table 5.9 – Indexes of risk with internal insulation
(moisture content in the wall substrate, drying from saturation and RH at the critical interface).

				INTERNAL INSULATION					
Wall:				**PORTO S**	**PORTO N**	**LISBON SW**	**BOLOGNA W**	**BOLOGNA E**	**LISBON N**
Climatic parameter (WDR/solar r.):				0.31	0.28	0.13	0.06	0.06	0.03
S_d	A_{w_ins}	$\lvert 10*s_d - A_{w\_ins}\rvert$	SYSTEM	Moisture content in the wall substrate – risk indexes					
0.08	**0.00**	0.79	**S_MW**	3%	6%	0%	2%	4%	4%
0.39	2.04	1.90	**S5**	2%	6%	1%	1%	3%	4%
0.54	2.64	2.79	**S1**	1%	5%	2%	1%	3%	4%
0.39	**0.00**	3.94	**S5_Aw**	2%	6%	2%	3%	3%	4%
0.65	1.32	5.19	**S3**	1%	5%	2%	1%	2%	4%
2.03	2.04	18.23	**S5_mu**	2%	6%	3%	1%	5%	12%
2.03	**0.00**	20.27	**S5_A_mu**	1%	15%	9%	17%	5%	12%
2.03	**0.00**	20.27	**S_EPS**	2%	15%	8%	17%	6%	13%
				Drying from saturation – risk indexes					
0.08	**0.00**	0.79	**S_MW**	3%	3%	1%	11%	16%	3%
0.39	2.04	1.90	**S5**	2%	2%	0%	-2%	0%	1%
0.54	2.64	2.79	**S1**	3%	3%	6%	14%	17%	8%
0.39	**0.00**	3.94	**S5_Aw**	3%	3%	15%	70%	76%	20%
0.65	1.32	5.19	**S3**	3%	3%	10%	28%	31%	12%
2.03	2.04	18.23	**S5_mu**	3%	3%	0%	0%	2%	1%
2.03	**0.00**	20.27	**S5_A_mu**	6%	6%	36%	124%	134%	46%
2.03	**0.00**	20.27	**S_EPS**	26%	26%	43%	142%	149%	47%
				RH at critical interface – risk indexes					
0.08	**0.00**	0.79	**S_MW**	30%	38%	4%	3%	11%	7%
0.39	2.04	1.90	**S5**	18%	20%	0%	0%	2%	0%
0.54	2.64	2.79	**S1**	10%	10%	0%	0%	0%	0%
0.39	**0.00**	3.94	**S5_Aw**	19%	18%	2%	0%	2%	3%
0.65	1.32	5.19	**S3**	6%	6%	0%	0%	0%	0%
2.03	2.04	18.23	**S5_mu**	33%	37%	0%	1%	0%	0%
2.03	**0.00**	20.27	**S5_A_mu**	46%	17%	3%	1%	0%	0%
2.03	**0.00**	20.27	**S_EPS**	54%	39%	4%	1%	0%	0%

	*Risk assessment – ranking scales:				
	High risk	Low risk	Neutral	Low benefit	High benefit
Moisture content in the wall substrate	17%	9%	0%	/	/
Drying from saturation	149%	75%	0%	-2%	/
RH at critical interface	54%	27%	0%	/	/

Notation: Climatic parameter: ratio annual sum of WDR[mm/a] divided by the annual solar radiation [kWh/m^{2}a]; sd: equivalent-air-thickness [m], Aw_ins: capillary water absorption coefficient of the insulation layer [kg/ (m^2 h)].

*** Risk assessment – ranking scales:** the values reported in the scale represent the upper and lower limit of the intervals of risk and benefit, respectively. The class "neutral" is constituted by one value only, namely 0%.

The first two indexes have the same meaning as in the matrix presented for external insulation systems. The latter one represents the increase of hours that the critical interface is found at a high RH level. Thus, the higher the index the longer the time the critical interface is found to be at a high RH.

At the top of the table, the walls considered are reported, which are organized according to a climate parameter, namely the ratio WDR/solar radiation. In the same table, the thermal insulation systems are ordered according to the parameter $|10s_{d\_system} - A_{w\_ins}|$. The first term refers to the s_d of the complete system and the second one to the A_w of the insulation material. The two properties are adopted with opposite signs to account for the different impacts they have on the behaviour of walls. Indeed, a high A_{w_insn} helps the wall to dry thanks to the capillary-active nature of the insulation, which helps absorb and redistribute liquid water towards the indoor facing surface. On the contrary, a high s_d of the system reduces the inward drying through vapour diffusion. A factor of 10 was introduced to account that under operational conditions, the vapour permeability of the system appears more relevant than the capillary water absorption of the insulation, according to the results obtained.

To help synthesize the results, the s_d of the insulation systems and the Aw of insulation materials are also reported in the table. The values of s_d exceeding 2m are indicated in bold, and the A_w of non-capillary-active insulation materials is also indicated in bold. Solutions having more moderate hygric properties are underlined. In addition, a scale from green to red is adopted to rank the results, with red indicating the maximum level of risk and green the best decrease of risk. The assessment scales are shown at the bottom of the table.

The indexes of risk show that solutions with the lowest hygric parameter $|10s_{d\_system} - A_{w\_insulation}|$ lead to the lowest risk of moisture increase and reduced drying. In particular, S_MW appears to provide very reduced risks. Nonetheless, this type of insulation can lead to a high risk of condensation at the critical interface, in the walls of Porto. This result shows that having very vapour permeable systems, based on non-capillary-active and non-hygroscopic insulation materials, is not the best choice for internal insulation. This type of systems can indeed increase the risk of condensation at the critical interface. Thus, although S_MW does not lead to condensation in the simulations considered, it can result in serious problems in those parts of the walls subjected to stronger thermal gradients, due to thermal bridges or high moisture content (e.g. because of rising damp).

Systems having a high hygric parameter entail the highest moisture-related risks, especially when based on a hydrophobic insulation layer. All systems having an s_d>2m, lead to high risk of moisture accumulation and high humidity at the critical interface, in at least one of the walls considered. When the same s_d is combined with a non-hydrophobic insulation layer, risks are more moderate, but still very relevant.

On the contrary, systems with a lower s_d, namely below 0.7m, are found to provide good results, when the insulation layer has a non-neglectable A_w and hygroscopicity. Specifically, thermal mortar-based systems, having an s_d below 0.7m, are the solutions entailing the more moderate risks, among all the systems considered.

Overall, it seems recommendable to avoid solutions with an s_d higher than 2m, especially when based on hydrophobic insulation materials. Because of condensation issues, also very permeable solutions should be avoided, if based on hydrophobic and non-hygroscopic insulation materials. On the contrary, thermal mortar-based systems, having an s_d lower than 0.7m, appear as a suitable solution for moderating moisture-related risks involved in the adoption of internal insulation systems to retrofit historic walls.

5.6.3. THERMAL PERFORMANCE WITH INTERIOR OR EXTERIOR INSULATION

In Table 5.10, the reductions of winter heat losses obtained with the different thermal insulation solutions, under dynamic conditions, are reported.

Table 5.10 – Indexes of performance, reduction of winter heat losses with external or internal insulation.

Wall:			**PORTO S**	**PORTO N**	**LISBON SW**	**BOLOGNA W**	**BOLOGNA E**	**LISBON N**
Side	U-value [W/(m²K)]	System	Reduction of heat losses in winter – performance indexes					
EXT	*2.01*	S4	-22%	-23%	-30%	-26%	-17%	-18%
INT	*2.01*	S3	-30%	-30%	-28%	-26%	-19%	-20%
EXT	*1.75*	S2	-22%	-24%	-29%	-29%	-21%	-20%
INT	*1.75*	S1	-37%	-36%	-33%	-32%	-23%	-25%
EXT	*1.27*	S5	-45%	-44%	-41%	-39%	-30%	-32%
INT	*1.27*	S5	-48%	-47%	-43%	-42%	-32%	-34%
EXT	*0.84*	S_MW	-59%	-58%	-59%	-54%	-43%	-48%
INT	*0.84*	S_MW	-60%	-60%	-57%	-54%	-43%	-46%
EXT	*0.84*	S_EPS	-60%	-58%	-60%	-54%	-44%	-47%
INT	*0.84*	S_EPS	-60%	-60%	-57%	-55%	-44%	-45%

* Performance indexes – ranking scales:

	Risk	Neutral	Low benefit	Medium benefit	High benefit
Reduction of heat losses in winter	/	0%	-20%	-40%	-60%

* **Performance indexes – ranking scales:** the values reported in the scale represent the upper and lower limit of the intervals of risk and benefit, respectively. The class "neutral" is constituted by one value only, namely 0%.

Walls and insulation systems are both ordered according to their U-values, calculated under stationary conditions and 80% RH. As expected, insulation solutions with lower thermal transmittance lead to higher reductions of heat losses. Thus, the best performance is obtained with the use of S_MW and S_EPS. With these systems, no relevant difference is observed when they are adopted at the interior or exterior side of walls.

With thermal mortar-based systems, the best results are obtained with S5, which has the lowest thermal transmittance and the minimum A_w*s_d. No relevant difference is observed when S5 is adopted as exterior or interior insulation, even in walls exposed to high WDR. This is the result of its good hygric behaviour, which does not lead to water accumulation in the insulation nor in the wall. In addition, the thermal mortar used in S5 (i.e., A3) has a more moderate dependency of thermal conductivity on moisture content, than the other thermal mortars (A1 and A2). Systems S1 and S2, based on thermal mortar A1, and S3-S4, based on thermal mortar A2, give noticeably lower benefits when applied at the external side of walls, in façades exposed to relevant WDR. This outcome appears to be the result of the water intake in the insulation systems, moisture accumulation in the wall, and the high dependency of the thermal conductivity of the insulation materials on moisture content.

Overall, thermal mortars appear interesting for adoption in historic walls having U-values above 0.8W/(m².K). Indeed, a very moderate thickness (4 cm) of thermal mortars resulted in a reduction of heat losses between 17 and 48%, during winter. However, only S5 appears to provide performance that is comparable with traditional insulation solutions as MW and EPS, providing reductions in the range

30-48% the former system and 43-61% the latter two. This difference seems mainly related to the different thermal conductivity of the insulation materials, indeed system S5 has a 50% higher U-value than MW and EPS based solutions.

5.6.4. COMPREHENSIVE ASSESSMENT

In this study, three types of historic massive walls were considered. Different insulation systems, based on thermal mortars, Mineral wool and EPS were taken into analysis and their effect on the performance of the walls was observed. In addition, a small parametric study (systems S5_A_w, S5_mu and S5_A_w_mu) was performed to evaluate the impact of the hygric properties of the insulation on the performance of the retrofitted walls.

Concerning moisture-related risks, the outcomes of the study led to the following observations:

- The result of the intervention depends on the hygric properties of the insulation solution adopted. Based on the side of the intervention, some solutions appeared to be riskier than others. Additionally, solutions with a s_d higher than 2m, having a hydrophobic and non-hygroscopic insulation layer, such as S_EPS, appeared to be the riskiest for both the interventions on the interior and the exterior surface of walls. This result is mainly determined by the detrimental effect that this type of solution has on the drying ability of walls.

- External insulation is less risky than the interior.
  The adoption of interior insulation does not lead to any benefit in terms of moisture content in the walls. In fact, internal insulation does not reduce the intake of moisture and, what is more, it reduces the wall temperature during the heating period, resulting in a reduced drying, as largely explained in the literature. However, the risks entailed by the intervention can be kept under control if a suitable solution is chosen. On the contrary, the adoption of external insulation offers one relevant benefit. Indeed, external insulation can reduce the rainwater intake of the wall, if the system adopted has lower capillary absorption than the original render. Indeed, the highest reductions of moisture content were observed in walls exposed to high WDR loads.

- The impact of external thermal insulation systems on the water content of walls depends on the effect they have on the wetting and drying of the components. Systems with s_d and A_w that do not comply with the recommendation of German standard on the parameter s_d*A_w, determined the worst moisture contents in the walls, leading to moisture accumulation in some of the case studies analysed. In addition, systems exceeding the limit s_d of 2m, can have detrimental effects on the drying ability of walls, especially when relying on hydrophobic insulation materials. Hence, external insulation systems that do not comply with the restrictions defined in the German standard on rain-protective stuccos and coatings, i.e. A_w*s_d < 0.2 and s_d < 2m, should be avoided. The German standard also sets a limit on the maximum A_w acceptable, namely 0.5 $kg.m^{-2}.h^{-0.5}$. Although no solution which such a high A_w was considered, this restriction seems logically recommendable. Furthermore, the best results were found with systems having very moderate A_w and s_d, namely A_w < 0.10 $kg/(m^2.h^{0.5})$ and s_d < 1m, which are the threshold values mentioned in the EAD for ETICS.
  Overall, S_MW emerged as a very good solution for application on the exterior side of walls, thanks to its high vapour permeability and very low water absorption coefficient. Similarly, also thermal mortar-based system S5 appeared suitable for the intervention.

- For internal insulation solutions, the s_d of the system emerged as a very important property to consider, while also the A_w of the insulation layer appeared to have relevance. Systems having a low s_d, and a non-hydrophobic, hygroscopic insulation layer appeared to provide good performance. Best results were obtained when these systems had an $|10\ s_d - A_{w\_insulation}| < 5$ (with $A_{w\_insulation}$ in $kg.m^{-2}.h^{-0.5}$ and s_d in m).

- Internal insulation systems that comply with the aforementioned indications, but have a hydrophobic insulation layer, such as S_MW, can provide good performance in terms of drying and water content in retrofitted walls. Nonetheless, it emerged that the hydrophobic and non-hygroscopic nature of the insulation layer, leads to a higher risk of condensation at the critical interface. For this reason, interior insulation systems which have a hygroscopic and capillary-active insulation layer, appear preferable to hydrophobic ones, when retrofitting thick historic walls. Overall, systems with low s_d (s_d <0.7m) and relevant $A_{w\_insulation}$ ($A_{w\_insulation} > 1\ kg.m^{-2}.h^{-0.5}$), namely thermal mortar-based solutions S1, S5 and S3, appeared to work better than S_MW and seemed suitable for the intervention.

In terms of thermal performance, the following considerations can be made:

- the adoption of relatively-thin insulation systems, namely about 4cm thick, resulted in interesting reductions of heat losses through massive masonry walls, during winter. Reductions in the range 20-70% are observed in walls having original U values between 0.85 and 1.75 $W/(m^2K)$. The best thermal performance is obtained with the systems having the lowest thermal transmittance, as expected. Namely, 40-60% reductions were obtained with EPS and MW, and 30-50% with thermal-mortar based system S5.
- For traditional, non-capillary-active insulation materials (MW and EPS), application at the exterior or interior side of walls did not appear to lead to relevant changes in the dynamic thermal performance obtained, which show very similar reductions of $Q_{loss,\%}$ to the ones theoretically calculated with the stationary U-value at 80%RH (discrepancy of 2-10%). On the contrary, noticeable differences were observed when thermal mortar-based systems are applied at the external or internal side of walls. This is the result of the capillary active nature of the materials and the dependency of their thermal conductivity on moisture content. Thus, lower performance was generally found when the systems were applied at the exterior side, in walls exposed to relevant WDR. Anyway, depending on the hygric properties of the systems, this difference can be more or less moderate. Indeed, system S5 showed a very small difference in performance when applied at the internal or external side of walls, namely up to 3%, which does not appear relevant. This outcome is the consequence of the good hygric properties of the system (which complies with EAD maximum values of A_w and s_d), the low free water saturation of the insulation, and the moderate dependency of the thermal conductivity of the thermal mortar on water content. Furthermore, this system provides for thermal performances that are very close to the ones expected from stationary calculations, with a maximum difference lower than 15%, thus showing similar behaviour to more common insulation solutions based on hydrophobic materials such as EPS and MW.

5.7. LIMITATIONS OF THE STUDY

It seems important to underline some limitations of the study, which appear particularly relevant for considerations on moisture-related risks.

First, the simulations performed consider one-dimensional processes. Thus, they account for the plane behaviour of perfect walls, while room corners, cracks in walls, window recesses, and other thermal bridges areas, where the temperature can get very low during the cold season, are disregarded. Thus, the recommendations of this study would need further validation through analyses that account for thermal bridges. Furthermore, the risk considered are limited, and future studies should also evaluate the effect of the recommended insulation solutions on risks like degradation of embedded wooden beam ends, and mould growth on the internal and the external surface of walls. For the latter evaluation, simulations which account for detailed counter radiation data would be suitable, to correctly estimate night-time overcooling.

Additionally, the simulations consider each layer as made of a homogeneous material, hence mortar joints between stones and bricks are not considered. Also, the effect of hygric interfaces is omitted.

The outdoor climates considered are characterized by mild winter temperatures, for colder climates risks correlated to water freezing might be necessary. The interior and exterior climates considered, as well as the type of walls, seem representative for temperate countries but more scenarios should be accounted for to obtain more generally applicable recommendations.

This study considers massive walls, with a minimum thickness of 60cm. In this scenario, the rainwater absorbed by the wall is not expected to reach its interior surface. On the contrary, walls with a thickness below 20-30cm might experience high humidity near the interior surface of walls, due to rainwater penetration. In this case, the recommendations here provided for interior insulation, are not applicable.

The considerations drawn are mainly referred to the hygric properties of entire systems and on those of the insulation layer, an outcome that is based on a very limited parametric study. It would be interesting to have future studies aimed at evaluating how the hygric properties of the coating, insulation layer, and entire system do impact the behaviour of retrofitted components.

Finally, the considerations drawn in this study assume that interventions on historical walls adopt a very moderate thickness of insulation. This is clearly not always the case. Thus, when thicker insulation solutions are adopted, different parameters might be suitable for the recommendations.

5.8. CONCLUSION

In this chapter, three types of historic massive walls located in temperate climates with mild winter conditions and several insulation solutions were considered.

The hygrothermal behaviour of the walls before and after the retrofit was analysed and three moisture-related risks were considered (moisture increase in the wall substrate, reduced drying and condensation behind internal insulation). Results showed that some thermal insulation solutions are riskier than others, depending on their hygric properties and the side of the intervention. Specifically, it emerged that external insulation solutions complying with the limitations defined in German standard, $A_w * s_d < 0.2$ $kg.m^{-1}.h^{-0.5}$ and $s_d < 2m$, should be preferred. Thus, it is recommendable to adopt vapour permeable insulation solutions with low absorption coefficients, such as systems based on hydrophobic mineral wool or thermal mortar-based system S5. The adoption of internal insulation appeared to lead to higher risks than external. Vapour permeable solutions that do not rely on a hydrophobic insulation layer appear recommendable to moderate the risk entailed by the intervention. In particular, thermal mortar-based insulation solutions, with an $s_d<0.7m$, appeared more recommendable.

This analysis also allowed to observe the importance of simulating the drying of walls from high water content. Indeed, some drawbacks might be overlooked if only typical moisture content and operational conditions are considered. For instance, solutions with an $s_d>2m$ and a hydrophobic insulation layer can perform well under typical conditions, but they have detrimental effects on the drying ability of walls. Thus, the use of these solutions should be discouraged. Indeed, historic and traditional walls are typically made of porous materials and have no capillary breaks. As a consequence, high moisture levels may occur in some parts of the walls, due to damages in the envelope, pipe leakage, rising damp or even floods. In these areas, solutions that reduce the drying ability of walls may lead to trapped moisture and increased rising damp, with the degradation risks and increased heat losses that those entail.

Finally, the analysis on winter-heat-losses indicated that a very small thickness of insulation can result in a relevant reduction of winter heat losses, in massive historic walls. Reductions of 40-60% were obtained with systems based on EPS and hydrophobic mineral wool, while a decrease of 20-50% was reached with one of the thermal mortar-based solutions considered (S5). This result points out that thermal mortars with modern formulations can be competitive with traditional insulation materials, and they appear promising for adoption in traditional and historic walls with U-values higher than 0.80 W/m^2K. The efficacy of thermal mortars is further investigated in the following chapter, by means of whole-building numerical simulations. These tools are applied to evaluate the impact of thermal mortar-based systems on thermal comfort and energy demands during the entire year, thus aiming at accounting not only for the winter benefits, but also for the overheating risks during warm and hot seasons.

5.9. REFERENCES

Hamid, Abdul Akram, and Petter Wallentén. 2017. “Hygrothermal Assessment of Internally Added Thermal Insulation on External Brick Walls in Swedish Multifamily Buildings.” *Building and Environment*. doi:10.1016/j.buildenv.2017.05.019.

Alev, Üllar, Targo Kalamees, Marko Teder, and Martti-Jaan Miljan. 2014. “Air Leakage and Hygrothermal Performance of an Internally Insulated Log House.” In *The 10th Nordic Symposium on Building Physics (NSB 2014)*, Lund, Sweden. 2014.

Amorim, Mafalda, Vasco Peixoto de Freitas, Isabel Torres, Tomasz Kisilewicz, and Umberto Berardi. 2020. “The Influence of Moisture on the Energy Performance of Retrofitted Walls.” *MATEC Web of Conferences*. doi:10.1051/matecconf/202032201035.

ASHRAE. 2014. “ASHRAE Guideline 14-2014 Measurement of Energy and Demand Savings.”

Banfill, P. F.G. 2021. “Hygrothermal Simulation of Building Performance: Data for Scottish Masonry Materials.” *Materials and Structures/Materiaux et Constructions* 54 (4). doi:10.1617/s11527-021-01759-x.

Barreira, E., M. L. Simões, J. M.P.Q. Delgado, and I. Sousa. 2017. “Procedures in the Construction of a Test Reference Year for Porto-Portugal and Implications for Hygrothermal Simulation.” *Sustainable Cities and Society* 32 (December 2016): 397–410. doi:10.1016/j.scs.2017.04.013.

Barreira, Eva, and V. P. de Freitas. 2013. “Experimental Study of the Hygrothermal Behaviour of External Thermal Insulation Composite Systems (ETICS).” *Building and Environment*. doi:10.1016/j.buildenv.2013.02.001.

Blocken, Bert, and Jan Carmeliet. 2004. “A Review of Wind-Driven Rain Research in Building Science.” *Journal of Wind Engineering and Industrial Aerodynamics* 92 (13). doi:10.1016/j.jweia.2004.06.003.

Browne, D. 2012. “The SPAB Research Report 3: The SPAB Hygrothermal Modelling-Interim Report.” *Society for the Protection of Ancient Buildings (SPAB): London, UK*.

CEN. 2017. “EN 16883:2017 - ‘Conservation of Cultural Heritage. Guidelines for Improving the Energy Performance of Historic Buildings.’”

Damas, Ana Leonor, Rosário Veiga, and Paulina Faria. 2016. “Caraterização de Argamassas Antigas de Portugal – Contributo Para a Sua Correta Conservação.” In *Congresso Ibero-Americano “Património, suas Matérias e Imatérias,* Lisbon, Portugal.

DIN - Deutsches Institut für Normung. 2018. "DIN 4108-3:2018-10 - 'Thermal protection and energy economy in buildings - Part 3: Protection against moisture subject to climate conditions - Requirements, calculation methods and directions for planning and construction'"

EOTA - European Organisation for Technical Approvals. 2020. "EAD 040083-00-0404:2020 - 'European Assessment Document. External Thermal Insulation Composite Systems (ETICS) with renderings'".

Ferreira, Cláudia. 2015. “Inércia Higroscópica Em Museus Instalados Em Edifícios Antigos - Utilização de Técnicas Passivas No Controlo Da Humidade Relativa Interior.” (PhD Thesis). FEUP: Porto,

Portugal.

Finken, Gholam Reza, Søren Peter Bjarløv, and Ruut Hannele Peuhkuri. 2016. "Effect of Façade Impregnation on Feasibility of Capillary Active Thermal Internal Insulation for a Historic Dormitory - A Hygrothermal Simulation Study." *Construction and Building Materials* 113: 202–214. doi:10.1016/j.conbuildmat.2016.03.019.

Freitas, Teresa Stingl, Ana Sofia Guimarães, Staf Roels, Vasco Freitas, and Andrea Cataldo. 2020. "Is the Time-Domain Reflectometry (TDR) Technique Suitable for Moisture Content Measurement in Low-Porosity Building Materials?" *Sustainability (Switzerland)* 12 (19). doi:10.3390/SU12197855.

Grunewald, J, U Ruisinger, and P Häupl. 2006. "The Rijksmuseum Amsterdam–Hygrothermal Analysis and Dimensioning of Thermal Insulation." In *3rd International Building Physics Conference—Research in Building Physics and Building Engineering*, Canada.

Hägerstedt, Olof, and Jesper Arfvidsson. 2010. "Comparison of Field Measurements and Calculations of Relative Humidity and Temperature in Wood Framed Walls." In *Thermophysics 2010*, Brno, Czech Republic.

Hegger, Manfred, Volker Auch-Schwelk, Matthias Fuchs, and Thorsten Rosenkranz. 2013. *Construction Materials Manual*. Walter de Gruyter: Berlin, Germany.

IBP - Fraunhofer Institute for Building Physics. 2018. "WUFI, Product Overview." Accessed March 29, 2021. https://wufi.de/en/software/product-overview/.

IBP - Fraunhofer Institute for Building Physics. 2007. "WUFI Passes Benchmark Test of EN 15026, Fraunhofer Institute for Building Physics." Accessed March 29,2021. https://wufi.de/en/2015/04/09/benchmark-test-of-en-15026/.

Jerman, Miloš, and Robert Černý. 2012. "Effect of Moisture Content on Heat and Moisture Transport and Storage Properties of Thermal Insulation Materials." *Energy and Buildings*. doi:10.1016/j.enbuild.2012.07.002.

Kaczorek, D. 2018. "Hygrothermal Assessment of Internally Insulated Brick Wall Based on Numerical Simulation." In *IOP Conference Series: Materials Science and Engineering*. doi:10.1088/1757-899X/415/1/012013.

Kunzel, H M, Th Schmidt, and A Holm. 2002. "Exterior Surface Temperature of Different Wall Constructions: Comparison of Numerical Simulation and Experiment." *Proceedings 11. Symposium for Building Physics,* TU Dresden, Germany, September 2002.

Künzel, Hartwig M. 1998. "Effect of Interior and Exterior Insulation on the Hygrothermal Behaviour of Exposed Walls." *Materials and Structures/Materiaux et Constructions*. doi:10.1007/bf02486471.

Künzel, Hartwig M., Helmut Künzel, and Andreas Holm. 2004. "Rain Protection of Stucco Facades." In *Proceedings of the Thermal Performance of the Exterior Envelopes of Whole Buildings IX–International Conference,* Florida, USA.

Künzel, Hartwig M. 1995. *Simultaneous Heat and Moisture Transport in Building Components One- and Two-Dimensional Calculation Using Simple Parameters . Physics*. Vol. 1995. doi:ISBN v.3-8167-4103-7.

Lisitano, Ivana Mattea, Deborah Laggiard, Stefano Fantucci, Valentina Serra, Carla Bartolozzi, Enrique Manuel Blanco Lorenzo, and Patricia Sabín Díaz. 2018. "Energy in Cultural Heritage: The Case Study of Monasterio de Santa Maria de Monfero in Galicia." In *REHABEND*, Caceres, Spain, May 15-18, 2018

Little, Joseph, Calina Ferraro, and Benat Aregi. 2015. *Technical Paper 15: Assessing Risks in Insulation Retrofits Using Hygrothermal Software Tools Heat and Moisture Transport in Internally Insulated Stone Walls*. *Technical Paper 15*. Historic Environment Scotland: Edinburgh, Scotland. doi:10.13140/RG.2.1.2493.3844.

Lucchi, Elena. 2017. "Thermal Transmittance of Historical Brick Masonries: A Comparison among Standard Data, Analytical Calculation Procedures, and in Situ Heat Flow Meter Measurements." *Energy and Buildings*. doi:10.1016/j.enbuild.2016.10.045.

Martin, Krus, and Thierry Nouidui1and Sedlbauer Klaus. 2009. "Application of Software Tools for Moisture Protection of Buildings in Different Climate Zones Special Example: Control of Air Humidifier in a Cold Climate for High Comfort and No Risk of Mould Growth in Building Room." In *Heating, Ventilating and Air-Conditioning,* Sisimiut, Groenland.

METEOTEST, Meteonorm - Version 6.0. Meteotest: Bern, Switzerland.

Mundt-Petersen, S. Olof, and Lars Erik Harderup. 2013. "Validation of a One-Dimensional Transient Heat and Moisture Calculation Tool under Real Conditions." In *Thermal Performance of the Exterior Envelopes of Whole Buildings - 12th International Conference,* Florida, USA.

Pina Dos Santos, Carlos A., and Rodrigo Rodrigues. 2010. ITE 54—Coeficientes de transmissão térmica de elementos opacos da envolvente dos edifícios. LNEC, Lisboa (in Portuguese). ISBN: 9789724921808

Ruiz, Germán Ramos, and Carlos Fernández Bandera. 2017. "Validation of Calibrated Energy Models: Common Errors." *Energies*. doi:10.3390/en10101587.

Stahl, Thomas, Karim Ghazi Wakili, Severin Hartmeier, Emil Franov, Walter Niederberger, and Mark Zimmermann. 2017. "Temperature and Moisture Evolution beneath an Aerogel Based Rendering Applied to a Historic Building." *Journal of Building Engineering* 12. Elsevier: 140–146. doi:10.1016/j.jobe.2017.05.016

Stöckl, Beate, Daniel Zirkelbach, and Hartwig M Künzel. 2014. "Hygrothermal Simulation of Green Roofs-New Models and Practical Application." In *Nordic Symposium on Building Physics (NSB),* Lund, Sweden.

Torres, M. Isabel M., and Vasco Peixoto de Freitas. 2007. "Treatment of Rising Damp in Historical Buildings: Wall Base Ventilation." *Building and Environment*. doi:10.1016/j.buildenv.2005.07.034.

Vacek, Simon, and Radovan Kostelník. 2019. "Case study of application of capillary active thermal insulation systems used as an interior insulation for historical buildings." In *Proceedings of the International Conference of Buildings and Environments*, Bratislava, Slovakia.

Veiga, Rosário, M., Ana Fragata, Ana Luisa Velosa, Ana Cristian Magalhães, and Goreti Margalha. 2010. "Lime-Based Mortars: Viability for Use as Substitution Renders in Historical Buildings."

International Journal of Architectural Heritage. doi:10.1080/15583050902914678.

Veiga, Rosário. 2013. "Conservation of Historic Renders and Plasters: From Laboratory to Site." *RILEM Bookseries*. doi:10.1007/978-94-007-4635-0_16.

Velosa, A L, and Rosário Veiga. 2016. "Argamassas Do Património Histórico: Conhecer Para Conservar e Reabilitar." In *Congresso internacional sobre patologia e reabilitação de estruturas*, Porto, Portugal.

Vereecken, Evy, and Staf Roels. 2015. "Capillary Active Interior Insulation: Do the Advantages Really Offset Potential Disadvantages?" *Materials and Structures* 48 (9). Springer: 3009–3021. doi:10.1617/s11527-014-0373-9

Vereecken, Evy, Liesje Van Gelder, Hans Janssen, and Staf Roels. 2015. "Interior Insulation for Wall Retrofitting–A Probabilistic Analysis of Energy Savings and Hygrothermal Risks." *Energy and Buildings* 89. Elsevier: 231–244. doi: 10.1016/j.enbuild.2014.12.031

Villmann, B. 2014. "Time-Dependent Moisture Distribution in Drying Cement Mortars – Results of Neutron Radiography and Inverse Analysis of Drying Tests." *Restoration of Buildings and Monuments*. doi:10.12900/rbm14.20.1-0004.

Zhao, Jianhua, John Grunewald, Ulrich Ruisinger, and Shuo Feng. 2017. "Evaluation of Capillary-Active Mineral Insulation Systems for Interior Retrofit Solution." *Building and Environment* 115. Elsevier Ltd: 215–227. doi:10.1016/j.buildenv.2017.01.004.

6

THERMAL INSULATION FOR HISTORIC WALLS: the effect on thermal comfort and energy demands

6.1. INTRODUCTION

Adopting thermal insulation in thermally heavy envelopes can be counterproductive, because of the detrimental effect on thermal inertia.

This throwback is particularly important when climates with warm and hot summers are considered, which is generally the case in southern European countries. For this reason, it is good practice to adopt numerical simulations to forecast the effect of thermal retrofits on indoor comfort and energy demands, accounting for the effect of the retrofit throughout the entire year. Furthermore, numerical simulations allow for a very detailed analysis, that can be tailored to account for the specific building characteristics and orientation, local climate, HVAC usage habits, occupancy and ventilation patterns.

For this aim, whole-building simulations are a very proper tool, and they are adopted in this chapter to evaluate how different thermal insulation solutions can affect the overall thermal behaviour of a test reference room. The room represents one of the spaces observed in the case studies and the model is validated against the hygrothermal data measured on-site, in that space. The validated model is adopted to study the effect of different thermal insulation solutions on thermal comfort and energy demands. The solutions adopted are based on thermal mortars and they are compared to more traditional solutions, such as hydrophobic mineral wool and expanded polystyrene. Insulation solutions are considered applied on the interior and exterior sides of walls, separately. Three climates are taken into considerations: Porto, Lisbon and Bologna.

The goal of this chapter is to evaluate how a relatively-thin layer of insulation can affect thermal comfort and energy demands in a room having monumental dimensions and thermally heavy walls, which is subjected to periodical occupancy patterns typical of buildings with public use. The main question addressed is whether the benefits provided by thermal insulation outweigh the throwbacks. Additionally, the efficacy of thermal mortars is compared to more common solutions and the importance of the side of the application is considered to evaluate if internal or external insulation appears preferable.

6.2. NUMERICAL MODEL AND VALIDATION

In this section, the software adopted for whole-building simulation is presented, and the reasons for the choice are explained. The basics of the software, its input and output are also briefly discussed.
A test reference room is chosen for the study and the input adopted to model its hygrothermal behaviour are explained. The methodology followed for the calibration and validation of the numerical model is then defined. Finally, the results obtained in the calibration and validation of the model are presented.

6.2.1. SOFTWARE

6.2.1.1. CHOICE OF THE SOFTWARE WUFI PLUS

The market and the academic world offer several tools for performing whole building hygrothermal simulations. WUFI Plus is hereby chosen because of its use of hourly data, detailed analysis of moisture transfer, and because it accounts for the effect of moisture content on the thermal conductivity of porous materials. Furthermore, it is largely adopted for simulations in traditional and historic buildings.

For instance, the software has already been adopted to model a historic church in Lisbon, and it was found to provide better results than Energy Plus, for that case study (Coelho, Entradas Silva and Henriques, 2019). It was also adopted to study the impact of tourism on the indoor humidity of a historic monastery (Silva and Henriques, 2021), the influence of paper and wooden collections on humidity stability and energy consumption in historic museums (Kupczak *et al.*, 2018), and the energy use in a historic Library (Radoń *et al.*, 2018). Furthermore, it was used to evaluate relative humidity fluctuations in a historic building (Kilian, Holm and Radon, 2008), possible energy retrofits in a historic case study in Palermo (Genova, Fatta and Vinci, 2017), and the influence of microclimate control scenarios in a historic art gallery (Sadłowska-Sałęga *et al.*, 2018). It was also considered for evaluating the suitability of numerical simulations to represent the hygrothermal behaviour in historic churches (Sadłowska-Sałęga and Radoń, 2020) and analysing the effect of climate change and energy-efficient retrofits on a historic church (Coelho, Entradas Silva and Henriques, 2020). It was also used for studying controlled ventilation in Historic Buildings (Antretter *et al.*, 2013) and for evaluating the effect of hygroscopic finishing on indoor relative humidity in historic buildings adopted as museums (Ferreira, Freitas and Delgado, 2019).

Furthermore, it was adopted for a study on the use of interior insulation in historic houses, in the climate of Porto (Magalhães, De Freitas and Alexandre, 2018). In this investigation, insulation appeared to be ineffective for improving the thermal behaviour of an apartment located in a historic building, both in free fluctuation and with intermittent heating. At the same time, the authors underlined that different building typologies, as well as the use of external insulation, should be further studied to evaluate the

efficacy of insulation in different types of historic buildings (Magalhães and De Freitas, 2017). This investigation aims at helping address this gap in the literature, providing for the effect of insulation on energy demands and thermal comfort in historic buildings adopted as public libraries.

6.2.1.2. BASICS OF THE SOFTWARE

Wufi Plus is a whole-building simulation software (IBP, 2018), meaning that it allows simulating the behaviour of whole buildings or parts of them (e.g. single rooms). The software relies on a holistic hygrothermal model (Holm *et al.*, 2004) that combines thermal building simulations and hygrothermal envelope calculations (Holm, Kuenzel and Sedlbauer, 2003), as schematically shown in Figure 6.1.

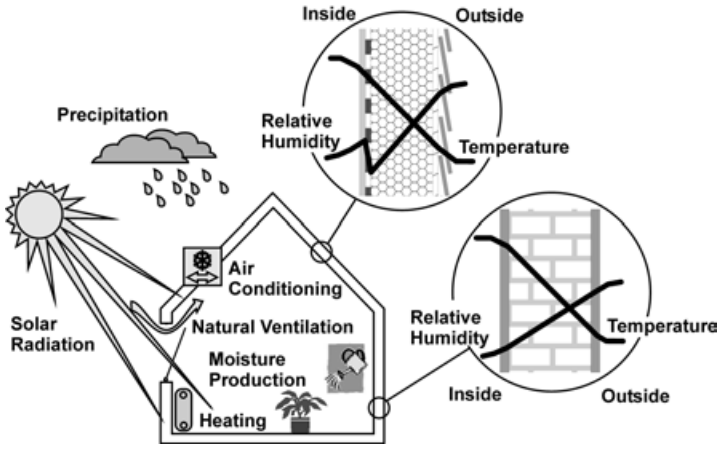

Figure 6.1 – Schematic representation of the parameters considered in WUFI Pro calculation model (outdoor weather, indoor heat and moisture loads and transient behaviour of envelope components) from Holm et al. (2004).

The model uses a finite element (volume) discretization. Construction components are discretized in a finite number of small volumes and each one is simplified as a node in the calculation algorithm (Magalhães and Freitas, 2020). The equations adopted for hygrothermal transport through the components are the same as in WUFI Pro, which were introduced in Chapter 5. The indoor environment is discretized in zones, defined in the inputs. Each zone represents a space with homogeneous temperature and relative humidity, and it is usually adopted to model one room of the building. Also the zones are simplified as nodes for the sake of calculations.

The heat and moisture exchange between zones and building components is calculated according to the equations presented in Holm, Kuenzel and Sedlbauer (2003). Very briefly, the heat balance at the zone node (room-level) considers the heat exchanged via conduction with the envelope surface, internal gains (people, lights, equipment), heat flux exchanged because of ventilation and air change rates (mix of indoor air with outdoor air). The heat balance determines the change in indoor air temperature in the

zone. Moisture transfer in the zone-node accounts for the moisture exchange between the envelope surfaces and the air volume in the zone, the air change rate due to infiltration and natural ventilation, moisture gains and losses due to occupancy and use of HVAC systems. The moisture balance determines the change in indoor air absolute moisture ratio, in the zone.

The inputs required for WUFI Plus simulations are synthesised in Figure 6.2. Those are outdoor climate parameters (which are the same defined in the chapter on mono-dimensional simulations), indoor heat and moisture sources due to occupancy, use and capacity of HVAC systems and ventilation, and envelope parameters, such as geometry, materials and orientation.

WUFI Plus provides the results of the simulations in terms of hygrothermal conditions of the building envelope, energy consumptions and indoor climate. In this work, two indoor climate outputs (air temperature and relative humidity) are used for the calibration and validation of the models. Whereas, indoor operative temperature and energy use for heating and cooling are the outputs considered in the comparative study on thermal insulation solutions. These parameters are adopted to evaluate the effect of insulation on thermal comfort and energy demands.

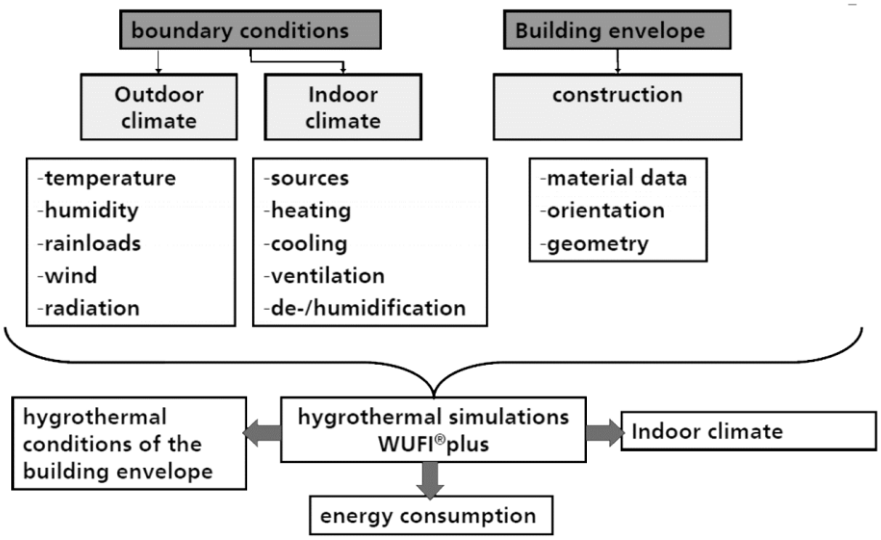

Figure 6.2 – Inputs and outputs of WUFI Plus (IBP, 2010).

6.2.2. CALIBRATION AND VALIDATION OF THE MODEL

In this section, the concepts of calibration and validation of a model are introduced, and a methodology is chosen for performing the two steps. A test reference room is selected from one of the case studies, its characteristics are defined and the input adopted to model the room are presented.

Then the results obtained in the validation and calibration of the model are provided. The validated model is then adopted for the comparative study on insulation, in the following section.

6.2.2.1. METHODS FOR CALIBRATION AND VALIDATION

Even though a generally shared method does not exist for validating hygrothermal simulations of historic buildings, the general approach relies on comparing microclimatic parameters measured in-situ versus those obtained in the simulations (Huerto-Cardenas *et al.*, 2020). The evaluation is generally performed with statistical indexes for the estimation of the error or considering the frequency of the absolute errors, with "error" indicating the difference between the simulated and measured hourly data. After these analyses, the models are largely referred to as "calibrated", "validated" or both.

Calibration is the process of adjusting physical parameters in the computational model to improve the agreement with experimental data (Oberkampf and Roy, 2010). A standard for calibrations based on indoor climate parameters does not exist yet, but ASHRAE Guideline 14 (ASHRAE, 2014), which is originally defined for energy simulations, is generally considered. A model is calibrated when it complies with the indications of the guideline on the statistical quantification of the error (Caro and Sendra, 2020). The statistical indexes considered are the cumulative variation of the root mean squared error (CV_{RMSE}), mean bias error (MBE) and the coefficient of determination (R^2) (Posani *et al.*, 2020). According to the Guideline, the three parameters should respectively fall under ±10%, 30% and over 0.75 for models calibrated against hourly measurements. Nonetheless, it is common practice to consider a model calibrated once it complies with the restrictions on the first two parameters only, i.e. the CV_{RMSE}, and the MBE (Havinga and Schellen, 2019; Kompatscher *et al.*, 2019, 2020, 2021).

Validation is the process of assessing the physical accuracy of the model via comparing simulated and experimental results (Oberkampf and Roy, 2010). An extensive review of validated hygrothermal models for historic buildings is provided by Huerto-Cardenas *et al.* (2020). The authors observed that, in most researches, a model is considered validated when the simulated data-set shows a very high share of residuals (90%–95%) within intervals of error ranging 1-2°C for temperature, 5- 10% for relative humidity and 1-2 g/kg for specific humidity. For instance, in a study on a historical archive (Kompatscher *et al.*, 2019), most of the results obtained for a validated model (one room) had differences within ±1°C, ±4% and ± 0.5 g/kg, from the hourly measurements of air temperature, relative humidity and specific humidity respectively. For a historic building (Magalhães and De Freitas, 2017) and museum (Ferreira, 2015) located in Porto, the final errors were all below 1°C and 4.5% air temperature and relative humidity. Kramer, Schijndel and Schellen (2017) validated the model of a historic museum with ±2°C, ±4% maximum errors for 90% of the air temperature and relative humidity data. What is more, given the lack of a general reference, a newly developed method proposed three categories for models-accuracy assessment through climatic parameters: excellent, acceptable and low (Rajčić, Skender and Damjanović, 2018). In this methodology, cumulative differences within ± 5% and ±1°C

are evaluated as excellent, while they are acceptable in the ranges ±10% relative humidity, ±3°C temperature of the air.

Finally, it is good practice to calibrate/validate the simulations while considering both periods of the building under use and in free fluctuation (Kompatscher *et al.*, 2019). The first assessment helps to observe if the model well represents regular conditions (accounting for the occupancy load and the use of HVAC systems), whereas the second provides information about the correct representation of the building envelope and boundary conditions.

Based on the outcomes of the literature, the following choices are made. Calibration is performed considering ASHRAE limits CV_{RMSE} <5% and MBE < 20%. Validation is based on the cumulative errors obtained at residual 95%, with values within ±1°C, ±5% RH indicating an excellent accuracy of the model and in the range ±3°C, ±10% RH indicating acceptable performance. In this study, a first calibration is performed by considering air temperature and relative humidity during a period of free fluctuation. During free fluctuation, indoor climate depends only on outdoor climate and envelope characteristics, because of the lack of ventilation, occupancy and use of HVAC systems. Thus the indoor climate monitoring performed during the covid closure, which consists of about two weeks of data in April 2020, was used to calibrate envelope-related parameters. Specifically, The U-value of windows and the infiltration rate were slightly modified to optimize simulation results, based on the CV_{RMSE} and MBE. Then, the model is calibrated considering one year of operational conditions, namely April 2019-April 2020. Realistic occupancy, ventilation patterns, as well as reasonable use of heating were considered, varying within some fixed ranges of values. After the calibration process, the simulation results are compared to the indoor air temperature and relative humidity measured on-site and the model is considered calibrated and validated when complying with the criteria previously defined.

6.2.2.2. CHARACTERISTICS OF THE TEST REFERENCE ROOM AND INPUT DATA ADOPTED IN THE SIMULATION MODEL

The space selected for the numerical simulation is one of the monitored rooms in the Municipal Library of Porto. This space appears particularly suitable as a test reference room for the study because it has monumental dimensions, as typical of rooms in historic buildings, plus it is conditioned with a heating system and it is a public space opened for the users of the library.

The room has a floor area of about 360 m^2 and is double-height. It is located on an intermediate floor, above the ground floor and below the attic. It has three walls exposed to outdoor weather, while the other two are partitional elements against other two conditioned rooms, as shown in Figure 6.3.

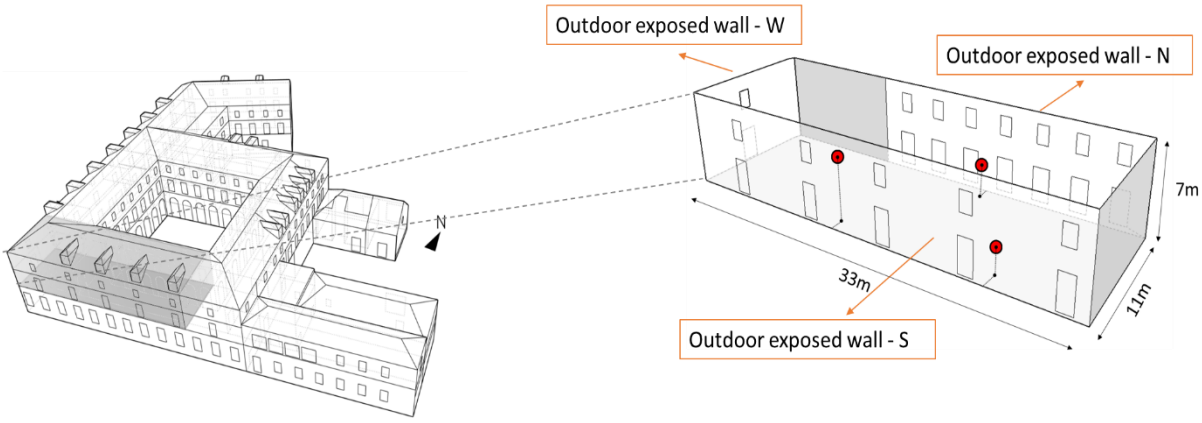

Figure 6.3 – Reference room for the study. On the right, its position inside the Municipal Library of Porto, on the left the room dimensions, the outdoor-facing walls and the position of the three dataloggers adopted in the monitoring (red points).

The test room is modelled as one zone with homogeneous temperature and relative humidity.

Assuming that the conditioned space adjacent to the room have similar indoor hygrothermal conditions, the partitional walls, as well as the floor and the ceiling are modelled as adiabatic components. The walls stratigraphy is the one shown in the previous chapter, namely 90cm-thick granite walls, plastered and rendered. The windows are modelled according to the typology observed on-site, namely wooden frames and single glazing. The main parameters adopted for walls and windows are reported in Table 6.1.

Internal heat gains were considered only during opening hours, thus accounting for the intermittent pattern of occupancy of the public building. Employee and users presence was determined by visual observation. Consequently, the occupancy was simplified considering a maximum of 20 people, and a minimum of 2. The heat and moisture gains due to occupation were approximated considering the indications of WUFI database for a seated person, working in the office (which are based on ASHRAE 55 IEA ANNEX 41), i.e. about 99W and 35g/h for each individual. Casual heat gains due to lighting and computers in the rooms were approximated with 15W/m^2 (Curado and Freitas, 2019).

The heating system was adopted with a set-point between 18°C and 23°C. The heating system located in the room indeed relies on manual regulation and it is subjected to periodical variations. The heating strategy is modelled according to the fluctuations of temperatures experimentally observed, being it mainly used only during opening hours in November-December and March. The heating seems to be often adopted continuously in January-February, with reduced capacity during closing hours, and turned off from Saturday evening until Sunday evening, when preheating is used to prepare the room for the reopening of Monday morning.

Ventilation was estimated with an air change rate of 0.5 ACH (Air Change per Hour) throughout the entire year, between 9 and 9:30, thus representing the air change before the opening of the library to the public. An additional ventilation of maximum 0.8 ACH was also considered during part of the opening hours. An infiltration rate of 0.1 ACR was also accounted, a value similar to the infiltration considered in the literature for a historic building hosting a museum (Ferreira, de Freitas and Delgado, 2019) and it is a value consistent with the infiltration observed in an extensive experimental investigation in historic churches, ranging 0.1-1.0 ACH (Schellen, 2002). More detailed information is provided in Table 6.1.

Table 6.1 – Main input data adopted in the calibrated and validated simulation model.

Walls:			
	Lime plaster - 3cm μ=12,λ=0.7 W/mk, C=850 J/(kg.K)	Granite - 90cm μ=70, λ= 2.3 W/mK, c=850 J/(kg.K)	Lime render -3cm μ=12,λ=0.7 W/mK, c=850 J/(kg.K)
Windows			
	U-value=2.87	Frame factor=0.7	
Opening time			
	Monday	Tuesday-Friday	Saturday
15th July - 15th Sept	10AM-18PMPM	10AM-18PMPM	10AM-18PMPM
16th Sept - 14th July	10AM-18PMPM	9:30AM-7:30PMAM	10AM-18PMPM
Closed on Sunday and days April 21and 25, December 24,25,29,31 and January1			
Internal loads			
People seated, reading: Lighting:	2-20 people	Heat: 99W/person Heat: 15 W/m^2	Moisture: 35g/h/person
Heating			
Maximum capacity Setpoint	12 Kw 18-23°C		
Use	11th Nov - 1st Jan: During opening hours	1st Jan - 1st March: During opening hours and often during closing time, with reduced capacity.	1st Mar-15th March: During opening hours
Natural ventilation			
Infiltration ACH Windows	0.1 h^{-1} 0.5 ACR 0-0.8 ACR	all year all year: 9-9:30h Variable during opening hours	

The outdoor climate is based on the climatic data obtained from a local meteorological station, as already explained in the previous chapter. During the calibration of the model, a better fit was observed when adopting the outdoor temperature registered by the meteorological station of FEUP, which is closer to the case study considered. Thus the final outdoor climate used in the simulation is the one already presented in the previous chapter, with the air temperature measured by the meteorological station of FEUP (Faculty of Engineering of the University of Porto, Porto, Portugal).

6.2.2.3. RESULTS OF THE MODEL CALIBRATION AND VALIDATION

Calibration and validation are based on the comparison between indoor air temperature and relative humidity simulated and measured on-site.

The hygrothermal data measured on-site were presented in Chapter 3. As already shown, in the room hereby considered as a reference, three hygrothermal sensors were installed, and their positions are schematically reported in Figure 6.3. The indoor climate is simplified by considering the average of the hourly data obtained by the three singular sensors.

In Figure 6.4 the results obtained with the calibrated model, under free fluctuation, are presented. In the same picture the data measured on-site, in the same period (31/03/2020-16/04/2020), are reported. Results appear in good agreement, with errors ranging ±1°C and ±7.5% for temperature and relative humidity respectively. Although the simulations appear to overestimate the fluctuation of the indoor climate parameters, the statical evaluation of the error shows that the NMBE and CV comply with the limits defined by ASHRAE.

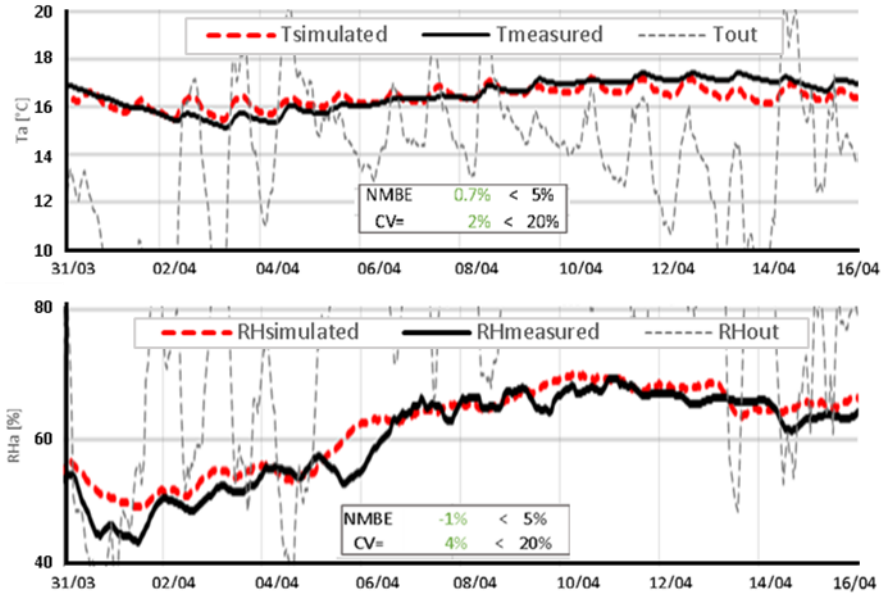

Figure 6.4 – Temperature and Relative humidity in the indoor air during a period of free fluctuation: simulated and measured data. Outdoor temperature and relative humidity from a local meteo-station are also displayed.

The results obtained during a complete year of operational conditions, namely April 2019 - April 2020, are reported in Figure 6.5. The measured and simulated data of indoor air temperature appear very similar, while relative humidity data show higher discrepancies. The statistical evaluation of the error, which is reported in the same image, complies with the criteria defined for the calibration.

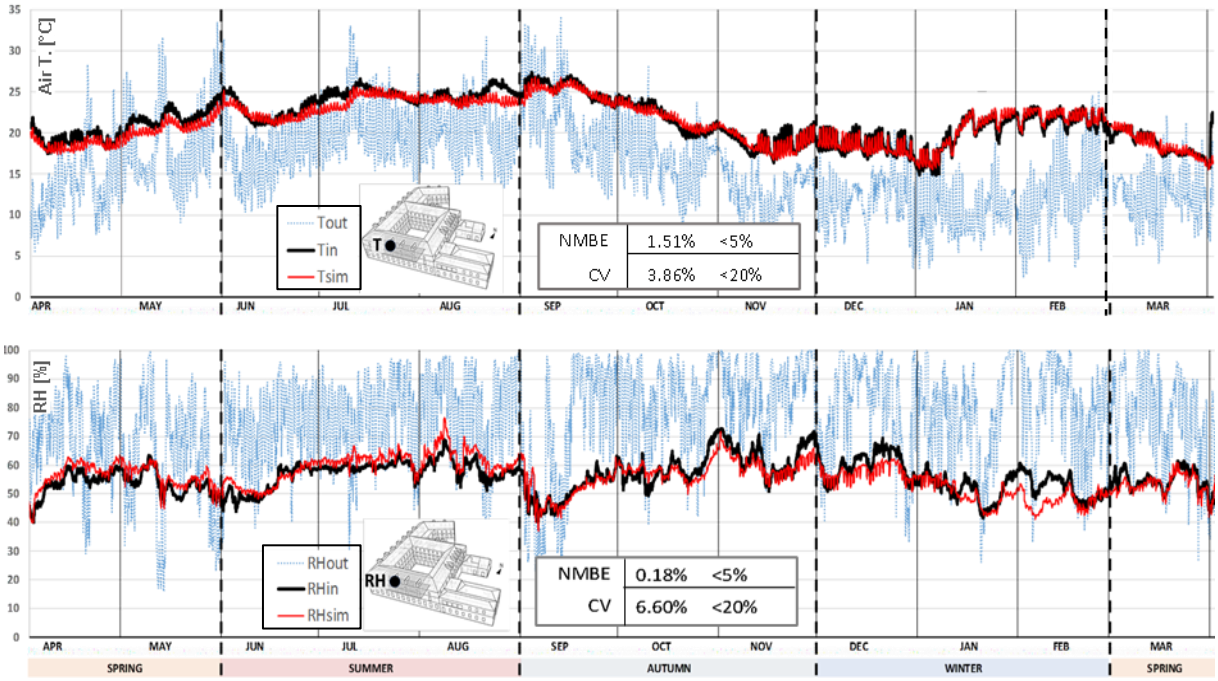

Figure 6.5 – Temperature and Relative humidity in the indoor air during one year of operational conditions: simulated and measured data. Outdoor temperature and relative humidity from a local meteo-station are also displayed.

Detailed results are reported in Figure 6.6 for one week for each season.

Each graph represents one week from Monday to Sunday, thus all days are subjected to use and occupation except the last day of each week.

During the weeks represented for August and March, a very good fit can be observed, with the overall shape of the data simulated and measured showing very similar trends. Nonetheless, the simulated temperature tends to experience stronger night falls than the measured data. Furthermore, in the simulation results of August, the model seems to slightly overestimate indoor relative humidity.

The week-data from November clearly shows a period of intermittent use of heating. It is observable that the model tends to underestimate indoor temperature during this week. This outcome seems the result of the setpoint assumed in the simulation, which was set between 19°C and 20°C, whereas in the real use of heating the setpoint was manually adjusted in situ, with setpoint temperatures occasionally exceeding 20°C. Anyway, the difference observed seems acceptable since it is below 1°C.

In January, a continuous heating strategy is adopted, with a reduced capacity of the systems at night and a complete shut down of the systems from Saturday afternoon until Sunday afternoon. The heating was turned on in the late afternoon every Sunday, for a pre-heating necessary before the re-opening of Monday morning. In this case, a very good agreement is observed between measured and simulated data, with the model slightly overestimating the temperature during Sunday.

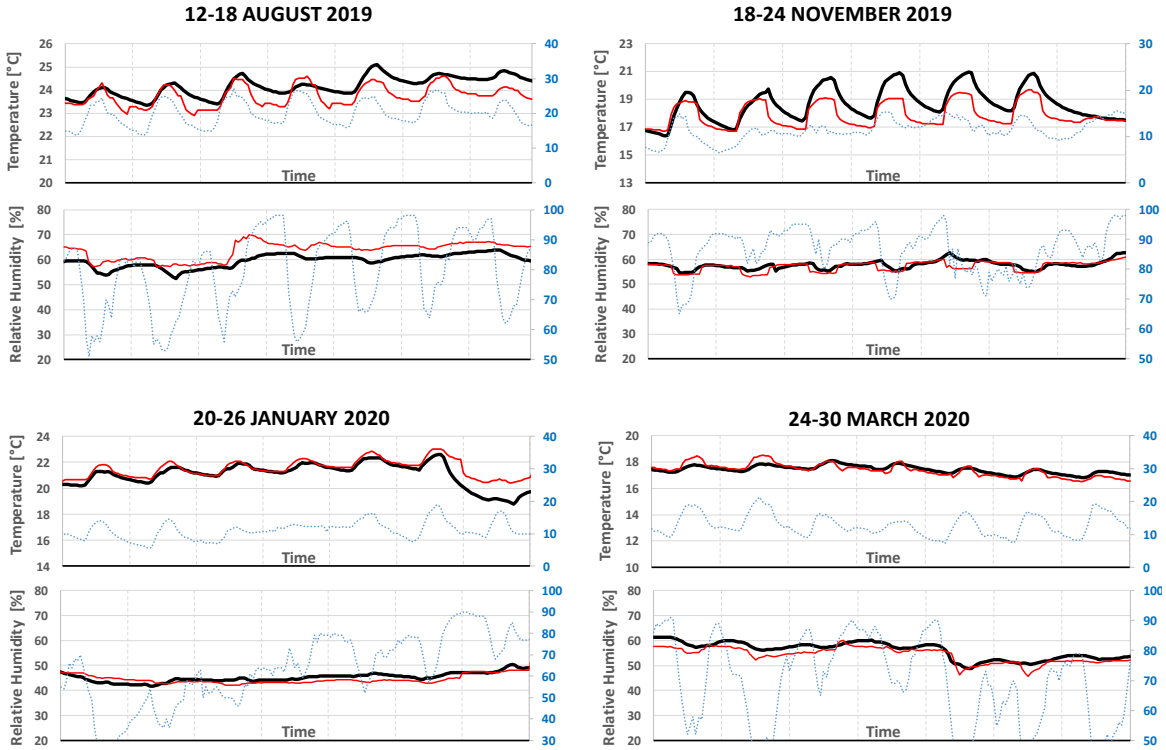

Figure 6.6 – Focus on the results obtained during one week (7days, Monday to Friday) of each season. Temperature and Relative humidity in the indoor air, simulated and measured, and outdoor data from a local meteo-station.

The relative frequency of the differences observed between the simulated and measured values is displayed in Figure 6.7. It emerges that the simulation model tends to overestimate indoor temperature and relative humidity. The 95th percentile of the errors stays within the limits ±2°C and ±8% for temperature and relative humidity, respectively. Hence the accuracy of the model seems acceptable.

Overall, the model defined is considered calibrated and validated.

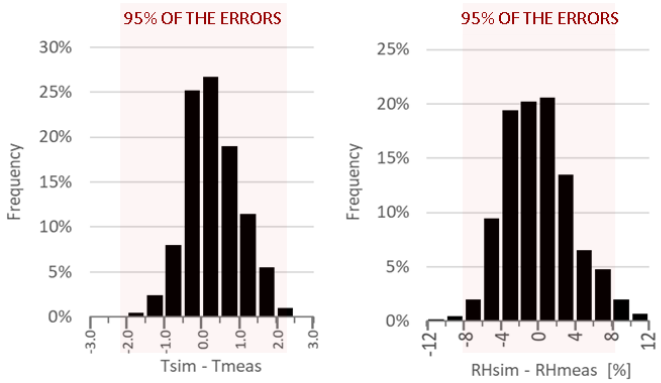

Figure 6.7 – Relative frequency of the difference between simulated and measured values of temperature and relative humidity of the indoor air.

6.3. COMPARATIVE STUDY: INFLUENCE OF DIFFERENT INTERIOR AND EXTERIOR INSULATION SOLUTIONS ON THERMAL COMFORT AND REDUCTIONS OF ENERGY DEMANDS IN THE CLIMATES OF PORTO, LISBON AND BOLOGNA.

Thermal comfort and energy demands depend on a large variety of parameters, for instance, the thermal transmittance of the envelope and its thermal inertia, the orientation of the room and its localization in the building (intermediate floor, attic, underground, or ground-facing floor), the ventilation and conditioning. In this study, only few parameters are considered for the comparative study, namely various insulation systems, different positions of the insulation, and different outdoor climates.
The test reference room is first considered under free fluctuation, and the results are evaluated in terms of indoor comfort. Then the test reference room is considered under intermittent conditioning and the results are analysed in terms of energy demands. Free fluctuation conditions and intermittent conditioning are chosen because they seem representative of typical situations in southern European countries. It is indeed not uncommon to have alternating periods of intermittent conditioning and free fluctuation in this aerea, because of the relatively mild climates and because of the lack of motivation to heat, which is quite high in southern Europe and especially in Portugal (Magalhães and Freitas, 2017). Overall, the comparative study aims to evaluate if adopting a relatively-thin layer of insulation is effective for reducing thermal discomfort and energy demands in the test reference room, in three temperate climates. The efficacy of thermal mortars is compared to that of two more common materials such as mineral wool and expanded polystyrene. Thermal insulation systems are applied on the interior or exterior side of walls, to evaluate if there is one side of application that appears to work generally better than the other.

In this section of the chapter, the input parameters adopted in the comparative study are explained, as well as the method adopted for evaluating thermal comfort and energy demands.

6.3.1. INPUT PARAMETERS

The comparative study relies on the variation of three input parameters: the type of insulation, the type of conditioning, and the outdoor climate. In total, 66 scenarios are considered, as schematically shown in Figure 6.8.

The reference scenario always consists of the un-retrofitted test reference room, meaning that no insulation is adopted on the walls. The insulation systems considered are the thermal mortar-based oness characterized in Chapter 4, i.e. S1, S2, S3, S4, and S5. In addition, two systems based on more common insulation materials, namely EPS and hydrophobic mineral wool (S_EPS and S_MW) are considered for the sake of comparison. The characteristics and hygrothermal properties of all these systems were

explained in detail in the previous chapter. In the simulations, five systems are adopted at the exterior side of the walls, and five at the interior. All insulation systems have a 4cm-thick insulation layer.

The adoption of insulation at both the exterior and interior sides of walls is not considered because it does not seem a viable solution for historic buildings.

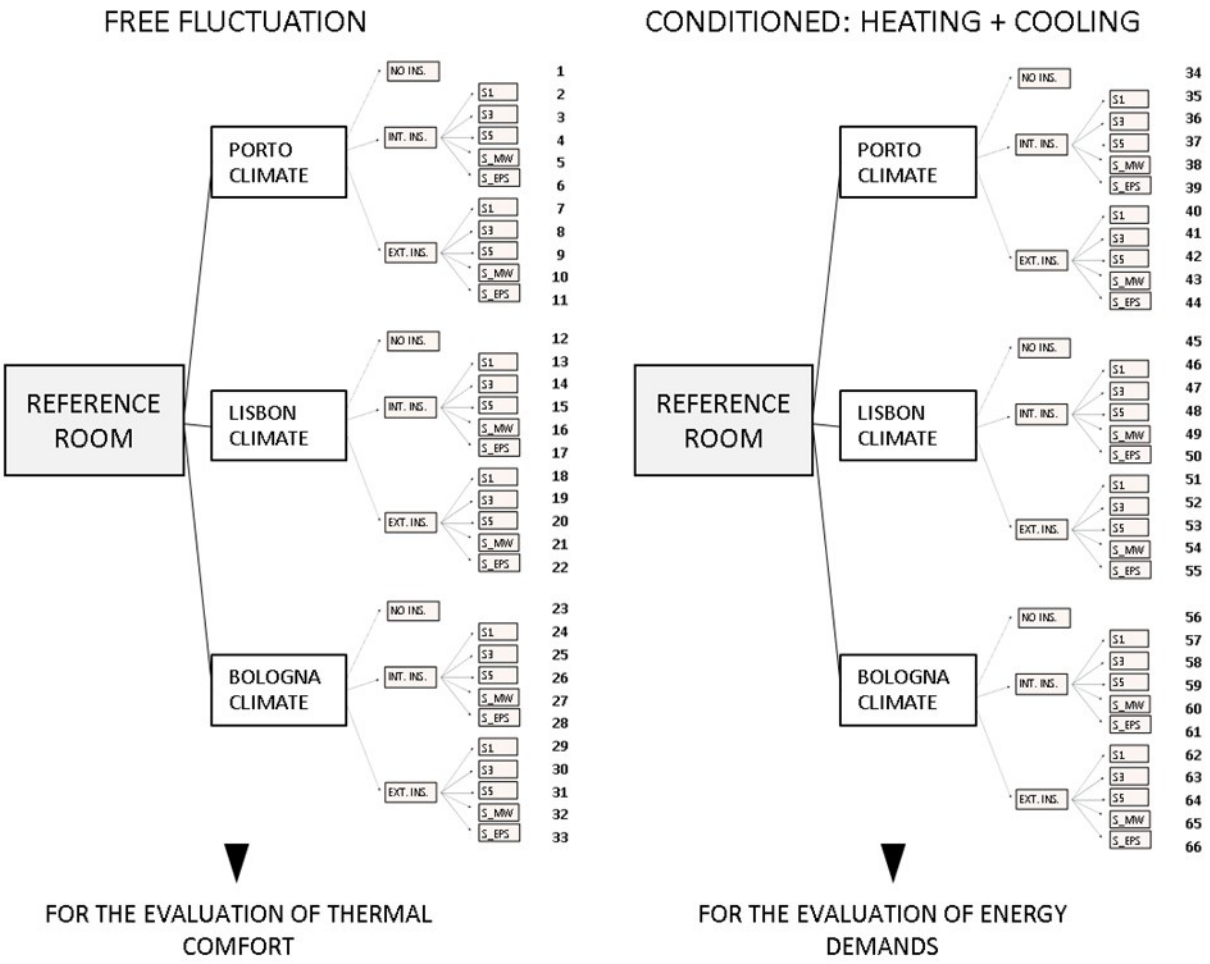

Figure 6.8 –Simulation-set for the comparative study.

Two types of conditioning strategies are considered, intermittent and absent. In the first case, the building is subjected to the conditioning of heating and cooling systems that are operative only during opening hours and rely on static set-points. In the second scenario, the room is left under free fluctuation. Those two situations represent two extremes, namely heating and cooling systems adopted along the whole year, and not adopted at all. This choice is not representative of typical conditions observed in the case studies, where periods of free fluctuation and conditioning were alternated. Nonetheless, the simulations allow having an overall view of the effect of insulation on energy demands and thermal

comfort in extreme scenarios, which allows deriving some observations for buildings with an intermediate strategy of conditioning.

Three outdoor climates are considered, namely those of Porto, Lisbon and Bologna. This choice allows considering temperate climates with noticeable differences in average winter and summer temperatures. To consider typical climatic conditions, the datasets adopted are the Test reference Years (TRY) for the different cities. For Porto the TRY adopted is the one defined by Barreira *et al.* (2017), while for Lisbon and Bologna the file are those provided in WUFI database. For Bologna, the file considered refers to Modena, which is located at a 35km-distance from Bologna. The courses of temperature in the three TRYs considered are presented in figure 6.9.

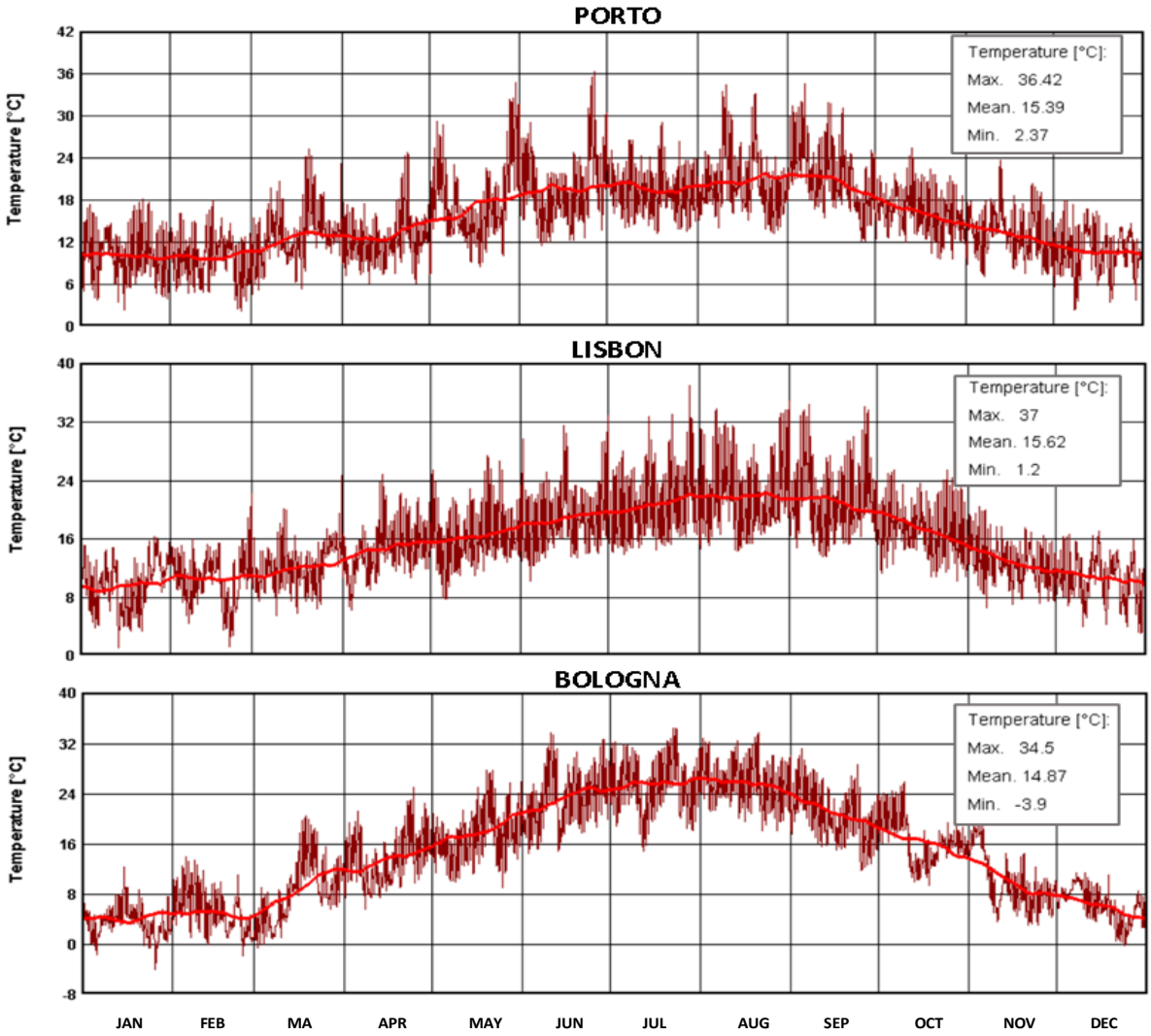

Figure 6.9 –Temperature in the TRY considered for Porto, Lisbon and Bologna. The darker line represents the ourly data of temperature, and the lighter red line indicates the 30-day moving average values.

According to the graphics of outdoor temperature, Bologna has lower winter temperatures than Porto and Lisbon, being the 30-day moving average below 8°C for a relevant part of winter in the former case and always above it in the latter ones. Bologna also has an averagely higher summer temperature, with a 30-day moving average that gets above 24 °C. Bologna has the lowest temperature among the cities considered, and Lisbon has the highest temperature peak.

To consider average, typical use conditions, some parameters are assumed as fixed, in the free fluctuation and conditioned scenarios. These parameters are defined in Table 6.2. Among them, there is one parameter that depends also on the climate considered, which is the heating and cooling capacity of the systems. The systems considered are ideal and they should be able to provide enough power for conditioning the indoor space. In the Portuguese climates, the maximum capacity considered is 12kW, while a much higher one is considered in Bologna because of the higher energy needs related to the more extreme climate conditions, namely 30 kW.

Table 6.2 – Parameters adopted in the simulations for the comparative study.

Free fluctuation	**Conditioned**
Internal gains from occupancy	
7 people: total heat gain: 693 W, total moisture gain: 245g/h Schedule: 10 AM-6PM, Monday-Saturday	
Natural ventilation	
Infiltration ACH: 0.1 h^{-1}	
Windows: 0.5 ACR all year (9-9:30 AM)	
Additional ventilation: 0.5 ACR 15th May - 1th July (10 AM-2PM) 0.8 ACR 1th July-15th Sep (10 AM-6PM)	Additional ventilation: None
Heating and cooling	
None	- Capacity: 12 kW in Portuguese climates, 30kW in Bologna - Setpoint : 20°C (heating) and 25°C (cooling) - Schedule: 10 AM-6PM, Monday-Saturday

6.3.2. THERMAL COMFORT - ASSESSMENT METHOD

Comfort is defined as a state of mind that expresses satisfaction with the environmental conditions (Hens, 2012).

Thermal Comfort is strongly related to the thermal balance of the body. This balance is influenced by environmental parameters like air temperature and mean radiant temperature, and by personal parameters. Generally, air temperature and mean radiant temperature are combined in a parameter called operative temperature (Hensen, 1990), which is the one considered in this study. Assuming that air speed is below 0.4 m/s, the operative temperature can be calculated as the arithmetic mean of air temperature and mean radiant temperature (Hensen, 1990).

The evaluation and quantification of thermal comfort have been widely studied over time and several models are provided in the literature. The most important difference lies in the distinction between classic and adaptive models.

Classic methods rely on the analytical approach to thermal comfort, as explained by Fanger's model. This method is explained in the international standard for comfort assessment EN ISO 7730:2005. It considers that the sensation of thermal comfort is influenced by several factors like the metabolic rate (developed activity) of the building users and their clothing, air velocity, air temperature, relative humidity and mean radiant temperature in the room. The model allows evaluating the comfort level for a specific static context, where the environmental and personal factors are known. Since the end of the 1990s, a new approach has gained popularity (Hens, 2012), i.e. the adaptive comfort model, which takes into consideration that thermal comfort also depends on the ability of users to adapt to environmental conditions.

The classic approach gives a strict criterion and an operative temperature to aim to, thus promoting a high use of HVAC systems for reaching a static target environment. This type of approach is not aligned with the current global focus on energy efficiency and reduction of CO_2 emissions. On the contrary, adaptive models are more suitable for reducing energy demands in buildings. These models are indeed more tolerant as they consider that users can adapt to indoor climate variations. Adaptive models are considered to well represent thermal comfort in real, dynamic environments and they are adopted in the European standard EN 16798-1:2019 – "Energy performance of buildings. Ventilation for buildings - Indoor environmental input parameters for design and assessment of energy performance of buildings addressing indoor air quality, thermal environment, lighting and acoustics. Module M1-6". In the aforementioned standard, indoor thermal comfort is defined according to the formula:

$$T_{OC} = 18PM,8 + 0,33 \times T_{RM} \ ,$$

where T_{OC} indicates the operative temperature of comfort and T_{RM} represents the running mean outdoor temperature of the day:

$$T_{RM} = (T_{n-1} + 0.8\ T_{n-2} + 0.6\ T_{n-3} + 0.5\ T_{n-4} + 0.4\ T_{n-5} + 0.3\ T_{n-6} + 0.2\ T_{n-7})\ /3.8 \ ,$$

with $T_{n\text{-}i}$ being the running mean outdoor temperature, referred to i-days before the one analysed.

The standard outlines that for buildings in free-running conditions, these equations can be used to define indoor operative temperature of comfort and that all operative temperatures that fall in the range of ± 3°C from the T_{OC} are acceptable in buildings belonging to Category II (which is the one of rehabilitated buildings). Further limits are introduced in this study, i.e. a minimum temperature of 18 °C and a maximum of 32 °C, as indicated in the standard for rooms with a "sedentary-use" with cooling appliances. The limits defined with the two models are schematically indicated in Figure 6.10.

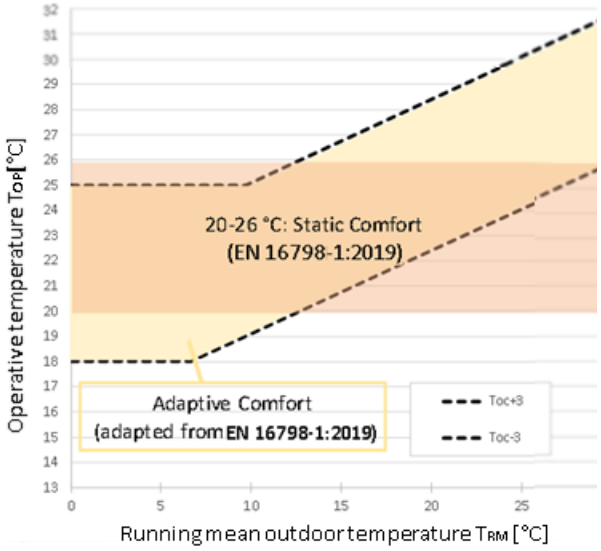

Figure 6.10 – Operative comfort temperature in te static comfort model, and correlation between it and outdoor running temperature in the Adaptive comfort model considered.

Operative temperature is one of the outputs of the simulation software adopted in the study. In this investigation, thermal comfort is evaluated by comparing the hourly output of T_{OP} obtained in the simulations to the operative temperature of comfort defined with the static and adaptive models. Furthermore, thermal comfort is quantified accounting only for the operative temperature during opening hours, thus when occupancy is expected in the library.

Four indexes are defined, based on Sicurella, Evola and Wurtz (2012):

- Hours of overheating and undercooling [%], which respectively represent the time during which operative temperature is found to be above or under the range defined with the comfort model, thus representing the temporal extension of discomfort;
- Index of overheating and undercooling discomfort [ºC.h], obtained as the sum of the hours of discomfort multiplied by the corresponding thermal distance from the limit of comfort-T_{OC}, thus representing the intensity of discomfort.

Additionally, the total sum of annual discomfort hours and indexes is calculated, to account for the total temporal extension and intensity of discomfort during the entire year.

To synthesize the results of the simulations and help the discussion, the annual discomfort observed with the retrofitted configurations is compared to the un-retrofitted one, and the results obtained in the various retrofitted configurations are expressed as a percentage of the discomfort in the un-retrofitted scenario. Finally, the correlation between the performance obtained and the thermal resistance of the thermal insulation solutions adopted, as well as their side of application, is evaluated.

At the end of the study, the annual results obtained in terms of discomfort hours and indexes are synthesized in a matrix of performance.

6.3.3. ENERGY DEMANDS - ASSESSMENT METHOD

As previously introduced, the use of heating and cooling systems consider an intermittent schedule. Namely, the conditioning is simplified by accounting for continuous use during 9am - 6pm from Monday to Saturday, with the set-point temperature of 20°C for heating and 25°C for cooling.

The energy demands are evaluated by accounting for the hourly energy use [KW.h] for heating and cooling, separately. Then the cumulative heating and cooling energy are evaluated. Finally, the total energy use due to the combination of heating and cooling systems is considered. To synthesize the results of the simulations and help the discussion, the annual energy use observed with the retrofitted configurations is compared to the un-retrofitted one, and the results are correlated to the U-value of the walls.

At the end of the study, the annual results obtained in terms of total energy demands with the different insulation solutions are collected in a matrix of performance to help define overall conclusions.

6.4. RESULTS OF THE COMPARATIVE STUDY

In this section, the results of the comparative study are presented.

First, the effect of thermal insulation on indoor air temperature, in a room under free fluctuation located in Porto, is analyzed and discussed. This step allows to qualitatively observe how thermal insulation impacts heat losses during cold periods and how it affects thermal inertia, especially during hot and warm seasons.

Then, thermal comfort is considered. The annual fluctuation of operative temperature in the test reference room under free fluctuation, with retrofitted and un-retrofitted walls, in three climates, is

analysed. The impact of insulation on thermal comfort is qualitatively evaluated by comparing operative temperature to the comfort limits defined with the adaptive and static models. The results are then assessed considering only opening hours. Thermal comfort during opening hours is quantified with the two models, in terms of hours and indexes of annual undercooling, overheating and total discomfort. Finally, the correlation between thermal comfort and thermal resistance of the insulation systems is analysed.

Energy demands are subsequently considered. The annual fluctuation of operative temperature is observed in the intermittently conditioned test room, in three climates, with and without thermal insulation. This parameter allows observing if the conditioning systems can maintain indoor target conditions during opening hours. Then the cooling and heating energy adopted in each simulated room is considered, and the annual energy use is quantified in terms of heating, cooling and total conditioning. Finally, the correlation between energy use and the U-value of the walls is assessed.

Overall, this section allows for a comparison between the effect of different insulation solutions, applied on the external or internal side of walls, in three temperate climates, in terms of thermal comfort and energy demands.

6.4.1. INDOOR AIR TEMPERATURE UNDER FREE FLUCTUATION

The indoor air temperature observed in the test reference room under free fluctuation, in the climate of Porto (simulated scenarios 1-11), is reported in Figure 6.11. In the graphic, the black line represents the temperature in the reference room when no insulation is considered, while coloured oned indicate the results obtained with 10 different insulation solutions.

All thermal insulation systems lead to a beneficial increase in indoor air temperature during the cold season. At the same time, the counterproductive effect in summer is also evident, with all insulation solutions determining higher indoor temperatures than in the un-retrofitted scenario. In addition, the solutions with the highest thermal resistance, namely S_EPS and S_MW, are found to determine the highest peaks of temperature in the warm season. On the other hand, these solutions give the best results during the cold period. More moderate results are observed with thermal mortars, due to their lower thermal performance.

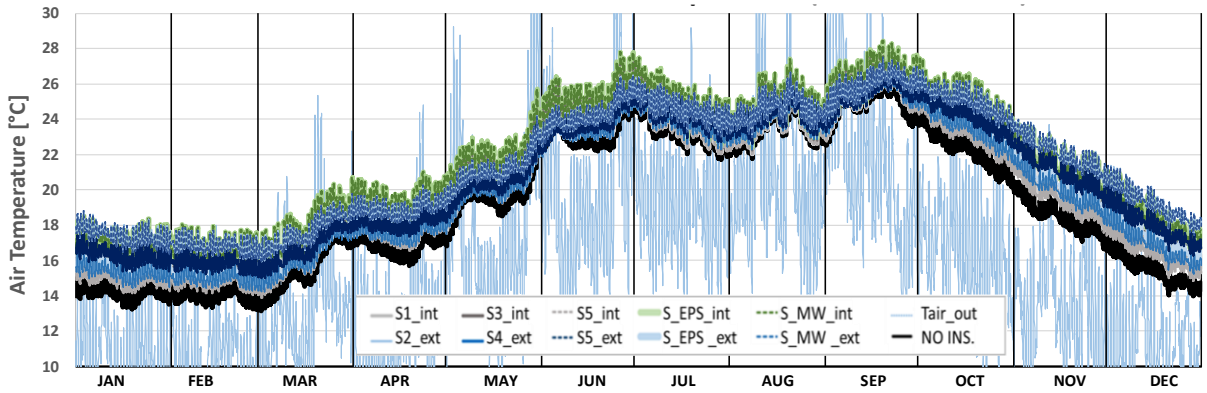

Figure 6.11 – Indoor air temperature in the test room under free fluctuation, in the climate of Porto, considering the walls with and without thermal insulation, and outdoor temperature in light blue.

Detailed results are provided for one week during each season, in Figure 6.12. Since not all the graphics start on a Monday, the occupancy is also reported in the graphics, with Sunday being the only day with no occupancy in all graphics.

The indoor air temperature observed in March 17-24 is below 20°C for all scenarios considered, while in the period 6th-13th December some of the insulation solutions allow reaching temperatures above this value. In these two periods, all retrofitted configurations provide wormer and more comfortable conditions than the un-retrofitted scenario. S_EPS, S_MW and S5 give a more relevant increase of temperature than other solutions, probably because of their higher thermal resistance. With the aforementioned solutions, indoor temperatures are above 18°C for a significant share of the opening hours, while they are never above 18°C in the original configuration. In addition, when internal insulation is adopted, indoor temperature results to experience stronger fluctuation than with exterior solutions. This outcome is probably due to the effect of thermal insulation on decoupling the thermal mass of walls from that of the air in the room.

This effect of internal insulation leads to having a higher increase in indoor temperature when there are internal heat gains due to occupancy. Nonetheless, internal insulation leads to lower temperatures than exterior insulation for most of the time, during 6th-13th December. This outcome suggests that decoupling the thermal mass of indoor air from walls can give lower benefit than disadvantage, during part of the cold periods. The disadvantage consists in the reduction of walls thermal inertia, which can contribute to mitigating indoor temperature during night falls. Indeed, internal insulation gives lower minimum temperatures during night during the December week, even when it leads to similar or higher peaks in daytime temperatures, than external solutions.

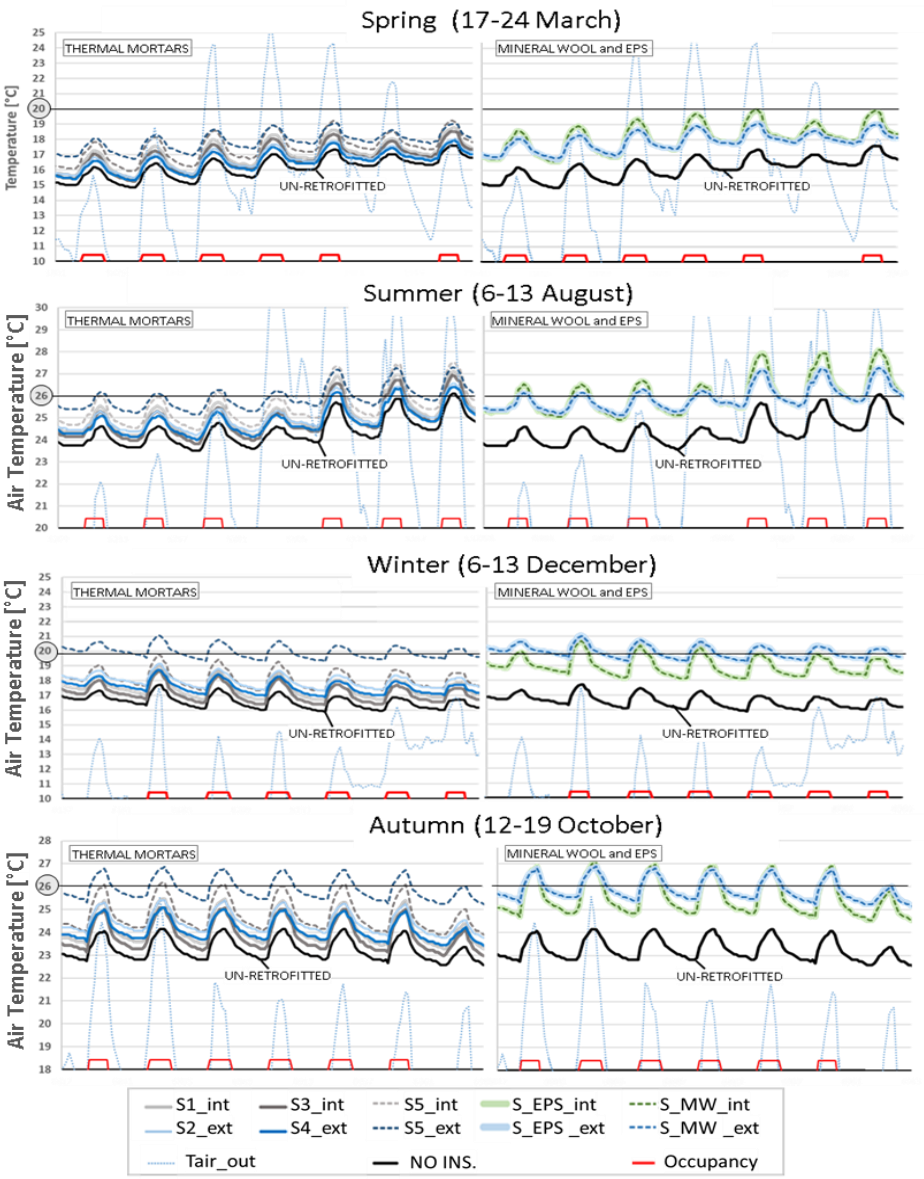

Figure 6.12 – Indoor air temperature in the Test room, in simulated scenarios 1-11,and outdoor temperature in light blue. Detailed view of one week during each season. On the left results obtained with thermal mortars or no insulation, on the right those given by EPS and MW or no insulation.

As expected, during hot and warm periods, thermal insulation can determine higher problems of overheating-discomfort. In August, the number of hours with an indoor temperature above 26°C is higher with insulation than in the un-retrofitted configuration. In October, such high levels are reached only with S_MW, S_EPS, and S5. The maximum peaks are observed with internal insulations based on EPS and mineral wool. This seems the result of the higher thermal resistance of these insulation solutions and their effect on reducing the benefits of thermal inertia. During the days that have no occupancy and no natural ventilation (Sunday, closure day), the different thermal inertia of the various configurations

is particularly evident. Internal insulation gives stronger fluctuations of indoor temperature rather than exterior one, thus suggesting that the former reduce the effects of thermal inertia to a stronger degree than external insulation.

Finally, in all seasons Mineral wool and EPS lead to almost identical indoor temperature, which is coherent with their similar thermal properties.

Overall, results show that in massive granite walls the adoption of a relatively-thin layer of insulation, suc as 4cm, can lead to relevant changes in indoor air temperature. All insulation solutions lead to reduced heat losses through the envelope, resulting in higher temperatures during cold periods. Thermal insulation also appears to lead to higher temperatures during summer, because of the detrimental effect on thermal inertia. Additionally, results appear to depend on the thermal resistance and side of application of the insulation solution. The higher the thermal resistance of the insulation is, the stronger the changes in indoor temperature get. Finally, applying insulation on the interior side of walls results in stronger fluctuation of indoor air temperature than with external insulation. This outcome seems related to the effect of internal insulation of decoupling the thermal mass of the wall from that of indoor air. During winter this results in stronger increase of indoor temperature during occupancy, while in summer it can lead to higher peaks of temperature due to the reduced thermal inertia of the envelope.

6.4.2. THERMAL COMFORT

6.4.2.1. OPERATIVE TEMPERATURE

In Figure 6.13, the operative temperature obtained under free fluctuation in the test room, in three climates, with different insulation solutions or no insulation is reported.

The results in black are those of the un-retrofitted room, while the coloured lines indicate different insulation solutions. In addition, dashed red lines are adopted to specify the maximum and minimum thermal comfort conditions, according to the adaptive model. Similarly, the yellow area indicates the range of comfort according to the static model.

In the climates of Porto and Lisbon, the un-retrofitted room appears to offer comfortable conditions during the entire summer, according to the adaptive model. Whereas, overheating discomfort appears relevant in the climate of Bologna, even when the un-retrofitted room is considered. In the climate of Porto, despite the increase of operative temperature entailed by insulation, thermal mortars do not lead to any relevant overheating discomfort, according to the adaptive model. On the contrary, S_EPS and S_MW seldom exceed the limit considered for adaptive comfort. Similarly, in Lisbon, some insulation solutions result in overheating discomfort, with S_EPS and S_MW giving the highest discomfort. In

Bologna, the operative temperature can get very high, with values being above 30°C all-time in August with all retrofit solutions. Thermal insulation solutions result in continuous overheating discomfort for more than one month, in Bologna.

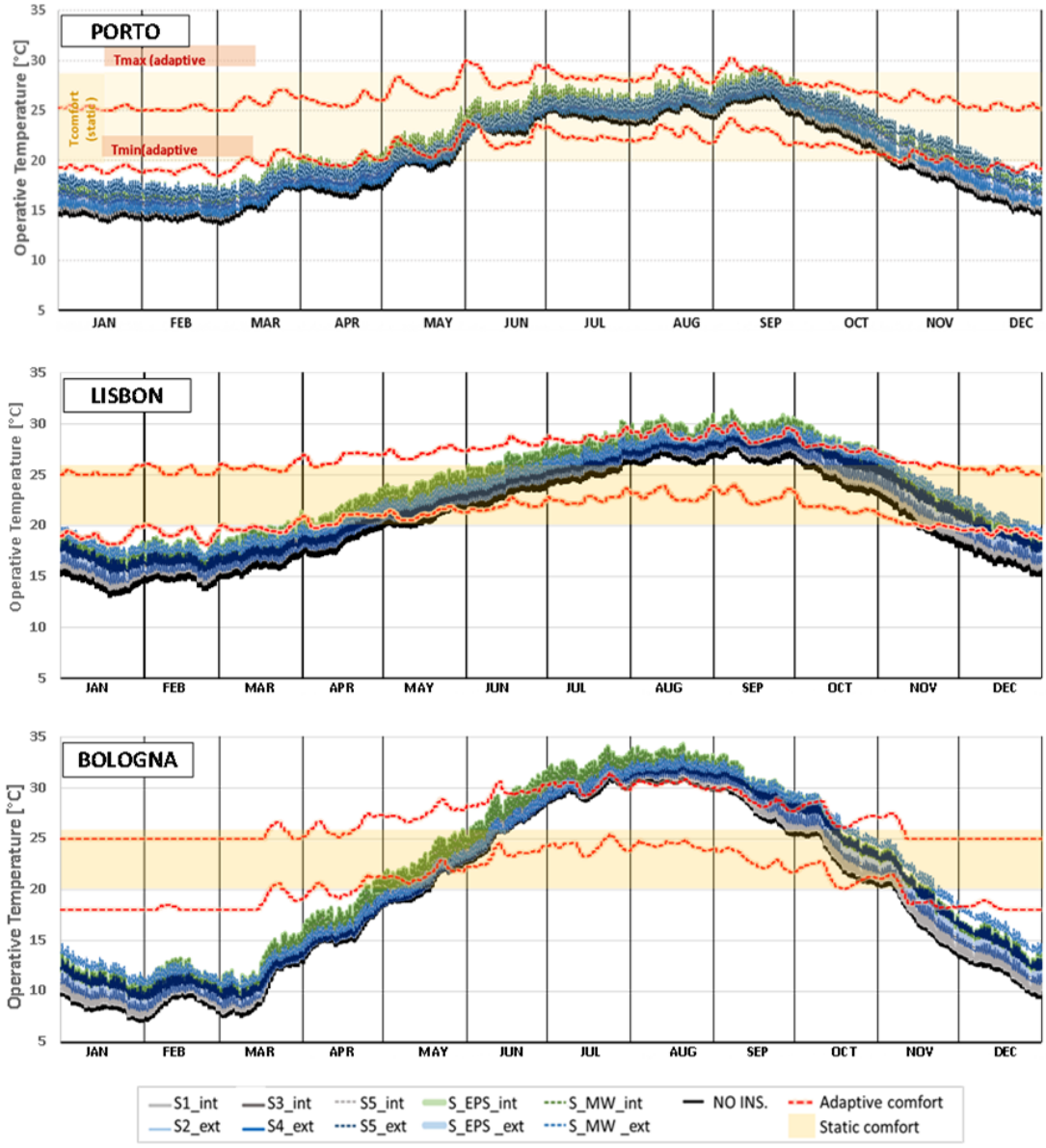

Figure 6.13 – Operative temperature in the Test room under free fluctuation, in the climate of Porto, Lisbon and Bologna.

During the cold season, Bologna has the coldest outdoor environment, with consequent lower operative temperature than in Lisbon and Porto, where winter conditions are milder. Even though a relevant increase of operative temperature can be observed in the retrofitted scenarios, during winter, the operative temperature stays below the adaptive comfort limit for a very long time in the three climates,

showing that the insulation systems considered are unable to provide a comfortable environment when no heating systems are adopted.

Bologna emerges as the climate leading to the highest thermal discomfort, due to the cold winter and hot summer conditions, which are more extreme than in the Portuguese climates.

The results obtained during opening hours only are plotted against the running mean outdoor temperature in Figure 6.14 and thereby compared to the limits of static and adaptive comfort.

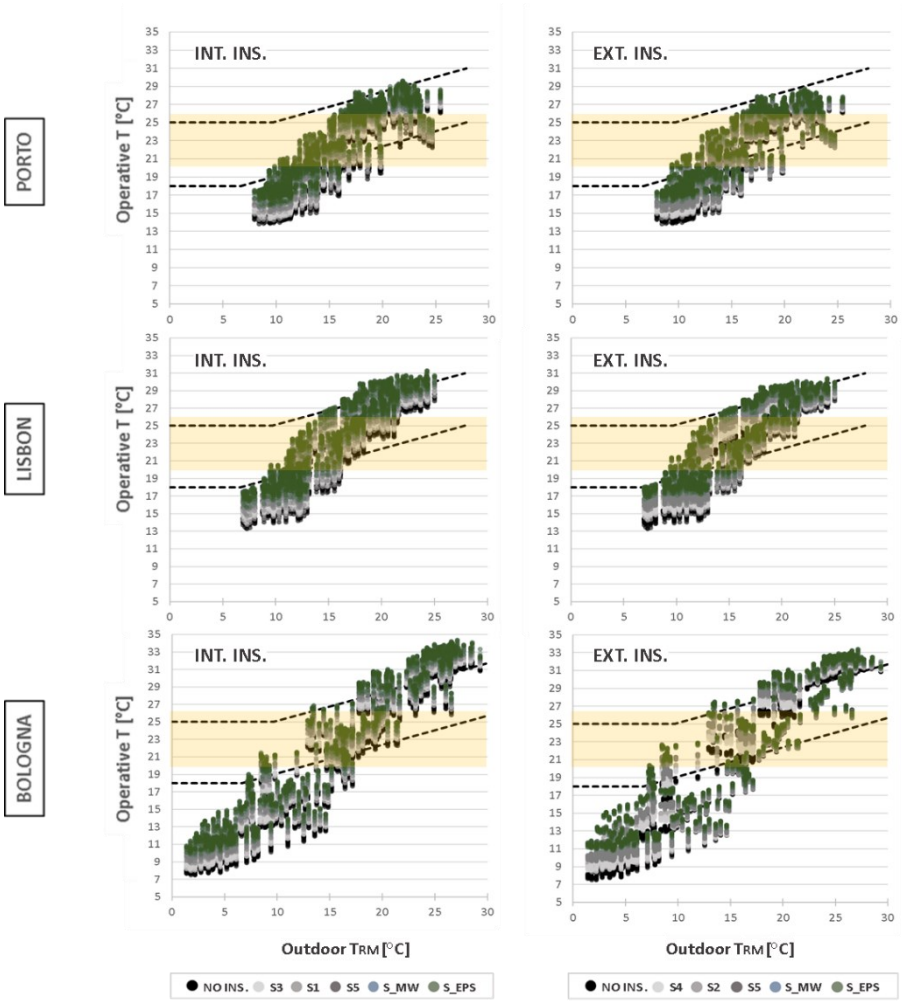

Figure 6.14 – Operative temperature during opening hours, in comparison with static and adaptive comfort limit.

During opening hours, a large share of data shows uncomfortable indoor conditions when free fluctuation is considered. Discomfort appears especially high in Bologna, where operative temperature data are much further from comfort limits than in Portuguese climates, especially in winter.

In the climate of Porto, comfort is provided much more often than in the other climates, during warm and hot periods, with the operative temperature rarely exceeding the maximum limit of the adaptive

model. In Lisbon and Bologna, the higher the thermal resistance of the insulation, the higher the overheating discomfort. Additionally, internal insulation appears to give higher overheating discomfort during opening hours, compared to external insulation. For instance, it is clear that more results exceed the adaptive comfort limit in Porto when internal insulation is adopted, and in Lisbon and Bologna internal insulation leads to a higher number of hours above 30°C and 33°C, respectively.

During cold periods, the test room has undercooling discomfort for a long time in all climates, which is consistent with the fact that no heating systems are considered under free-floating conditions. Anyway, the use of insulation decreases the intensity of discomfort by rising the operative temperature relevantly. The increase observed during opening hours is up to about 4°C in the Portuguese climates and almost 5°C in Bologna. In addition, it emerges that the intensity of undercooling discomfort during opening hours is much higher in Bologna than in the other climates, because of the very low operative temperature observed.

6.4.2.2. QUANTIFICATION OF DISCOMFORT

The thermal discomfort during opening hours is hereby evaluated in terms of annual discomfort hours and index, considering both the static and adaptive model.

The results obtained in terms of undercooling and overheating discomfort are reported in Figures 6.15 and 6.16, respectively. In each graph, the value observed in the un-retrofitted scenario is represented with a black column and labelled with the value of discomfort hours or index. The other columns indicate the values observed in the retrofitted scenarios. They are represented in proportion to the first black column and labelled with their value, expressed as a percentage of the amount in the un-retrofitted scenario. The percentages are rounded to the nearest multiple of 5%. When the un-retrofitted scenario has no discomfort, the values obtained in the retrofitted configurations are labelled with their absolute values.

Considering undercooling discomfort, the hours and indexes appear to be in the same order of magnitude when calculated with the static or adaptive method. In the un-retrofitted scenarios, the hours of undercooling observed with the adaptive method are higher than with the static one. This outcome is consistent with the fact that during mild periods some undercooling discomfort can be detected with the adaptive model, but not with the static one. Indeed, when the outdoor running temperature is above 13°C, the minimum temperature of adaptive comfort is above the static limit of 20°C, resulting in some additional discomfort hours during mild periods. On the contrary, the undercooling indexes are lower with the adaptive model, since it allows for lower temperatures during cold periods, namely a comfort temperature below 20°C when the running mean outdoor temperature is lower than 13°C. In addition,

the discomfort hours observed in Bologna, are similar to those detected in the Portuguese climates, but the discomfort indexes are much higher in the former climate. This outcome indicates that even though the period of discomfort might be similar, its intensity is much more relevant in Bologna than in the other two climates.

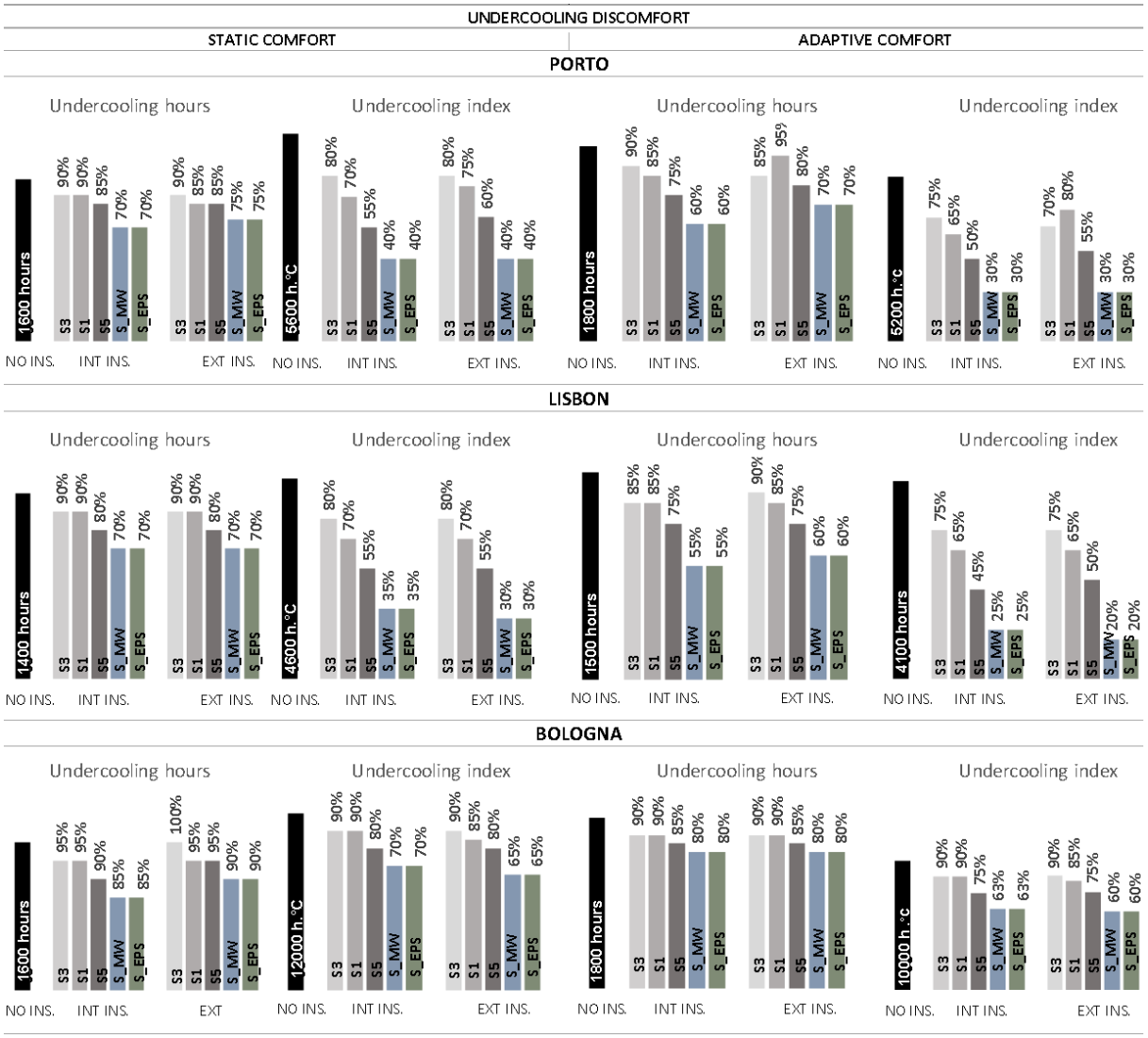

Figure 6.15 – Undercooling hours and index in the un-retrofitted and retrofitted scenarios.

Results show that all insulation solutions reduce undercooling hours and index, with best results given by the systems with the highest thermal resistance, namely S_EPS and S_MW. Additionally, it seems that the highest reductions of discomfort hours and index are provided in climates with milder winter temperatures, namely Lisbon and Porto, with Lisbon having the best percentual improvements.

The use of a very relatively-thin layer of thermal insulation appears very promising for reducing the

intensity of undercooling discomfort. With S_EPS and S_MW, the discomfort index is reduced to be 20%-40% of the original amount in the Portuguese climates and 60-70% in Bologna's. Similarly, the hours of discomfort decrease to 55%-75% in the Portuguese climates, which seems very relevant. In the climate of Bologna, more moderate benefits are observed, with discomfort hours being reduced by 10%-20% only. Thermal mortar-based system S5 seems quite competitive with S_EPS and S_MW. Indeed, it provides for a final amount of discomfort hours and indexes down to 75% and 45% of the unretrofitted configuration, respectively. The other thermal mortar-based systems, namely S1, S2, S3 and S4, are less effective. These systems lead up to a maximum decrease of discomfort hours and indexes of 15% and 35%, respectively. Such results are obtained with the adaptive model in the climate of Lisbon, while a much lower decrease is observed in the climate of Bologna, where the maximum reduction obtained is of 10% for discomfort hours and 15% for discomfort index.

In sum, a 4cm-thick layer of insulation appears to offer great potential for reducing undercooling discomfort, especially when systems with high thermal resistance, such as S_MW and S_EPS are adopted. Thermal mortar S5 offers very competitive results and thus thermal mortars with high thermal resistance appear promising for the intervention, especially if they have good thermal conductivity, e.g. as low as the one of S5 and down to those of EPS and MW.

Overheating discomfort is Reported in Figure 6.16. Contrary to what was observed with undercooling, the total hours of discomfort are higher with the static model rather than the adaptive one. This outcome is consistent with the fact that the adaptive model allows for higher operative temperature during warm and hot periods, namely when running mean outdoor temperature is above 13°C.
With the static model, the un-retrofitted room has some discomfort hours in all climates, and the amount increases with all thermal insulation solutions. On the contrary, considering the adaptive model, the un-retrofitted room does not present discomfort hours in the climates of Porto and Lisbon. Nonetheless, some thermal insulation systems lead to having some, thus creating a problem that did not exist before the thermal retrofit. The increase of overheating seems to depend on the thermal resistance of the insulation system, meaning that the higher the resistance the stronger the overheating discomfort. The increase is especially high in the climate of Porto, where the hours and index of overheating are low before the retrofit, and they get to almost quintuplicate and decuplicate respectively when S_MW and S_EPS are used as interior insulation, considering the static model. In all cases, internal insulation leads to equal or higher overheating hours and indexes than exterior insulation.

The discomfort hours and indexes observed in Bologna are relevantly higher than in the Portuguese climates.

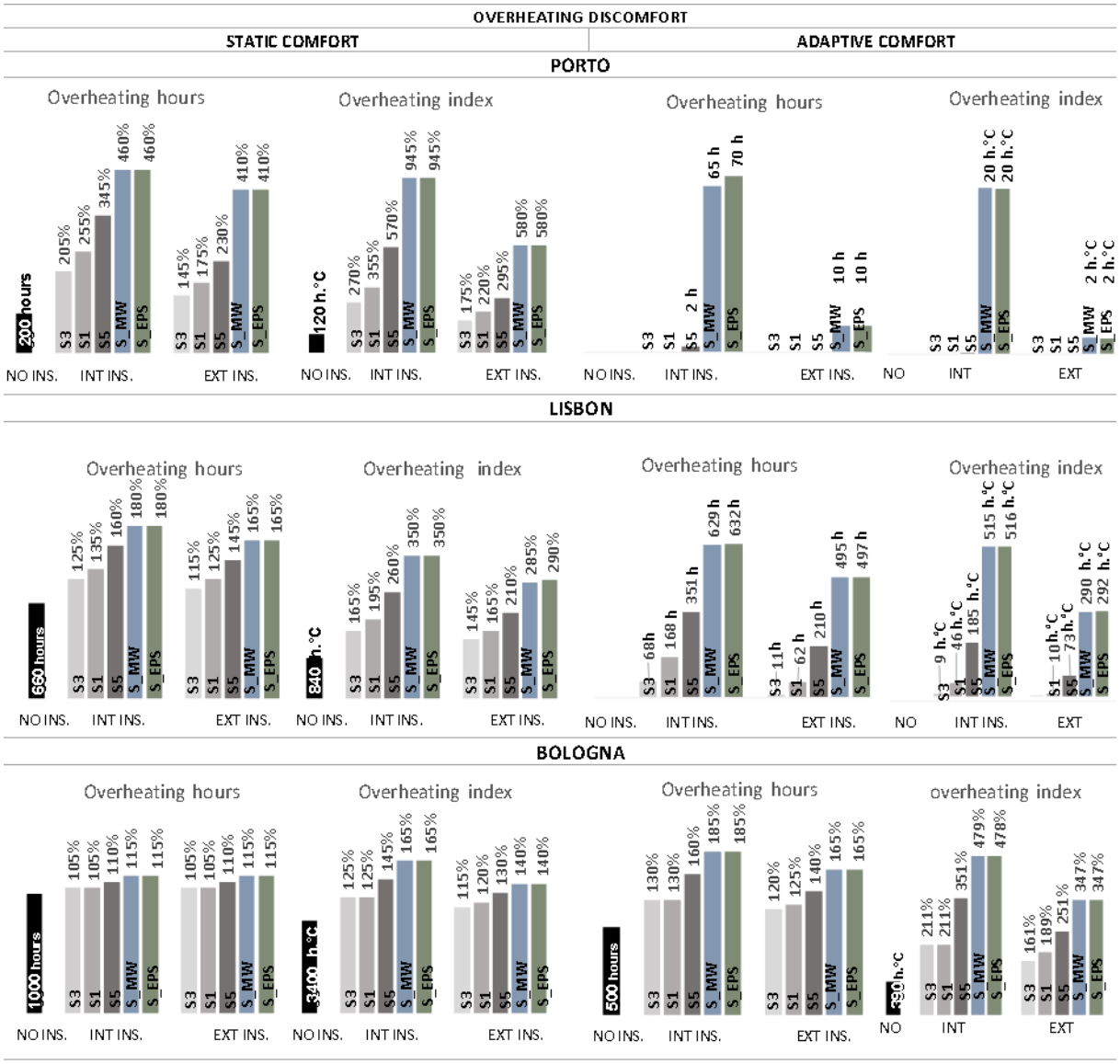

Figure 6.16 – Overheating hours and index in the un-retrofitted and retrofitted scenarios.

The total discomfort was calculated as the sum of those due to overheating and undercooling. The results are presented in Figure 6.17.

Total discomfort is higher in Bologna than in the other two climates. This difference is moderate in terms of discomfort hours, and very relevant in terms of discomfort index. With both the adaptive and static model, the change in discomfort hours due to the adoption of insulation does not seem relevant, with maximum differences in the order of 5-10% in most cases. The only exception is the test room in the climate of Porto, which experience a very relevant decrease of discomfort hours according to the adaptive model, with reductions of 10-25% with thermal mortars and 40-60% with S_EPS and S_MW. In all climates, discomfort indexes are subjected to a much more relevant change in discomfort intensity,

with the best result observed in the climate of Porto, probably because of the lower problems of overheating generated in this climate. As expected, the best results are observed with the adaptive model, with indexes reduction of 20-70% in Porto, 25-70% in Lisbon and 10-30% in Bologna. This outcome suggests that the higher the problems of overheating, the lower reduction of total comfort are obtained.

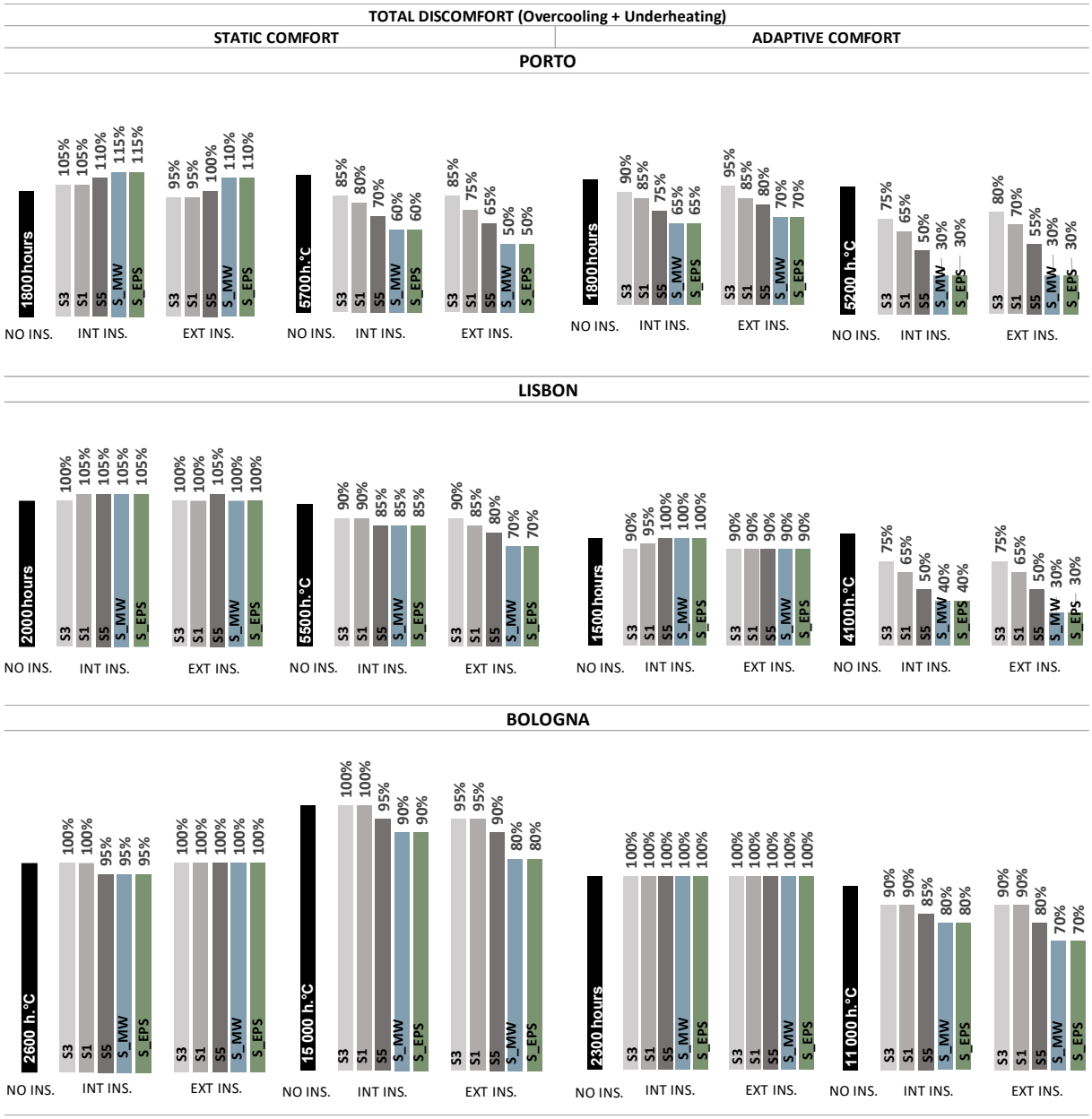

Figure 6.17 – Discomfort (overheating + undercooling) hours and index in the un-retrofitted and retrofitted scenarios.

In addition, it can be noticed that the higher the thermal resistance of the insulation, the best the reduction of discomfort index. Depending on the climate, insulation type, and comfort model considered, it seems

at times better to adopt internal insulation and at times exterior one.

The results obtained in terms of total discomfort show that thermal insulation may relevantly reduce the intensity of discomfort in the three climates considered, while it is generally not effective in terms of reducing its temporal extension.

6.4.2.3. CORRELATION BETWEEN DISCOMFORT AND RETROFIT SOLUTIONS (THERMAL RESISTANCE AND SIDE OF THE APPLICATION)

Some general patterns emerged from the quantification of discomfort, namely that the higher the thermal performance of the insulation the higher the overheating discomfort, the lower the undercooling one and the better reduction of total discomfort. Additionally, overheating appeared to be generally higher with internal insulation than external systems.

To evaluate these patterns in detail, the correlation between discomfort and thermal performance of the insulation, as well as the side of the application, was evaluated. The discomfort was considered in terms of indexes because insulation appeared to have a much more relevant impact on the former parameter rather than on the discomfort hours. The dependency of discomfort indexes on the U-value of walls (retrofitted and not) and the thermal resistance of insulation was considered and a better correlation was found using the latter parameter. Thus, this last connection is the one hereby presented.

A strong parabolic correlation ($R2 \geq 0.98$) was found between discomfort indexes and thermal resistance of the insulation systems when internal and external insulation were considered separately. These results are shown in Figure 6.18, and they confirm the overall patterns previously observed. Indeed, the correlations indicate that the higher the thermal resistance of the insulation, the lower the undercooling and total discomfort intensity, and the stronger the overheating discomfort. The different effect of internal and external insulation does not seem very relevant in terms of undercooling. On the contrary, the side of application of the insulation is very significant of overcooling discomfort in all climates, with internal insulation increasing overheating discomfort to a larger extent. Finally, accounting for the total discomfort due to both overheating and overcooling, the different side of application of insulation does not seem very relevant in the Portuguese climates, although the static model indicates the tendency of external insulation to provide better results. In Bologna, the side of application appears significant, probably due to the higher problems of overheating. In this case, the tendency of results suggests that exterior insulation gives lower discomfort than interior one.

Finally, all the correlations observed with the adaptive model have a positive coefficient for the quadratic variable, thus indicating a parabola that opens upwards. This type of correlation suggests that the higher the thermal resistance of the insulation, the smaller the proportional benefits get.

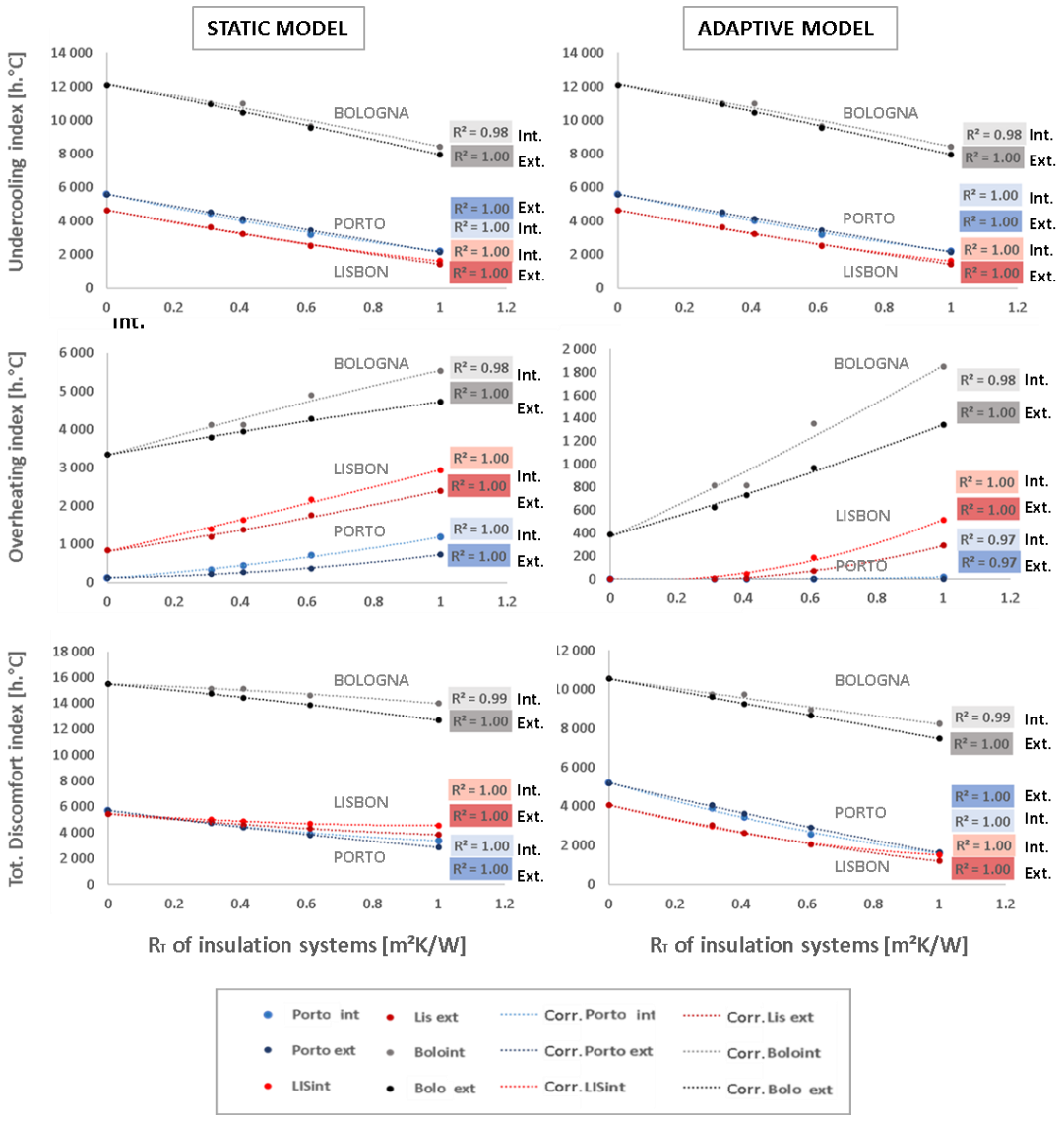

Figure 6.18 – Correlation between annual underccoling, overheating and total discomfort indexes and thermal resistance of the insulation layer adopted.

6.4.3. ENERGY DEMANDS

6.4.3.1. OPERATIVE TEMPERATURE

In Figure 6.19, the operative temperature observed in the conditioned test room before and after different retrofits is shown. In the same picture, red dotted lines are used to indicate the setpoint temperature of the heating and cooling systems.

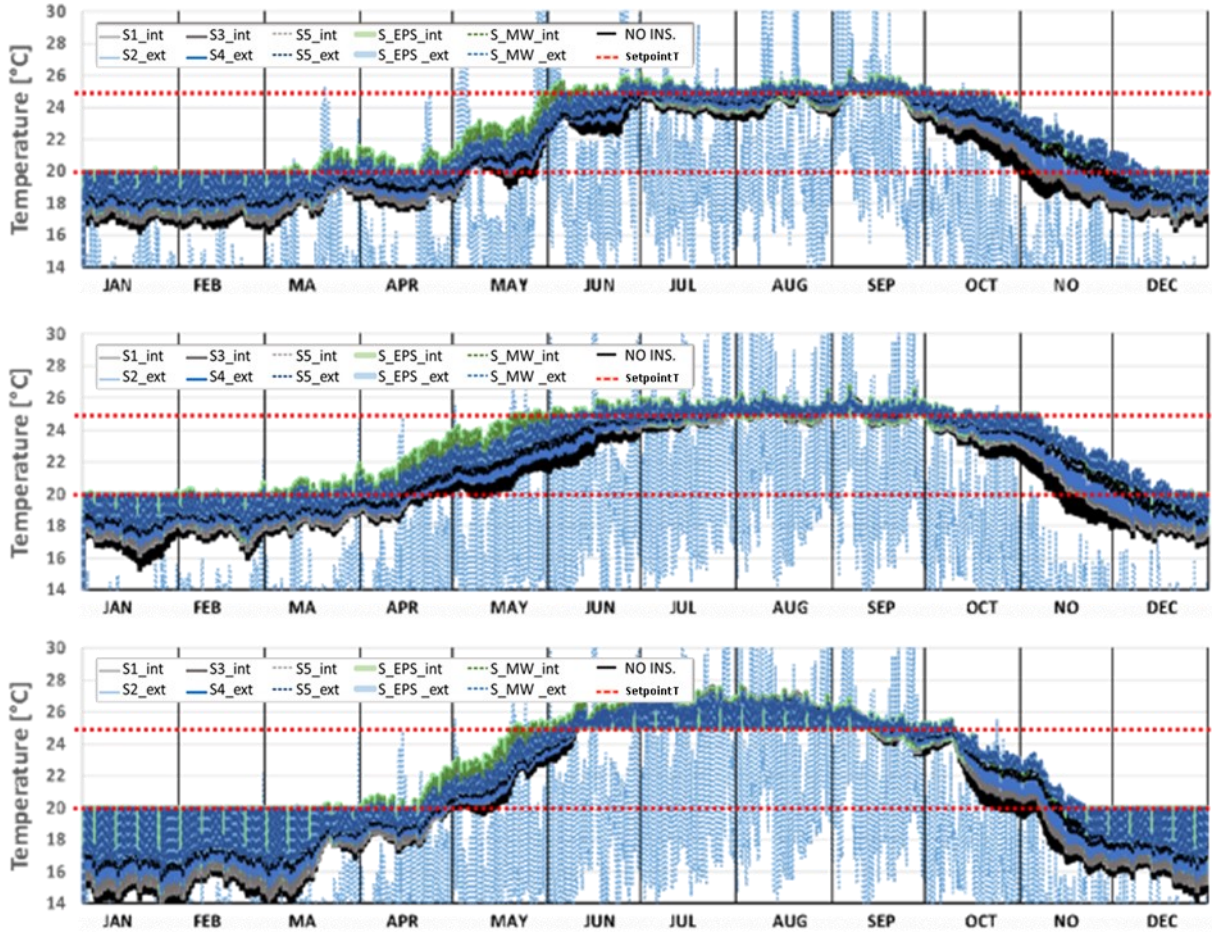

Figure 6.19 – Operative temperature in the conditioned Test room, in the climate of Porto, Lisbon and Bologna.

The graphics of operative temperature show that with intermittent heating the operative temperature can get very low during closing hours, especially in Bologna where winter is colder. The period of heating seems similar in the three climates, which is roughly from November to April. In the climate of Lisbon, the test rooms have a slighter smaller period of heating, which starts later than in the other two climates, i.e. around the middle of November. On the contrary, in the climate of Porto, the heating period is slightly longer, with some of the test rooms being heated also in the beginning of May.

In Bologna, the period of heating is in between that of the two Portuguese climates, but the energy needed is likely to be much higher. Indeed, during closing hours the operative temperature gets much lower and hotter, respectively in the cold and hot seasons, than in the Portuguese climates.

6.4.3.2. QUANTIFICATION OF ENERGY USE

In Figure 6.20 the cumulative energy use for heating, cooling, as well as for the total conditioning is displayed.

As expected, the test rooms located in the climate of Bologna have the highest energy use for heating and cooling. In the two Portuguese climates, the yearly total energy use is similar, i.e. around 12.10^3 kW.h in the un-retrofitted scenario, with test rooms located in Porto having higher heating demands than those in Lisbon, while the latter ones have higher cooling needs. The graphics show that insulation has a strong effect on reducing heating demands. The increase of cooling determined by the insulation seems lower than the reduction created in heating needs, especially in the climate of Bologna.

In all climates, insulation appears to relevantly reduce the energy needs for overall conditioning.

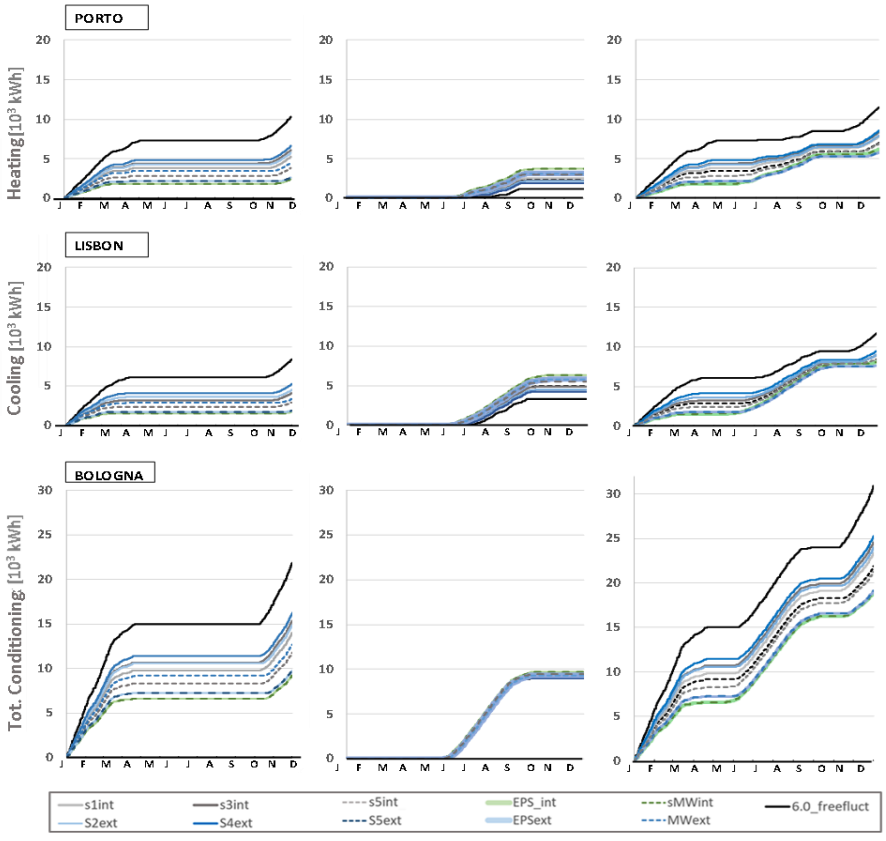

Figure 6.20 – Cumulative energy use in the conditioned Test room, in the climate of Porto, Lisbon and Bologna.

In Figure 6.21 the annual energy demands for heating, cooling and total conditioning are reported for all the simulated scenarios. The results obtained with the un-retrofitted test room are represented in black and their value is reported with 2 significant digits. Retrofitted configurations are represented with coloured bars and their energy demands are reported as a percentage of that in the un-retrofitted scenario, with the percentage expressed as a multiple of 5%.

The histograms show that the use of internal insulation gives better or equal results to external insulation, in terms of heating demands, but the differences are very moderate, namely in the order of 5-10%. On the contrary, internal insulation gives worse results for the cooling demands. This effect does not seem very relevant in the climate of Bologna, where the increase of cooling due to insulation is of maximum 10%, and the differences between external and internal solutions are in the order of 5%. In Portuguese climates, the increase of cooling and the different effect of internal and external insulation is much more relevant. The differences observed due to the side of the intervention can be related to the fact that adopting internal insulation decouples the thermal mass of indoor air from that of the wall. This effect is positive for reducing the heat absorbed by walls during the heating season but counterproductive in terms of thermal inertia, which increases cooling demands.

Considering the energy for the overall conditioning, compatible results are obtained when thermal mortar S5 is adopted at the exterior or interior side of the walls. With systems S_MW and S_EPS, external insulation appears more effective than interior one. This result is consistent with the fact that these solutions give compatible results for heating demands when adopted at the interior and exterior side of walls, while they are preferable at the exterior side for cooling. Thermal mortar-based insulation systems S1 and S2 give better or comparable performance when adopted as interior insulation. All considered, it seems that the preference for internal or external insulation depends on both the climate and the type of system adopted. Nonetheless, the differences observed do not seem very relevant since they are all in the order of magnitude of 5%. For this reason, the adoption of internal or external insulation seems quite interchangeable in terms of annual energy demands, in the scenarios considered.

Overall the adoption of a 4cm-thick insulation layer appears very effective for reducing energy demands in the test room analysed, especially in Porto and Bologna, whereas the benefits are lower in Lisbon. In the former two climates, the reduction of annual conditioning is in the range 20-40% and 30-50% in Bologna and Porto, respectively. In Lisbon, the reduction is of about 25-35%.

Thermal mortar-based solutions appear promising, especially S5, which has the best thermal resistance, since it provides for reductions of 30-40% in the climates considered. The outcomes presented suggest that if more advanced thermal mortars are used, such as those containing aerogel, reductions in the order of 30-50% could be achieved (based on the values found in literature), i.e. as strong as with S_MW and S_EPS.

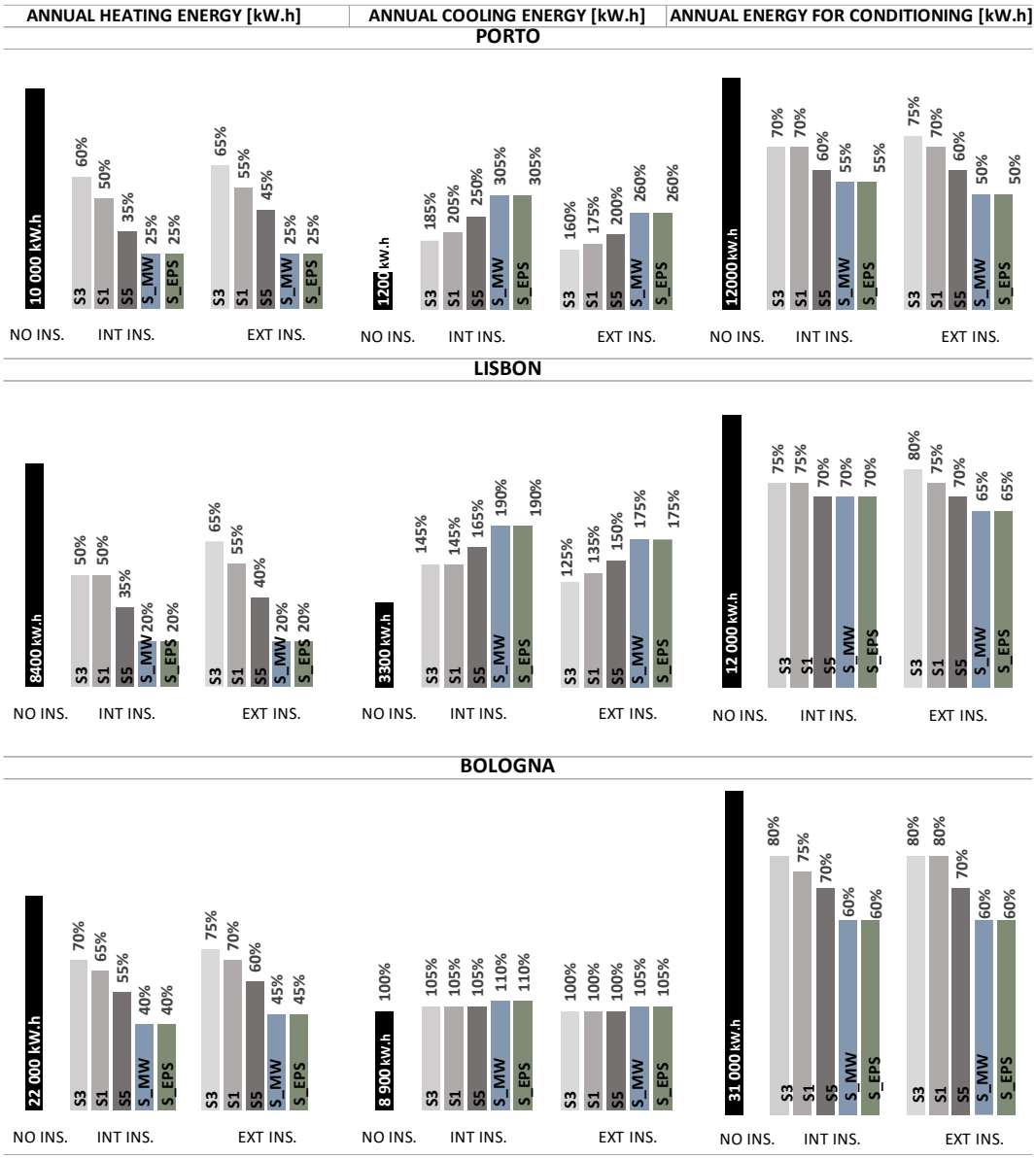

Figure 6.21 – Annual energy for heating, cooling, and overall conditioning in the simulated scenarios.

6.4.3.3. CORRELATION BETWEEN ENERGY USE AND RETROFIT SOLUTIONS (U-VALUE AND SIDE OF THE APPLICATION)

The results obtained in terms of annual heating, cooling and total conditioning suggest that the effect of the retrofit depends on the side of the intervention and on the thermal performance of the insulation solution adopted. These correlations were evaluated by considering the dependency of energy demands on the thermal resistance of insulation and on the U-value of walls. The latter analysis showed stronger correlations, thus it is the one hereby considered.

A strong parabolic correlation (R^2>0.98) was found between the two parameters, when internal and external insulation were considered separately, as shown in Figure 6.22.

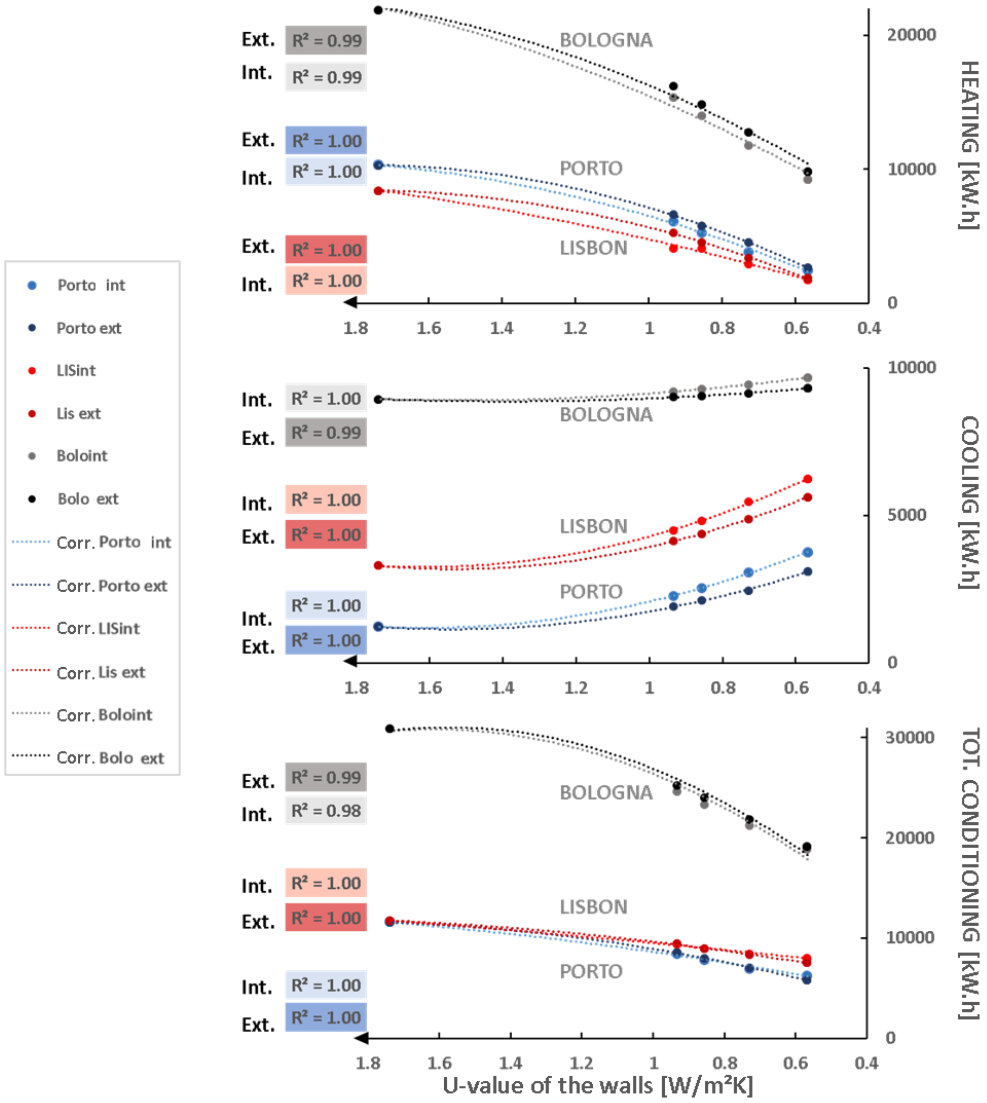

Figure 6.22 – Correlation between annual energy for heating, cooling, and overall conditioning and the U-value of the walls in the simulated scenarios.

The correlation observed allow to extrapolate the following observations. Heating and cooling demands are strongly influenced by the changes in the U-value of walls. Namely, reducing the U-value of walls leads to lower heating demands and higher cooling demands. Internal and external insulation have a different impact on heating and cooling demands, being internal one better for reducing heating demands and worse for moderating cooling demands. The annual energy demand for conditioning decreases in all climates, with the best results provided in Bologna and Porto, probably because of the high heating

demands. The strongest absolute reductions are observed in Bologna, which is probably the result of the very high total energy demands of the un-retrofitted room in this climate.

The correlations observed with the total energy demands suggest that external insulation is preferable in Portuguese climates, whereas interior performs better in Bologna. Nonetheless, for the range of U-values considered, the difference between the use of internal and external insulation seems neglectable.

Finally, all correlations have a negative coefficient for the quadratic variable, thus indicating a parabola that opens downwards. This type of correlation suggests that the benefit of insulation on total energy demands gets proportionally more relevant when lower U- values are obtained.

6.5. SYNTHESIS OF RESULTS

The results obtained in terms of energy demands and thermal discomfort in the retrofitted scenarios are synthesized in a matrix, which is reported in Figure 6.23.

		S4ext	S3int	S2ext	S1int	S5ext	S5int	S_MWext	S_EPSext	S_MWint	S_EPSint
ENERGY											
ANNUAL ENERGY FOR CONDITIONING	POR	74%	73%	69%	68%	61%	60%	50%	50%	54%	54%
	LIS	80%	80%	76%	76%	71%	72%	64%	64%	68%	68%
	BOLO	82%	80%	78%	76%	71%	69%	62%	62%	61%	61%
DISCOMFORT											
DISCOMFORT INDEX - AD.	POR	78%	75%	70%	66%	56%	50%	31%	31%	31%	31%
	LIS	75%	74%	65%	65%	50%	50%	30%	29%	38%	38%
	BOLO	68%	66%	57%	56%	42%	41%	23%	23%	30%	30%
DISCOMFORT INDEX - ST.	POR	83%	84%	77%	78%	67%	69%	50%	50%	59%	60%
	LIS	88%	92%	84%	89%	79%	86%	70%	70%	84%	84%
	BOLO	88%	92%	84%	89%	78%	85%	69%	69%	82%	82%
DISCOMFORT HOURS - AD.	POR	94%	90%	87%	86%	79%	76%	69%	69%	64%	65%
	LIS	89%	91%	88%	94%	91%	98%	92%	92%	98%	98%
	BOLO	87%	82%	82%	78%	77%	73%	59%	59%	62%	62%
TOT DISCOMFORT HOURS - ST.	POR	96%	103%	96%	106%	99%	112%	112%	112%	114%	113%
	LIS	100%	102%	100%	103%	103%	107%	100%	100%	105%	105%
	BOLO	99%	101%	100%	103%	102%	106%	100%	100%	105%	105%

Abbreviations: AD. - Adaprive model, ST. – Static model

Ranking scale	High Benefit	Low Benefit	neutral	Low Risk	High Risk
	20-60%	60-100%	100%	100-105%	**105-115%**

Figure 6.23– Matrix of performance: energy demands and thermal comfort with different thermal insulation solutions.

In the matrix, the performance observed with the different insulation solutions are reported as a percentage of those in the un-retrofitted scenario. A colour scale from green to red is adopted to indicate the benefit and risk of the interventions. Each column of the matrix represents the results obtained with one thermal insulation solution. Thermal insulation solutions are ordered from left to right according to their thermal resistance, from low to high. For solutions having the same thermal resistance, external insulation is put before interior one.

The synthesis of results shows that in the three climates considered, it is convenient to adopt thermal insulation to reduce energy demands of intermittently heated buildings and improve indoor thermal comfort under free fluctuation, according to the adaptive model. Considering the stricter limits set by the static model, most insulation solutions appear to lead to an increase in the hours of thermal discomfort. Given that the increase of discomfort time is always below 15%, and that the discomfort intensity appears more relevantly reduced, the increase of discomfort hours seems neglectable.

Overall, reductions between 8% and 50% are observed in terms of annual energy demands for conditioning. Better results are obtained with insulation having higher thermal resistance, and the difference between using insulation on the interior or exterior surface of walls does not seem relevant. Best results are obtained in the climate of Porto, where cooling demands are much lower than heating ones. In terms of annual discomfort, index reductions in the range 22%-77% are observed with the adaptive model and decreases of 8%-50% are found with the static model.

The decrease of discomfort intensity observed with the adaptive and static models are quite in agreement, both showing that insulation always leads to overall benefits and that the higher the thermal resistance of the solution, the lower the intensity of annual discomfort. With the first model, the best results are found in Bologna and Porto while with the static model much better results are found in Porto than in the other two climates. The fact that the adaptive model gives noticeably better results in Bologna than the static one is due to the higher temperatures allowed by the former one during summer. The decrease of discomfort intensity shows that for thermal comfort, S_MW and S_EPS generally perform better if applied at the exterior side of walls, with a difference up to 15% in the percentual reduction of discomfort, depending on the side of application. For thermal mortars, the static model shows better results with external insulation, while the adaptive model suggests that interior solutions are preferable. This difference seems the result of the much higher temperature of comfort considered in the adaptive model. However, very small differences due to the side of application are observed, up to 7%, it thus seems not relevant.

6.6. LIMITATIONS OF THE STUDY

Before outlining the overall conclusions of the study, it seems important to underline some limitations of it.

The simulations hereby presented account for energy use by considering ideal heating and cooling systems. The conclusion derived might be not applicable for situations where heating and cooling systems differ from each other, for instance relying on pieces of equipment with very different performances.

The thermal insulation solutions considered have a small thickness and a maximum thermal resistance of 1 m^2.K/W, which are typical features of solutions suitable for historic buildings, due to the geometrical limitations implied by this type of intervention. The results obtained cannot be extended to insulation solutions having much higher thermal resistance, as suggested by the parabolic correlation observed in the study.

The results obtained refer to Granite walls with a thickness of 1.2m, having a U-value of about 1.4 W/(m^2.K). Since the gains of insulation are related to the reduction of heat losses through the walls, lower benefits can be expected when massive walls with lower U-value are considered, and better ones when walls with worse thermal performance are evaluated.

6.7. CONCLUSION

In this chapter, a room located in the case study of Porto was adopted as a test reference room for a comparative study on the effect of thermal insulation on thermal comfort and energy demands. The room was modelled through a whole-building hygrothermal simulation tool and the model was calibrated and validated against the hygrothermal data measure on site. This model is representative of a room having massive stonework walls and monumental dimensions, located on an intermediate floor, with intermittent occupancy due to the usage, i.e. public library.

The model was adopted to study thermal comfort under free fluctuation, and energy demands for intermittent conditioning. The results obtained appear representative for southern countries, and especially Portugal, where the lack of motivation to heat tends to lead to conditioning strategies that rely on intermittent conditioning and free fluctuation periods.

Five types of insulation materials were considered, namely three types of thermal mortars and two more common materials such as mineral wool and expanded polystyrene. Thermal insulation systems based on these materials were considered for applications on the interior and exterior sides of walls. Three temperate climates were considered, namely the ones of Lisbon, Porto and Bologna, i.e. cities located in southern European countries. The results obtained led to the following conclusions.

When considering massive walls and a very relatively-thin layer of insulation, such as 4cm-thick one, noticeable benefits can be found. On one hand, the effect of insulation reduces heating demands and undercooling discomfort, on the other, it increases cooling needs and overheating discomfort. In the scenarios considered, the benefits of thermal insulation overweighted the drawbacks. Annual energy demands for conditioning were found to be reduced by 32% to 50% with mineral wool and EPS, and by 18-40% with thermal mortars. Best results were found in the climate of Porto, probably because of its mild summer temperatures which moderate the disadvantages of adopting insulation. In this climate,

energy demands were reduced by 26-50% with the use of thermal insulation, while intensity of thermal discomfort was decreased by 32-70%, according to the adaptive model.

System S5, which is the thermal mortar-based solution with the best thermal conductivity among those considered, provided for lower but comparable performance to S_EPS and S_MW. System S5 provided for reduction of energy demands in the range of 28-40% and reduction of discomfort indexes of 44-59% (adaptive model), which seems very promising. These outcomes show that thermal mortars with low thermal conductivity are competitive with traditional insulation materials and effective for application in historic buildings with massive walls. Furthermore, results suggest that thermal mortars with advanced formulations (e.g. containing aerogel) might offer benefits as high as typical solutions based on EPS and mineral wool.

It is well known that interior insulation has a stronger detrimental effect than exterior one on thermal inertia, leading to higher cooling demands and overheating discomfort. Nonetheless, considering the results of a complete year of simulations, the differences obtained between internal and external insulation were not very relevant. In terms of decrease of annual energy demands, the differences between internal and external insulation were always lower than 5%. For the intensity of thermal discomfort, results obtained with thermal mortars applied at different sides of the wall were of maximum 7%. With mineral wool and expanded polystyrene higher difference were observed, up to 15%, and exterior insulation seemed preferable.

A strong parabolic correlation was found between discomfort index and thermal resistance of insulation, for internal and external solutions. These correlations showed that the higher the resistance the stronger the increase of overheating discomfort, and the decrease of annual undercooling intensity. The parabolic nature of the correlations also suggested that the higher the thermal resistance of the insulation, the smaller the proportional benefit gets, in terms of total discomfort intensity. Similarly, strong parabolic relations were found between the U-value of walls and energy demands. These correlations showed that the lower the U-value (i.e., the better the thermal resistance) the lower the heating needs and the higher the cooling demands. In terms of total conditioning demands, the parabolic nature of the correlations shows that the benefit of insulation gets proportionally more relevant when lower U- values are obtained.

Overall, it appears convenient to adopt thermal insulation in spaces with similar characteristics to the one analysed, if they are intermittently conditioned or in free fluctuation. This result seems reasonably extendable to those spaces that are at times intermittently conditioned and at times left under free fluctuation. On the contrary, thermal insulation might be counterproductive in buildings equipped with heating systems only. In this case, heating demands are reduced but summer discomfort is increased,

which appeared especially detrimental in Porto since the un-retrofitted configuration has no relevant overheating discomfort, whereas it does with some insulation solutions. Thus, the thermal retrofit could require the installation of new cooling systems or very uncomfortable summer conditions. For buildings with prolonged summer closure, e.g. 2-3 weeks in the middle of the hot season, the situation might be different and the overheating problems might be less relevant.

6.8. REFERENCES

ASHRAE. 2014. 'ASHRAE Guideline 14-2014 Measurement of Energy and Demand Savings'.

Antretter, Florian, Sarah Kosmann, Ralf Kilian, Andreas Holm, Fabian Ritter, and Barbara Wehle. 2013. 'Controlled Ventilation of Historic Buildings: Assessment of Impact on the Indoor Environment via Hygrothermal Building Simulation', in *Hygrothermal Behavior, Building Pathology and Durability*. Springer. p. 93-111.

Barreira, Eva, M. L. Simões, J. M.P.Q. Delgado, and I. Sousa. 2017. 'Procedures in the construction of a test reference year for Porto-Portugal and implications for hygrothermal simulation', *Sustainable Cities and Society*, 32. doi: 10.1016/j.scs.2017.04.013.

Caro, Rosana, and Juan José Sendra. 2020. 'Evaluation of indoor environment and energy performance of dwellings in heritage buildings. The case of hot summers in historic cities in Mediterranean Europe', *Sustainable Cities and Society*. doi: 10.1016/j.scs.2019.101798.

CEN . 2019. "EN 16798-1:2019 - ' Energy performance of buildings. Ventilation for buildings - Indoor environmental input parameters for design and assessment of energy performance of buildings addressing indoor air quality, thermal environment, lighting and acoustics. '".

oelho, Guilherme B. A., Hugo Entradas Silva, and Fernando M. A. Henriques. 2019. ' Development of a three-dimensional hygrothermal model of a historic building in WUFI ® Plus vs EnergyPlus', *MATEC Web of Conferences*. doi:10.1051/matecconf/201928202079.

Coelho, Guilherme B.A., Hugo Entradas Silva, and Fernando M.A. Henriques. 2020. 'Impact of climate change in cultural heritage: from energy consumption to artefacts' conservation and building rehabilitation', *Energy and Buildings*. doi: 10.1016/j.enbuild.2020.110250.

Curado, António, and V. P. Freitas. 2019. 'Influence of thermal insulation of facades on the performance of retrofitted social housing buildings in Southern European countries', *Sustainable Cities and Society*, 48. doi: 10.1016/j.scs.2019.101534.

Ferreira, Claudia, V. P. Freitas, and Delgado, J. M. P. Q. 2019. 'The Influence of Hygroscopic Materials on the Fluctuation of Relative Humidity in Museums Located in Historical Buildings', *Studies in Conservation*. doi: 10.1080/00393630.2019.1638666.

Ferreira, Claudia S. F. M. 2015. *Inércia higroscópica em museus instalados em edifícios antigos - Utilização de técnicas passivas no controlo da humidade relativa interior*. PhD Thesis, FEUP: Porto, Portugal. In Potuguese.

Genova, Enrico, Giovanni Fatta, and Calogero Vinci. 2017. 'The Recurrent Characteristics of Historic Buildings as a Support to Improve their Energy Performances: The Case Study of Palermo', in *Energy Procedia*. doi: 10.1016/j.egypro.2017.03.207.

Havinga, Lisanne, and Henk Schellen. 2019. 'The impact of convective vapour transport on the hygrothermal risk of the internal insulation of post-war lightweight prefab housing', *Energy and Buildings*, 204. doi: 10.1016/j.enbuild.2019.109418.

Hens, Hugo. 2012. *Building Physics: Heat, Air and Moisture*. *Building Physics: Heat, Air and Moisture*. KG: Berlin, Germany. ISBN:9783433030271. doi:10.1002/9783433602379.

Hensen, J. L. M. . 1990. 'Literature review on thermal comfort in transient conditions', *Building and Environment*, 25. 4 . doi: 10.1016/0360-1323. 90. 90004-B.

Holm, Andreas, Jan Radon, Hartwig Künzel, and Klaus Sedlbauer. 2004. 'Description of the IBP holistic hygrothermal model', *IEA ANNEX*, 41.

Holm, Andreas, Hartwig M Kuenzel, and Klaus Sedlbauer. 2003. 'The hygrothermal behaviour of rooms: combining thermal building simulation and hygrothermal envelope calculation', *Eighth International IBPSA Conference*, Eindhoven, Netherlands. 11 – 14 August 2003.

Huerto-Cardenas, H. E., F. Leonforte, N. Aste, C. Del Pero, G. Evola, V. Costanzo, and E. Lucchi. 2020. 'Validation of dynamic hygrothermal simulation models for historical buildings: State of the art, research challenges and recommendations', *Building and Environment*. doi: 10.1016/j.buildenv.2020.107081.

IBP - Fraunhofer Institute for Building Physics. 2018. "WUFI, Product Overview." Accessed March 29, 2021. https://wufi.de/en/software/product-overview/.

IBP - Fraunhofer Institute for Building Physics. 2010. 'Fundamentals of WUFI®plus - Presentation of the seminar: Simultaneous Calculation of Transient Hygrothermal Conditions of Indoor Spaces and Building Envelopes.' Documentation from IBP seminar, IBP: Germany.

Kilian, Ralf, Andreas Holm, and Jan Radon. 2008. 'The King's House on the Schachen – Indoor

Climate Analysis of a Cultural Heritage Building', in *8th Symposium on Building Physics in the Nordic Countries*. Copenhagen, Denmark .June 16-18, 2008.

Kompatscher, K., R. P. Kramer, B. Ankersmit, and H. L. Schellen. 2019. 'Intermittent conditioning of library archives: Microclimate analysis and energy impact', *Building and Environment*. doi: 10.1016/j.buildenv.2018.10.013.

Kompatscher, Karin, Bart Ankersmit, Edgar Neuhaus, Marcel A.P. van Aarle, Jos W.M. van Schijndel, and Henk L. Schellen. 2020. 'Experimental and Numerical Analysis of a Novel Display Case Design: Case Study of the Renovated Anne Frank House', *Studies in Conservation*, 65. 5. . doi: 10.1080/00393630.2019.1703401.

Kompatscher, Karin, Rick P. Kramer, Bart Ankersmit, and Henk L. Schellen. 2021. 'Indoor airflow distribution in repository design: Experimental and numerical microclimate analysis of an archive', *Buildings*, 11. 4. . doi: 10.3390/buildings11040152.

Kramer, Rick, Jos van Schijndel, and Henk Schellen. 2017. 'Dynamic setpoint control for museum indoor climate conditioning integrating collection and comfort requirements: Development and energy impact for Europe', *Building and Environment*. doi: 10.1016/j.buildenv.2017.03.028.

Kupczak, Arkadiusz, Agnieszka Sadłowska-Sałęga, Leszek Krzemień, Joanna Sobczyk, Jan Radoń, and Roman Kozłowski. 2018. 'Impact of paper and wooden collections on humidity stability and energy consumption in museums and libraries', *Energy and Buildings*. doi: 10.1016/j.enbuild.2017.10.005.

Magalhães, S. A., and V. P. Freitas. 2017. 'A complementary approach for energy efficiency and comfort evaluation of renovated dwellings in Southern Europe', in *Energy Procedia*. doi: 10.1016/j.egypro.2017.09.717.

Magalhães, S. A., and V. P. Freitas. 2020. *Comparação do índice de desconforto passivo com a classe energética de edifícios de habitação reabilitados do sul da europa*. FEUP.

Magalhães, S. A., V. P. Freitas, and J. L. Alexandre. 2018. 'Energy Certification Label vs. Passive Discomfort Index for existing dwellings', in *IOP Conference Series: Materials Science and Engineering*. doi: 10.1088/1757-899X/415/1/012021.

Oberkampf, William L, and Christopher J Roy. 2010. *Verification and validation in scientific computing*. Cambridge University Press. ISBN 978-0-521-11360-1.

Posani, Magda, M.R. Veiga, V. P. Freitas, K. Kompatscher, and H. Schellen. 'Dynamic Hygrothermal Models for Monumental, Historic Buildings with HVAC Systems: Complexity shown through a case study', in *E3S Web of Conferences*. EDP Sciences, 172, 15007.

https://doi.org/10.1051/e3sconf/202017215007

Radoń, J., P. Sadłowska-Sałęga, K. Wąs, A. Gryc, and A. Kupczak. 2018. 'Energy use optimization in the building of National Library', in *IOP Conference Series: Materials Science and Engineering*. doi: 10.1088/1757-899X/415/1/012029.

Rajčić, Vlatka, Ana Skender, and Domagoj Damjanović. 2018. 'An innovative methodology of assessing the climate change impact on cultural heritage', *International Journal of Architectural Heritage*. Taylor & Francis, 12. 1, pp. doi: 21–35. 10.1080/15583058.2017.1354094

Sadłowska-Sałęga, A., J. Radoń, J. Sobczyk, and K. Wąs. 2018. 'Influence of microclimate control scenarios on energy consumption in the Gallery of the 19th-Century Polish Art in the Sukiennice . the former Cloth Hall. of the National Museum in Krakow', in *IOP Conference Series: Materials Science and Engineering*. doi: 10.1088/1757-899X/415/1/012026.

Sadłowska-Sałęga, Agnieszka, and Jan Radoń. 2020. 'Feasibility and limitation of calculative determination of hygrothermal conditions in historical buildings: Case study of st. Martin church in Wiśniowa', *Building and Environment*. doi: 10.1016/j.buildenv.2020.107361.

Schellen, H.. 2002. *Heating monumental churches: indoor climate and preservation of cultural heritage*. PhD Thesis. Tue: Eindhoven, Netherlands.

Sicurella, Fabio, Gianpiero Evola, and Etienne Wurtz. 2012. 'A statistical approach for the evaluation of thermal and visual comfort in free-running buildings', *Energy and Buildings*. doi: 10.1016/j.enbuild.2011.12.013.

Silva, Hugo Entradas, and Fernando M.A. Henriques. 2021. 'The impact of tourism on the conservation and IAQ of cultural heritage: The case of the Monastery of Jerónimos . Portugal. ', *Building and Environment*. doi: 10.1016/j.buildenv.2020.107536.

7

CONCLUSIONS AND FUTURE WORKS

This research thesis provided a detailed description of the steps followed for investigating the topic of "Thermal insulation solutions for historic buildings: Feasibility, Efficacy, Compatibility".

The focus of the research was put on thermal insulation for massive historic walls, since this type of intervention appeared to be an open question in the literature. The topic was investigated for the context of southern Europe, considering temperate climates with mild winters and warm or hot summers, such as those of Porto, Lisbon and Bologna. The type of buildings considered is public libraries i.e., buildings with public use and temporary occupation. All buildings considered adopt heating systems during winter, and the results hereby presented are not extendable to unheated buildings, where moisture-related risks in walls might become much more relevant.

The question addressed in the research were the following:

- Is it feasible to adopt thermal insulation on historic walls? When is it reasonable to do so? Are there solutions that appear suitable for the scope, on the market?
- Do feasible insulation solutions appear compatible with historic walls? Is it possible to define some recommendations for choosing solutions that are compatible with historic walls, in the context considered?
- Are feasible solutions effective for reducing thermal discomfort and energy demands, when massive historic walls and temperate climates are taken into account? Is one side of the application (exterior/interior) preferable to the other?

Thus, this work aims to define if it is possible to identify feasible, compatible and effective thermal insulation solutions for retrofitting building components belonging to the cluster of "thick, massive walls of historic buildings having intermittent occupancy, heating systems, and located in areas with temperate climates with warm or hot summers".

In this chapter, the work performed in the doctoral research is summed up. First, a brief synthesis of the chapters previously presented is provided. Then, based on the results obtained in the research, some remarks and recommendations are hereby outlined. Finally, the main conclusions of this doctoral investigation are presented and some suggestions for future works are offered.

7.1. SYNTHESIS OF SINGLE CHAPTERS

In this paragraph, a brief synthesis of the work presented in the single chapters of the thesis is provided.

The **first chapter** introduced the significance of improving energy efficiency and thermal comfort in historic buildings. Additionally, in this chapter thermal insulation for historic walls was identified as an interesting research topic, due to its complex feasibility and the open questions on its efficacy and compatibility. Public libraries were selected for the investigation since they represent a type of building where conditioning systems may be intensively applied and where guaranteeing thermal comfort appears important. Furthermore, they appear representative of public buildings such as communal offices and public offices in general, and also of private buildings having a moderate number of users, whose main activity is sedentary and occupation patterns are temporary, such as banks and private offices. In this chapter the research gap was addressed and the goals of the research were defined.

The literature review was presented in the **second chapter**. It allowed defining the types of insulation solutions existing in literature, as well as thermal insulation materials commonly adopted. Results showed that thermal mortars, mineral wool and EPS are thermal insulation materials widely considered for post-insulating historic walls, both on the interior and exterior sides of walls. The feasibility of post-insulating historic walls was then discussed, considering the international charters on conservation and restoration of cultural heritage and the principles thereby outlined. The same references were used to discuss the different impacts of internal and external insulation on the significance of historic buildings. Then, feasibility was considered from the constructional point of view. This last analysis allowed to identify thermal mortars as a very feasible solution for interventions on historic walls, as opposed to insulation materials offered in boards and blankets. For this reason, thermal mortars were chosen to be the focus of the research.

The literature review on efficacy showed that the thermal performance of thermal insulation is usually evaluated at the material, component or building level. For insulation materials, the main parameter considered is thermal conductivity, and the lower the better. From this point of view, some thermal mortars appear to have competitive thermal performance to more common insulation materials, such as those adopted for ETICS (External Thermal Insulation Composite System). Indeed, modern thermal

mortars can offer thermal conductivity lower than 0.065 W/(m.K). Thermal mortars containing advanced materials such as aerogel can have thermal conductivity even lower than 0.026 W/(m.K). Nonetheless, thermal mortars can have also higher thermal conductivity, namely up to 0.2 W/(m.K), thus their efficacy depends on the specific composition taken into account. At the component level, the U-value under static conditions can be considered, which can give a rough indication of the reduction of energy losses obtainable in the wall during the cold season, thanks to the use of thermal insulation. Nonetheless, it does not take into account the effect of thermal mass of massive walls, and it does not account for the effect of moisture accumulation on thermal performance, which can become very relevant in porous walls exposed to wind-driven rain. These parameters can be accounted for in mono-dimensional dynamic hygrothermal simulations, which can provide for a more accurate representation of the reduction of winter heat losses. Finally, the efficacy of insulation can be evaluated at the whole-building level. In this case, the tools adopted are whole-building dynamic hygrothermal simulations, which can be applied to the entire building or part of it (e.g. one room). These simulations allow accounting for not only the effect of thermal mass of walls and moisture content in the components, but also for the effect of thermal inertia during summer. These tools allow evaluating the impact of insulation on thermal comfort and energy demands, under realistic operational conditions. In addition, the literature indicates that interior insulation can lead to higher overheating discomfort and higher cooling demands than exterior insulation, due to its stronger detrimental effect on thermal inertia. On the contrary, it can lead to higher thermal comfort in the cold season and stronger reductions of heating demands in intermittently conditioned buildings, due to the effect of de-coupling the thermal mass of indoor air from that of walls. Thus, it is not possible to define if internal or external insulation is more effective, since they both give benefits and drawbacks. Based on the outcomes of this chapter, whole-building simulations were chosen for studying the impact of insulation on thermal comfort and energy demands of buildings. In addition, the information obtained led to choose case studies located in temperate climates with warm/hot summers and equipped with heating systems. The first choice is related to the need to investigate the effect of insulation on overheating risks, the second is for evaluating the actual potential of insulation for reducing energy demands.

In terms of compatibility, the literature showed that the main hazards involved in thermal retrofits are moisture-related, thus the main concern emerged to be physical compatibility, from the hygric point of view. In addition, it emerged that moisture-related degradation risks can be assessed with mono-dimensional dynamic hygrothermal simulations. Thus, this type of simulation was chosen to perform the compatibility assessment in this research. Capillary water absorption and water vapour permeability emerged as the main parameters to be considered, since they rule the processes of wetting and drying. A classification was proposed, to rank the capillary water absorption and vapour permeability of thermal insulation materials, based on the comparison with traditional materials typically adopted in historic

envelops. This ranking is considered to give an indication of the potential effect of the material when applied on a historic wall. Three types of hygric behaviour were observed for insulation materials: vapour permeable and capillary active ones (e.g. cellulose and hydrophilic mineral wool), vapour permeable materials with low/moderately low capillary water absorption (e.g. most natural fibres and hydrophobic mineral wool), and materials having low/moderately low values for both capillary absorption and vapour permeability (e.g. petrochemical materials and Vacuum Insulation Panels). On the contrary, thermal mortars appeared to be able to offer different hygric behaviours depending on their formulations. The literature indicates that no common methodology exists for recommending compatible insulation solutions, being it dependent to the specific context taken into consideration. Nonetheless, it also seemed conceivable to define solutions that appear compatible for a specific intervention (interior or exterior insulation) in defined clusters of situations. For this reason, the Ph.D. research was chosen to address the specific cluster of "thick walls of historic buildings with temporary occupation, located in areas with temperate climates with warm or hot summers and mild winters, where heating systems are adopted".

In the **third chapter**, the case studies selected for investigation were presented and the monitoring campaign performed on their indoor hygrothermal conditions was presented, as well as some additional measurements such as the superficial temperature of walls and vertical thermal stratification in one case study. The three case studies were selected to belong to the cluster previously defined. They are historic buildings converted to the use of public libraries, and they are located in Porto, Lisbon and Bologna. Some background information concerning the history of the buildings were presented in this chapter, as well as the main technical characteristics needed for numerical simulations, such as the geometry, materials and hygrothermal data measured on-site. The Outdoor climatic data obtained from meteorological stations were also presented, since they constitute fundamental information for numerical simulations too. The climate of Lisbon emerged to have the mildest winter temperatures, while Porto has the most moderate summer temperatures among the climates considered. Bologna appeared to offer the most extreme conditions, being colder than Portuguese climates in winter, and hotter in summer. Based on the data obtained in the indoor monitoring campaign, the use of heating was observed in almost all rooms considered, and also summer conditioning was detected in several spaces. In all cases conditioning was intermittent, and also heating was so for at least part of the heating period. Despite the use of heating and cooling systems, all monitored rooms appear to offer uncomfortable indoor air temperatures for a relevant part of the year. Thus, the buildings considered appeared suitable for studying potential solutions for improving thermal comfort and reducing energy demands.

In **chapter four**, the hygrothermal characterization of some insulation solutions based on thermal mortars was presented. Three thermal mortars were chosen from those available on the market. They were selected for providing low capillary water absorption and high vapour permeability, according to the ranking presented in chapter two. The thermal mortars considered contained cork or expanded polystyrene aggregates, and they have declared thermal conductivities in the range 0.045-0.080 W/(m.K). Five systems based on these insulation materials were considered. Their composition was defined according to the instructions of the manufacturers. Two systems were designed for exterior applications, two for interior ones, and the last one for both applications. The results obtained in the experimental campaign considered samples of single and painted materials, according to the European standard for thermal mortars EN 998-1:2017. Also layered samples of combined materials and complete systems, as indicated in the EOTA European Guidelines for External thermal insulation composite systems (ETICS) with renderings (EAD 040083-00-0404:2020). The outcomes of the study were used to define a complete database of hygrothermal properties to be used as input in the numerical simulations. In addition, the results were used to compare the properties observed with the samples aligned with EN 998-1 and EOTA guidelines. Results show a strong dependency of the thermal conductivity of thermal mortars on water content, $\lambda(w)$. Layered samples of thermal mortars were found to have relevantly lower water absorption coefficient than standard samples of single materials, which seemed the effect of the application by layers and of the interfacial phenomena. In addition, it emerged that paints may have very different effect on the vapour permeability of samples when applied on specimens of singular materials or layered ones. For this reason, the necessity of testing not only single materials but also complete systems emerged. In addition, it was recommended to add some specific hygric properties obtained from layered samples of complete insulation systems based on thermal mortars, in their technical sheets. Namely, the resistance to water vapour for all systems, and also the capillary water absorption for external insulation solutions.

The **fifth chapter** presented a comparative study on the moisture-related risks and winter heat losses in three massive masonry walls retrofitted with thermal insulation, considering two orientations of walls. More in detail, the walls of the three case studies were analysed. Hygrothermal simulations were qualitatively validated by comparing the simulated superficial temperatures of the walls with the data measured on-site. Then simulations were run considering the thermal mortar-based insulation systems characterized in chapter four, and more common insulation, namely based on hydrophobic mineral wool and expanded polystyrene. Insulation was alternatively adopted on the interior or exterior surface of the walls. Then a small sensitivity study was performed to evaluate the impact of capillary absorption coefficient and vapour permeability of thermal mortar on the performance of the entire insulation system. Three moisture-related risks were considered: increase of moisture content in the wall substrate,

reduction of drying and condensation between internal insulation and the wall. Results showed that some thermal insulation solutions are riskier than others, depending on their hygric properties and the side of the intervention. Specifically, it emerged the importance of the hygric properties of complete insulation systems, for external application. Solutions complying with the limitations defined in the German standard for stuccos and coatings seemed to perform better than the others. Thus, it appeared recommendable to adopt vapour permeable insulation solutions with low absorption coefficients, such as systems based on hydrophobic mineral wool or thermal mortar-based system S5. The adoption of internal insulation appeared riskier than the external one. Vapour permeable solutions that do not rely on a hydrophobic insulation layer appeared recommendable. In particular, thermal mortar-based insulation solutions, with an s_d<0.7m, showed good results. This chapter also allowed observing the importance of simulating the drying of walls from high water content. Indeed, some drawbacks might be overlooked if only typical moisture content and operational conditions are considered. Finally, the analysis of winter heat-losses indicated that a very small thickness of insulation can result in a relevant reduction of winter heat losses, in massive historic walls. Reductions of 40-60% were obtained with systems based on EPS and hydrophobic mineral wool, while a decrease of 20-50% was reached with one of the thermal mortar-based solutions considered (S5). These results point out that thermal mortars with modern formulations can be competitive with more common insulation materials, and they appear promising for adoption in traditional and historic walls with U-values higher than 0.80 W/(m^2.K).

The efficacy of thermal mortars was further investigated in **chapter six**, by means of whole-building numerical simulations. One test reference room was selected in the case study of Porto, because of its monumental dimensions, which are typical of rooms located in historic constructions. The model was calibrated and validated against the hygrothermal data measured on-site. Then simulations were run to evaluate the impact of thermal mortar-based insulation systems, in comparison to more commonly adopted systems, such as those based on hydrophobic mineral wool and expanded polystyrene. Results showed that insulation decreases the intensity of undercooling discomfort and heating demands while increasing overheating and cooling demands. Considering the entire year, it appeared convenient to adopt thermal insulation to reduce energy demands for intermittently conditioned buildings (reductions between 8% and 50%) and decrease the intensity of the annual thermal discomfort under free fluctuation (decreases of 22%-77% and 8%-50% with the adaptive and static model, respectively). Strong parabolic correlations were observed between discomfort intensity and thermal resistance of the internal or external insulation solutions (separately). Similarly, strong parabolic correlations were found between energy demands and U-value of walls, considering interior and exterior insulation separately. These results show that the higher the thermal resistance of the insulation, the better the annual benefits, for insulation solutions having up to 1 (m^2.K/W). In addition, the positive coefficient observed in the

correlations elaborated for annual total discomfort with the adaptive model suggests that the higher the thermal resistance considered, the lower the proportional benefit. Likewise, the correlations observed for annual energy demands for intermittent conditioning showed that the higher the U-value of the wall the higher the proportional benefit obtainable with insulation.

In terms of thermal mortars performance, they were found to reduce energy demands of 20-40% and discomfort index by 20-60%, according to the adaptive model, which appears relevant. Thermal mortar-based system S5 was found to provide competitive performance to mineral wool and expanded polystyrene, providing energy reductions of about 30-40% the former and 30-50% the latters. In terms of discomfort intensity, S5 led to reductions in the order of 40-60% while the other two insulation systems resulted in decreases around 60-80%, according to the adaptive model. These outcomes show not only that thermal mortars can be competitive with more common insulation solutions, but that modern formulations with low thermal conductivity, such as those involving aerogel, might give thermal performance as good as those of hydrophobic mineral wool and expanded polystyrene, or even better.

7.2. FINAL REMARKS AND RECOMMENDATIONS

The literature review and the original work performed via laboratory testing and numerical simulations allow formulating some remarks and recommendations that can be useful for professionals working in academia and industry.

Most outcomes regard the feasibility, compatibility and efficacy of thermal insulation solutions for adoption in the cluster of "thick walls of historic buildings with temporary occupation, located in areas with temperate climates with warm or hot summers and mild winters, where heating systems are adopted". Other outputs concern procedures for testing and certifying thermal mortar-based insulation solutions.

7.2.1. FEASIBILITY OF THE INTERVENTION AND SUITABILITY OF THERMAL MORTARS

Concerning the feasibility of adopting thermal insulation to retrofit historic walls, some overall indications emerged from the literature:

- In existing construction, on-site inspections are generally needed and typically mandatory for heritage buildings, to gain awareness and information on existing components and their state of

conservation. Walls may present high initial moisture levels and various types of damage, which should be critically evaluated and eventually resolved to avoid post-intervention problems. Furthermore, for historic buildings, the first phase of recognition of the significance and specific values of the construction is preferable and typically mandatory for listed buildings. Based on the significance of the construction, its characteristics and the information obtained on-site (if possible), the feasibility of the intervention can be evaluated.

- Intervention is excluded for surfaces holding cultural or tangible values or subjected to integral protection. When these circumstances do not occur, insulation may be installed, especially if the original rendering or plastering is so damaged that it needs to be replaced. It is generally preferable to use internal insulation over external solutions to maintain the exterior appearance of buildings. Nonetheless, external interventions may be feasible if the appearance of the façade is reconstructed to conserve the identity of the building, especially for constructions whose importance is related to the cultural value of "groups of buildings" or landscape and not to the single building. It may also be preferable when valuable features are internal, such as decorative internal plasters.

- Interventions that cause dimensional changes at window and door openings or where original surface details are valuable should be avoided. In all cases, the original proportions and spatial perception of the building and its parts should be preserved by adopting moderate thicknesses of insulation. Thus, solutions providing good thermal performance with a small thickness of insulation appear more viable than other solutions. Furthermore, insulations offering a wide range of available thicknesses appear to be preferable.

- Thermal mortars appear as a very feasible and potentially effective solution for historic walls because of several reasons. Unlike insulation boards and blankets, they do not need any anchoring points or adhesive layers. They offer great flexibility for the thickness, which can be easily adapted to the dimensional restriction that the intervention may require, and it can be adjusted near valuable decorations to leave them clearly visible. They adapt to uneven surfaces and provide gap-filling abilities, consequently allowing for continuous contact between the insulation layer and the substrate, even in the case of irregularities, cracks and other damages which are quite commonly found in historic components. Thermal mortars can be applied by mechanical spraying, noticeably easing the intervention. In addition, they are more able than insulation boards and blankets to offer a similar texture to the original renders and plasters.

In addition, it seems useful to recall that the nomenclature "thermal insulating mortar" or, simplifying, "thermal mortar", indicates a mortar with thermal insulation properties, namely a thermal conductivity

lower than 0.2 W/(m.K) at 10°C, according to standard EN 998-1:2017. Thermal mortars can be applied on the external or internal side of building components, and they may be referred to as thermal renders or thermal plasters, respectively in the former and latter cases. Generally, thermal mortars are designed to be covered with a regularization layer and/or a finishing layer. The composite solutions can be referred to as thermal plastering /rendering systems or as thermal mortar-based systems.

7.2.2. COMPATIBILITY OF THERMAL INSULATION SOLUTIONS WITH HISTORIC WALLS

A challenging aspect of interventions on historic constructions is represented by the compatibility of the new materials with the original components.

The literature review conducted on this topic led to defining the following remarks:

- Traditional constructions are typically porous and capillary-active, and they are typically not equipped with waterproofing layers that are common in modern constructions (e.g., capillary breaks, vapour-proof membranes, vented cavities…). As a consequence, traditional walls generally absorb liquid water (e.g., rain and rising damp), and thanks to their hygric properties they are generally able to buffer it and let it dry out with time. In this context, post-insulation represents a very complex intervention because it can alter the original moisture dynamics of historic walls, leading to trapped moisture. The main hazards introduced by the intervention are moisture-related, thus the main compatibility concern lies in the physical compatibility, from the hygric point of view. Capillary water absorption and water vapour permeability emerged as the main material properties to consider for evaluating physical compatibility.

- It appears that a general criterion for choosing compatible insulation solutions for historic walls does not exist. This lack is likely to be related to the dependency of moisture-related risks on the specific type of intervention (internal or external insulation), component type (masonry wall, wooden structure, ...), geometry (thickness of the element) and boundary conditions (e.g., interior and exterior climates, exposure to wind-driven rain) considered. However, it seems possible to define specific clusters of situations for which, at a preliminary-design stage, some solutions appear more compatible than others. For this reason, this study focused on the cluster of "thick, massive walls of historic buildings having intermittent occupancy, heating systems, and located in areas with temperate climates with warm or hot summers".

In addition, the original work performed through dynamic hygrothermal simulations at the wall level allowed to observe the effect of various insulation solutions on the moisture dynamics of different walls. The study showed that the outcomes of the intervention depend on the hygric properties of the thermal insulation solution adopted, and it led to formulating the following remarks and recommendations:

- When both external and internal insulation are suitable for the intervention, the former one is preferable. The adoption of interior insulation does not lead to any benefit in terms of moisture content in the walls. Indeed, it does not reduce the intake of water in the wall and, what is more, it reduces the wall temperature during the heating period, resulting in a reduction of drying. On the contrary, the adoption of external insulation offers one relevant benefit. It can reduce the rainwater intake of the wall if the system adopted has lower capillary absorption than the original render, thus having a very beneficial effect on the moisture content of walls.

- Thermal insulation systems with an s_d higher than 2m, should be avoided for both interventions, especially when they rely on a hydrophobic insulation layer, such as expanded polystyrene. In fact, these systems can have detrimental effects on the drying ability of walls, which can result in increased rising damp and trapped moisture in some parts of walls, e.g. those that experience high moisture content.

- When analysing the impact of insulation on moisture dynamics of historic walls it seems important to simulate the drying of walls from high water content. This scenario aims at reproducing the effect of insulation on those areas of the walls that might experience high moisture content due to occurrences as damages in the envelop, rising damp, pipe leakages and floods. For these parts of walls, some drawbacks of the intervention might be overlooked if only typical moisture content and operational conditions are considered.

For external insulation systems:

- The impact of external thermal insulation systems on the water content of walls depends on the effect they have on the wetting and drying of the components. The German standard on rain-protective stuccos and coatings emerged as a very good reference for evaluating the impact of relatively-thin thermal insulation systems on historic masonry walls. Based on the restrictions defined in this standard and the numerical work performed in this research, solutions that exceeded the following two limitations should be avoided: $A_w * s_d < 0.2$ kg/(m.h$^{0.5}$) and $s_d < 2$m. Where the parameters A_w and s_d refer to complete thermal insulation systems, and not to singular materials or layers. Thermal insulation solutions exceeding the recommended $A_w * s_d$ might result in moisture accumulation in walls.

- The German standard also sets a limit on the maximum A_w acceptable, namely 0.5 kg/(m^2.h$^{0.5}$). Although no solution with such a high A_w was considered in this study, this restriction seems reasonably recommendable.

- Stricter limitations on the A_w and s_d of complete insulation solutions are defined in the EOTA European Guidelines for External thermal insulation composite systems (ETICS) with renderings (EAD 040083-00-0404:2020). In the numerical work presented in this thesis, the best reduction of moisture-related risks was observed with systems having low A_w and s_d, namely those complying with the aforementioned restrictions. Thus, solutions that comply with the following limitations appear preferable, when possible: namely $A_w < 0.10$ kg/(m^2.h$^{0.5}$) and $s_d < 1$m.

- Overall, the system based on hydrophobic mineral wool (S_MW) emerged as a very good solution for application on the exterior side of walls, thanks to its high vapour permeability and very low water absorption coefficient. Similarly, also thermal mortar S5 appeared suitable for the intervention.

- Systems with an s_d higher than 2m, which rely on a hydrophobic insulation layer (e.g. expanded polystyrene), should be avoided for interventions on historic walls. In fact, they can have detrimental effects on the drying ability of walls.

For interior thermal insulation solutions:

- The s_d of the complete system and the A_w of the insulation layer emerged as important parameters for the compatibility of the intervention. Systems having a low s_d, and an insulation material with relevant A_w appear preferable, especially when they comply with the following recommendation: $s_d < 2$m and $|10\ s_d - Aw\_insulation| < 5$ (with A_w in kg.m^{-2}.h$^{-0.5}$ and s_d in m).
  Internal insulation systems that comply with the aforementioned indications, but have a hydrophobic insulation layer (e.g. hydrophobic mineral wool), can provide for good performance in terms of drying and water content in retrofitted walls. Nonetheless, they can lead to a higher risk of condensation at the critical interface compared to more capillary-active solutions. Interior insulation systems that have a hygroscopic and capillary-active insulation layer, appear preferable.

- Thermal plastering solutions complying with the aforementioned recommendations, while also respecting the following limits, were found to be very recommendable solutions: $s_d < 0.7$m for the complete system and $A_{w\_insulation} > 1$ kg.m^{-2}.h$^{-0.5}$ in the thermal mortar.

7.2.3. EFFICACY OF THERMAL INSULATION SOLUTIONS AND POTENTIAL OF THERMAL MORTARS

The efficacy of thermal insulation can be evaluated at the material, component and building level.

These three levels were investigated in detail in this work, with a focus on thermal mortars since they emerged as very feasible and suitable solutions for applications on historic walls. On one hand, the laboratory characterization on materials concerned only thermal mortar-based insulation systems. On the other, numerical simulations considered thermal mortars in comparison with more common insulation materials such as hydrophobic mineral wool and expanded polystyrene (EPS). The original research performed through experimental and numerical analyses allowed for defining the following remarks concerning the efficacy of thermal mortars:

- In this study, three thermal mortars were considered, and laboratory tests show higher thermal conductivity than declared by manufacturers, for all of them. Nonetheless, all insulation materials complied with the requirement of EN 998-1 for thermal mortars, namely a maximum thermal conductivity of 0.02 $W.m^{-1}.K^{-1}$. Hence, all thermal mortars showed much better thermal conductivity ($\lambda_{10°C,dry}$= 0.130-0.065 $W.m^{-1}.K^{-1}$) than typical renders and plasters based on gypsum, lime and cement (approximative range: 0.4 – 1.0 $W.m^{-1}.K^{-1}$), and they thus appear interesting for substituting original renders and plasters when a complete replastering is needed.
  In addition, the mortar with the lowest thermal conductivity (A3) complies with the threshold value defined in EOTA guidelines for ETICS (0.065 $W.m^{-1}.K^{-1}$). Thus, despite offering moderate thermal performance, this solution appeared to be competitive with more common insulation materials, such as those typically adopted for ETICS.

- The dynamic hygrothermal simulations performed at the wall level showed that the adoption of relatively-thin insulation systems, namely about 4cm thick, can result in interesting reductions of winter heat losses through massive masonry walls, during winter. Reductions in the range 20-70% were observed in walls having original U-values ≥ 0.85 $W.m^{-2}.K^{-1}$. The best thermal performance was obtained with the systems based on insulation materials with the lowest thermal conductivity, as expected. Namely, 40-60% reductions were obtained with expanded polystyrene and hydrophobic mineral wool, and 30-50% with thermal-mortar A3 (system S5). This outcome shows that thermal mortars with modern formulations can offer a very interesting performance and be competitive with more common insulation materials. Additionally, the results obtained suggest that thermal mortars with advanced formulations, which can provide for thermal conductivity as low as 0.04 W/(m.K), would determine a reduction of heat losses as high as mineral wool and expanded polystyrene, or even higher for insulation mortars with lower thermal conductivity.

- Mono-dimensional simulations also showed that for common, non-capillary-active insulation materials (hydrophobic mineral wool and expanded polystyrene), the side of the application does not relevantly impact winter heat losses through the retrofitted walls. In fact, maximum differences in the order of 3% were found when this type of insulation was applied at the interior or exterior side of walls. On the contrary, noticeable differences were observed with thermal mortar-based systems, based on the side of the application of insulation. This is the result of the capillary active nature of the materials and the dependency of their thermal conductivity on moisture content, which can lead to reduced thermal performance when the insulation is applied on the exterior side of walls, if exposed to relevant WDR. Anyway, depending on the hygric properties of the systems, this difference can be more or less moderate.

  Indeed, in terms of winter heat losses reduction, thermal mortar-based system S5 showed very small differences when applied at the internal or external side of walls, namely up to 3%. This outcome is likely to be the consequence of the good hygric properties of the system, (which complies with EOTA maximum values $A_w < 0.10$ kg/(m^2.h$^{0.5}$) and $s_d < 1$m), the low free saturation water content of the thermal mortar, and the moderate dependency of its thermal conductivity on water content. The other two thermal mortars considered, A1 and A2, give higher differences of thermal performance based on the side of the application. In detail, the first one gave differences of up to 8% while the second one resulted in a maximum difference of 18%, but this high magnitude of differences was observed only in the walls located in Porto, where wind-driven rain is very high. On the contrary, when applied on the walls of Bologna, where the annual load of wind-driven rain is more moderate, or in Lisbon, where winter conditions are milder, all thermal mortars give differences of up to 5%.

  These outcomes indicate that thermal mortars can offer very good thermal performances even when adopted on the exterior side of walls, despite the dependency of their thermal conductivity on water content and their capillary-active nature. Unrelevant losses of thermal performance can be expected if the thermal-mortar based insulation solutions are adopted on walls exposed to moderate wind-driven rain or if a suitable coating system is adopted to moderate rainwater intake.

- Simulations at the room level confirmed that even when considering thick massive walls, a relatively-thin layer of insulation can have noticeable effects on thermal comfort and energy demands.

  On one hand, the effect of insulation reduces heating demands and undercooling discomfort, on the other, it increases cooling needs and overheating discomfort. In the scenarios considered, the benefits of thermal insulation overweighted the drawbacks. Annual energy demands for conditioning were found to be reduced by 32%-50% with mineral wool and EPS, and by 18-40%

with thermal mortars. Considering the static and adaptive comfort models, decreases of 60%-80% and 15%-50%, respectively, were found in the annual discomfort indexes when adopting expanded polystyrene and mineral wool. With thermal mortars, the same indexes were found to be reduced by 20-60 % and 10-30%, respectively. Best results were observed in the climate of Porto, probably because of its mild summer temperatures which moderate the disadvantages of adopting insulation. In this climate, energy demands were reduced by 26-50% with the use of thermal insulation, while the intensity of thermal discomfort was decreased by 32-70%, according to the adaptive model.
System S5, which is based on thermal mortar A3 (λ=0.065 $W.m^{-1}.K^{-1}$), provided for lower but comparable performance to systems based on mineral wool and expanded polystyrene. In fact, it led to reductions of energy demands in the range of 28-40% and a decrease of total discomfort indexes of 44-59% (adaptive model), which seem very promising. These outcomes show that thermal mortars with low thermal conductivity are competitive with more common insulation materials and promising for application in historic buildings with massive walls. Furthermore, results suggest that thermal mortars with advanced formulations (e.g., containing aerogel) might offer benefits as high as typical solutions based on EPS and mineral wool, or even higher if thermal conductivities lower than 0.04 $W.m^{-1}.K^{-1}$ are provided.

- As expected, interior insulation showed a stronger detrimental effect than exterior one on thermal inertia, leading to higher cooling demands and overheating discomfort. On the contrary, interior insulation emerged as more effective than exterior one for decreasing heating demands, but not always for decreasing undercooling discomfort intensity. When considering the whole year, the two effects tend to compensate each other in terms of energy demands in intermittently heated buildings, resulting in disregardable differences (lower than 5%). For the intensity of thermal discomfort, differences were found to be more relevant. Results obtained with thermal mortars applied at different sides of the wall were of a maximum of 7%. With mineral wool and expanded polystyrene higher differences were observed, namely up to 15%, and exterior insulation seemed preferable.

- A strong parabolic correlation was found between discomfort index and thermal resistance of insulation, for internal and external solutions. These correlations showed that the higher the resistance the stronger the increase of overheating discomfort, and the decrease of annual undercooling intensity. The parabolic nature of the correlations also suggested that the higher the thermal resistance of the insulation, the smaller the proportional benefit gets, in terms of total discomfort intensity. Similarly, strong parabolic relations were found between the U-value of walls and energy demands. These correlations showed that the stronger the decrease of U-value obtained with the retrofit, the lower the heating needs and the higher the cooling demands. In terms of total

conditioning demands, the parabolic nature of the correlations shows that the benefit of insulation gets proportionally more relevant when lower U- values are obtained.

- Whole building simulations showed that it was convenient to adopt thermal insulation in the test room considered, both when intermittently conditioned and in free fluctuation. Thus, despite having a negative effect during the warm and hot periods, insulation appeared to offer higher benefits than throwbacks. Hence, the outcomes of the simulations performed at the room level show that the effect of adopting insulation on massive walls can be beneficial in terms of total energy demands for conditioning and thermal comfort when the entire year is considered, in spaces with temporary occupancy, and intermittent conditioning or no conditioning at all. This result seems reasonably extendable to a room that is at times intermittently conditioned and at times left under free fluctuation.

  On the contrary, thermal insulation might be counterproductive in buildings equipped with heating systems only. In this case, heating demands are reduced but summer discomfort is increased. Thus, the thermal retrofit could determine very uncomfortable summer conditions. Thus, the intervention might result in the need for additional cooling, provided by passive bioclimatic strategies, or even new cooling devices when passive strategies are not sufficient. based For buildings with prolonged summer closure, e.g. 2-3 weeks in the middle of the hot season, the situation might be different and the overheating problems might be less relevant.

7.2.4. LABORATORY TESTS ON THE HYGROTHERMAL PROPERTIES OF THERMAL-MORTAR BASED SYSTEMS

The experimental campaign performed in this doctoral research to characterize the hygrothermal properties of thermal mortar-based insulation systems considered tests on different types of samples, which were based on two different regulations. The first type of samples consisted of single or painted materials, following the European specifications for mortars for masonry – EN 998-1:2017. The other type was represented by tile samples prepared by layers, thus better representing real applications and complete insulation systems, according to the indications of the EOTA European Guidelines for External thermal insulation composite systems (ETICS) with renderings (EAD 040083-00-0404:2020).

The results obtained led to the following observations and recommendations:

- The use of layered-tile and standard samples can result in very different results, in terms of the resistance of paint to water vapour diffusion. For instance, with silicate-based paint C2, the sd observed with standard samples was 4-times higher than the one obtained with layered tiles, at dry conditions. This outcome is coherent with a previous study that observed that the resistance of paints to vapour diffusion can noticeably depend on the substrate adopted.

- Relevant reductions of capillary water absorption can be observed when tile layered samples of thermal mortars are adopted, instead of standard ones. In this work, differences up to 75% were observed in the A_w of thermal mortars, when adopting different types of samples. Similar differences were also observed in previous studies, which indicate that sample preparation can affect the physical properties of mortars, especially when they are applied on porous supports (for example the previously hardened layer) that can absorb water from the fresh mortar applied. Furthermore, in samples prepared by successive layers, the effect of hygric resistances at the interfaces between layers may further contributed to reducing the capillary water absorption coefficient of the specimens.

- These outcomes show that complete insulation systems may have very different moisture transport properties than expected from the characterization of single materials. Thus, it seems recommendable to add some information concerning the behaviour of complete systems, as whole units, in the technical sheets of thermal mortar-based insulation solutions: namely the s_d for all systems, and also the A_w for those designed for outdoor exposure. As observed in numerical simulations, the properties of complete systems have a relevant impact on the moisture dynamics of walls, and they can be used to evaluate the compatibility of the solutions for the applications on historic components. Thus, this additional information would allow designers to make a more informed choice and to better forecast the outcomes of the intervention, potentially leading to reduced degradation risks and improved durability of the retrofitted components.

Relevant differences were found between the declared and measured properties of lime-cork mortars, especially in terms of thermal conductivity, which ranged from 60% higher to more than twice the declared value. The increase observed was considered to be the result of the following circumstances: the lack of efficacy of the air-entraining admixtures, or the application of mortars by spatula. The last concern led to formulate the following observation and recommendation:

- Thermal mortars are sensitive to manipulation, and it is expected that they provide better performance when applied by mechanical spraying. It is indeed expected that spray application does improve the entrance of air into the fresh mortar, resulting in higher porosity and, consequently,

lower thermal conductivity of the hardened materials. A high amount of entrained air may also reduce the capillary water absorption, as large voids (above capillary range) work as water barriers.

- If strong differences are systematically found between the properties of thermal mortars applied by mechanical spraying and by spatula, it would be useful to provide some correlated indications in the technical sheets of the materials, when they are designed to be applied with both techniques.

7.3. CONCLUSIONS

Retrofitting historic heritage plays a crucial role in sustainable development. Having comfortable, retrofitted buildings that are suitable for being kept in use means reducing the need for new constructions and the CO_2 emissions that building them would entail. Furthermore, heritage buildings represent a non-renewable, irreplaceable resource that we have the duty to deliver to future generations. For this reason, adapting, keeping in use and preserving historic buildings appears to be a key element in the field of sustainability, as already emphasized by the United Nations in the 2030 Agenda for Sustainable Development.

Several solutions are provided in the literature, and, among the others, the use of thermal insulation appears as a very debated intervention whose outcomes are difficult to predict. On one hand, the feasibility of the intervention is limited by the significance and characterising features of the building. On the other, the compatibility of the intervention depends on several factors that depend on the building, the climate and the side of the intervention. As a consequence, a shared criterion for choosing suitable solutions does not exist yet. Additionally, the efficacy of adopting a relatively-thin layer of insulation on massive masonry walls is not known, especially considering that it can have counterproductive effects during hot and warm periods.

The literature review performed in this research allowed observing that it is feasible to adopt thermal insulation on historic walls, depending on the context considered. Hence, some recommendations concerning the viability of the intervention were defined, considering heritage conservation needs and the constructional point of view. In addition, thermal mortars were identified as very suitable solutions, for several reasons e.g., their adaptability to uneven surfaces and gap-filling abilities.

Thermal mortars were investigated through experimental tests and numerical simulation. The outcomes allowed observing the importance of testing not only single materials but also complete insulation systems. Indeed, it was noticed that the layered structure of thermal mortar-based insulation systems can result in reduced water absorption coefficients and higher resistance to vapour permeability than expected, due to interface phenomena and application of materials on porous substrates. Based on these observations, some recommendations were defined concerning testing procedures for the certification

of thermal rendering and plastering systems, as well as concerning the data reported in their technical documentation.

The importance of the hygric properties of complete insulation systems emerged also in the simulations performed at the wall level. Simulations were adopted to evaluate the compatibility of insulation solutions with historic walls. The literature indicates that the main compatibility concern regards the effect of insulation on the original moisture dynamics of historic walls. Thus, compatibility was studied by considering moisture-related degradation risks. Results showed the importance of the resistance to water vapour permeability of complete systems, both for applications on the interior and exterior sides of walls, in terms of s_d. Also, capillary water absorption (A_w) was found to be an important parameter. For internal insulation, the capillary water absorption of the insulation material was found to be very relevant, whereas for external insulation the A_w of complete insulation systems emerged as very significant. Based on the outcomes of the simulations, some recommendations were defined for evaluating the compatibility of insulation solutions at the design stage of intervention projects. The recommendations focused on interventions on the cluster of "thick walls of historic buildings with temporary occupation, located in areas with temperate climates with warm or hot summers and mild winters, where heating systems are adopted".

Efficacy was evaluated at the component and room levels, through dynamic hygrothermal simulations. Results showed that the adoption of a relatively-thin layer of insulation on thick historic walls can have a relevant effect on reducing winter heat losses through the components. Reductions in the range 20-70% were observed in walls having original U-values between 0.85 and 1.75 W/(m^2.K), in the climates of Porto, Lisbon and Bologna. More in detail, Reductions in the range 40-60% were obtained with expanded polystyrene and hydrophobic mineral wool, and between 30% and 50% with one thermal-mortar based insulation system (S5). This outcome shows that thermal mortars with modern formulations can offer very interesting performance and be competitive with more common insulation materials. Additionally, the outcomes of the study suggest that thermal mortars with advanced formulations, which can provide for thermal conductivity as low as 0.04 W/(m.K), could determine a reduction of heat losses as high as mineral wool and expanded polystyrene, or even higher if lower thermal conductivity is provided.

Furthermore, results obtained in terms of total annual energy demands and thermal comfort in one reference room, showed that the adoption of insulation can be relevantly beneficial when walls with high U-values, such as 1.75 W/(m^2.K), are considered. In the climates of Porto, Lisbon and Bologna, the benefits of thermal insulation appeared to overweight the drawbacks. Annual energy demands for conditioning were found to be reduced by 32%-50% with mineral wool and expanded polystyrene, and by 30-40% with one thermal mortar-based system (S5). Similarly, the total discomfort intensity resulted

to be reduced by 70-80% with the first two solutions, and 50-60% with the thermal mortar, considering the adaptive model, and of respectively 15-50% and 15-35%, accounting for the static model. These outcomes show that thermal mortars with low thermal conductivity are competitive with more common insulation materials and they can be very effective for application in the cluster considered, for spaces having intermittent conditioning or no conditioning at all. Furthermore, results suggest that thermal mortars with advanced formulations (e.g. containing aerogel) might offer benefits as high as typical solutions based on EPS and mineral wool, or even higher if thermal conductivities lower than 0.04 W/(m.K) are provided.

Finally, internal insulation appeared to have a worse effect than exterior one during warm and hot periods, in terms of both cooling demands and thermal comfort. On the contrary, internal insulation appeared more effective than exterior one during the heating season, for the heating demands, but not always for decreasing undercooling discomfort. In terms of energy demands in the intermittently heated scenario, the pro and cons of the different sides of the intervention appear to balance each other, resulting in disregardable differences, namely up to 5%. For discomfort intensity, differences appeared more relevant, up to 15%, and external insulation emerged as preferable for buildings in free fluctuation.

7.4. FUTURE WORKS

Some concerns, which are not addressed in this research are anyway recognized to be very important to fully understand the potential and hazards related to insulation solutions for historic walls. Those issues should be addressed in future research, i.e. sustainability of the insulation solutions adopted, adhesion to the substrate, fire safety, economic payback of the interventions, their reversibility and their effects on the response of buildings to future climate changes.

The simulations performed in this work consider the plane behaviour of perfect walls, while room corners, cracks in walls, window recesses, and other thermal bridges areas, where the temperature can get very low during the cold season, are disregarded. Thus, the recommendations and outcomes defined in this work would benefit from further validation through analyses that account for thermal bridges.

Compatibility assessment considered three types of moisture-related degradation risks. Future studies regarding the effect of the recommended insulation solutions on risks like degradation of embedded wooden beam ends, and mould growth on the internal and the external surface of walls would provide useful information to complement this work. For the latter evaluation, simulations which account for detailed counter radiation data would be suitable, to correctly estimate night-time overcooling.

The behaviour of retrofitted walls depends on several parameters which strongly influence moisture related risks. Some parameters that are not studied in detail in this work are the thickness of walls (here assumed as massive 60-90cm) and their substrate material (here fixed as granite, limestone and bricks). It would be interesting to have future sensitive analyses that account for the influence of these two parameters on moisture-related risks. Considering a wider number of case studies would also serve the purpose of further verifying the applicability of the recommendations of this study for the cluster of "thick, massive walls of historic buildings having intermittent occupancy, heating systems, and located in areas with temperate climates with warm or hot summers".

Similarly, future sensitive analysis could evaluate the effect of insulation on thermal comfort and energy demands, when different rooms are considered. For instance, the effect of parameters as the orientation of the room, different thickness of walls, different location of the room in the building, different geometries, different thickness of insulation materials, various strategies of ventilation and heating patterns could be studied in detail.

This study disregards the existence of hygric resistances between successive layers of the insulation systems and between systems and walls, which is a very common assumption in numerical hygrothermal simulations. These resistances may have relevant effects on rainwater intake and on the drying of walls, thus future more detailed studies could evaluate if the presence of hygric resistances does noticeably alter the moisture-related risks observed in this study. An experimental campaign of the hygric properties of thermal mortars applied on different substrates also seems to offer a very interesting potential for evaluating how the application of thermal mortars on porous walls does affect their properties, in comparison to those observed on tests on standard samples prepared in metallic moulds.

ANNEXES

ANNEX I
Evaluation of T-RH sensors Performances

I.1 HOBO DATALOGGERS

A 24 hours cycle was set in the Climate chamber of LFC at FEUP, which was characterized by 4 steady states, with Temperature ranging from 35 °C to 10°C and Relative Humidity from 50 % up to 80 %, as reported in the graphic at the top of Figure I.1.

The results obtained with HOBO dataloggers, with a sampling interval of 10minuts, are shown in the second graphic of Figure I.1.

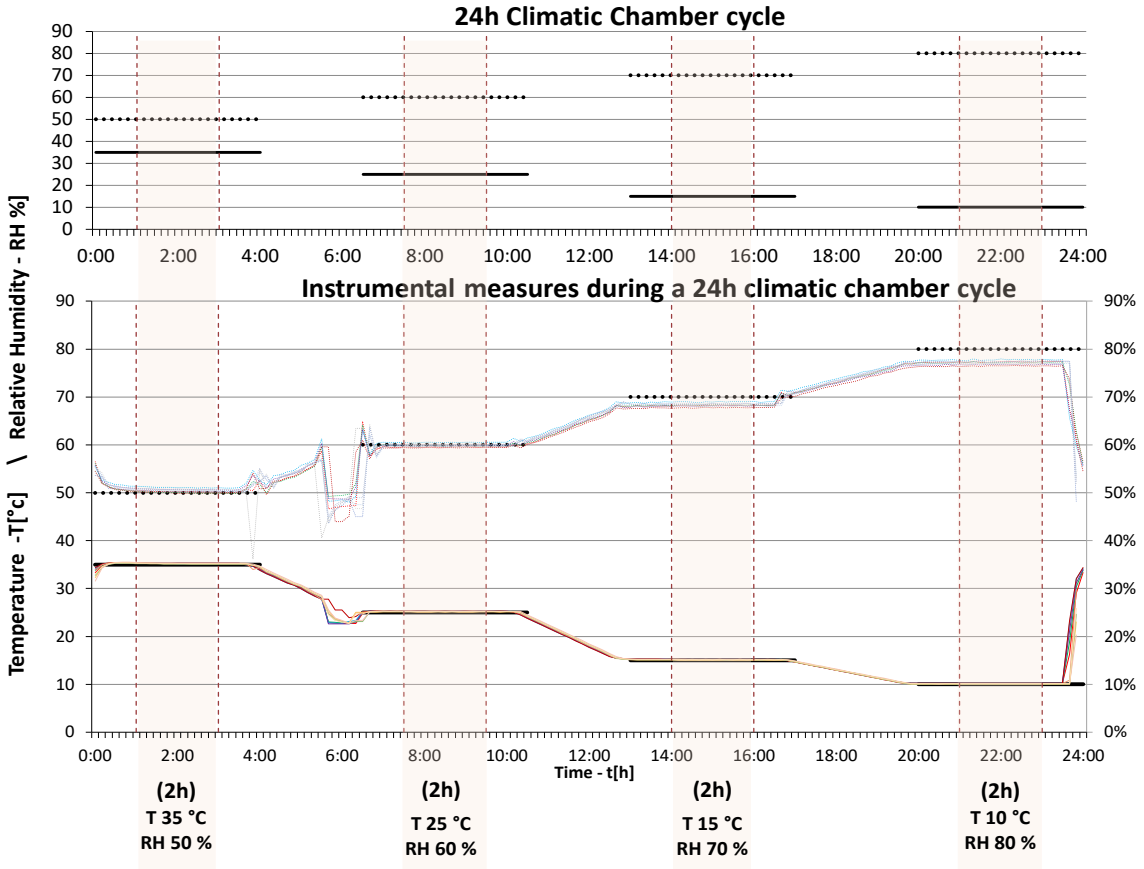

Figure I.1– From top to bottom: the cycle defined in the climatic chamber and the data measured with HOBO dataloggers.

The climate chamber was programmed to maintain stable conditions of Temperature and Relative Humidity for steps of 4 hours. In order to avoid the unstable states, it was safely decided to consider the two hours in the middle of each interval only, for evaluating the difference between the data measured with HOBO dataloggers and the T, RH set in the climatic chamber. The synthetic outcome of this comparison (maximum relative and absolute errors) are illustrated in Table I.1.

The maximum absolute errors obtained are 0.43 °C for Temperature and 3.62% for Relative humidity, which appear acceptable (less than 0.5°C and 5%, Mesas-Carrascosa *et al.*, 2016).

Table I.1 – Difference between measured data and the climatic chamber programmed Temperature/Relative Humidity. In red are reported the maximum relative and absolute errors.

T	**RH**	**T**	**RH**	**T**	**RH**	**T**	**RH**
35	**50%**	**25**	**60%**	**15**	**70%**	**10**	**80%**
T - % error	**R H - % error**	**T - % error**	**RH - % error**	**T - % error**	**RH - % error**	**T - % error**	**RH - % error**
1.23%	2.68%	1.23%	1.13%	1.65%	3.36%	2.47%	4.53%
T - abs. error	**RH - abs.error**	**T - abs. error**	**RH - abs.error**	**T - abs. error**	**RH - abs.error**	**T - abs. error**	**RH - abs.error**
0.43 °C	1.34%	0.31 °C	0.68%	0.25 °C	2.35%	0.25 °C	3.62%

I.2 ELTEK SENSORS

Eltek sensors for air T, RH and superficial temperature were left in a closed wooden container for 24 hours, the results obtained are shown in Figure I.2. Several devices were adopted in the monitoring campaign, but only the results obtained from 4 sensors for air temperature and relative humidity, and 4 sensors for superficial temperature were used in the research, and thus presented in the thesis.

The maximum difference found between Eltek and HOBO equipment results were about 1.1 °C and 8% RH, which was considered acceptable for the scope of the research.

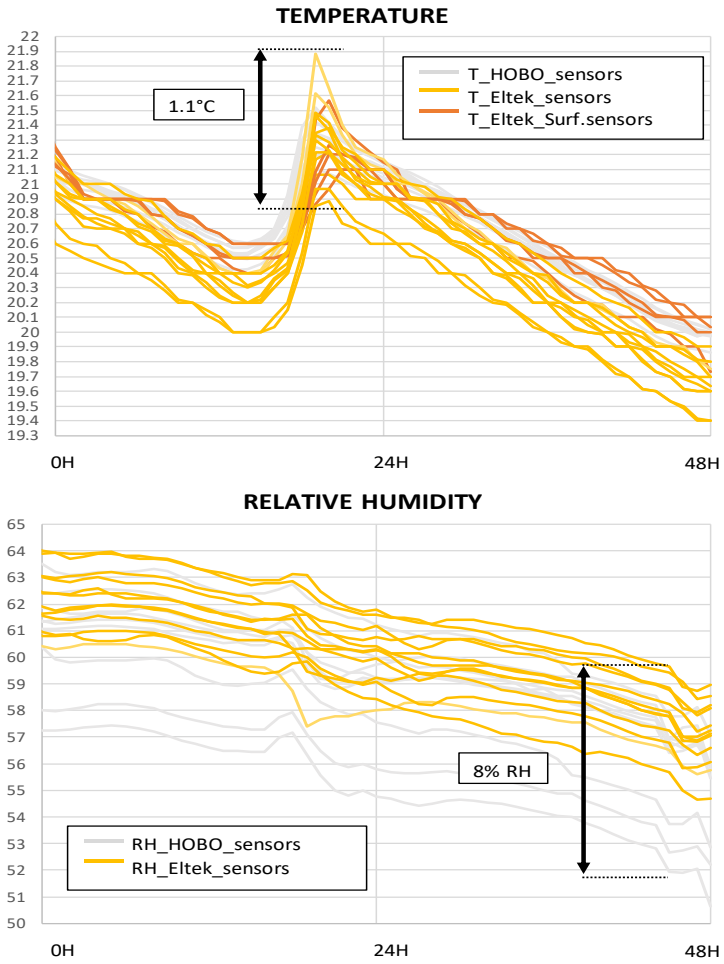

Figure I.2 –Results obtained in 48h of monitoring when all HOBO and Eltek sensors were left together in a closed container.

I.3 References

Mesas-Carrascosa, F. J., Verdú Santano, D., Meroño de Larriva, J. E., Ortíz Cordero, R., Hidalgo Fernández, R. E., & García-Ferrer, A. 2016. "Monitoring heritage buildings with open source hardware sensors: A case study of the mosque-cathedral of Córdoba." *Sensors* 16.10: 1620.

ANNEX II

II.1. WUFI PRO - BASICS OF THE NUMERICAL MODEL

The software relies on Künzel's (1995) differential equations for the simultaneous transport of heat and moisture (1,2). In WUFI Pro these equations are discretised by means of an implicit finite volume method and iteratively solved (Martin and Klaus, 2009).

$$\frac{\partial H}{\partial \theta}\frac{\partial \theta}{\partial t} = \frac{\partial}{\partial x}\left(\lambda \frac{\partial \theta}{\partial x}\right) + h_v \frac{\partial}{\partial x}\left(\frac{\delta_a}{\mu}\frac{\partial}{\partial x}(\varphi\, p_{sat})\right) \qquad (1)$$

Heat transport equation

$$\left(\rho_w \frac{\partial u}{\partial \varphi}\right)\frac{\partial \varphi}{\partial t} = \frac{\partial}{\partial x}\left(\rho_w D_w \frac{\partial u}{\partial \varphi}\frac{\partial \varphi}{\partial x}\right) + \frac{\partial}{\partial x}\left(\frac{\delta_a}{\mu}\frac{\partial}{\partial x}(\varphi\, p_{sat})\right) \qquad (2)$$

Moisture transport equation

In the equations:

- H is the enthalpy of the moist material, H = (ρ_m c_m+ u ρ_w c_w) θ , where ρ_m and c_m are the bulk density [kg/m^3] and specific heat capacity [J/(kg K)] of the dry material, u is the volumetric water content in the moist material [m^3/m^3], ρ_w and c_w are the bulk density [kg/m^3] and the specific heat capacity [J/(kg K)] of water
- θ and φ are the temperature [ºC] and the relative humidity [-]
- t and x are the temporal [s] and spatial (position in the component cross section) [m] variables
- λ is the thermal conductivity of the moist material [W/(m ºC)]
- h_v is the evaporation enthalpy of water [J/kg]
- δ_a is the vapour permeability of still air [kg/(m s Pa)] and μ is the vapour resistance factor of the material [-]
- p_{sat} is the water vapour saturation pressure [Pa]
- Dw is the liquid conduction coefficient [m^2/s].

The left-hand sides of the equations consist of the storage terms and on the right-hand side, the transport terms are introduced. Temperature and Relative humidity are adopted as driving potentials of heat and moisture transport.

Heat storage comprises the heat capacity of the dry material (ρ_m c_m) and the heat capacity of the moisture that it contains (u ρ_w c_w). Heat transport is the sum of thermal conduction through the moist material (λ(u). $\partial\theta/\partial$x) and vapour enthalpy flow ($h_v \frac{\partial}{\partial x}\left(\frac{\delta_a}{\boldsymbol{\mu}}\frac{\partial}{\partial x}(\varphi\, p_{sat})\right)$).

Moisture storage is described by the derivative of the moisture storage function. Moisture transport accounts for liquid transport through surface diffusion and capillary conduction ($\rho_w D_w \frac{\partial u}{\partial \varphi}\frac{\partial \varphi}{\partial x}$), and for water vapour diffusion ($\frac{\delta_a}{\mu}\frac{\partial}{\partial x}(\varphi\, p_{sat})$).

For heat and moisture exchange through the external surface of the walls, two factors are very important: solar radiation and wind-driven rain.

At the external surface of the walls, WUFI Pro accounts for the heat absorbed by the component surface exposed to solar short-wave radiation as (Manfred and Schmidt, 2008):

$$I = a\, I_s \quad (3)$$

where I is the short wave radiation [W/m^2] at the component surface, obtained as the normal component of the short wave radiation incident on the surface, I_s [W/m^2] (that accounts for direct, diffuse and reflected-by-the-ground solar radiation), multiplied by the short-wave absorption coefficient of the component's surface, a [-]. In this study, all systems adopted at the exterior side of the wall, as well as current finishings, are characterized by a bright colour. For this reason, all external surfaces are assigned with a short-wave absorption coefficient of 0.4.

For wind-driven rain (WDR) calculations, WUFI Pro adopts the formula:

$$R_{wdr} = R_h (R_1 + R_2 V \cos \psi) \quad (4)$$

where R_{wdr} is the WDR intensity (mm/h), Rh is the rainfall on horizontal surfaces (mm/h), R_1 is the coefficient dependent on the surface inclination, R_2 is the coefficient dependent on the vertical distance of the component from the ground (s/m), V is the average hourly wind speed at 10 meters height (m/s), and ψ is the angle between the wind direction and the normal to the façade (°) (Nascimento *et al.*, 2016). For the walls analysed, the calculations are performed by considering vertical components ($R_1 = 0$) located at a height up to10m from the ground ($R_2 = 0.07$).

II.2. LIMITATIONS OF THE SIMULATION MODEL

According to the online support provided for the software family WUFI (IBP-Fraunhofer Institute for Building Physics, 2009) some simplifications were introduced in the model to make the calculations viable. Those simplifications entail the following limitations:

- WUFI Pro considers one-dimensional processes.
  Thus, it accounts for the plane behaviour of perfect walls and it does not refer to room corners, cracks in walls, window recesses, and other thermal bridges areas where the temperature can get very low during the cold season. It does not account for joints in the wall construction or the connection areas between the wall and other building components.
- The main heat and moisture transport phenomena are considered but some relevant ones are disregarded, such as convective heat and vapour transport by air flows;
- The interfacial hygric resistance between layers, which can reduce moisture transport considerably, is disregarded;
- The moisture storage function is simplified with one curve and it can be not representative for materials that have a strong hygroscopic hysteresis;

- The enthalpy flows resulting from the transport of liquid water across a temperature differential are ignored, which means that in the calculation cold rainwater does not cool the surface of the building component;
- The heat transfer coefficients at the surface are treated as constant or exhibiting a simple predefined dependence on wind speed.

II.3. INFORMATION ON THE CALCULATIONS PERFORMED TO EVALUATE THE U-VALUE OF COMPONENTS IN CHAPTER 5

The U-value, or thermal transmittance, of a building component, defines its ability to transmit heat under steady-state conditions: it indeed quantifies the heat that passes through one square meter of the wall when 1°C difference is applied at the boundary layers of air. For most building materials, the transmittance grows when the relative humidity increases, therefore two U-values are calculated, one refers to dry conditions and the other accounts for a relative humidity of 80%.

The calculation of the U-values is based on the indications of standard UNI EN 1745:2020 - 'Masonry and Masonry Products. Methods for Determining Thermal Properties', as shown in the following equations:

$$U - value = \frac{1}{Rsi + \sum Ri + Rse} \quad [W/(m^2.K)]$$

$$Ri = \frac{t_i}{\lambda_i} \quad [m^2.K/W]$$

where U-value is the thermal transmittance of the component, R_{si} and R_{se} are the resistances at the interior and exterior surface of the component, and ΣR_i is the sum of the thermal resistances of the single layers composing the building element. Each thermal resistance is calculated as the thickness of the layer, in m, divided by the thermal conductivity of the material composing the layer. For calculations at dry conditions the dry thermal conductivity is considered, for calculations at 80%RH the corresponding thermal conductivity is accounted.

Thermal resistances of the surfaces where approximated considering horizontal heat fluxes through vertical components and the suggestions provided in WUFI software: R_{se} =0.059 m^2K/W, R_{si} = 0.125 m^2K/W.

II.4. SENSITIVITY STUDY: THE INFLUENCE OF ORIENTATION AND LOCALIZATION ON MOISTURE ACCUMULATION IN A MASSIVE MASONRY WALL EXPOSED TO OUTDOOR CLIMATE.

In the case of massive walls exposed to outdoor climate without special rain protection, dynamic moisture equilibrium is governed by the alternating events of rain and sunshine (Künzel, 1998), which respectively influence the wetting and drying of the walls. Indeed, wind-driven rain is the main responsible for water intake in walls exposed to outdoor climate (Künzel, Künzel and Holm, 2004;

Guizzardi et al., 2015), whereas the exposure to direct solar radiation increases the superficial temperature of walls and, consequently, their drying process. More in detail, a rise in superficial temperature determines a higher saturation pressure at the component surface, thus increasing the period of time when drying conditions occur, i.e. when saturation pressure at the wet wall surface is greater than the vapour pressure in the air (Barreira and de Freitas, 2013).

Thus, the orientation of the wall, and its consequent exposition to different rain and solar loads strongly influences its moisture content. For this reason, two preliminary sensitivity analyses are performed to define the most important orientations to consider, as shown in Figure II.1.

The two studies account for a massive brick wall (1m-thick) exposed to different orientations in the three different climates. In the first study, the behaviour of the wall for one year, at dynamic equilibrium, is considered and its moisture content is analyzed. The second one considers the walls at their saturation water content and the following five years of drying.

Based on the results, one exposure is chosen to maximize water contents and it is expected to be the one exposed to maximum annual loads of wind-driven rain. The other exposure is chosen as exposed to smaller loads of wind-driven rain and more moderate moisture contents.

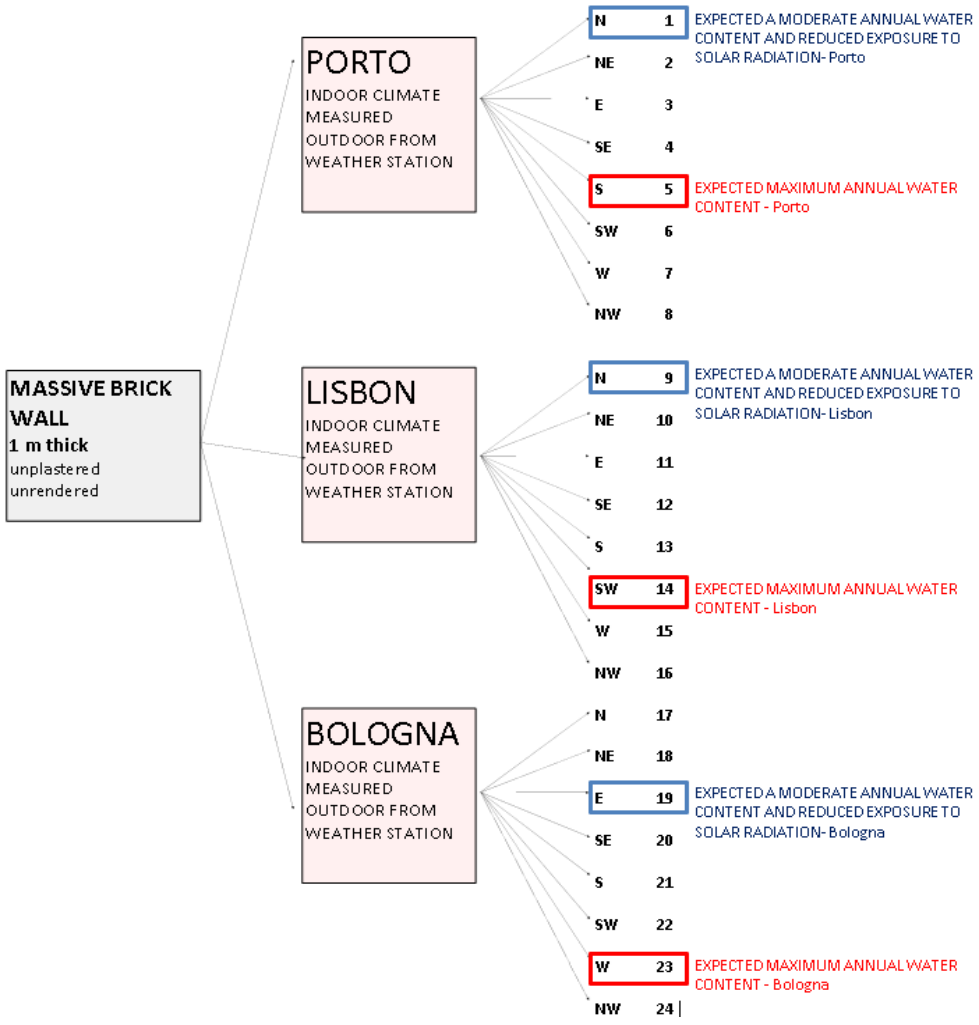

Figure II.1 – Planned simulation-set for the preliminary sensitivity analysis.

The results obtained for the sum of hourly water contents in a 1m-thick brick wall, exposed accordingly to several orientations, in the climate of Porto, Lisbon and Bologna are shown in Figure II.2.

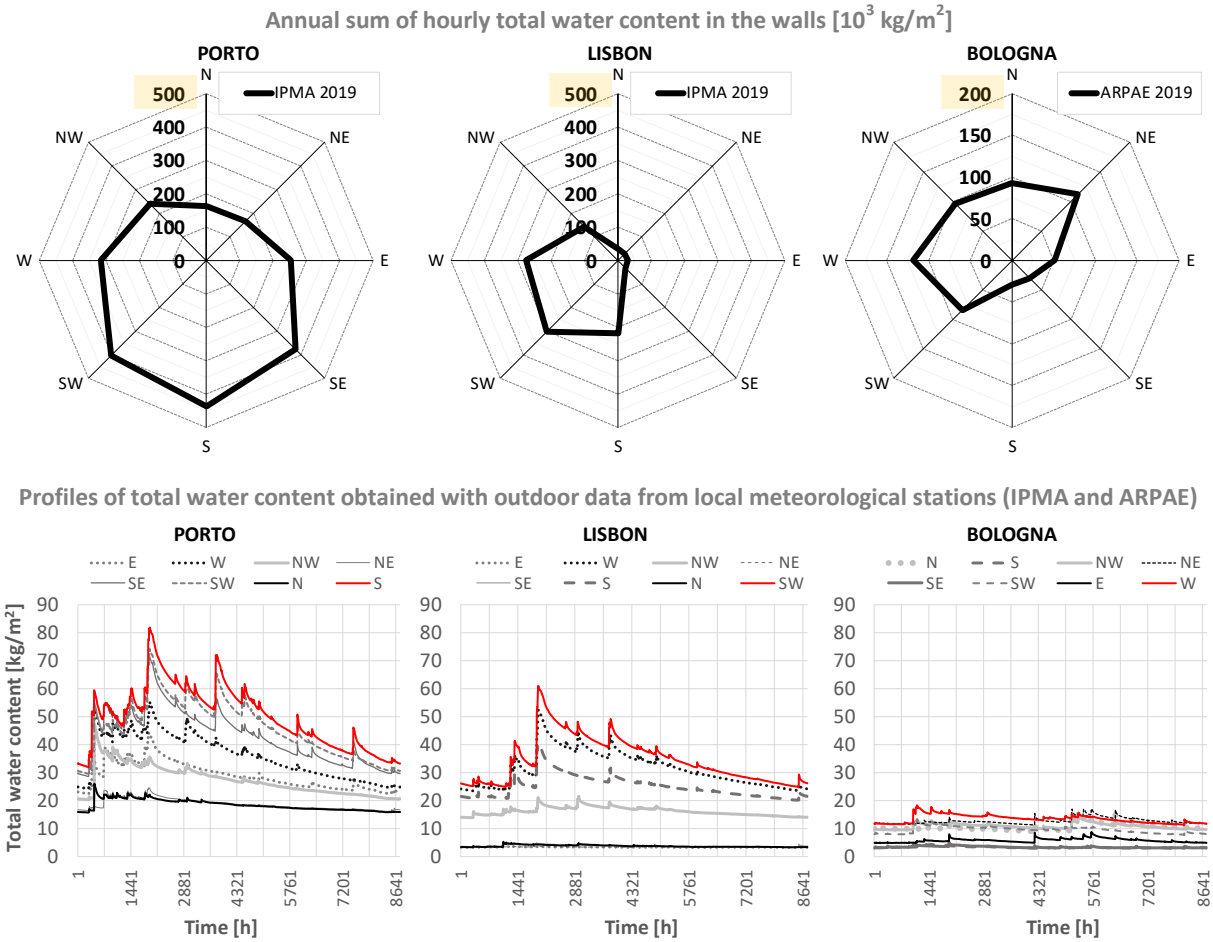

Figure II.2 – Water content in 1m thick brick walls, exposed to different orientations, in Porto, Lisbon and Bologna. At the top: sum of hourly water contents according to the climate obtained via IPMA and ARPAE meteorological stations. At the bottom: hourly profiles of total water content, where the red lines represent the profile of the wall orientation that maximise the annual water content and continuous black lines indicates a wall orientation that leads to very moderate water contents.

It emerges that:

- The results of moisture content in walls strongly depend on the outdoor climate considered;
- Different orientations lead to great differences in water contents and indicate that the maximum water contents (annual sum of hourly contents) are the ones of walls exposed to the maximum annual load of wind-driven rain;
- the maximum water contents (annual sum of hourly contents) are found for walls oriented to South, South-West and West in Porto, Lisbon and Bologna, respectively. Various orientations appear to minimize moisture content in walls, for the simulations, those are selected as North-oriented for Porto and Lisbon and East oriented for Bologna;
- The three climates have very different wind-driven rain loads which result in high differences in water contents. In Porto, the maximum water content in an exposed brick wall, 1-m thick, is about

80 kg/m^2 which is much higher than in the other two climates, indeed in Lisbon it is about 25% lower and in Bologna it is about a quarter of it;

- Porto has relevant annual wind-driven rain loads in all directions, indeed the annual sum of hourly water contents found for a wall exposed to minimum wind-driven rain load in Porto (N-oriented wall) is higher than in a wall exposed to maximum wind-driven rain in Bologna (W-oriented wall).

The results obtained for the drying curves of a 1m-thick brick wall, with several orientations, in the climate of Porto, Lisbon and Bologna are shown in Figure II.3.

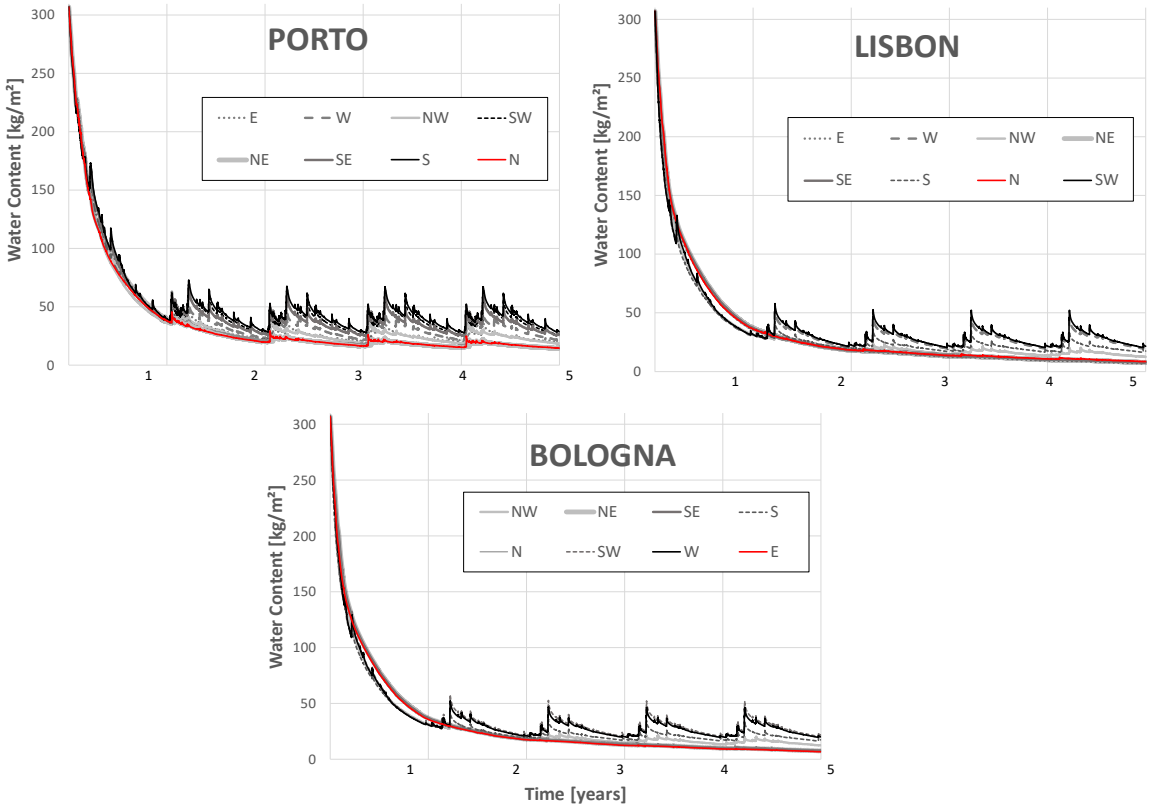

Figure II.3 – Water content in 1m thick brick walls during drying from initial free water saturation content. The walls are exposed to different orientations, in the climate of Porto, Lisbon and Bologna. Continuous black and red lines indicate the water content in walls respectively exposed to high and low wind-driven rain, respectively.

It emerges that:

- The drying curves obtained for different climates show similar behaviours, with walls exposed to high loads of wind-driven rain (S, SW, W for Porto, Lisbon and Bologna respectively) reaching equilibrium moisture content in about 2 years while North-oriented walls continue their drying also afterwards;
- In the first year of drying, walls exposed to low solar radiation, like the North-oriented wall in Lisbon and the North or East-oriented walls in Bologna, appear to experience slower drying than South and West oriented ones. In Porto this trend is not found, probably because of the high

influence of rain on the water content during the drying process, which makes the water content curves to be all very similar in the first year of drying.

Based on the outcomes of this sensitivity study, the following orientations were chosen for the study on the hygrothermal behaviour of retrofitted walls (Chater 5), to observe higher and lower exposure to moisture accumulation, as well as higher and lower exposure to WDR:

- North and South for Porto;
- North and South-West for Lisbon;
- East and West for Bologna.

II.5. COMPLEMENTARY SIMULATIONS: MOISTURE ACCUMULATION IN LISBON WALLS WHEN DIFFERENT COATINGS ARE ADOPTED FOR THERMAL-MORTAR BASED SYSTEMS.

In Chapter 5, the hygrothermal behaviour of massive walls retrofitted with various thermal insulation solutions was evaluated.

Very different results were obtained when adopting different thermal mortar-based insulation systems on the exterior side of walls. Namely, good performance was obtained with S5 and bad ones with systems S2, and S4. The latter two systems resulted in moisture accumulation in the SW-oriented wall in Lisbon. The different behaviour of the external insulation systems was considered to be strongly dependent on the coating adopted on the insulation layer. This assumption is hereby investigated with some complementary simulations. The three thermal mortars A1, A2, and A3 are adopted with different coating, namely B1+C2 and B2. The Aw and sd of the systems are synthesized in Figure II.4. All systems finished with B2, i.e. S5, A1+B2,A2+B2, fall inside the hyperbola $A_w * s_d = 0.2$ kg.m^{-1}.h$^{-0.5}$, whereas all systems finished with B1+C2 exceed this limit.

Results obtained in terms of moisture content under operational conditions are reported in Figure II.5. All thermal mortars do not lead to relevant moisture increase when covered with mortar B2. On the contrary, they lead to a noticeable increase (and even accumulation in SW-oriented wall) when finished with B1+C2. Thus, coating B1+C2 seems a risky choice. The results obtained further confirm that systems exceeding the recommended hyperbola should be avoided.

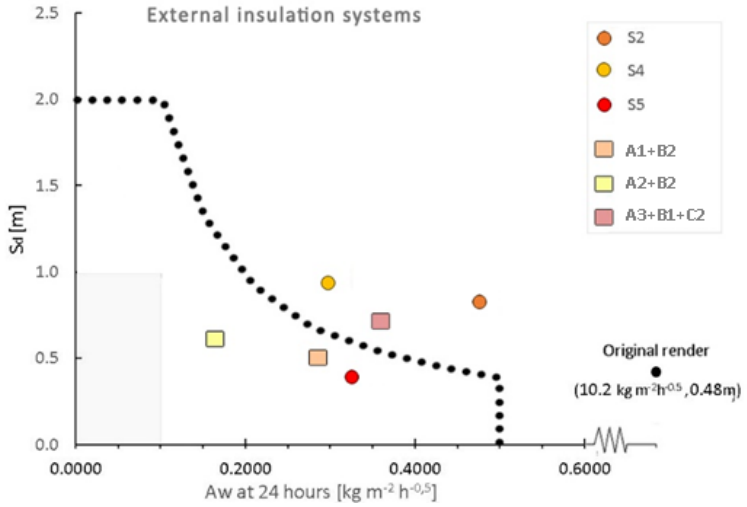

Figure II.4 – Equivalent air layer thickness (s_d) and capillary absorption coefficient (A_w) of external insulation systems and original render. Study on different coating for thermal mortar-based insulation systems S1, S3, S5.

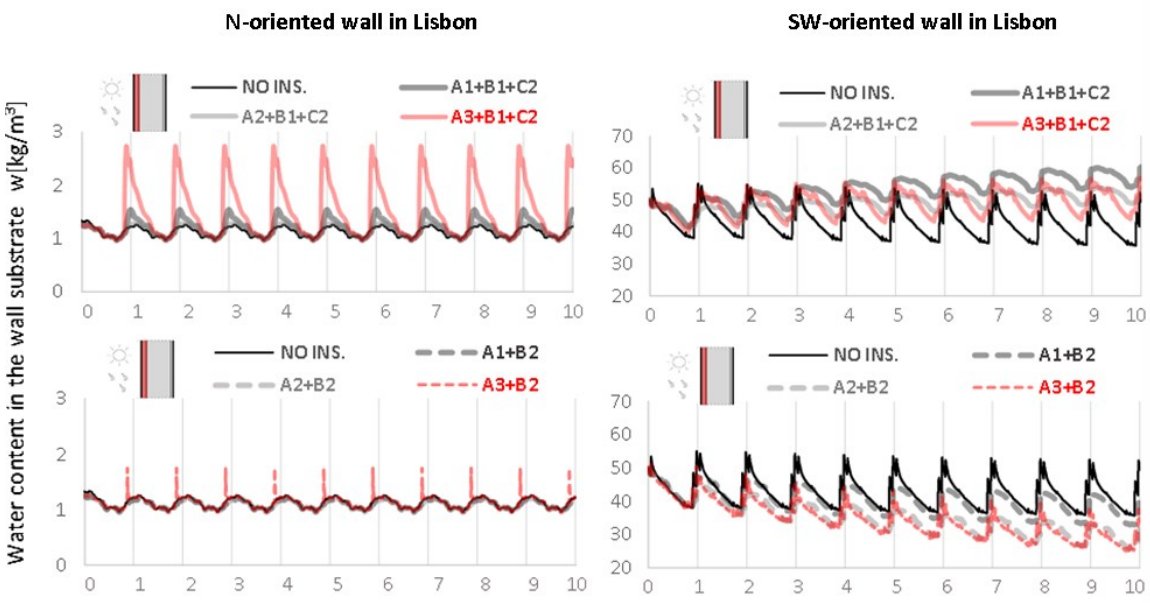

Figure II.5 – Water content in the wall substrate of the original and retrofitted walls (exterior insulation based on thermal mortars adopted with different coatings).